ADP/ATP carrier activity and mitochondrial translation-dependent regulation of oxidative phosphorylation in *Saccharomyces cerevisiae*

By

Oluwaseun Basit Ogunbona

A dissertation submitted to Johns Hopkins University School of Medicine in conformity with the requirements for the degree of Doctor of Philosophy

Baltimore, Maryland

March, 2018

ABSTRACT

The mitochondrial carrier family is a group of transport proteins that are mostly localized to the inner mitochondrial membrane where they facilitate the movements of various solutes across the membrane. Although these carriers represent potential targets for therapeutic application, research on the mitochondrial carrier family has not progressed commensurately. The ADP/ATP carrier is the most studied of mitochondrial carriers and is referred to as the paradigm of the family. Since it was first reported about two decades ago, a long-standing mystery in the field is how the absence of the major mitochondrial ADP/ATP carrier in yeast, Aac2p, results in a specific defect in cytochrome *c* oxidase (COX; complex IV) activity. In light of the recent demonstration that Aac2p physically associates with respiratory supercomplexes (RSCs), the possibility emerged that the activity of the complex may be dependent on its association with Aac2p. Therefore, this work was done to understand the mechanism of regulation of complex IV activity by the ADP/ATP carrier in yeast (*Saccharomyces cerevisiae*). By using a transport-dead pathogenic *AAC2* point mutant discovered in a patient with hypertrophic cardiomyopathy and mild myopathy, we sought to determine whether the reduced COX activity is due to absence of the interaction between Aac2p and components of the respiratory chain and/or the absence of Aac2p function (ADP/ATP transport). Using a battery of biochemical and molecular biology techniques, we uncovered a translation-dependent regulation of cytochrome *c* oxidase biogenesis that is provided by Aac2p function. Importantly, the steady state levels of mitochondrial genome-encoded complex IV subunits, which form the catalytic core of the complex, are significantly reduced when Aac2p function is missing, irrespective of the status of its association with respiratory supercomplexes. This decrease

in COX subunit amounts is not caused by a reduction in the mitochondrial DNA copy number or the level of its transcripts and does not reflect a defect in complex IV assembly. Instead, the absence of Aac2p activity results in an aberrant pattern of the mitochondrial translation. These results point to a direct functional link between Aac2p mediated transport and normal mitochondrial translation that is critical for the biogenesis of cytochrome *c* oxidase and optimal oxidative phosphorylation by extension.

Dissertation Readers:

Steven M. Claypool, Ph.D.
Director, Cellular and Molecular Physiology Graduate Program
Associate Professor of Physiology
Johns Hopkins University School of Medicine
725 North Wolfe Street, Hunterian 207
Baltimore, MD, 21205
[Faculty Sponsor and Reader]

Brian O' Rourke, Ph.D.
Vice Chair of Basic and Translational Research, Department of Medicine
Director, Bernard Laboratory of Fundamental Research in Preventive Cardiology
Professor of Medicine
720 Rutland Avenue, Ross 1060
Baltimore, MD, 21205
[Reader]

ACKNOWLEDGEMENTS

As a new arrival to the United States struggling with the attending jet lag and cultural shock, I found it very hard to conceptualize molecular concepts when I first started this journey at Johns Hopkins in the summer of 2013. Everyone needs help in the beginning as they say, and I was fortunate to have people who were determined and committed to help me succeed in this new career path.

I am extremely indebted to my advisor and mentor, Dr Steven Claypool for many reasons. He has provided all the needed support, guidance and training for me to develop as a scientist and to ensure I successfully transition to my next career step. He is always helpful, ever tolerant and one of the most supportive people I have ever met or known. From the skype-gone-bad interview when we first met and which I and Steve will never stop to remind each other about, till the time in future when he will truly be proud of me as an eminent physician-scientist, I am always assured of Steve's constant support of my life goals and aspiration. I could not have wished for a better mentor and he made this daunting graduate school task an easy ride, and I am so grateful for that and for every extracurricular support I received from him.

My thesis committee members, Dr Rajini Rao, Dr Natasha Zachara and Dr Brian O' Rourke, have been very supportive and contributory to my thesis project. They provided quality guidance to ensure that I succeed with my thesis project which initially proved to be very complex and complicated. Their constructive criticisms of my research plan brought fresh insights and ideas, and their supportive comments concerning the research progress updates made completion of my thesis project possible. I could not have done it without them. More so, I am grateful to my thesis reader, Dr O' Rourke, for the unparalleled

interest he took in my project and for working to ensure that my thesis is read promptly so that it was submitted on time.

There is no denying the support of all my colleagues at the Claypool lab. They all made the environment conducive for making productive scientific discussions, generating insightful hypotheses and performing excellent and highly reproducible experiments that make science both fun and rigorous at the Mitochondrial Phospholipid Research Center *aka* the Claypool lab. The lab was such a close-knit family and I can't take all their help for granted. Dr Ouma Onguka (Ouma) is one of the most instrumental in ensuring my success as a PhD student for he patiently taught me and trained me in the fundamentals of bench research. In addition to Ouma, Drs Matthew Baile, Yawen Lu and Elizabeth Calzada were senior graduate students in the lab when I joined. They all accepted me, taught me a lot of research techniques and never got tired of answering my numerous questions as a new member of the family. Nevertheless, Dr Selvaraju Kandasamy, Michelle Acoba, Pingdewinde Sam, Erica Avery and my mentee, Alex Rodriguez (Johns Hopkins University undergrad), who joined the lab sometimes after I did, contributed immeasurably to my thesis research.

I sincerely appreciate all my teachers from kindergarten all through to graduate school. How I wish Mrs. Philomena Mary Peters, who founded my elementary school, Mrs P. O Ojetunde, my high school principal, and Dr Sunny Gbenebitse, one of my favorite medical school teachers who gave me the first-ever formal lecture on physiology/medicine, were alive today. I am sure they will be very happy to know the flag is still flying. May their memories be eternal.

Dr William Bill Guggino, Madeline McLaughlin, Marsha Miller, LaTanya Heath, Catherine (Cathy) Will, Sylvia Stuart, Busayo Awe, Dr Jan Hoh, Dr Thomas Woolf, Dr Svetlana Lutsenko, Dr Guang William Wong, Dr Marcus Seldin, Dr Roger Reeves, Dr Frank Bosmans, Dr Jen Pluznick, Dr Peter Espenshade, Dr Namandje Bumpus, Dr Daniel Teraguchi, Dr Tilak Rathnanather, Dr Timothy Amukele, Dr Mario Amzel, Tammy Hubbe, Dr Michael J Borowitz, Francis K Fordjour and Dr Daniel Raben, all of the Johns Hopkins Medical Institution (JHMI), have supported me in one or more ways during my training at Hopkins. In the same vein, I am grateful for the support of all my teachers at the University of Lagos and Lagos University Teaching Hospital, Nigeria that prepared me for graduate degree particularly Professors Winifred Ayinke Mankanjuola, Olusoga A Sofola, Chikodi N Anigbogu, Smith I Jaja, Olufeyi Adegoke, Abraham A Osinubi, Mike Ibeabuchi, Aderonke Samuel, Wellington Oyibo, Adekunbiola Banjo, Fatimah Abdulkareem, Esther O Agbaje, Alani S Akanmu, Emmanuel Olanrewaju Bandele, Cyril Chukwu, Andrew Toyin Olagunju, Ahmed Kolade Oloyo, Foluso Ebun Afolabi Lesi, and Ifeoma P Okafor.

I have been helped and favored by a lot of people and I will not be able to list the name of everyone here. A number of people gave me financial and moral support during the period of my application for the PhD program. A lot of people received me when I arrived the United States and ensured my acclimatization was smooth. Many offered me a shoulder to lean on during times of stress and disappointments. Many opened the doors of their office and homes to accommodate all my requests. Many blessed me and my family with gifts and supported us during wedding, baby's arrival and other celebrations. I am very grateful and appreciate everyone.

I thank my parents-in-law, Moses and Margaret Ibiloye for their unwavering support and constant advice. They are an important addition to my life and they have been wonderful as parents to me and my beautiful wife, and as grandparents to our handsome son.

I am highly grateful to my parents, Dola and Adijat Ogunbona for the nurture, structure and future they gave my life. They are my foundation and pillar and standing on their shoulders enabled me to see life further. Now, I could not agree more with them that education is indeed the best legacy. They set me on the path to be a doctor of medicine that I could not recover from and taught me to be compassionate and patient in life. Being a medical doctor was enough for life's ambition but I have gone a little bit farther. It was not easy but it will be worth it all in the end.

On a final note, I am extremely indebted to my wife and the mother of our son, Oreoluwa Elnathan, for her constant love, support and encouragement during the period of my doctoral research. Elizabeth Ayooluwa will always hold a special place in my heart for accepting and loving me in spite of my flaws and shortcomings. I can't thank her enough. Without her, I could not have achieved this feat. It is because of her unquantifiable sacrifice that I could be a husband, father and student all at once and for this I am very thankful to have her by my side. There is no pretending that I love her and I will forever love her.

TABLE OF CONTENTS

LIST OF TABLES

LIST OF FIGURES

Chapter 1

Introduction

The Mitochondrial Carrier Family: Emerging Roles in the Biogenesis of Cytochrome *c* oxidase

1.1 SOLUTE CARRIER FAMILY (SLC)

Transport of substrates across biological membranes between and among organelles is an important feature of eukaryotic cells. The **S**o**L**ute **C**arrier (SLC) family, the second largest family of membrane proteins, is a large group of membrane transport proteins; in humans, there are 456 known members that are grouped into 65 subfamilies (Höglund, Nordström, Schiöth, & Fredriksson, 2011; Perland & Fredriksson, 2017). SLCs allow the movement of solutes—such as amino acids, ions, nucleotides, sugars and drugs—across biological membranes. The family includes functionally related proteins that allow transport and exchange of solutes across cell membranes. Transport can be facilitative by simply allowing solutes to move across a membrane according to their relative gradient on either side. Additionally, SLCs can mediate secondary active transport by coupling the downhill flow of a substrate, typically an ion, to the uphill movement of another substrate against its relative gradient across a membrane. Primary active transporters, ion channels and aquaporins are not included in the SLC family. The SLC family is structurally diverse as the criterion for inclusion in its ranks is being an integral membrane protein that transports a solute. However, within an individual family, members often share more than 20% sequence homology (Hediger et al., 2004). Table 1.1 describes the current list of SLC family members based on http://slc.bioparadigms.org and the references that review each subfamily. Families SLC53-65 are newly registered, and are based on a work presented at the BioMedical Transporters 2017 conference in Lausanne, Switzerland.

1.2 MITOCHONRIAL CARRIER FAMILY (SLC25)

Across the inner mitochondrial membrane, the Solute Carrier 25 (SLC25) family of transporters transport solutes into and out of the mitochondrion, although a number of

the members of this family are localized to other cellular organelles such as chloroplasts and peroxisomes (Bedhomme et al., 2005; Visser, van Roermund, Waterham, & Wanders, 2002). The mitochondrial carrier family (MCF) is the largest SLC subfamily and all members are encoded by the nuclear genome. As such, they are synthesized by cytoplasmic ribosomes and need to be imported from the cytosol to their final location. 35 members have been identified in yeast, 58 members in *Arabidopsis thaliana*, and 53 members have been identified in humans with about a third of these orphanized with no substrate(s) yet identified, as summarized in Table 1.2 (F. Palmieri & Pierri, 2010). Tissue distribution can vary from ubiquitous expression (e.g. SLC25A6 (Stepien, Torroni, Chung, Hodge, & Wallace, 1992)) to tissue-specific expression (e.g. SLC25A31 (Dolce, Scarcia, Iacopetta, & Palmieri, 2005; Rodić et al., 2005)).

SLC25 members are generally characterized by the presence of a tripartite structure (Figure 1.1) of approximately 300 amino acids, six conserved transmembrane regions, and the three-fold repeated MCF signature motif, P-X-[DE]-X-X-[RK]. Although they vary in size and nature of shuttled substrates, most members catalyze the exchange of one solute for another (antiport), couple the transport of one solute with another (symport), or facilitate the transport of a solute (uniport). Because of their sequence similarity, it is assumed that the transport mechanism is similar for the extended family.

1.2.1 Physiology of MCF

MCF is a family of functionally diverse proteins. Members transport a wide range of solutes across the inner mitochondrial membrane (IMM) and are important bridges linking many biochemical pathways in the cytosol and the mitochondrial matrix (F. Palmieri, 2014). Solutes transported include protons, nucleotides, amino acids, carboxylic

acids, inorganic ions, and cofactors. Their fundamental role in enabling metabolic compartmentalization cannot be overemphasized. SLC25 family members are involved in metabolic pathways such as heme synthesis and metal homeostasis (SLC25A28, SLC25A37, SLC25A38), fatty acid metabolism (SLC23A1, SLC25A20), amino acid metabolism (SLC25A13, SLC25A18, SLC25A22), nucleic acid metabolism (SLC25A19, SLC25A26, SLC25A33, SLC25A36), urea production (SLC25A2, SLC25A15) (LeMoine & Walsh, 2015; Shayakul, Clémençon, & Hediger, 2013; Shayakul & Hediger, 2004), oxidative phosphorylation (SLC25A3, SLC25A4, SLC25A5, SLC25A6, **SLC25A31**) and heat generation (SLC25A7, SLC25A9). In the next two sections, the physiology of select SLC25 members is briefly discussed to illustrate the diversity of cellular functions in which its members participate.

1.2.1.1 Mitoferrins are fundamental to Iron transport

Mitochondria are highly involved in the regulation of cellular iron. Iron is essential for mitochondrial function (Levi & Rovida, 2009). It is important in the heme biosynthetic pathway in the reaction step of ferrous iron incorporation into protoporphyrin IX catalyzed by ferrochetalase (Ponka, 1997). Heme is needed for synthesis of the mitochondrial cytochromes which are electron carriers critical for OXPHOS. In addition, iron-sulfur cluster biogenesis occurs in the mitochondrial matrix and is tightly linked to many other cellular processes such as heme biosynthesis, ribosome assembly, DNA synthesis, and translation initiation (Lill, 2009; Lill & Mühlenhoff, 2008). *SLC25A28* and *SLC25A37* encode Mitoferrin 2 (MFRN2) and Mitoferrin 1 (MFRN1), respectively, which are involved in iron import into the mitochondrion. In zebrafish and mammals, MFRN1 is expressed predominantly in hematopoietic tissues whereas MFRN2, with 65% amino acid

identity to its paralog is widely expressed (Amigo et al., 2011; Shaw et al., 2006). MFRN2 has about 38% identity to Mrs3p and Mrs4p (Shaw et al., 2006), two yeast transporters originally identified as suppressors of an intron splicing defect (Waldherr et al., 1993) that have since been associated with iron transport (Foury & Roganti, 2002). Yeast lacking Mrs3p and Mrs4p exhibit poor growth in iron-depleted conditions (Foury & Roganti, 2002). *MFRN1* loss of function of in mice and zebrafish results in reduced iron uptake into mitochondria and defective hemoglobinization (Shaw et al., 2006). Using 3T3 fibroblasts and mouse embryonic stem cells, it was shown that MFRN2 and MFRN1 are both involved in mitochondrial iron uptake in non-erythroid cells (Paradkar, Zumbrennen, Paw, Ward, & Kaplan, 2009). Heme synthesis is extremely compromised when both transporters are silenced and overexpression of one can functionally compensate for the loss of the other in non-erythroid cells (Paradkar et al., 2009). These results indicate the fundamental importance of these proteins in mitochondrial iron metabolism in erythroid and non-erythroid cells.

1.2.1.2 UCPs provide a pathway for proton leakage

The uncoupling proteins (UCPs) are regulated mitochondrial proteins known to transport protons, anions or other mitochondrial substrates (Fedorenko, Lishko, & Kirichok, 2012; Jezek, Jabůrek, & Garlid, 2010; Monné et al., 2018; Porter, 2012). Six UCP homologues have been discovered in humans - UCP1 or thermogenin (Heaton, Wagenvoord, Kemp, & Nicholls, 1978), UCP2 (Fleury et al., 1997), UCP3 (Boss et al., 1997), UCP4 (Mao et al., 1999), UCP5 or BMCP1 for brain mitochondrial carrier protein 1 (Sanchis et al., 1998), and UCP6 or KMCP1 for kidney mitochondrial carrier protein 1 (Haguenauer et al., 2005). UCPs uncouple OXPHOS from ATP synthesis; they dissipate

proton gradients by allowing protons that have been pumped into the intermembrane space by respiratory complexes to flow back into the mitochondrial matrix without being utilized for ATP synthesis. The translocation of hydrogen ion by UCPs requires fatty acids and this activity is inhibited by purine nucleotides such as GDP. However, there is controversy regarding the role of fatty acids in activating the uncoupling process that is directly pertinent to the putative UCP transport mechanism. There are currently two models of how UCP transports protons and anions in a process that involves or is regulated by fatty acids, as extensively reviewed (Jezek, Holendová, Garlid, & Jaburek, 2018). According to the fatty acid cycling mechanism, UCPs carry protons across the IM bound to fatty acids, which are flipped between membrane leaflets and subject to protonation and deprotonation events that in the net dissipate the proton gradient (Jabůrek, Varecha, Jezek, & Garlid, 2001; Jezek et al., 2018; Jezek et al., 2010; Jezek, Modrianský, & Garlid, 1997a, 1997b; Kamp & Hamilton, 1992; Kamp, Hamilton, & Westerhoff, 1993; Kamp, Zakim, Zhang, Noy, & Hamilton, 1995). This model is validated by a nuclear magnetic resonance and functional mutagenesis studies on UCP2 which provided molecular and structural support for this protonophoretic model (Berardi & Chou, 2014). The other mechanism, referred to as the fatty acid shuttling-carrier mechanism, has recently been experimentally disproven (Jezek et al., 2018). According to this model, originally advanced following a patch clamp study on UCP1 (Fedorenko et al., 2012), the protonated fatty acid must remain bound by hydrophobic interactions with UCP and shuttle hydrogen ion across the inner mitochondrial membrane through the protein (Jezek et al., 2018).

UCP1 is thought to be exclusively found in brown adipose tissue and is the only UCP responsible for adaptive adrenergic non-shivering thermogenesis (Golozoubova et al.,

2001; Matthias et al., 2000; Nicholls, Bernson, & Heaton, 1978; Porter, 2008). As such, it is firmly established that UCP1 functions as a true uncoupling protein that utilizes the electrochemical gradient produced by the respiratory chain to produce heat instead of ATP. Also, there seems to be a close relationship between mitochondrial reactive oxygen species (ROS) and UCP1-dependent thermogenesis although whether or not superoxide modulates UCP1 function is debated (Chouchani, Kazak, & Spiegelman, 2017; Echtay et al., 2002; Silva et al., 2005). Nonetheless, work with *ucp1* knockout (*ucp1*$^{-/-}$) mice has established that UCP1 is a target of redox modification *in vivo* (Chouchani et al., 2016). A recent study showed that brown adipose tissue (BAT) from *ucp1*$^{-/-}$ mice have reduced respiratory chain proteins and increased host defense signaling following exposure to cold (Kazak et al., 2017). Intriguingly, BAT-derived mitochondria from *ucp1*$^{-/-}$ mice are more sensitive to calcium overload in a ROS-dependent manner (Kazak et al., 2017). Thus, though UCP1 is traditionally linked to thermogenesis, it is very clear that UCP1 function extends beyond thermogenesis.

UCP2-5 are not involved in thermogenesis even though they provide mild uncoupling which may be protective against oxidative stress (Jezek et al., 2018). UCP2 is widely expressed (Fleury et al., 1997; Gimeno et al., 1997) and has numerous pathophysiological roles. For instance, due to its ability to reduce reactive oxygen species generation, UCP2 participates in both host immunity and the inflammatory response (Arsenijevic et al., 2000; Mattiasson & Sullivan, 2006; Nègre-Salvayre et al., 1997). In addition, UCP2 has been implicated in body mass regulation, glucose metabolism, and carcinogenesis (Derdak et al., 2008; Horimoto et al., 2004; Li, Nichols, Nathan, & Zhao, 2013; Li et al., 2015; Mattiasson & Sullivan, 2006; Sreedhar, Petruska, Miriyala,

Panchatcharam, & Zhao, 2017; Vozza et al., 2014; C. Y. Zhang et al., 2001). UCP3 is expressed mainly in the skeletal muscle and brown adipose tissue, and minimally in the heart (Boss et al., 1997; A. Vidal-Puig, Solanes, Grujic, Flier, & Lowell, 1997) where it is important for ROS attenuation but not body mass regulation or fatty acid metabolism (A. J. Vidal-Puig et al., 2000). Indeed, mitochondria from mice with lower levels of UCP3 have increased ROS production and oxidative damage further suggesting that UCP3 protects against ROS and oxidative damage (Brand et al., 2002). UCP4 is predominantly expressed in the nervous system including different regions of the brain, the spinal cord, hair cells of the inner ear, and Merkel cells in the skin (Liu et al., 2006; Smorodchenko, Rupprecht, Fuchs, Gross, & Pohl, 2011; Smorodchenko et al., 2009). UCP4 overexpressing neuronal cell lines have reduced oxidative phosphorylation with a corresponding increase in glucose uptake and glycolysis (Liu et al., 2006). These metabolic changes correlate with a drop in ROS production, a reduced tendency for calcium overload and an overall increased resistance to apoptosis (Liu et al., 2006). Overexpression of UCP4 in pre-adipocyte cell lines stimulates their proliferation, inhibits their differentiation into adipocytes and protects them against apoptosis (M. Zhang et al., 2006). Furthermore, impaired insulin sensitivity and mitochondrial biogenesis, decreased mtDNA level and increased ROS production occurs in adipocyte cell lines overexpressing UCP4 suggesting a global negative impact of UCP4 on mitochondrial function (Gao et al., 2010). However, in UCP4 overexpressing L6 myocytes, insulin sensitivity was improved with no change in intracellular ROS production, mtDNA levels or mitochondrial biogenesis (Gao et al., 2011). Regulated UCP4 expression, therefore, seems to be critical for optimal mitochondrial and cellular function.

UCP5 is expressed principally in the central nervous system and has three different forms (long form, UCP5L with 325 amino acids; short form, UCP5S with 322 amino acids; and short insert form, UCP5S1 with 353 amino acids) (Ramsden et al., 2012). UCP5 overexpression in human SH-SY5Y cells increases proton leak, reduces mitochondrial membrane potential and ATP production and increases oxygen consumption (Kwok et al., 2010). UCP6 has not been well studied. To date, it is associated with carcinogenesis (Nohara et al., 2012) and its expression in the kidney cortex is increased following pro-oxidant states (Haguenauer et al., 2005).

1.2.2 Pathology of MCF

MCF provide substrates for various biochemical processes in the cell. Consistent with their diverse and fundamental roles in metabolism, the absence or dysfunction of assorted MCF family members are associated with a wide variety of disorders including hematologic, neurologic, and cardiac diseases. Underlying many of these disorders is a defect in OXPHOS leading to disturbed mitochondrial energy metabolism that manifests in a wide variety of clinical signs and symptoms. A number of systemic diseases caused by SLC25 members is discussed briefly and Table 1.3 displays a summary of MCF-involved diseases clustered by presentation.

Mitochondrial carriers encoded by *SLC25A28*, *SLC25A37*, and *SLC25A38* are important for heme synthesis which requires cellular iron, glycine and succinyl CoA (Figure 1.2). Since red blood cells are very sensitive to defects in heme synthesis, dysfunction in any of these mitochondrial carriers causes anemia (Xu, Barrientos, & Andrews, 2013). The erythroid specific SLC25A38, which based on its requirement for erythropoiesis was initially predicted to encode an amino acid carrier capable of

transporting glycine, is now regarded as a glycine transporter (Fernández-Murray et al., 2016; Guernsey et al., 2009; Lunetti et al., 2016). Pathogenic mutations in *SLC25A38* and knockdown experiments in zebrafish implicate the carrier in the etiology of congenital sideroblastic anemia (Guernsey et al., 2009) (OMIM 610819). Mutations in the carrier are the second most common cause of inherited sideroblastic anemia and may account for about a fifth of all cases (Harigae & Furuyama, 2010; Horvathova, Ponka, & Divoky, 2010). As previously discussed, *SLC25A28* and *SLC25A37*, which encode the mitoferrins, are critical for iron homeostasis. Although no human mutations have been described for these carriers, MFRN1 has been shown to be important for heme synthesis in erythroid cells (Shaw et al., 2006).

SLC25A46 encodes a novel outer mitochondrial membrane protein, is widely expressed in the nervous system (Haitina, Lindblom, Renström, & Fredriksson, 2006), and mutated numerous neurological diseases including optic atrophy spectrum disorder, Charcot-Marie-Tooth type 2, Leigh syndrome, progressive myoclonic ataxia, and lethal congenital pontocerebellar hypoplasia (Abrams et al., 2015; Terzenidou et al., 2017; Wan et al., 2016) (OMIM 610826). Insight into each of these neurological diseases is hampered by the fact that SLC25A46 is also an orphan member of the MCF whose substrate(s) has not been defined (F. Palmieri & Monné, 2016). However, given its unusual localization to the outer membrane, whether SLC25A46 functions as a transporter or instead has novel activities that are unrelated to its SLC25 membership remains an open question.

Mitochondrial energy production is high in cardiac tissue and it is unsurprising that many mitochondrial carriers have been associated with cardiac disease, manifested in most cases as hypertrophic cardiomyopathy. Mutations in *SLC25A4* (*aka* adenine nucleotide

translocase-1; ANT1) are responsible for both the autosomal dominant and recessive cardiomyopathic type mitochondrial DNA depletion syndromes (OMIM 617184 and 615418 respectively) (Echaniz-Laguna et al., 2012; Körver-Keularts et al., 2015; L. Palmieri et al., 2005; Thompson et al., 2016),. Mutations in *SLC25A3* that encodes the phosphate carrier (PiC) cause either hypertrophic cardiomyopathy and impaired function of other organs such as skeletal muscle (Mayr et al., 2007; Mayr et al., 2011) or isolated cardiomyopathy (Bhoj et al., 2015). Interestingly, in the latter case (Bhoj et al., 2015), the mutations discovered in *SLC25A3* were a mix of a single nucleotide change and a stretch of indels, both of which could potentially impact the two mammalian isoforms of the protein (Bhoj et al., 2015; Seifert, Ligeti, Mayr, Sondheimer, & Hajnóczky, 2015). Carnitine-acylcarnitine translocase deficiency resulting from many different mutations in *SLC25A20* results in a multi-systemic disorder that includes cardiomyopathy as one of its clinical features (OMIM 212138) (Iacobazzi et al., 2004; Pande et al., 1993; Stanley et al., 1992). A genome-wide association study reported an association between UCP5 gene variants and the formation of atherosclerotic plaques suggesting that UCP5 has a protective role against atherosclerosis (Dong et al., 2011). Furthermore, UCP5 expression is increased in embolic stroke and multiple infarction brain lesions probably due to upregulation brought about by chronic ischemic stress (Nakase, Yoshida, & Nagata, 2007). However, since UCP5, like SLC25A38 and SLC25A46, is an orphan MCF, the underlying pathogenic mechanism is very much unclear at this time.

1.2.3 Challenges to Research on MCF

Mitochondrial carriers, and solute carriers in general, perform a central role in metabolism and their association with a myriad of diseases makes them attractive

candidates for basic and translational research. However, it has been noted that this area of research has not grown in commensurate proportion to its size or the potential gold mine it affords (César-Razquin et al., 2015). Most of these carriers are yet to be fully characterized and many of them remain totally uncharacterized. A number of technical factors have hampered growth of research focused on the extended membership of the SLC family that of course includes the MCF. A huge technical hurdle is the systemic absence of validated antibodies specific to most of these proteins. Further, many of the available antibodies are too weak to detect endogenous proteins whose expression is likely low and in general, many of the available reagents have not been rigorously characterized and validated (e.g. absence of signal with appropriate negative controls such as knockout cells). Compounding issues is the fact that many SLC members appear to have low immunogenicity which likely stems from the fact that they are polytopic membrane proteins that often display high interspecies conservation. Finally, transport assays are tedious to perform and somewhat limited by the volume of substrates available and/or required to de-orphanize a SLC protein.

Interestingly, a number of carriers have been shown to display substrate promiscuity by transporting more than one type of solute (Fiermonte, Paradies, Todisco, Marobbio, & Palmieri, 2009). Two members in *Arabidopsis thaliana*, AtUCP1 and AtUCP2, previously thought to be uncoupling proteins and therefore named as such were recently assigned the function of transporting amino acids, dicarboxylates, phosphate, sulfate, and thiosulfate (Monné et al., 2018). The Pi carrier in mammals, SLC25A3, was originally described as a phosphate symporter (Seifert et al., 2015; Wohlrab & Flowers, 1982) whose mutation is associated with fatal childhood diseases (Bhoj et al., 2015; Mayr

et al., 2007). Pic2p, originally thought to be a second albeit minor Pi carrier in yeast, actually functions as a Cu^{++} transporter responsible for the import of copper, required for cytochrome *c* oxidase assembly, into the mitochondrial matrix (Vest, Leary, Winge, & Cobine, 2013). Similarly, SLC25A3, which shares 65% similarity with Pic2p, was recently shown to have a conserved role for copper transport *in vivo* and *in vitro* (Boulet et al., 2017; Vest et al., 2013).

Apparent functional redundancy is another recurring feature of mitochondrial carriers (Taylor, 2017). For example, mitochondrial nucleotide homeostasis not only involves the ADP/ATP carriers (SLC25A4, SLC25A5, SLC25A6 and SLC25A31) but also is influenced by the ATP-Mg/Pi carriers (SLC25A23, SLC25A24, and SLC25A25). There is still a lot of unknowns regarding how all of these different transporters maintain the nucleotide pool across the inner mitochondrial membrane (IMM). It has been suggested that different mammalian ADP/ATP carrier isoforms, which do not transport AMP, may have different preferred transport modes i.e. ATP *vs* ADP. For instance, based on its high expression in cancer cells, SLC25A5 (also called adenine nucleotide translocase-2; ANT2) was postulated to preferentially import ATP made by glycolysis, an activity that maintains the mitochondrial membrane potential and by extension, other essential mitochondrial functions (Chevrollier et al., 2005; Giraud, Bonod-Bidaud, Wesolowski-Louvel, & Stepien, 1998; Stepien et al., 1992). However, it was recently demonstrated in a range of cancer cells that the uptake of ATP is in fact completely independent of the activity of any ADP/ATP carrier isoform (Maldonado et al., 2016). As such, it remains unresolved whether the different ANT isoforms do or do not have distinct transport activities and/or substrate preferences. Also unclear is how the calcium-dependent ATP-Mg/Pi carriers,

which were originally thought to preferentially transport ATP but since demonstrated to also transport other adenine nucleotides (Fiermonte et al., 2004), interface with the ADP/ATP carriers to modulate mitochondrial nucleotide homeostasis. As research progresses in this area, the substrate(s) transported by many of these proteins will be identified which will provide foundational information as to their physiological roles.

1.3 The ADP/ATP carrier protein

Eukaryotic cells make energy in the form of ATP in the mitochondrial matrix and the ATP is translocated through the impermeable IMM to power many processes in the cell. The ADP/ATP carriers (AAC) provide the means of transport of ATP and its precursor ADP, across the IMM. Under physiological conditions, 1 molecule of ADP from the cytosol is exchanged for 1 molecule of matrix-localized ATP by the activity of the ADP/ATP carrier. AAC, referred to as adenine nucleotide translocase (ANT) in humans, is a notable MCF member as it was the first to have its amino acid sequenced (Aquila, Misra, Eulitz, & Klingenberg, 1982) and its 3D structure solved (Pebay-Peyroula et al., 2003). Similar to all members of the MCF and regarded as a paradigm for this family, AACs are nuclear-encoded, integral membrane proteins with approximately 300 amino acids arranged into three repeats linked by two loops on the cytosolic side. There are two transmembrane α-helices in each repeat connected together by a long loop on the matrix side, giving the carrier a three-fold pseudosymmetry (F. Palmieri, 2013).

One of the most abundant proteins in the IMM, AACs are encoded by multiple different genes in both unicellular and multicellular eukaryotes. There are three yeast AAC isoforms and four human ANT isoforms. The human ANT isoforms overlap in their expression pattern but exhibit tissue-specificity. ANT1 is the most equivalent to yeast

Aac2p and the predominant isoform in the heart and skeletal muscle (Stepien et al., 1992). *ANT2* is mostly expressed in regenerative tissues such as the kidney and liver, *ANT3* is ubiquitously expressed at low baseline levels, and *ANT4* is selectively expressed in the testis (Doerner et al., 1997; Dolce et al., 2005; Dupont & Stepien, 2011; Kim et al., 2007; Rodić et al., 2005; Stepien et al., 1992). Aac2p is the most abundant of all three isoforms in yeast and the only one absolutely required for oxidative phosphorylation and growth on respiratory carbon sources (Lawson, Gawaz, Klingenberg, & Douglas, 1990). Aac1p and Aac3p are minor isoforms in yeast that under normal growth conditions, are undetectable at the protein level. Aac1p expression is repressed in hypoxic conditions (Gavurníková, Sabova, Kissová, Haviernik, & Kolarov, 1996) and Aac3p expression is induced in anaerobic situations (Sabová, Zeman, Supek, & Kolarov, 1993).

AAC has been a subject of many controversies in the field of mitochondrial biology. First, the oligomeric status of the OXPHOS machinery has been much debated over the past 18 years. Originally thought to consist of individual complexes in a functional chain, the advent of Blue-Native Polyacrylamide Gel-Electrophoresis (BN-PAGE) (Schägger & von Jagow, 1991), a gentle electrophoretic technique for analysis protein-protein interactions, facilitated the discovery and ultimate acceptance that the respiratory complexes interact to form higher-order supramolecular complexes of varying stoichiometry that are referred to as respiratory supercomplexes (RSCs) (Acín-Pérez, Fernández-Silva, Peleato, Pérez-Martos, & Enriquez, 2008; Cruciat, Brunner, Baumann, Neupert, & Stuart, 2000; Gu et al., 2016; Letts, Fiedorczuk, & Sazanov, 2016; Moreno-Lastres et al., 2012; Schägger & Pfeiffer, 2000; Wu, Gu, Guo, Huang, & Yang, 2016). The RSCs are conserved despite differences in composition across different species. For

example, in yeast which lack complex I, RSCs form composed of complexes III and IV whereas in mammals, RSCs consist of complexes I, III, and IV (Schägger & Pfeiffer, 2000). Nevertheless, there is still some controversy as to their functional and physiological relevance. Recently it was demonstrated that the respiratory supercomplexes (RSC) are functional entities (Barrientos & Ugalde, 2013; Lapuente-Brun et al., 2013) whose structures have since provided novel insight into the potential benefits that they may confer (Althoff, Mills, Popot, & Kühlbrandt, 2011; Dudkina, Kudryashev, Stahlberg, & Boekema, 2011; Genova & Lenaz, 2014; Gu et al., 2016; Letts, Fiedorczuk, & Sazanov, 2016; Schäfer, Dencher, Vonck, & Parcej, 2007; Wu, Gu, Guo, Huang, & Yang, 2016). Functional benefits of RSCs that have been suggested but not yet proven include: improved electron transfer efficiency and reduced ROS generation, each stemming from a substrate channeling based mechanism; increased metabolic flexibility resulting from changes in RSC composition; and finally, enhanced stability and functionality of all participating complexes in the specific context of the protein-dense inner mitochondrial membrane (Barrientos & Ugalde, 2013; Milenkovic, Blaza, Larsson, & Hirst, 2017).

About ten years ago, a new functional entity was shown to interact with yeast RSCs: Aac2p (Claypool, Oktay, Boontheung, Loo, & Koehler, 2008; Dienhart & Stuart, 2008). This association was recently shown to be evolutionarily conserved as two distinct human ANT isoforms also form complexes with RSCs (Lu et al., 2017). Functionally, this conserved interaction could benefit both RSCs and the AACs. Specifically, the electrogenic exchange of ATP_{in}/ADP_{out} by AAC/ANT is positively influenced by the membrane potential ($\Delta\Psi$) across the IM (Krämer & Klingenberg, 1980) which of course is established by the electron transport chain. Similarly, by dissipating the electrical gradient, productive

AAC/ANT transport makes it easier for RSCs to pump protons. As such, it is reasonable to hypothesize that this known functional synergy is further enhanced by being physically associated. Additional work is needed to test this provocative hypothesis.

AACs interacts with the respiratory supercomplexes in the presence of cardiolipin, a unique phospholipid found exclusively in the mitochondrion (Claypool et al., 2008). Available structures of AAC/ANTs depict three tightly bound cardiolipin molecules per monomer (Beyer & Klingenberg, 1985; Pebay-Peyroula et al., 2003; Ruprecht et al., 2014). In the absence of cardiolipin, Aac2p function is impaired and Aac2p assembly is drastically altered (Claypool et al., 2008; Jiang et al., 2000). The absence of cardiolipin also destabilizes the RSCs (Pfeiffer et al., 2003; M. Zhang, Mileykovskaya, & Dowhan, 2002), including its association with Aac2p (Claypool et al., 2008). That Aac2p assembly and function is CL-dependent has led to the hypothesis that the assembly and function of AAC/ANTs may be the "Achilles heel" of a multitude of cardiolipin-based diseases (Claypool, 2009; Klingenberg, 2008). The structural changes in RSCs and Aac2p that occur in the absence of cardiolipin have clear functional consequences (Claypool et al., 2008). However, the relative contribution of each structural change— impaired assembly of RSCs, Aac2p, or RSC-Aac2p— that occurs in the absence of cardiolipin to the associated mitochondrial dysfunction has not been established.

It has also been hotly debated whether the protein exists and/or functions as a monomer or dimer. Mitochondrial carriers were originally accepted to exist and function as homo-dimers (Capobianco, Ferramosca, & Zara, 2002; Dyall, Agius, De Marcos Lousa, Trezeguet, & Tokatlidis, 2003; Klingenberg, 1981; Kotaria, Mayor, Walters, & Kaplan, 1999; Lin, Hackenberg, & Klingenberg, 1980; Nury et al., 2005; Palmisano et al., 1998;

Postis, De Marcos Lousa, Arnou, Lauquin, & Trézéguet, 2005; Schroers, Burkovski, Wohlrab, & Krämer, 1998; Trézéguet et al., 2000). A number of studies, motivated by the crystal structures (Kunji & Harding, 2003; Pebay-Peyroula et al., 2003; Ruprecht et al., 2014) have challenged this initial view. Using a variety of biochemical, biophysical and structural studies, the Kunji lab has provided evidence that AAC functions, and in fact exists in the IMM, as monomers (Bamber, Harding, Butler, & Kunji, 2006; Bamber, Harding, Monné, Slotboom, & Kunji, 2007; Bamber, Slotboom, & Kunji, 2007; Kunji & Crichton, 2010; Kunji & Harding, 2003). However, the functional significance of AACs interaction with the RSCs, whether the interaction occurs as monomeric or oligomeric units, what subunits of the respiratory complexes are involved in the interaction, and whether or not the RSCs facilitate AACs' oligomerization are outstanding questions in need of experimental answers.

The absence of Aac2p in yeast impairs oxidative phosphorylation (Claypool et al., 2008; Dienhart & Stuart, 2008; Fontanesi et al., 2004; Heidkämper, Müller, Nelson, & Klingenberg, 1996; Müller, Basset, Nelson, & Klingenberg, 1996). Prior mutagenic studies of Aac2p suggested that the OXPHOS machinery is dependent on Aac2p function and/or expression (Müller et al., 1996; Müller, Heidkämper, Nelson, & Klingenberg, 1997). More recently, several groups, including ours, reported similar findings of specific reduction in cytochrome *c* oxidase activity in yeast strains lacking Aac2p (Claypool et al., 2008; Dienhart & Stuart, 2008; Fontanesi et al., 2004; Heidkämper et al., 1996; Müller et al., 1996). It remains to be determined, however, how the absence of Aac2p results in a specific defect in cytochrome *c* oxidase activity. Mechanistically, Aac2p nucleotide transport

activity and/or its interaction with the RSCs may be important for optimal cytochrome *c* oxidase activity.

1.4 Mitochondrial translation

The vast majority of mitochondrial proteins are translated in the cytosol and thereafter have to be imported into the mitochondrion. For those proteins encoded by the mitochondrial genome (mtDNA), mitochondria have retained a dedicated, dual-origin translational machinery whose architecture is similar to that of bacteria. Consistent with this bacterial origin, mitochondrial translation is pharmacologically unaffected by cycloheximide, an inhibitor of cytosolic translation, and is instead sensitive to antibiotics such as puromycin. Eight polypeptides in yeast and thirteen polypeptides in humans are encoded by mtDNA and produced via mitochondrial translation. Apart from genes for these polypeptides, the mtDNA also encodes a set of transfer (t)RNAs, ribosomal (r) RNAs and in yeast, the RNA component of the mitochondrial RNAse P (Towpik, 2005; Walker & Engelke, 2008). The mitochondrial translational cycle is subdivided into four steps—initiation, elongation, termination and recycling—and nuclear encoded polypeptide factors are required at different steps for optimal mitochondrial translation (Kehrein, Bonnefoy, & Ott, 2013; Smits, Smeitink, & van den Heuvel, 2010; Towpik, 2005). An example of a nuclear-encoded factor in yeast is the mitochondrial translation initiation factor 3 (mIF3p), the *Saccharomyces cerevisiae* homolog of the bacterial translation initiation factor 3 (IF3). Its function is conserved and overlaps with human mIF3p (Atkinson et al., 2012; Kuzmenko et al., 2014), and its absence in yeast disrupts mitochondrial translation (Kuzmenko et al., 2016). In addition, a number of translational activators directly interacting with mRNAs of mitochondrial encoded polypeptides are necessary to optimize

the translation of a specific mtDNA-encoded polypeptide e.g. synthesis of Cox1p is affected when Mss51p is absent or limiting (Barrientos, Zambrano, & Tzagoloff, 2004; Fontanesi, Clemente, & Barrientos, 2011; Perez-Martinez, Broadley, & Fox, 2003; Perez-Martinez, Butler, Shingu-Vazquez, & Fox, 2009; Siep, van Oosterum, Neufeglise, van der Spek, & Grivell, 2000).

Translation of mitochondrial proteins is tightly coupled to their assembly into respiratory complexes in a manner similar to a mechanism described as "controlled by epistasy of synthesis" (CES) that exists in the biogenesis of photosynthetic protein complexes (Choquet et al., 2001; Towpik, 2005). For example, in yeast, Cox1p synthesis is tightly coupled to the assembly of respiratory complex IV which helps to balance the production of subunits with their assembly into the holoenzyme which in the net preserves mitochondrial proteostasis (Barrientos et al., 2004; Perez-Martinez et al., 2003; Soto, Fontanesi, Liu, & Barrientos, 2012; Towpik, 2005).

1.5 Emerging Roles in the Biogenesis of Cytochrome c oxidase

In yeast and in humans, there is an emerging link between the function of MCF members and cytochrome *c* oxidase biogenesis. For instance, it was shown that a destabilizing pathogenic mutation in *SLC25A46* impairs OXPHOS and Ascorbate/TMPD-dependent respiration and reduces steady state levels of complex IV subunits (Janer et al., 2016). These findings are consistent with a complex IV-specific assembly defect in *SLC25A46* mutant fibroblasts. At present, the mechanistic basis for the reduced steady state levels of complex IV subunits has not been determined. While it is not totally unexpected that MCF carriers play a role in the assembly of this intricate complex with subunit derived from two genomes (many SLC members provide substrates that serve as building blocks

needed for processes such as mitochondrial DNA replication, transcription, translation, and/or post-translational assembly of protein complexes), it is very surprising that these defects seem to specifically impact complex IV without significantly affecting the other OXPHOS complexes that are built from subunits expressed from both the nuclear and mitochondrial genomes.

Very recently, the yeast ortholog of the human *SLC25A38*, HEM25, important for heme synthesis as a mitochondrial glycine importer, was tested for its role in the stability of proteins of the respiratory complexes (Dufay, Fernández-Murray, & McMaster, 2017). Interestingly, while deletion of Hem25p compromises the steady state level of subunits of all the respiratory complexes except for complex V (ATP synthase), its absence is most detrimental on complex IV (Dufay et al., 2017). Intriguingly, the combined absence of Hem25p and Flx1p, the mitochondrial flavin adenine dinucleotide transporter (ortholog of human *SLC25A32*), further reduces the steady states level of subunits of the *hem25*Δ-affected respiratory complexes except complex IV (Dufay et al., 2017). These results are consistent with a model that Hem25p and Flx1p provide heme and FAD, respectively, which are required for the assembly of the respiratory chain complexes.

Furthermore, siRNA knockdown of the two isoforms of *SLC25A3*, *SLC25A3-A* and *SLC25A3-B*, in many different cell types results in reduced cytochrome *c* oxidase holoenzyme levels and activity (Boulet et al., 2017). When SLC25A3 is limiting, the steady state levels of COX4, a nuclear encoded subunit of cytochrome *c* oxidase, and mitochondrial copper are reduced (Boulet et al., 2017). Interestingly, COX4 abundance is rescued by copper supplementation (Boulet et al., 2017). Since copper is critical for the assembly of cytochrome *c* oxidase (Baile & Claypool, 2013; Diaz, 2010), defects in copper

import are likely to impair cytochrome *c* oxidase biogenesis. Nevertheless, SLC25A3 function may be modulated and/or linked to the assembly of cytochrome *c* oxidase via a pathway that is presently unidentified (Boulet et al., 2017).

Finally, the absence of Aac2p in yeast leads to a specific reduction of cytochrome *c* oxidase activity while the activity of complex III is unaffected (Dienhart & Stuart, 2008). The reduced complex IV activity likely stems from lower steady state levels of its subunits in the absence of Aac2p. These findings are consistent with the impaired OXPHOS activity that occurs when Aac2p expression is decreased or ablated (Claypool et al., 2008; Heidkämper et al., 1996; Müller et al., 1996; Müller et al., 1997). Intuitively, the mechanistic basis for the reduced steady state levels of complex IV subunits could derive from a defect in any step in its biogenesis that is regulated/modulated by and/or dependent on the nucleotide transport function of Aac2p. Alternatively, the conserved AAC/ANT-RSC interaction may itself be critical for robust cytochrome *c* oxidase expression, assembly, and/or function. Since the Aac2p and ANT1/ANT2 interactomes all included other SLC25 family members (Claypool et al., 2008; Lu et al., 2017), it is possible that these MCF-MCF interactions are critical for maintaining the abundance of metabolites that are needed for optimal mitochondrial translation and assembly of respiratory complexes. Future efforts focused on dissecting the functional significance of distinct aspects of the AAC/ANT interactome are likely to shed significant insight into how it supports complex IV biogenesis.

1.5 Summary

Mitochondrial carriers represent a vast array of transport proteins with essential biochemical and physiological functions. At the molecular level, the mechanistic basis for

their role(s) in the regulation of OXPHOS is still missing. Significant knowledge gaps exist in this area of research and discovery of new members and novel functions of existing members will give us a better understanding of their pathophysiological roles. Long term, such information may guide development of effective therapeutic strategies to correct or better manage disease resulting from their dysfunction. With recent advances in biomedical research such as the advent of gene editing technologies (e.g. CRISPR/Cas9), substantial and rapid progress in the field of solute carriers is anticipated.

1.6 Acknowledgements

We would like to thank Gergely Gyimesi (University of Bern, Switzerland) for providing more information on the SLC tables. This work was supported by the National Institutes of Health grant (R01HL108882) to S.M.C and a pre-doctoral fellowship from the American Heart Association (15PRE24480066) to O.B.O.

TABLES

Table 1.1 Abridged list of current SLC families[a].

SLC Subfamily	Description	Number of members	References
SLC1	High-affinity glutamate and neutral amino acid transporter family	7	(Gegelashvili et al., 2006; Kanai et al., 2013; Kanai & Hediger, 2003, 2004; Nakagawa & Kaneko, 2013)
SLC2	Facilitative GLUT transporter family	18 (including 4 pseudogene: SLC2A3P1, SLC2A3P2, SLC2A3P4, SLC2AXP1)	(Barron, Bilan, Tsakiridis, & Tsiani, 2016; Hevia et al., 2015; Mueckler & Thorens, 2013; Simpson et al., 2008; Uldry & Thorens, 2004)
SLC3	Heavy subunits of the heteromeric amino acid transporters	2	(Bergeron, Simonin, Bürzle, & Hediger, 2008; Fotiadis, Kanai, & Palacín, 2013; Palacín & Kanai, 2004; Schweikhard & Ziegler,

			2012; Verrey et al., 2004)
SLC4	Bicarbonate transporter family	10 (SLC4A6 and SLC4A7 are the same)	(Aalkjaer, Boedtkjer, Choi, & Lee, 2014; Alper, 2006; Alper, Chernova, & Stewart, 2001; Alper, Darman, Chernova, & Dahl, 2002; Gill & Boron, 2006; Parker & Boron, 2013; Pushkin & Kurtz, 2006; Romero, 2005; Romero, Chen, Parker, & Boron, 2013)
SLC5	Sodium glucose cotransporter family	12	(Bergeron et al., 2008; Wright, 2013)
SLC6	Sodium- and chloride-dependent neurotransmitter transporter family	22 (1 pseudogene SLCA10P)	(Pramod, Foster, Carvelli, & Henry, 2013)
SLC7	Cationic amino acid transporter/glycoprotein-associated family	15 (including 2 pseudogenes SLC7A5P1	(Bergeron et al., 2008; Fotiadis et al., 2013; Palacín & Kanai, 2004; Schweikhard & Ziegler,

		and SLC7A15P)	2012; Verrey et al., 2004)
SLC8	Na^+/Ca^{2+} exchanger family	4	(Blaustein & Lederer, 1999; DiPolo & Beaugé, 2006; Khananshvili, 2013; Quednau, Nicoll, & Philipson, 2004)
SLC9	Na^+/H^+ exchanger family	18 (including 5 pseudogenes)	(Donowitz, Ming Tse, & Fuster, 2013; Fuster & Alexander, 2014; Orlowski & Grinstein, 2004; Padan & Landau, 2016)
SLC10	Sodium bile salt cotransport family	7	(Claro da Silva, Polli, & Swaan, 2013; Geyer, Wilke, & Petzinger, 2006)
SLC25	Mitochondrial carrier family	60 (including 7 pseudogenes)	(Clémençon, Babot, & Trézéguet, 2013; Haitina et al., 2006; F. Palmieri, 2004, 2013; F. Palmieri & Monné, 2016)
SLC53	Phosphate carriers	1	

SLC54	Mitochondrial pyruvate carriers	3	
SLC55	Mitochondrial cation/proton exchangers	3	
SLC56	Sideroflexins	5	
SLC57	Non-imprinted in Prader-Willi/Angelman syndrome chromosome region (NiPA) -like magnesium transporter family	6	
SLC58	MagT-like magnesium transporter family	2	
SLC59	Sodium-dependent lysophosphatidylcholine symporter family	2	
SLC60	Glucose transporters	2	
SLC61	Molybdate transporter family	1	
SLC62	Pyrophosphate transporters	1	
SLC63	Sphingosine-phosphate transporters	3	
SLC64	Golgi $Ca2^{+}/H^{+}$ exchangers	1	
SLC65	Niemann-Pick C (NPC)-type cholesterol transporters	2	

[a]The SLC subfamily, description and numbers of members in each subfamily are shown. Further information on the SLC genes can be found at http://slc.bioparadigms.org.

Table 1.2: Current list of MCF members[a].

SLC name	Protein name	Substrates
SLC25A1	CIC (citrate carrier)	citrate, isocitrate, malate, phosphoenolpyruvate (PEP)
SLC25A2	ORC2 (ornithine carrier 2)	ornithine, citrulline, lysine, arginine, histidine
SLC25A3	PHC (phosphate carrier)	phosphate, Cu^{++}
SLC25A4	ANT1 (adenine nucleotide translocase-1)	ADP, ATP
SLC25A5	ANT2 (adenine nucleotide translocase-2)	ADP, ATP
SLC25A5P1	pseudogene	
SLC25A6	ANT3 (adenine nucleotide translocase-3)	ADP, ATP
SLC25A6P1	pseudogene	
SLC25A7	UCP1 (uncoupling protein 1)	H^+
SLC25A8	UCP2 (uncoupling protein 2)	H^+
SLC25A9	UCP3 (uncoupling protein 3)	H^+
SLC25A10	DIC (dicarboxylate carrier)	malate, phosphate, succinate, sulphate, thiosulphate
SLC25A11	OGC (oxoglutarate carrier)	2-oxoglutarate, malate

SLC25A12	AGC1 (aspartate / glutamate carrier 1)	aspartate, glutamate
SLC25A13	AGC2 (aspartate / glutamate carrier 2)	aspartate, glutamate
SLC25A14	UCP5 (uncoupling protein 5)	***Orphan***
SLC25A15	ORC1 (ornithine carrier 1)	ornithine, citrulline, lysine, arginine
SLC25A15P1	pseudogene	
SLC25A16	GDC (Graves' disease carrier)	***Orphan***
SLC25A17	Peroxisomal membrane protein PMP34	CoA, FAD, NAD+, AMP, ADP, PAP, dPCoA, FMN
SLC25A18	GC2 (glutamate carrier 2)	glutamate
SLC25A19	DNC (deoxynucleotide carrier)	thiamine pyrophosphate, thiamine monophosphate, (deoxy)nucleotides
SLC25A20	CAC (carnitine / acylcarnitine carrier)	carnitine, acylcarnitine
SLC25A20P1	pseudogene	
SLC25A21	ODC (oxoadipate carrier)	oxoadipate, oxoglutarate
SLC25A22	GC1 (glutamate carrier 1)	glutamate

SLC25A23	Calcium-binding mitochondrial carrier protein SCaMC-3	ATP-$Mg2^{+}$, ATP, ADP, AMP, Pi
SLC25A24	Calcium-binding mitochondrial carrier protein SCaMC-1	ATP-Mg^{2+}, ATP, ADP, AMP, Pi
SLC25A25	Calcium-binding mitochondrial carrier protein SCaMC-2	***Orphan***
SLC25A26	S-adenosylmethionine mitochondrial carrier protein (SAMC)	S-adenosyl-methionine, S-adenosyl-homocysteine
SLC25A27	UCP4 (uncoupling protein 4)	***Orphan***
SLC25A28	Mitoferrin 2 (Mfrn2)	Fe^{2+}
SLC25A29	ORNT3	ornithine, acylcarnitine
SLC25A30	Kidney mitochondrial carrier protein 1 or UCP6 (uncoupling protein 6)	***Orphan***
SLC25A31	AAC4, ANT4 (adenine nucleotide carrier 4)	ADP, ATP
SLC25A32	MFT	folate
SLC25A33	PNC1 (pyrimidine nucleotide carrier 1)	UTP

SLC25A34		***Orphan***
SLC25A35		***Orphan***
SLC25A36	PNC2 (pyrimidine nucleotide carrier 2)	pyrimidine nucleotides
SLC25A37	Mitoferrin 1 (Mfrn1)	Fe^{2+}
SLC25A38		glycine ?
SLC25A39		***Orphan***
SLC25A40		***Orphan***
SLC25A41	APC4	ATP-Mg / Pi
SLC25A42	Mitochondrial coenzyme A transporter	CoA, ADP, ATP, adenosine 3',5'-diphosphate, dPCoA
SLC25A43		***Orphan***
SLC25A44		***Orphan***
SLC25A45		***Orphan***
SLC25A46		***Orphan***
SLC25A47		***Orphan***
SLC25A48		***Orphan***
SLC25A49	Mitochondrial carrier homolog (MTCH) 1	***Orphan***
SLC25A50	MTCH2	***Orphan***
SLC25A51	Mitochondrial carrier triple repeat protein (MCART) 1	***Orphan***
SLC25A51P1	pseudogene	

SLC25A51P2	pseudogene	
SLC25A51P3	pseudogene	
SLC25A52	MCART2	***Orphan***
SLC25A53	MCART6	***Orphan***

[a]The SLC and protein names, and transported substrate(s) of each MCF member. Further information on the MCF can be found at http://slc.bioparadigms.org.

Table 1.3: Summary of known MCF-involved diseases clustered by systemic presentation.

System	Clinical presentation/disease and MCF member associated
Hematopoietic	**Sideroblastic anemia:** SLC25A38 OMIM 205950 (Guernsey et al., 2009; Harigae & Furuyama, 2010; Horvathova et al., 2010)
Metabolic	**Lactic acidosis:** SLC25A4 (Bakker et al., 1993; L. Palmieri et al., 2005; Thompson et al., 2016); SLC25A26 OMIM 616794 (Kishita et al., 2015) **Citrullinemia:** SLC25A13 OMIM 603471 and 605814 (Fiermonte et al., 2008; Kobayashi et al., 1999; Ohura et al., 2001; Tazawa et al., 2001; Yasuda et al., 2000) **Hydroxyglutaric aciduria:** SLC25A1 OMIM 615182 (Edvardson et al., 2013; Muntau et al., 2000; Nota et al., 2013) **Hyperornithinemia-Hyperammonemia-Homocitrullinuria (HHH) Syndrome:** SLC25A15 OMIM 603861 (Camacho et al., 1999; Debray et al., 2008; Miyamoto et al., 2001; Salvi et al., 2001; Tessa et al., 2009; Tsujino et al., 2000) **Hypoglycemia, Hyperammonemia:** SLC25A20 OMIM 212138 (Iacobazzi et al., 2004; Pande et al., 1993; Stanley et al., 1992) **Hypertryglyceridemia:** linkage to SLC25A40 (Rosenthal et al., 2013)

	Exercise intolerance: SLC25A32 OMIM 616839 (Hellebrekers et al., 2017; Schiff et al., 2016)
Cardiovascular	**Hypertrophic cardiomyopathy:** SLC25A4 OMIM 615418 (Echaniz-Laguna et al., 2012; Körver-Keularts et al., 2015; L. Palmieri et al., 2005), OMIM 617184 (Thompson et al., 2016); SLC25A3 OMIM 610773 (Bhoj et al., 2015; Mayr et al., 2007); SLC25A20 OMIM 212138 (Dong et al., 2015; Dong et al., 2011; Huizing et al., 1998; Iacobazzi et al., 2004; Nakase et al., 2007; Pande et al., 1993; Stanley et al., 1992; Van De Parre et al., 2008)
Pulmonary	**Respiratory insufficiency:** SLC25A26 OMIM 616794 (Kishita et al., 2015)
Musculoskeletal	**Myopathy:** SLC25A4 OMIM 615418 (Bakker et al., 1993; Echaniz-Laguna et al., 2012; Körver-Keularts et al., 2015; L. Palmieri et al., 2005), OMIM 617184 (Thompson et al., 2016); SLC25A3 OMIM 610773 (Mayr et al., 2007); SLC25A26 OMIM 616794 (Kishita et al., 2015); SLC25A32 (Hellebrekers et al., 2017) **Progressive External Ophthalmoplegia:** SLC25A4 OMIM 609283 (Kaukonen et al., 2000; Lamantea et al., 2002; Napoli et al., 2001)
Neurological	**Epileptic encephalopathy:** SLC25A12 OMIM 612949 (Falk et al., 2014; Wibom et al., 2009); SLC25A22 OMIM 609304 (Molinari et al., 2009; Molinari et al., 2005; Poduri et al., 2013)

	Microcephaly: SLC25A19 OMIM 607196 (Hellebrekers et al., 2017; Rosenberg et al., 2002) **Neuropathy:** Progressive polyneuropathy - SLC25A19 OMIM 613710 (Spiegel et al., 2009); Charcot-Marie-Tooth Disease – SLC25A46 OMIM 616505 (Abrams et al., 2015; Charlesworth et al., 2016; Janer et al., 2016; Wan et al., 2016) **Ataxia, Myoclonus, dysarthria:** SLC25A32 (Hellebrekers et al., 2017)
Gastrointestinal	**Cholestatic jaundice:** SLC25A13 OMIM 605814 (Ohura et al., 2001; Tamamori et al., 2002; Tazawa et al., 2001) **Hepatic Steatosis:** SLC25A13 OMIM 603471 (Komatsu et al., 2008)
General	**Progeroid syndrome:** SLC25A24 OMIM 612289 (Ehmke et al., 2017; Writzl et al., 2017)

FIGURES

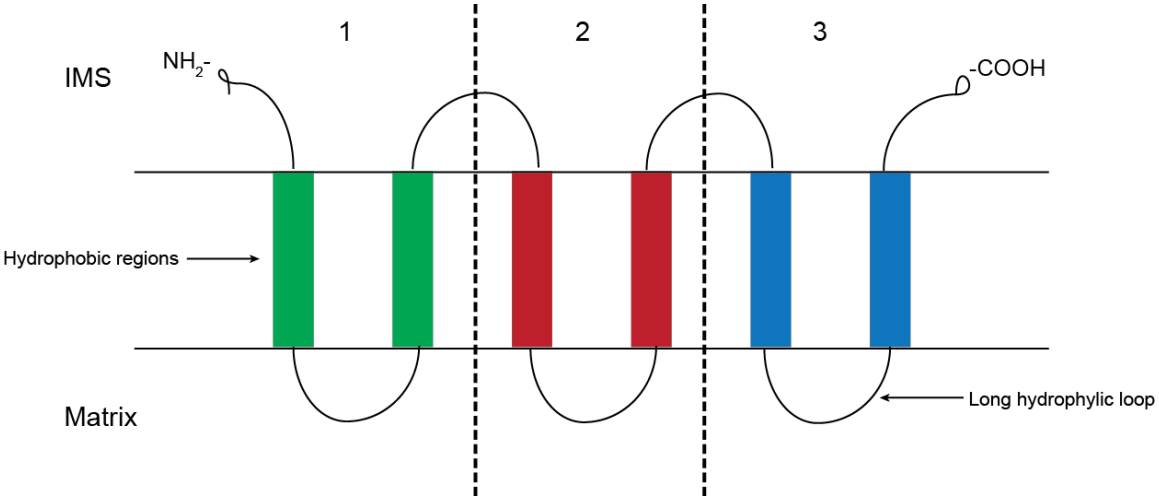

Figure 1.1: Schematic of the MCF tripartite structure. The structure of members of the mitochondrial carrier family can be seen as three similar parts/domains with approximately 100 amino acids each. In each part, there are two alpha-helix transmembrane segments connected by a long matrix localized hydrophilic loop. The NH_2- and COOH- terminal are on the IMS side of the inner mitochondrial membrane.

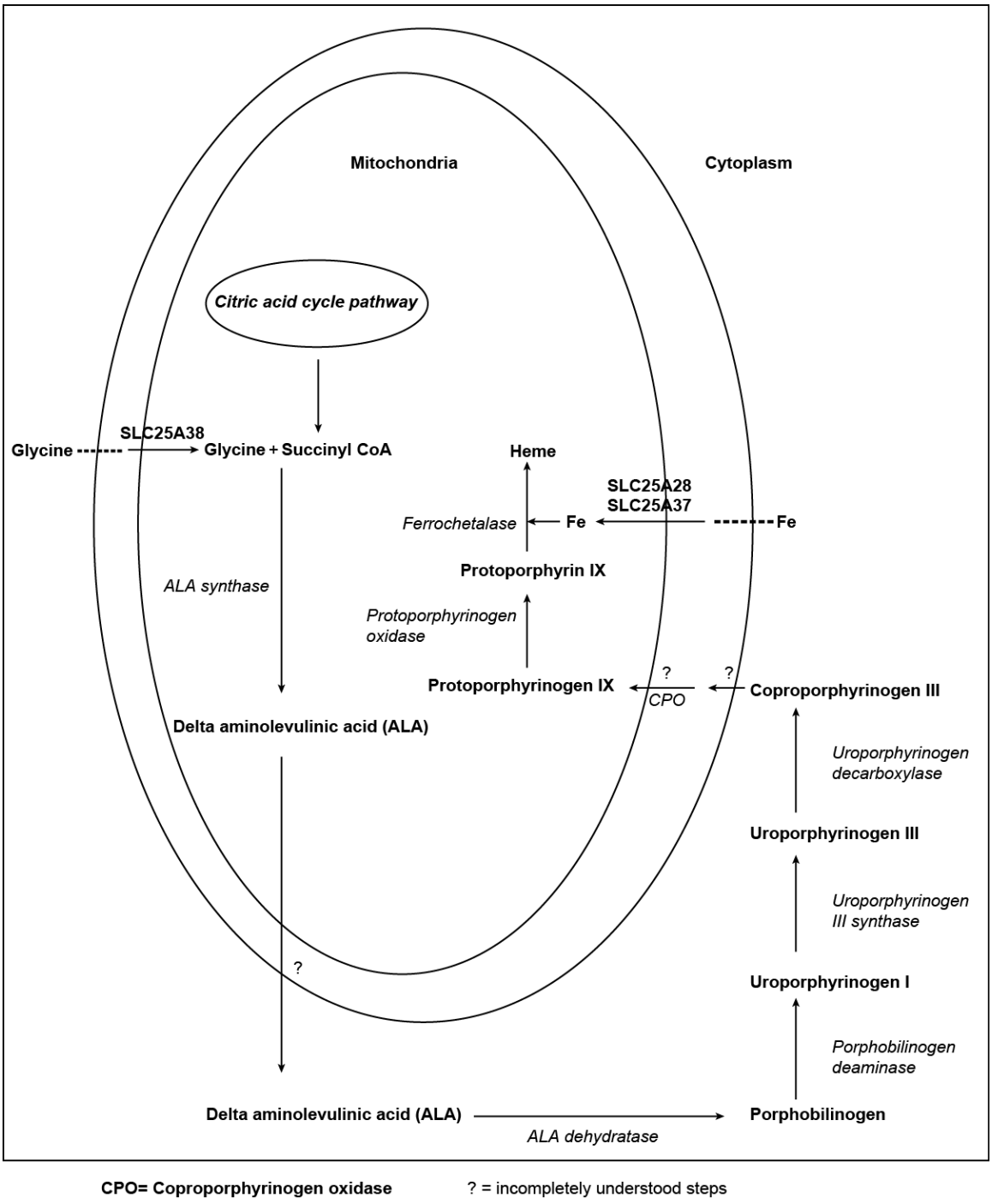

Figure 1.2: Overview of the Heme biosynthetic pathway. Three known MCF member are involved in the first and last step of heme biosynthesis. The first step of the pathway is the reaction of the condensation of glycine and succinyl-CoA to form ALA by ALA synthase. Glycine is transported across the inner mitochondrial membrane by SLC25A38. The last

step which generate heme from protoporphyrin IX by incorporation of ferrous ion is catalyzed by ferrochetalase. Iron crosses the inner mitochondrial membrane via the mitoferrins, SLC25A28 and SLC25A37.

1.6 References

Aalkjaer, C., Boedtkjer, E., Choi, I., & Lee, S. (2014). Cation-coupled bicarbonate transporters. *Compr Physiol, 4*(4), 1605-1637. doi:10.1002/cphy.c130005

Abrams, A. J., Hufnagel, R. B., Rebelo, A., Zanna, C., Patel, N., Gonzalez, M. A., . . . Dallman, J. E. (2015). Mutations in SLC25A46, encoding a UGO1-like protein, cause an optic atrophy spectrum disorder. *Nat Genet, 47*(8), 926-932. doi:10.1038/ng.3354

Acín-Pérez, R., Fernández-Silva, P., Peleato, M. L., Pérez-Martos, A., & Enriquez, J. A. (2008). Respiratory active mitochondrial supercomplexes. *Mol Cell, 32*(4), 529-539. doi:10.1016/j.molcel.2008.10.021

Alper, S. L. (2006). Molecular physiology of SLC4 anion exchangers. *Exp Physiol, 91*(1), 153-161. doi:10.1113/expphysiol.2005.031765

Alper, S. L., Chernova, M. N., & Stewart, A. K. (2001). Regulation of Na+-independent Cl-/HCO3- exchangers by pH. *JOP, 2*(4 Suppl), 171-175.

Alper, S. L., Darman, R. B., Chernova, M. N., & Dahl, N. K. (2002). The AE gene family of Cl/HCO3- exchangers. *J Nephrol, 15 Suppl 5*, S41-53.

Amigo, J. D., Yu, M., Troadec, M. B., Gwynn, B., Cooney, J. D., Lambert, A. J., . . . Paw, B. H. (2011). Identification of distal cis-regulatory elements at mouse mitoferrin loci using zebrafish transgenesis. *Mol Cell Biol, 31*(7), 1344-1356. doi:10.1128/MCB.01010-10

Aquila, H., Misra, D., Eulitz, M., & Klingenberg, M. (1982). Complete amino acid sequence of the ADP/ATP carrier from beef heart mitochondria. *Hoppe Seylers Z Physiol Chem, 363*(3), 345-349.

Arsenijevic, D., Onuma, H., Pecqueur, C., Raimbault, S., Manning, B. S., Miroux, B., . . . Ricquier, D. (2000). Disruption of the uncoupling protein-2 gene in mice reveals a role in immunity and reactive oxygen species production. *Nat Genet, 26*(4), 435-439. doi:10.1038/82565

Atkinson, G. C., Kuzmenko, A., Kamenski, P., Vysokikh, M. Y., Lakunina, V., Tankov, S., . . . Hauryliuk, V. (2012). Evolutionary and genetic analyses of mitochondrial translation initiation factors identify the missing mitochondrial IF3 in S. cerevisiae. *Nucleic Acids Res, 40*(13), 6122-6134. doi:10.1093/nar/gks272

Baile, M. G., & Claypool, S. M. (2013). The power of yeast to model diseases of the powerhouse of the cell. *Front Biosci (Landmark Ed), 18*, 241-278.

Bakker, H. D., Scholte, H. R., Van den Bogert, C., Ruitenbeek, W., Jeneson, J. A., Wanders, R. J., . . . Van Gennip, A. H. (1993). Deficiency of the adenine nucleotide translocator in muscle of a patient with myopathy and lactic acidosis: a new mitochondrial defect. *Pediatr Res, 33*(4 Pt 1), 412-417. doi:10.1203/00006450-199304000-00019

Bamber, L., Harding, M., Butler, P. J., & Kunji, E. R. (2006). Yeast mitochondrial ADP/ATP carriers are monomeric in detergents. *Proc Natl Acad Sci U S A, 103*(44), 16224-16229. doi:10.1073/pnas.0607640103

Bamber, L., Harding, M., Monné, M., Slotboom, D. J., & Kunji, E. R. (2007). The yeast mitochondrial ADP/ATP carrier functions as a monomer in mitochondrial membranes. *Proc Natl Acad Sci U S A, 104*(26), 10830-10834. doi:10.1073/pnas.0703969104

Bamber, L., Slotboom, D. J., & Kunji, E. R. (2007). Yeast mitochondrial ADP/ATP carriers are monomeric in detergents as demonstrated by differential affinity purification. *J Mol Biol, 371*(2), 388-395. doi:10.1016/j.jmb.2007.05.072

Barrientos, A., & Ugalde, C. (2013). I function, therefore I am: overcoming skepticism about mitochondrial supercomplexes. *Cell Metab, 18*(2), 147-149. doi:10.1016/j.cmet.2013.07.010

Barrientos, A., Zambrano, A., & Tzagoloff, A. (2004). Mss51p and Cox14p jointly regulate mitochondrial Cox1p expression in Saccharomyces cerevisiae. *EMBO J, 23*(17), 3472-3482. doi:10.1038/sj.emboj.7600358

Barron, C. C., Bilan, P. J., Tsakiridis, T., & Tsiani, E. (2016). Facilitative glucose transporters: Implications for cancer detection, prognosis and treatment. *Metabolism, 65*(2), 124-139. doi:10.1016/j.metabol.2015.10.007

Bedhomme, M., Hoffmann, M., McCarthy, E. A., Gambonnet, B., Moran, R. G., Rébeillé, F., & Ravanel, S. (2005). Folate metabolism in plants: an Arabidopsis homolog of the mammalian mitochondrial folate transporter mediates folate import into chloroplasts. *J Biol Chem, 280*(41), 34823-34831. doi:10.1074/jbc.M506045200

Berardi, M. J., & Chou, J. J. (2014). Fatty acid flippase activity of UCP2 is essential for its proton transport in mitochondria. *Cell Metab, 20*(3), 541-552. doi:10.1016/j.cmet.2014.07.004

Bergeron, M. J., Simonin, A., Bürzle, M., & Hediger, M. A. (2008). Inherited epithelial transporter disorders--an overview. *J Inherit Metab Dis, 31*(2), 178-187. doi:10.1007/s10545-008-0861-6

Beyer, K., & Klingenberg, M. (1985). ADP/ATP carrier protein from beef heart mitochondria has high amounts of tightly bound cardiolipin, as revealed by 31P nuclear magnetic resonance. *Biochemistry, 24*(15), 3821-3826.

Bhoj, E. J., Li, M., Ahrens-Nicklas, R., Pyle, L. C., Wang, J., Zhang, V. W., . . . Yudkoff, M. (2015). Pathologic Variants of the Mitochondrial Phosphate Carrier SLC25A3: Two New Patients and Expansion of the Cardiomyopathy/Skeletal Myopathy Phenotype With and Without Lactic Acidosis. *JIMD Rep, 19*, 59-66. doi:10.1007/8904_2014_364

Blaustein, M. P., & Lederer, W. J. (1999). Sodium/calcium exchange: its physiological implications. *Physiol Rev, 79*(3), 763-854. doi:10.1152/physrev.1999.79.3.763

Boss, O., Samec, S., Paoloni-Giacobino, A., Rossier, C., Dulloo, A., Seydoux, J., . . . Giacobino, J. P. (1997). Uncoupling protein-3: a new member of the mitochondrial carrier family with tissue-specific expression. *FEBS Lett, 408*(1), 39-42.

Boulet, A., Vest, K. E., Maynard, M. K., Gammon, M. G., Russell, A. C., Mathews, A. T., . . . Cobine, P. A. (2017). The mammalian phosphate carrier SLC25A3 is a mitochondrial copper transporter required for cytochrome c oxidase biogenesis. *J Biol Chem*. doi:10.1074/jbc.RA117.000265

Brand, M. D., Pamplona, R., Portero-Otín, M., Requena, J. R., Roebuck, S. J., Buckingham, J. A., . . . Cadenas, S. (2002). Oxidative damage and phospholipid fatty acyl composition in skeletal muscle mitochondria from mice underexpressing or overexpressing uncoupling protein 3. *Biochem J, 368*(Pt 2), 597-603. doi:10.1042/BJ20021077

Camacho, J. A., Obie, C., Biery, B., Goodman, B. K., Hu, C. A., Almashanu, S., . . . Valle, D. (1999). Hyperornithinaemia-hyperammonaemia-homocitrullinuria syndrome is caused by mutations in a gene encoding a mitochondrial ornithine transporter. *Nat Genet, 22*(2), 151-158. doi:10.1038/9658

Capobianco, L., Ferramosca, A., & Zara, V. (2002). The mitochondrial tricarboxylate carrier of silver eel: dimeric structure and cytosolic exposure of both N- and C-termini. *J Protein Chem, 21*(8), 515-521.

Charlesworth, G., Balint, B., Mencacci, N. E., Carr, L., Wood, N. W., & Bhatia, K. P. (2016). SLC25A46 mutations underlie progressive myoclonic ataxia with optic atrophy and neuropathy. *Mov Disord, 31*(8), 1249-1251. doi:10.1002/mds.26716

Chevrollier, A., Loiseau, D., Chabi, B., Renier, G., Douay, O., Malthiery, Y., & Stepien, G. (2005). ANT2 isoform required for cancer cell glycolysis. *J Bioenerg Biomembr, 37*(5), 307-316. doi:10.1007/s10863-005-8642-5

Choquet, Y., Wostrikoff, K., Rimbault, B., Zito, F., Girard-Bascou, J., Drapier, D., & Wollman, F. A. (2001). Assembly-controlled regulation of chloroplast gene translation. *Biochem Soc Trans, 29*(Pt 4), 421-426.

Chouchani, E. T., Kazak, L., Jedrychowski, M. P., Lu, G. Z., Erickson, B. K., Szpyt, J., . . . Spiegelman, B. M. (2016). Mitochondrial ROS regulate thermogenic energy expenditure and sulfenylation of UCP1. *Nature, 532*(7597), 112-116. doi:10.1038/nature17399

Chouchani, E. T., Kazak, L., & Spiegelman, B. M. (2017). Mitochondrial reactive oxygen species and adipose tissue thermogenesis: Bridging physiology and mechanisms. *J Biol Chem, 292*(41), 16810-16816. doi:10.1074/jbc.R117.789628

Claro da Silva, T., Polli, J. E., & Swaan, P. W. (2013). The solute carrier family 10 (SLC10): beyond bile acid transport. *Mol Aspects Med, 34*(2-3), 252-269. doi:10.1016/j.mam.2012.07.004

Claypool, S. M. (2009). Cardiolipin, a critical determinant of mitochondrial carrier protein assembly and function. *Biochim Biophys Acta, 1788*(10), 2059-2068. doi:10.1016/j.bbamem.2009.04.020

Claypool, S. M., Oktay, Y., Boontheung, P., Loo, J. A., & Koehler, C. M. (2008). Cardiolipin defines the interactome of the major ADP/ATP carrier protein of the mitochondrial inner membrane. *J Cell Biol, 182*(5), 937-950. doi:10.1083/jcb.200801152

Clémençon, B., Babot, M., & Trézéguet, V. (2013). The mitochondrial ADP/ATP carrier (SLC25 family): pathological implications of its dysfunction. *Mol Aspects Med, 34*(2-3), 485-493. doi:10.1016/j.mam.2012.05.006

Cruciat, C. M., Brunner, S., Baumann, F., Neupert, W., & Stuart, R. A. (2000). The cytochrome bc1 and cytochrome c oxidase complexes associate to form a single supracomplex in yeast mitochondria. *J Biol Chem, 275*(24), 18093-18098. doi:10.1074/jbc.M001901200

César-Razquin, A., Snijder, B., Frappier-Brinton, T., Isserlin, R., Gyimesi, G., Bai, X., . . . Superti-Furga, G. (2015). A Call for Systematic Research on Solute Carriers. *Cell, 162*(3), 478-487. doi:10.1016/j.cell.2015.07.022

Debray, F. G., Lambert, M., Lemieux, B., Soucy, J. F., Drouin, R., Fenyves, D., . . . Mitchell, G. A. (2008). Phenotypic variability among patients with hyperornithinaemia-hyperammonaemia-homocitrullinuria syndrome homozygous

for the delF188 mutation in SLC25A15. *J Med Genet, 45*(11), 759-764. doi:10.1136/jmg.2008.059097

Derdak, Z., Mark, N. M., Beldi, G., Robson, S. C., Wands, J. R., & Baffy, G. (2008). The mitochondrial uncoupling protein-2 promotes chemoresistance in cancer cells. *Cancer Res, 68*(8), 2813-2819. doi:10.1158/0008-5472.CAN-08-0053

Diaz, F. (2010). Cytochrome c oxidase deficiency: patients and animal models. *Biochim Biophys Acta, 1802*(1), 100-110. doi:10.1016/j.bbadis.2009.07.013

Dienhart, M. K., & Stuart, R. A. (2008). The yeast Aac2 protein exists in physical association with the cytochrome bc1-COX supercomplex and the TIM23 machinery. *Mol Biol Cell, 19*(9), 3934-3943. doi:10.1091/mbc.E08-04-0402

DiPolo, R., & Beaugé, L. (2006). Sodium/calcium exchanger: influence of metabolic regulation on ion carrier interactions. *Physiol Rev, 86*(1), 155-203. doi:10.1152/physrev.00018.2005

Doerner, A., Pauschinger, M., Badorff, A., Noutsias, M., Giessen, S., Schulze, K., . . . Schultheiss, H. P. (1997). Tissue-specific transcription pattern of the adenine nucleotide translocase isoforms in humans. *FEBS Lett, 414*(2), 258-262.

Dolce, V., Scarcia, P., Iacopetta, D., & Palmieri, F. (2005). A fourth ADP/ATP carrier isoform in man: identification, bacterial expression, functional characterization and tissue distribution. *FEBS Lett, 579*(3), 633-637. doi:10.1016/j.febslet.2004.12.034

Dong, C., Della-Morte, D., Cabral, D., Wang, L., Blanton, S. H., Seemant, C., . . . Rundek, T. (2015). Sirtuin/uncoupling protein gene variants and carotid plaque area and morphology. *Int J Stroke, 10*(8), 1247-1252. doi:10.1111/ijs.12623

Dong, C., Della-Morte, D., Wang, L., Cabral, D., Beecham, A., McClendon, M. S., . . . Rundek, T. (2011). Association of the sirtuin and mitochondrial uncoupling protein genes with carotid plaque. *PLoS One, 6*(11), e27157. doi:10.1371/journal.pone.0027157

Donowitz, M., Ming Tse, C., & Fuster, D. (2013). SLC9/NHE gene family, a plasma membrane and organellar family of Na^+/H^+ exchangers. *Mol Aspects Med, 34*(2-3), 236-251. doi:10.1016/j.mam.2012.05.001

Dufay, J. N., Fernández-Murray, J. P., & McMaster, C. R. (2017). SLC25 Family Member Genetic Interactions Identify a Role for HEM25 in Yeast Electron Transport Chain Stability. *G3 (Bethesda), 7*(6), 1861-1873. doi:10.1534/g3.117.041194

Dupont, P. Y., & Stepien, G. (2011). Computational analysis of the transcriptional regulation of the adenine nucleotide translocator isoform 4 gene and its role in spermatozoid glycolytic metabolism. *Gene, 487*(1), 38-45. doi:10.1016/j.gene.2011.07.024

Dyall, S. D., Agius, S. C., De Marcos Lousa, C., Trezeguet, V., & Tokatlidis, K. (2003). The dynamic dimerization of the yeast ADP/ATP carrier in the inner mitochondrial membrane is affected by conserved cysteine residues. *J Biol Chem, 278*(29), 26757-26764. doi:10.1074/jbc.M302700200

Echaniz-Laguna, A., Chassagne, M., Ceresuela, J., Rouvet, I., Padet, S., Acquaviva, C., . . . Mousson de Camaret, B. (2012). Complete loss of expression of the ANT1 gene causing cardiomyopathy and myopathy. *J Med Genet, 49*(2), 146-150. doi:10.1136/jmedgenet-2011-100504

Echtay, K. S., Roussel, D., St-Pierre, J., Jekabsons, M. B., Cadenas, S., Stuart, J. A., . . . Brand, M. D. (2002). Superoxide activates mitochondrial uncoupling proteins. *Nature, 415*(6867), 96-99. doi:10.1038/415096a

Edvardson, S., Porcelli, V., Jalas, C., Soiferman, D., Kellner, Y., Shaag, A., . . . Elpeleg, O. (2013). Agenesis of corpus callosum and optic nerve hypoplasia due to mutations in SLC25A1 encoding the mitochondrial citrate transporter. *J Med Genet, 50*(4), 240-245. doi:10.1136/jmedgenet-2012-101485

Ehmke, N., Graul-Neumann, L., Smorag, L., Koenig, R., Segebrecht, L., Magoulas, P., . . . Kornak, U. (2017). De Novo Mutations in SLC25A24 Cause a Craniosynostosis Syndrome with Hypertrichosis, Progeroid Appearance, and Mitochondrial Dysfunction. *Am J Hum Genet, 101*(5), 833-843. doi:10.1016/j.ajhg.2017.09.016

Falk, M. J., Li, D., Gai, X., McCormick, E., Place, E., Lasorsa, F. M., . . . Hakonarson, H. (2014). AGC1 Deficiency Causes Infantile Epilepsy, Abnormal Myelination, and Reduced N-Acetylaspartate. *JIMD Rep, 14*, 77-85. doi:10.1007/8904_2013_287

Fedorenko, A., Lishko, P. V., & Kirichok, Y. (2012). Mechanism of fatty-acid-dependent UCP1 uncoupling in brown fat mitochondria. *Cell, 151*(2), 400-413. doi:10.1016/j.cell.2012.09.010

Fernández-Murray, J. P., Prykhozhij, S. V., Dufay, J. N., Steele, S. L., Gaston, D., Nasrallah, G. K., . . . McMaster, C. R. (2016). Glycine and Folate Ameliorate Models of Congenital Sideroblastic Anemia. *PLoS Genet, 12*(1), e1005783. doi:10.1371/journal.pgen.1005783

Fiermonte, G., De Leonardis, F., Todisco, S., Palmieri, L., Lasorsa, F. M., & Palmieri, F. (2004). Identification of the mitochondrial ATP-Mg/Pi transporter. Bacterial

expression, reconstitution, functional characterization, and tissue distribution. *J Biol Chem, 279*(29), 30722-30730. doi:10.1074/jbc.M400445200

Fiermonte, G., Paradies, E., Todisco, S., Marobbio, C. M., & Palmieri, F. (2009). A novel member of solute carrier family 25 (SLC25A42) is a transporter of coenzyme A and adenosine 3',5'-diphosphate in human mitochondria. *J Biol Chem, 284*(27), 18152-18159. doi:10.1074/jbc.M109.014118

Fiermonte, G., Soon, D., Chaudhuri, A., Paradies, E., Lee, P. J., Krywawych, S., . . . Lachmann, R. H. (2008). An adult with type 2 citrullinemia presenting in Europe. *N Engl J Med, 358*(13), 1408-1409. doi:10.1056/NEJMc0707353

Fleury, C., Neverova, M., Collins, S., Raimbault, S., Champigny, O., Levi-Meyrueis, C., . . . Warden, C. H. (1997). Uncoupling protein-2: a novel gene linked to obesity and hyperinsulinemia. *Nat Genet, 15*(3), 269-272. doi:10.1038/ng0397-269

Fontanesi, F., Clemente, P., & Barrientos, A. (2011). Cox25 teams up with Mss51, Ssc1, and Cox14 to regulate mitochondrial cytochrome c oxidase subunit 1 expression and assembly in Saccharomyces cerevisiae. *J Biol Chem, 286*(1), 555-566. doi:10.1074/jbc.M110.188805

Fontanesi, F., Palmieri, L., Scarcia, P., Lodi, T., Donnini, C., Limongelli, A., . . . Viola, A. M. (2004). Mutations in AAC2, equivalent to human adPEO-associated ANT1 mutations, lead to defective oxidative phosphorylation in Saccharomyces cerevisiae and affect mitochondrial DNA stability. *Hum Mol Genet, 13*(9), 923-934. doi:10.1093/hmg/ddh108

Fotiadis, D., Kanai, Y., & Palacín, M. (2013). The SLC3 and SLC7 families of amino acid transporters. *Mol Aspects Med, 34*(2-3), 139-158. doi:10.1016/j.mam.2012.10.007

Foury, F., & Roganti, T. (2002). Deletion of the mitochondrial carrier genes MRS3 and MRS4 suppresses mitochondrial iron accumulation in a yeast frataxin-deficient strain. *J Biol Chem, 277*(27), 24475-24483. doi:10.1074/jbc.M111789200

Fuster, D. G., & Alexander, R. T. (2014). Traditional and emerging roles for the SLC9 Na+/H+ exchangers. *Pflugers Arch, 466*(1), 61-76. doi:10.1007/s00424-013-1408-8

Gao, C. L., Ni, Y. H., Liu, G., Chen, X. H., Ji, C. B., Qin, D. N., . . . Guo, X. R. (2011). UCP4 overexpression improves fatty acid oxidation and insulin sensitivity in L6 myocytes. *J Bioenerg Biomembr, 43*(2), 109-118. doi:10.1007/s10863-011-9344-9

Gao, C. L., Zhu, J. G., Zhao, Y. P., Chen, X. H., Ji, C. B., Zhang, C. M., . . . Guo, X. R. (2010). Mitochondrial dysfunction is induced by the overexpression of UCP4 in 3T3-L1 adipocytes. *Int J Mol Med, 25*(1), 71-80.

Gavurníková, G., Sabova, L., Kissová, I., Haviernik, P., & Kolarov, J. (1996). Transcription of the AAC1 gene encoding an isoform of mitochondrial ADP/ATP carrier in Saccharomyces cerevisiae is regulated by oxygen in a heme-independent manner. *Eur J Biochem, 239*(3), 759-763.

Gegelashvili, M., Rodriguez-Kern, A., Pirozhkova, I., Zhang, J., Sung, L., & Gegelashvili, G. (2006). High-affinity glutamate transporter GLAST/EAAT1 regulates cell surface expression of glutamine/neutral amino acid transporter ASCT2 in human fetal astrocytes. *Neurochem Int, 48*(6-7), 611-615. doi:10.1016/j.neuint.2005.12.033

Geyer, J., Wilke, T., & Petzinger, E. (2006). The solute carrier family SLC10: more than a family of bile acid transporters regarding function and phylogenetic relationships.

Naunyn Schmiedebergs Arch Pharmacol, 372(6), 413-431. doi:10.1007/s00210-006-0043-8

Gill, H. S., & Boron, W. F. (2006). Expression and purification of the cytoplasmic N-terminal domain of the Na/HCO3 cotransporter NBCe1-A: structural insights from a generalized approach. *Protein Expr Purif, 49*(2), 228-234. doi:10.1016/j.pep.2006.04.001

Gimeno, R. E., Dembski, M., Weng, X., Deng, N., Shyjan, A. W., Gimeno, C. J., . . . Tartaglia, L. A. (1997). Cloning and characterization of an uncoupling protein homolog: a potential molecular mediator of human thermogenesis. *Diabetes, 46*(5), 900-906.

Giraud, S., Bonod-Bidaud, C., Wesolowski-Louvel, M., & Stepien, G. (1998). Expression of human ANT2 gene in highly proliferative cells: GRBOX, a new transcriptional element, is involved in the regulation of glycolytic ATP import into mitochondria. *J Mol Biol, 281*(3), 409-418. doi:10.1006/jmbi.1998.1955

Golozoubova, V., Hohtola, E., Matthias, A., Jacobsson, A., Cannon, B., & Nedergaard, J. (2001). Only UCP1 can mediate adaptive nonshivering thermogenesis in the cold. *FASEB J, 15*(11), 2048-2050. doi:10.1096/fj.00-0536fje

Gu, J., Wu, M., Guo, R., Yan, K., Lei, J., Gao, N., & Yang, M. (2016). The architecture of the mammalian respirasome. *Nature, 537*(7622), 639-643. doi:10.1038/nature19359

Guernsey, D. L., Jiang, H., Campagna, D. R., Evans, S. C., Ferguson, M., Kellogg, M. D., . . . Samuels, M. E. (2009). Mutations in mitochondrial carrier family gene

SLC25A38 cause nonsyndromic autosomal recessive congenital sideroblastic anemia. *Nat Genet, 41*(6), 651-653. doi:10.1038/ng.359

Haguenauer, A., Raimbault, S., Masscheleyn, S., Gonzalez-Barroso, M.el M, Criscuolo, F., Plamondon, J., . . . Pecqueur, C. (2005). A new renal mitochondrial carrier, KMCP1, is up-regulated during tubular cell regeneration and induction of antioxidant enzymes. *J Biol Chem, 280*(23), 22036-22043. doi:10.1074/jbc.M412136200

Haitina, T., Lindblom, J., Renström, T., & Fredriksson, R. (2006). Fourteen novel human members of mitochondrial solute carrier family 25 (SLC25) widely expressed in the central nervous system. *Genomics, 88*(6), 779-790. doi:10.1016/j.ygeno.2006.06.016

Harigae, H., & Furuyama, K. (2010). Hereditary sideroblastic anemia: pathophysiology and gene mutations. *Int J Hematol, 92*(3), 425-431. doi:10.1007/s12185-010-0688-4

Heaton, G. M., Wagenvoord, R. J., Kemp, A., & Nicholls, D. G. (1978). Brown-adipose-tissue mitochondria: photoaffinity labelling of the regulatory site of energy dissipation. *Eur J Biochem, 82*(2), 515-521.

Hediger, M. A., Romero, M. F., Peng, J. B., Rolfs, A., Takanaga, H., & Bruford, E. A. (2004). The ABCs of solute carriers: physiological, pathological and therapeutic implications of human membrane transport proteinsIntroduction. *Pflugers Arch, 447*(5), 465-468. doi:10.1007/s00424-003-1192-y

Heidkämper, D., Müller, V., Nelson, D. R., & Klingenberg, M. (1996). Probing the role of positive residues in the ADP/ATP carrier from yeast. The effect of six arginine

mutations on transport and the four ATP versus ADP exchange modes. *Biochemistry, 35*(50), 16144-16152. doi:10.1021/bi960668j

Hellebrekers, D. M. E.I, Sallevelt, S. C. E.H, Theunissen, T. E. J., Hendrickx, A. T. M., Gottschalk, R. W., Hoeijmakers, J. G. J., . . . Smeets, H. J. M. (2017). Novel SLC25A32 mutation in a patient with a severe neuromuscular phenotype. *Eur J Hum Genet, 25*(7), 886-888. doi:10.1038/ejhg.2017.62

Hevia, D., González-Menéndez, P., Quiros-González, I., Miar, A., Rodríguez-García, A., Tan, D. X., . . . Sainz, R. M. (2015). Melatonin uptake through glucose transporters: a new target for melatonin inhibition of cancer. *J Pineal Res, 58*(2), 234-250. doi:10.1111/jpi.12210

Horimoto, M., Resnick, M. B., Konkin, T. A., Routhier, J., Wands, J. R., & Baffy, G. (2004). Expression of uncoupling protein-2 in human colon cancer. *Clin Cancer Res, 10*(18 Pt 1), 6203-6207. doi:10.1158/1078-0432.CCR-04-0419

Horvathova, M., Ponka, P., & Divoky, V. (2010). Molecular basis of hereditary iron homeostasis defects. *Hematology, 15*(2), 96-111. doi:10.1179/102453310X12583347009810

Huizing, M., Wendel, U., Ruitenbeek, W., Iacobazzi, V., IJlst, L., Veenhuizen, P., . . . Palmieri, F. (1998). Carnitine-acylcarnitine carrier deficiency: identification of the molecular defect in a patient. *J Inherit Metab Dis, 21*(3), 262-267.

Höglund, P. J., Nordström, K. J., Schiöth, H. B., & Fredriksson, R. (2011). The solute carrier families have a remarkably long evolutionary history with the majority of the human families present before divergence of Bilaterian species. *Mol Biol Evol, 28*(4), 1531-1541. doi:10.1093/molbev/msq350

Iacobazzi, V., Pasquali, M., Singh, R., Matern, D., Rinaldo, P., Amat di San Filippo, C., . . . Longo, N. (2004). Response to therapy in carnitine/acylcarnitine translocase (CACT) deficiency due to a novel missense mutation. *Am J Med Genet A, 126A*(2), 150-155. doi:10.1002/ajmg.a.20573

Jabůrek, M., Varecha, M., Jezek, P., & Garlid, K. D. (2001). Alkylsulfonates as probes of uncoupling protein transport mechanism. Ion pair transport demonstrates that direct H(+) translocation by UCP1 is not necessary for uncoupling. *J Biol Chem, 276*(34), 31897-31905. doi:10.1074/jbc.M103507200

Janer, A., Prudent, J., Paupe, V., Fahiminiya, S., Majewski, J., Sgarioto, N., . . . Shoubridge, E. A. (2016). SLC25A46 is required for mitochondrial lipid homeostasis and cristae maintenance and is responsible for Leigh syndrome. *EMBO Mol Med, 8*(9), 1019-1038. doi:10.15252/emmm.201506159

Jezek, P., Holendová, B., Garlid, K. D., & Jaburek, M. (2018). Mitochondrial uncoupling proteins: subtle regulators of cellular redox signaling. *Antioxid Redox Signal*. doi:10.1089/ars.2017.7225

Jezek, P., Jabůrek, M., & Garlid, K. D. (2010). Channel character of uncoupling protein-mediated transport. *FEBS Lett, 584*(10), 2135-2141. doi:10.1016/j.febslet.2010.02.068

Jezek, P., Modrianský, M., & Garlid, K. D. (1997a). A structure-activity study of fatty acid interaction with mitochondrial uncoupling protein. *FEBS Lett, 408*(2), 166-170.

Jezek, P., Modrianský, M., & Garlid, K. D. (1997b). Inactive fatty acids are unable to flip-flop across the lipid bilayer. *FEBS Lett, 408*(2), 161-165.

Jiang, F., Ryan, M. T., Schlame, M., Zhao, M., Gu, Z., Klingenberg, M., . . . Greenberg, M. L. (2000). Absence of cardiolipin in the crd1 null mutant results in decreased mitochondrial membrane potential and reduced mitochondrial function. *J Biol Chem, 275*(29), 22387-22394. doi:10.1074/jbc.M909868199

Kamp, F., & Hamilton, J. A. (1992). pH gradients across phospholipid membranes caused by fast flip-flop of un-ionized fatty acids. *Proc Natl Acad Sci U S A, 89*(23), 11367-11370.

Kamp, F., Hamilton, J. A., & Westerhoff, H. V. (1993). Movement of fatty acids, fatty acid analogues, and bile acids across phospholipid bilayers. *Biochemistry, 32*(41), 11074-11086.

Kamp, F., Zakim, D., Zhang, F., Noy, N., & Hamilton, J. A. (1995). Fatty acid flip-flop in phospholipid bilayers is extremely fast. *Biochemistry, 34*(37), 11928-11937.

Kanai, Y., Clémençon, B., Simonin, A., Leuenberger, M., Lochner, M., Weisstanner, M., & Hediger, M. A. (2013). The SLC1 high-affinity glutamate and neutral amino acid transporter family. *Mol Aspects Med, 34*(2-3), 108-120. doi:10.1016/j.mam.2013.01.001

Kanai, Y., & Hediger, M. A. (2003). The glutamate and neutral amino acid transporter family: physiological and pharmacological implications. *Eur J Pharmacol, 479*(1-3), 237-247.

Kanai, Y., & Hediger, M. A. (2004). The glutamate/neutral amino acid transporter family SLC1: molecular, physiological and pharmacological aspects. *Pflugers Arch, 447*(5), 469-479. doi:10.1007/s00424-003-1146-4

Kaukonen, J., Juselius, J. K., Tiranti, V., Kyttala, A., Zeviani, M., Comi, G. P., . . . Suomalainen, A. (2000). Role of adenine nucleotide translocator 1 in mtDNA maintenance. *Science, 289*(5480), 782-785.

Kazak, L., Chouchani, E. T., Stavrovskaya, I. G., Lu, G. Z., Jedrychowski, M. P., Egan, D. F., . . . Spiegelman, B. M. (2017). UCP1 deficiency causes brown fat respiratory chain depletion and sensitizes mitochondria to calcium overload-induced dysfunction. *Proc Natl Acad Sci U S A, 114*(30), 7981-7986. doi:10.1073/pnas.1705406114

Kehrein, K., Bonnefoy, N., & Ott, M. (2013). Mitochondrial protein synthesis: efficiency and accuracy. *Antioxid Redox Signal, 19*(16), 1928-1939. doi:10.1089/ars.2012.4896

Khananshvili, D. (2013). The SLC8 gene family of sodium-calcium exchangers (NCX) - structure, function, and regulation in health and disease. *Mol Aspects Med, 34*(2-3), 220-235. doi:10.1016/j.mam.2012.07.003

Kim, Y. H., Haidl, G., Schaefer, M., Egner, U., Mandal, A., & Herr, J. C. (2007). Compartmentalization of a unique ADP/ATP carrier protein SFEC (Sperm Flagellar Energy Carrier, AAC4) with glycolytic enzymes in the fibrous sheath of the human sperm flagellar principal piece. *Dev Biol, 302*(2), 463-476. doi:10.1016/j.ydbio.2006.10.004

Kishita, Y., Pajak, A., Bolar, N. A., Marobbio, C. M., Maffezzini, C., Miniero, D. V., . . . Wedell, A. (2015). Intra-mitochondrial Methylation Deficiency Due to Mutations in SLC25A26. *Am J Hum Genet, 97*(5), 761-768. doi:10.1016/j.ajhg.2015.09.013

Klingenberg, M. (1981). Membrane protein oligomeric structure and transport function. *Nature, 290*(5806), 449-454.

Klingenberg, M. (2008). The ADP and ATP transport in mitochondria and its carrier. *Biochim Biophys Acta, 1778*(10), 1978-2021. doi:10.1016/j.bbamem.2008.04.011

Kobayashi, K., Sinasac, D. S., Iijima, M., Boright, A. P., Begum, L., Lee, J. R., . . . Saheki, T. (1999). The gene mutated in adult-onset type II citrullinaemia encodes a putative mitochondrial carrier protein. *Nat Genet, 22*(2), 159-163. doi:10.1038/9667

Komatsu, M., Yazaki, M., Tanaka, N., Sano, K., Hashimoto, E., Takei, Y., . . . Kobayashi, K. (2008). Citrin deficiency as a cause of chronic liver disorder mimicking non-alcoholic fatty liver disease. *J Hepatol, 49*(5), 810-820. doi:10.1016/j.jhep.2008.05.016

Kotaria, R., Mayor, J. A., Walters, D. E., & Kaplan, R. S. (1999). Oligomeric state of wild-type and cysteine-less yeast mitochondrial citrate transport proteins. *J Bioenerg Biomembr, 31*(6), 543-549.

Krämer, R., & Klingenberg, M. (1980). Modulation of the reconstituted adenine nucleotide exchange by membrane potential. *Biochemistry, 19*(3), 556-560.

Kunji, E. R., & Crichton, P. G. (2010). Mitochondrial carriers function as monomers. *Biochim Biophys Acta, 1797*(6-7), 817-831. doi:10.1016/j.bbabio.2010.03.023

Kunji, E. R., & Harding, M. (2003). Projection structure of the atractyloside-inhibited mitochondrial ADP/ATP carrier of Saccharomyces cerevisiae. *J Biol Chem, 278*(39), 36985-36988. doi:10.1074/jbc.C300304200

Kuzmenko, A., Atkinson, G. C., Levitskii, S., Zenkin, N., Tenson, T., Hauryliuk, V., & Kamenski, P. (2014). Mitochondrial translation initiation machinery: conservation and diversification. *Biochimie, 100*, 132-140. doi:10.1016/j.biochi.2013.07.024

Kuzmenko, A., Derbikova, K., Salvatori, R., Tankov, S., Atkinson, G. C., Tenson, T., . . . Hauryliuk, V. (2016). Aim-less translation: loss of Saccharomyces cerevisiae mitochondrial translation initiation factor mIF3/Aim23 leads to unbalanced protein synthesis. *Sci Rep, 6*, 18749. doi:10.1038/srep18749

Kwok, K. H., Ho, P. W., Chu, A. C., Ho, J. W., Liu, H. F., Yiu, D. C., . . . Ho, S. L. (2010). Mitochondrial UCP5 is neuroprotective by preserving mitochondrial membrane potential, ATP levels, and reducing oxidative stress in MPP+ and dopamine toxicity. *Free Radic Biol Med, 49*(6), 1023-1035. doi:10.1016/j.freeradbiomed.2010.06.017

Körver-Keularts, I. M., de Visser, M., Bakker, H. D., Wanders, R. J., Vansenne, F., Scholte, H. R., . . . van den Bosch, B. J. (2015). Two Novel Mutations in the SLC25A4 Gene in a Patient with Mitochondrial Myopathy. *JIMD Rep, 22*, 39-45. doi:10.1007/8904_2015_409

Lamantea, E., Tiranti, V., Bordoni, A., Toscano, A., Bono, F., Servidei, S., . . . Zeviani, M. (2002). Mutations of mitochondrial DNA polymerase gammaA are a frequent cause of autosomal dominant or recessive progressive external ophthalmoplegia. *Ann Neurol, 52*(2), 211-219. doi:10.1002/ana.10278

Lawson, J. E., Gawaz, M., Klingenberg, M., & Douglas, M. G. (1990). Structure-function studies of adenine nucleotide transport in mitochondria. I. Construction and genetic

analysis of yeast mutants encoding the ADP/ATP carrier protein of mitochondria. *J Biol Chem, 265*(24), 14195-14201.

LeMoine, C. M., & Walsh, P. J. (2015). Evolution of urea transporters in vertebrates: adaptation to urea's multiple roles and metabolic sources. *J Exp Biol, 218*(Pt 12), 1936-1945. doi:10.1242/jeb.114223

Letts, J. A., Fiedorczuk, K., & Sazanov, L. A. (2016). The architecture of respiratory supercomplexes. *Nature, 537*(7622), 644-648. doi:10.1038/nature19774

Levi, S., & Rovida, E. (2009). The role of iron in mitochondrial function. *Biochim Biophys Acta, 1790*(7), 629-636. doi:10.1016/j.bbagen.2008.09.008

Li, W., Nichols, K., Nathan, C. A., & Zhao, Y. (2013). Mitochondrial uncoupling protein 2 is up-regulated in human head and neck, skin, pancreatic, and prostate tumors. *Cancer Biomark, 13*(5), 377-383. doi:10.3233/CBM-130369

Li, W., Zhang, C., Jackson, K., Shen, X., Jin, R., Li, G., . . . Zhao, Y. (2015). UCP2 knockout suppresses mouse skin carcinogenesis. *Cancer Prev Res (Phila), 8*(6), 487-491. doi:10.1158/1940-6207.CAPR-14-0297-T

Lill, R. (2009). Function and biogenesis of iron-sulphur proteins. *Nature, 460*(7257), 831-838. doi:10.1038/nature08301

Lill, R., & Mühlenhoff, U. (2008). Maturation of iron-sulfur proteins in eukaryotes: mechanisms, connected processes, and diseases. *Annu Rev Biochem, 77*, 669-700. doi:10.1146/annurev.biochem.76.052705.162653

Lin, C. S., Hackenberg, H., & Klingenberg, E. M. (1980). The uncoupling protein from brown adipose tissue mitochondria is a dimer. A hydrodynamic study. *FEBS Lett, 113*(2), 304-306.

Liu, D., Chan, S. L., de Souza-Pinto, N. C., Slevin, J. R., Wersto, R. P., Zhan, M., . . . Mattson, M. P. (2006). Mitochondrial UCP4 mediates an adaptive shift in energy metabolism and increases the resistance of neurons to metabolic and oxidative stress. *Neuromolecular Med, 8*(3), 389-414. doi:10.1385/NMM:8:3:389

Lu, Y. W., Acoba, M. G., Selvaraju, K., Huang, T. C., Nirujogi, R. S., Sathe, G., . . . Claypool, S. M. (2017). Human adenine nucleotide translocases physically and functionally interact with respirasomes. *Mol Biol Cell, 28*(11), 1489-1506. doi:10.1091/mbc.E17-03-0195

Lunetti, P., Damiano, F., De Benedetto, G., Siculella, L., Pennetta, A., Muto, L., . . . Capobianco, L. (2016). Characterization of Human and Yeast Mitochondrial Glycine Carriers with Implications for Heme Biosynthesis and Anemia. *J Biol Chem, 291*(38), 19746-19759. doi:10.1074/jbc.M116.736876

Maldonado, E. N., DeHart, D. N., Patnaik, J., Klatt, S. C., Gooz, M. B., & Lemasters, J. J. (2016). ATP/ADP Turnover and Import of Glycolytic ATP into Mitochondria in Cancer Cells Is Independent of the Adenine Nucleotide Translocator. *J Biol Chem, 291*(37), 19642-19650. doi:10.1074/jbc.M116.734814

Mao, W., Yu, X. X., Zhong, A., Li, W., Brush, J., Sherwood, S. W., . . . Pan, G. (1999). UCP4, a novel brain-specific mitochondrial protein that reduces membrane potential in mammalian cells. *FEBS Lett, 443*(3), 326-330.

Matthias, A., Ohlson, K. B., Fredriksson, J. M., Jacobsson, A., Nedergaard, J., & Cannon, B. (2000). Thermogenic responses in brown fat cells are fully UCP1-dependent. UCP2 or UCP3 do not substitute for UCP1 in adrenergically or fatty scid-induced thermogenesis. *J Biol Chem, 275*(33), 25073-25081. doi:10.1074/jbc.M000547200

Mattiasson, G., & Sullivan, P. G. (2006). The emerging functions of UCP2 in health, disease, and therapeutics. *Antioxid Redox Signal, 8*(1-2), 1-38. doi:10.1089/ars.2006.8.1

Mayr, J. A., Merkel, O., Kohlwein, S. D., Gebhardt, B. R., Böhles, H., Fötschl, U., . . . Sperl, W. (2007). Mitochondrial phosphate-carrier deficiency: a novel disorder of oxidative phosphorylation. *Am J Hum Genet, 80*(3), 478-484. doi:10.1086/511788

Mayr, J. A., Zimmermann, F. A., Horváth, R., Schneider, H. C., Schoser, B., Holinski-Feder, E., . . . Sperl, W. (2011). Deficiency of the mitochondrial phosphate carrier presenting as myopathy and cardiomyopathy in a family with three affected children. *Neuromuscul Disord, 21*(11), 803-808. doi:10.1016/j.nmd.2011.06.005

Milenkovic, D., Blaza, J. N., Larsson, N. G., & Hirst, J. (2017). The Enigma of the Respiratory Chain Supercomplex. *Cell Metab, 25*(4), 765-776. doi:10.1016/j.cmet.2017.03.009

Miyamoto, T., Kanazawa, N., Kato, S., Kawakami, M., Inoue, Y., Kuhara, T., . . . Tsujino, S. (2001). Diagnosis of Japanese patients with HHH syndrome by molecular genetic analysis: a common mutation, R179X. *J Hum Genet, 46*(5), 260-262. doi:10.1007/s100380170075

Molinari, F., Kaminska, A., Fiermonte, G., Boddaert, N., Raas-Rothschild, A., Plouin, P., . . . Colleaux, L. (2009). Mutations in the mitochondrial glutamate carrier SLC25A22 in neonatal epileptic encephalopathy with suppression bursts. *Clin Genet, 76*(2), 188-194. doi:10.1111/j.1399-0004.2009.01236.x

Molinari, F., Raas-Rothschild, A., Rio, M., Fiermonte, G., Encha-Razavi, F., Palmieri, L., . . . Colleaux, L. (2005). Impaired mitochondrial glutamate transport in autosomal

recessive neonatal myoclonic epilepsy. *Am J Hum Genet, 76*(2), 334-339. doi:10.1086/427564

Monné, M., Daddabbo, L., Gagneul, D., Obata, T., Hielscher, B., Palmieri, L., . . . Palmieri, F. (2018). Uncoupling proteins 1 and 2 (UCP1 and UCP2) from Arabidopsis thaliana are mitochondrial transporters of aspartate, glutamate and dicarboxylates. *J Biol Chem*. doi:10.1074/jbc.RA117.000771

Moreno-Lastres, D., Fontanesi, F., García-Consuegra, I., Martín, M. A., Arenas, J., Barrientos, A., & Ugalde, C. (2012). Mitochondrial complex I plays an essential role in human respirasome assembly. *Cell Metab, 15*(3), 324-335. doi:10.1016/j.cmet.2012.01.015

Mueckler, M., & Thorens, B. (2013). The SLC2 (GLUT) family of membrane transporters. *Mol Aspects Med, 34*(2-3), 121-138. doi:10.1016/j.mam.2012.07.001

Muntau, A. C., Röschinger, W., Merkenschlager, A., van der Knaap, M. S., Jakobs, C., Duran, M., . . . Roscher, A. A. (2000). Combined D-2- and L-2-hydroxyglutaric aciduria with neonatal onset encephalopathy: a third biochemical variant of 2-hydroxyglutaric aciduria? *Neuropediatrics, 31*(3), 137-140. doi:10.1055/s-2000-7497

Müller, V., Basset, G., Nelson, D. R., & Klingenberg, M. (1996). Probing the role of positive residues in the ADP/ATP carrier from yeast. The effect of six arginine mutations of oxidative phosphorylation and AAC expression. *Biochemistry, 35*(50), 16132-16143. doi:10.1021/bi960667r

Müller, V., Heidkämper, D., Nelson, D. R., & Klingenberg, M. (1997). Mutagenesis of some positive and negative residues occurring in repeat triad residues in the

ADP/ATP carrier from yeast. *Biochemistry, 36*(50), 16008-16018. doi:10.1021/bi9718671

Nakagawa, T., & Kaneko, S. (2013). SLC1 glutamate transporters and diseases: psychiatric diseases and pathological pain. *Curr Mol Pharmacol, 6*(2), 66-73.

Nakase, T., Yoshida, Y., & Nagata, K. (2007). Amplified expression of uncoupling proteins in human brain ischemic lesions. *Neuropathology, 27*(5), 442-447.

Napoli, L., Bordoni, A., Zeviani, M., Hadjigeorgiou, G. M., Sciacco, M., Tiranti, V., . . . Comi, G. P. (2001). A novel missense adenine nucleotide translocator-1 gene mutation in a Greek adPEO family. *Neurology, 57*(12), 2295-2298.

Nicholls, D. G., Bernson, V. S., & Heaton, G. M. (1978). The identification of the component in the inner membrane of brown adipose tissue mitochondria responsible for regulating energy dissipation. *Experientia Suppl, 32*, 89-93.

Nohara, K., Tateishi, Y., Suzuki, T., Okamura, K., Murai, H., Takumi, S., . . . Ito, T. (2012). Late-onset increases in oxidative stress and other tumorigenic activities and tumors with a Ha-ras mutation in the liver of adult male C3H mice gestationally exposed to arsenic. *Toxicol Sci, 129*(2), 293-304. doi:10.1093/toxsci/kfs203

Nota, B., Struys, E. A., Pop, A., Jansen, E. E., Fernandez Ojeda, M. R., Kanhai, W. A., . . . Salomons, G. S. (2013). Deficiency in SLC25A1, encoding the mitochondrial citrate carrier, causes combined D-2- and L-2-hydroxyglutaric aciduria. *Am J Hum Genet, 92*(4), 627-631. doi:10.1016/j.ajhg.2013.03.009

Nury, H., Dahout-Gonzalez, C., Trézéguet, V., Lauquin, G., Brandolin, G., & Pebay-Peyroula, E. (2005). Structural basis for lipid-mediated interactions between

mitochondrial ADP/ATP carrier monomers. *FEBS Lett, 579*(27), 6031-6036. doi:10.1016/j.febslet.2005.09.061

Nègre-Salvayre, A., Hirtz, C., Carrera, G., Cazenave, R., Troly, M., Salvayre, R., . . . Casteilla, L. (1997). A role for uncoupling protein-2 as a regulator of mitochondrial hydrogen peroxide generation. *FASEB J, 11*(10), 809-815.

Ohura, T., Kobayashi, K., Tazawa, Y., Nishi, I., Abukawa, D., Sakamoto, O., . . . Saheki, T. (2001). Neonatal presentation of adult-onset type II citrullinemia. *Hum Genet, 108*(2), 87-90.

Orlowski, J., & Grinstein, S. (2004). Diversity of the mammalian sodium/proton exchanger SLC9 gene family. *Pflugers Arch, 447*(5), 549-565. doi:10.1007/s00424-003-1110-3

Padan, E., & Landau, M. (2016). Sodium-Proton (Na(+)/H(+)) Antiporters: Properties and Roles in Health and Disease. *Met Ions Life Sci, 16*, 391-458. doi:10.1007/978-3-319-21756-7_12

Palacín, M., & Kanai, Y. (2004). The ancillary proteins of HATs: SLC3 family of amino acid transporters. *Pflugers Arch, 447*(5), 490-494. doi:10.1007/s00424-003-1062-7

Palmieri, F. (2004). The mitochondrial transporter family (SLC25): physiological and pathological implications. *Pflugers Arch, 447*(5), 689-709. doi:10.1007/s00424-003-1099-7

Palmieri, F. (2013). The mitochondrial transporter family SLC25: identification, properties and physiopathology. *Mol Aspects Med, 34*(2-3), 465-484. doi:10.1016/j.mam.2012.05.005

Palmieri, F. (2014). Mitochondrial transporters of the SLC25 family and associated diseases: a review. *J Inherit Metab Dis, 37*(4), 565-575. doi:10.1007/s10545-014-9708-5

Palmieri, F., & Monné, M. (2016). Discoveries, metabolic roles and diseases of mitochondrial carriers: A review. *Biochim Biophys Acta, 1863*(10), 2362-2378. doi:10.1016/j.bbamcr.2016.03.007

Palmieri, F., & Pierri, C. L. (2010). Mitochondrial metabolite transport. *Essays Biochem, 47*, 37-52. doi:10.1042/bse0470037

Palmieri, L., Alberio, S., Pisano, I., Lodi, T., Meznaric-Petrusa, M., Zidar, J., . . . Zeviani, M. (2005). Complete loss-of-function of the heart/muscle-specific adenine nucleotide translocator is associated with mitochondrial myopathy and cardiomyopathy. *Hum Mol Genet, 14*(20), 3079-3088. doi:10.1093/hmg/ddi341

Palmisano, A., Zara, V., Hönlinger, A., Vozza, A., Dekker, P. J., Pfanner, N., & Palmieri, F. (1998). Targeting and assembly of the oxoglutarate carrier: general principles for biogenesis of carrier proteins of the mitochondrial inner membrane. *Biochem J, 333 (Pt 1)*, 151-158.

Pande, S. V., Brivet, M., Slama, A., Demaugre, F., Aufrant, C., & Saudubray, J. M. (1993). Carnitine-acylcarnitine translocase deficiency with severe hypoglycemia and auriculo ventricular block. Translocase assay in permeabilized fibroblasts. *J Clin Invest, 91*(3), 1247-1252. doi:10.1172/JCI116288

Paradkar, P. N., Zumbrennen, K. B., Paw, B. H., Ward, D. M., & Kaplan, J. (2009). Regulation of mitochondrial iron import through differential turnover of mitoferrin 1 and mitoferrin 2. *Mol Cell Biol, 29*(4), 1007-1016. doi:10.1128/MCB.01685-08

Parker, M. D., & Boron, W. F. (2013). The divergence, actions, roles, and relatives of sodium-coupled bicarbonate transporters. *Physiol Rev, 93*(2), 803-959. doi:10.1152/physrev.00023.2012

Pebay-Peyroula, E., Dahout-Gonzalez, C., Kahn, R., Trézéguet, V., Lauquin, G. J., & Brandolin, G. (2003). Structure of mitochondrial ADP/ATP carrier in complex with carboxyatractyloside. *Nature, 426*(6962), 39-44. doi:10.1038/nature02056

Perez-Martinez, X., Broadley, S. A., & Fox, T. D. (2003). Mss51p promotes mitochondrial Cox1p synthesis and interacts with newly synthesized Cox1p. *EMBO J, 22*(21), 5951-5961. doi:10.1093/emboj/cdg566

Perez-Martinez, X., Butler, C. A., Shingu-Vazquez, M., & Fox, T. D. (2009). Dual functions of Mss51 couple synthesis of Cox1 to assembly of cytochrome c oxidase in Saccharomyces cerevisiae mitochondria. *Mol Biol Cell, 20*(20), 4371-4380. doi:10.1091/mbc.E09-06-0522

Perland, E., & Fredriksson, R. (2017). Classification Systems of Secondary Active Transporters. *Trends Pharmacol Sci, 38*(3), 305-315. doi:10.1016/j.tips.2016.11.008

Pfeiffer, K., Gohil, V., Stuart, R. A., Hunte, C., Brandt, U., Greenberg, M. L., & Schägger, H. (2003). Cardiolipin stabilizes respiratory chain supercomplexes. *J Biol Chem, 278*(52), 52873-52880. doi:10.1074/jbc.M308366200

Poduri, A., Heinzen, E. L., Chitsazzadeh, V., Lasorsa, F. M., Elhosary, P. C., LaCoursiere, C. M., . . . Walsh, C. A. (2013). SLC25A22 is a novel gene for migrating partial seizures in infancy. *Ann Neurol, 74*(6), 873-882.

Ponka, P. (1997). Tissue-specific regulation of iron metabolism and heme synthesis: distinct control mechanisms in erythroid cells. *Blood, 89*(1), 1-25.

Porter, R. K. (2008). Uncoupling protein 1: a short-circuit in the chemiosmotic process. *J Bioenerg Biomembr, 40*(5), 457-461. doi:10.1007/s10863-008-9172-8

Porter, R. K. (2012). Studies on the function and regulation of mitochondrial uncoupling proteins. *Adv Exp Med Biol, 748*, 171-184. doi:10.1007/978-1-4614-3573-0_7

Postis, V., De Marcos Lousa, C., Arnou, B., Lauquin, G. J., & Trézéguet, V. (2005). Subunits of the yeast mitochondrial ADP/ATP carrier: cooperation within the dimer. *Biochemistry, 44*(45), 14732-14740. doi:10.1021/bi051648x

Pramod, A. B., Foster, J., Carvelli, L., & Henry, L. K. (2013). SLC6 transporters: structure, function, regulation, disease association and therapeutics. *Mol Aspects Med, 34*(2-3), 197-219. doi:10.1016/j.mam.2012.07.002

Pushkin, A., & Kurtz, I. (2006). SLC4 base (HCO3 -, CO3 2-) transporters: classification, function, structure, genetic diseases, and knockout models. *Am J Physiol Renal Physiol, 290*(3), F580-599. doi:10.1152/ajprenal.00252.2005

Quednau, B. D., Nicoll, D. A., & Philipson, K. D. (2004). The sodium/calcium exchanger family-SLC8. *Pflugers Arch, 447*(5), 543-548. doi:10.1007/s00424-003-1065-4

Ramsden, D. B., Ho, P. W., Ho, J. W., Liu, H. F., So, D. H., Tse, H. M., . . . Ho, S. L. (2012). Human neuronal uncoupling proteins 4 and 5 (UCP4 and UCP5): structural properties, regulation, and physiological role in protection against oxidative stress and mitochondrial dysfunction. *Brain Behav, 2*(4), 468-478. doi:10.1002/brb3.55

Rodić, N., Oka, M., Hamazaki, T., Murawski, M. R., Jorgensen, M., Maatouk, D. M., . . . Terada, N. (2005). DNA methylation is required for silencing of ant4, an adenine

nucleotide translocase selectively expressed in mouse embryonic stem cells and germ cells. *Stem Cells, 23*(9), 1314-1323. doi:10.1634/stemcells.2005-0119

Romero, M. F. (2005). Molecular pathophysiology of SLC4 bicarbonate transporters. *Curr Opin Nephrol Hypertens, 14*(5), 495-501.

Romero, M. F., Chen, A. P., Parker, M. D., & Boron, W. F. (2013). The SLC4 family of bicarbonate (HCO_3^-) transporters. *Mol Aspects Med, 34*(2-3), 159-182. doi:10.1016/j.mam.2012.10.008

Rosenberg, M. J., Agarwala, R., Bouffard, G., Davis, J., Fiermonte, G., Hilliard, M. S., . . . Biesecker, L. G. (2002). Mutant deoxynucleotide carrier is associated with congenital microcephaly. *Nat Genet, 32*(1), 175-179. doi:10.1038/ng948

Rosenthal, E. A., Ranchalis, J., Crosslin, D. R., Burt, A., Brunzell, J. D., Motulsky, A. G., . . . Project, NHLBI GO Exome Sequencing. (2013). Joint linkage and association analysis with exome sequence data implicates SLC25A40 in hypertriglyceridemia. *Am J Hum Genet, 93*(6), 1035-1045. doi:10.1016/j.ajhg.2013.10.019

Ruprecht, J. J., Hellawell, A. M., Harding, M., Crichton, P. G., McCoy, A. J., & Kunji, E. R. (2014). Structures of yeast mitochondrial ADP/ATP carriers support a domain-based alternating-access transport mechanism. *Proc Natl Acad Sci U S A, 111*(4), E426-434. doi:10.1073/pnas.1320692111

Sabová, L., Zeman, I., Supek, F., & Kolarov, J. (1993). Transcriptional control of AAC3 gene encoding mitochondrial ADP/ATP translocator in Saccharomyces cerevisiae by oxygen, heme and ROX1 factor. *Eur J Biochem, 213*(1), 547-553.

Salvi, S., Santorelli, F. M., Bertini, E., Boldrini, R., Meli, C., Donati, A., . . . Dionisi-Vici, C. (2001). Clinical and molecular findings in hyperornithinemia-hyperammonemia-homocitrullinuria syndrome. *Neurology, 57*(5), 911-914.

Sanchis, D., Fleury, C., Chomiki, N., Goubern, M., Huang, Q., Neverova, M., . . . Ricquier, D. (1998). BMCP1, a novel mitochondrial carrier with high expression in the central nervous system of humans and rodents, and respiration uncoupling activity in recombinant yeast. *J Biol Chem, 273*(51), 34611-34615.

Schiff, M., Veauville-Merllié, A., Su, C. H., Tzagoloff, A., Rak, M., Ogier de Baulny, H., . . . Acquaviva-Bourdain, C. (2016). SLC25A32 Mutations and Riboflavin-Responsive Exercise Intolerance. *N Engl J Med, 374*(8), 795-797. doi:10.1056/NEJMc1513610

Schroers, A., Burkovski, A., Wohlrab, H., & Krämer, R. (1998). The phosphate carrier from yeast mitochondria. Dimerization is a prerequisite for function. *J Biol Chem, 273*(23), 14269-14276.

Schweikhard, E. S., & Ziegler, C. M. (2012). Amino acid secondary transporters: toward a common transport mechanism. *Curr Top Membr, 70*, 1-28. doi:10.1016/B978-0-12-394316-3.00001-6

Schägger, H., & Pfeiffer, K. (2000). Supercomplexes in the respiratory chains of yeast and mammalian mitochondria. *EMBO J, 19*(8), 1777-1783. doi:10.1093/emboj/19.8.1777

Schägger, H., & von Jagow, G. (1991). Blue native electrophoresis for isolation of membrane protein complexes in enzymatically active form. *Anal Biochem, 199*(2), 223-231.

Seifert, E. L., Ligeti, E., Mayr, J. A., Sondheimer, N., & Hajnóczky, G. (2015). The mitochondrial phosphate carrier: Role in oxidative metabolism, calcium handling and mitochondrial disease. *Biochem Biophys Res Commun, 464*(2), 369-375. doi:10.1016/j.bbrc.2015.06.031

Shaw, G. C., Cope, J. J., Li, L., Corson, K., Hersey, C., Ackermann, G. E., . . . Paw, B. H. (2006). Mitoferrin is essential for erythroid iron assimilation. *Nature, 440*(7080), 96-100. doi:10.1038/nature04512

Shayakul, C., Clémençon, B., & Hediger, M. A. (2013). The urea transporter family (SLC14): physiological, pathological and structural aspects. *Mol Aspects Med, 34*(2-3), 313-322. doi:10.1016/j.mam.2012.12.003

Shayakul, C., & Hediger, M. A. (2004). The SLC14 gene family of urea transporters. *Pflugers Arch, 447*(5), 603-609. doi:10.1007/s00424-003-1124-x

Siep, M., van Oosterum, K., Neufeglise, H., van der Spek, H., & Grivell, L. A. (2000). Mss51p, a putative translational activator of cytochrome c oxidase subunit-1 (COX1) mRNA, is required for synthesis of Cox1p in Saccharomyces cerevisiae. *Curr Genet, 37*(4), 213-220.

Silva, J. P., Shabalina, I. G., Dufour, E., Petrovic, N., Backlund, E. C., Hultenby, K., . . . Larsson, N. G. (2005). SOD2 overexpression: enhanced mitochondrial tolerance but absence of effect on UCP activity. *EMBO J, 24*(23), 4061-4070. doi:10.1038/sj.emboj.7600866

Simpson, I. A., Dwyer, D., Malide, D., Moley, K. H., Travis, A., & Vannucci, S. J. (2008). The facilitative glucose transporter GLUT3: 20 years of distinction. *Am J Physiol Endocrinol Metab, 295*(2), E242-253. doi:10.1152/ajpendo.90388.2008

Smits, P., Smeitink, J., & van den Heuvel, L. (2010). Mitochondrial translation and beyond: processes implicated in combined oxidative phosphorylation deficiencies. *J Biomed Biotechnol, 2010*, 737385. doi:10.1155/2010/737385

Smorodchenko, A., Rupprecht, A., Fuchs, J., Gross, J., & Pohl, E. E. (2011). Role of mitochondrial uncoupling protein 4 in rat inner ear. *Mol Cell Neurosci, 47*(4), 244-253. doi:10.1016/j.mcn.2011.03.002

Smorodchenko, A., Rupprecht, A., Sarilova, I., Ninnemann, O., Bräuer, A. U., Franke, K., . . . Pohl, E. E. (2009). Comparative analysis of uncoupling protein 4 distribution in various tissues under physiological conditions and during development. *Biochim Biophys Acta, 1788*(10), 2309-2319. doi:10.1016/j.bbamem.2009.07.018

Soto, I. C., Fontanesi, F., Liu, J., & Barrientos, A. (2012). Biogenesis and assembly of eukaryotic cytochrome c oxidase catalytic core. *Biochim Biophys Acta, 1817*(6), 883-897. doi:10.1016/j.bbabio.2011.09.005

Spiegel, R., Shaag, A., Edvardson, S., Mandel, H., Stepensky, P., Shalev, S. A., . . . Elpeleg, O. (2009). SLC25A19 mutation as a cause of neuropathy and bilateral striatal necrosis. *Ann Neurol, 66*(3), 419-424. doi:10.1002/ana.21752

Sreedhar, A., Petruska, P., Miriyala, S., Panchatcharam, M., & Zhao, Y. (2017). UCP2 overexpression enhanced glycolysis via activation of PFKFB2 during skin cell transformation. *Oncotarget, 8*(56), 95504-95515. doi:10.18632/oncotarget.20762

Stanley, C. A., Hale, D. E., Berry, G. T., Deleeuw, S., Boxer, J., & Bonnefont, J. P. (1992). Brief report: a deficiency of carnitine-acylcarnitine translocase in the inner mitochondrial membrane. *N Engl J Med, 327*(1), 19-23. doi:10.1056/NEJM199207023270104

Stepien, G., Torroni, A., Chung, A. B., Hodge, J. A., & Wallace, D. C. (1992). Differential expression of adenine nucleotide translocator isoforms in mammalian tissues and during muscle cell differentiation. *J Biol Chem, 267*(21), 14592-14597.

Tamamori, A., Okano, Y., Ozaki, H., Fujimoto, A., Kajiwara, M., Fukuda, K., . . . Yamano, T. (2002). Neonatal intrahepatic cholestasis caused by citrin deficiency: severe hepatic dysfunction in an infant requiring liver transplantation. *Eur J Pediatr, 161*(11), 609-613. doi:10.1007/s00431-002-1045-2

Taylor, E. B. (2017). Functional Properties of the Mitochondrial Carrier System. *Trends Cell Biol, 27*(9), 633-644. doi:10.1016/j.tcb.2017.04.004

Tazawa, Y., Kobayashi, K., Ohura, T., Abukawa, D., Nishinomiya, F., Hosoda, Y., . . . Saheki, T. (2001). Infantile cholestatic jaundice associated with adult-onset type II citrullinemia. *J Pediatr, 138*(5), 735-740. doi:10.1067/mpd.2001.113264

Terzenidou, M. E., Segklia, A., Kano, T., Papastefanaki, F., Karakostas, A., Charalambous, M., . . . Douni, E. (2017). Novel insights into SLC25A46-related pathologies in a genetic mouse model. *PLoS Genet, 13*(4), e1006656. doi:10.1371/journal.pgen.1006656

Tessa, A., Fiermonte, G., Dionisi-Vici, C., Paradies, E., Baumgartner, M. R., Chien, Y. H., . . . Santorelli, F. M. (2009). Identification of novel mutations in the SLC25A15 gene in hyperornithinemia-hyperammonemia-homocitrullinuria (HHH) syndrome: a clinical, molecular, and functional study. *Hum Mutat, 30*(5), 741-748. doi:10.1002/humu.20930

Thompson, K., Majd, H., Dallabona, C., Reinson, K., King, M. S., Alston, C. L., . . . Taylor, R. W. (2016). Recurrent De Novo Dominant Mutations in SLC25A4 Cause Severe

Early-Onset Mitochondrial Disease and Loss of Mitochondrial DNA Copy Number. *Am J Hum Genet, 99*(6), 1405. doi:10.1016/j.ajhg.2016.11.001

Towpik, J. (2005). Regulation of mitochondrial translation in yeast. *Cell Mol Biol Lett, 10*(4), 571-594.

Trézéguet, V., Le Saux, A., David, C., Gourdet, C., Fiore, C., Dianoux, A., . . . Lauquin, G. J. (2000). A covalent tandem dimer of the mitochondrial ADP/ATP carrier is functional in vivo. *Biochim Biophys Acta, 1457*(1-2), 81-93.

Tsujino, S., Kanazawa, N., Ohashi, T., Eto, Y., Saito, T., Kira, J., & Yamada, T. (2000). Three novel mutations (G27E, insAAC, R179X) in the ORNT1 gene of Japanese patients with hyperornithinemia, hyperammonemia, and homocitrullinuria syndrome. *Ann Neurol, 47*(5), 625-631.

Uldry, M., & Thorens, B. (2004). The SLC2 family of facilitated hexose and polyol transporters. *Pflugers Arch, 447*(5), 480-489. doi:10.1007/s00424-003-1085-0

Van De Parre, T. J., Martinet, W., Verheye, S., Kockx, M. M., Van Langenhove, G., Herman, A. G., & De Meyer, G. R. (2008). Mitochondrial uncoupling protein 2 mediates temperature heterogeneity in atherosclerotic plaques. *Cardiovasc Res, 77*(2), 425-431. doi:10.1093/cvr/cvm003

Verrey, F., Closs, E. I., Wagner, C. A., Palacin, M., Endou, H., & Kanai, Y. (2004). CATs and HATs: the SLC7 family of amino acid transporters. *Pflugers Arch, 447*(5), 532-542. doi:10.1007/s00424-003-1086-z

Vest, K. E., Leary, S. C., Winge, D. R., & Cobine, P. A. (2013). Copper import into the mitochondrial matrix in Saccharomyces cerevisiae is mediated by Pic2, a

mitochondrial carrier family protein. *J Biol Chem, 288*(33), 23884-23892. doi:10.1074/jbc.M113.470674

Vidal-Puig, A. J., Grujic, D., Zhang, C. Y., Hagen, T., Boss, O., Ido, Y., . . . Lowell, B. B. (2000). Energy metabolism in uncoupling protein 3 gene knockout mice. *J Biol Chem, 275*(21), 16258-16266. doi:10.1074/jbc.M910179199

Vidal-Puig, A., Solanes, G., Grujic, D., Flier, J. S., & Lowell, B. B. (1997). UCP3: an uncoupling protein homologue expressed preferentially and abundantly in skeletal muscle and brown adipose tissue. *Biochem Biophys Res Commun, 235*(1), 79-82. doi:10.1006/bbrc.1997.6740

Visser, W. F., van Roermund, C. W., Waterham, H. R., & Wanders, R. J. (2002). Identification of human PMP34 as a peroxisomal ATP transporter. *Biochem Biophys Res Commun, 299*(3), 494-497.

Vozza, A., Parisi, G., De Leonardis, F., Lasorsa, F. M., Castegna, A., Amorese, D., . . . Fiermonte, G. (2014). UCP2 transports C4 metabolites out of mitochondria, regulating glucose and glutamine oxidation. *Proc Natl Acad Sci U S A, 111*(3), 960-965. doi:10.1073/pnas.1317400111

Waldherr, M., Ragnini, A., Jank, B., Teply, R., Wiesenberger, G., & Schweyen, R. J. (1993). A multitude of suppressors of group II intron-splicing defects in yeast. *Curr Genet, 24*(4), 301-306.

Walker, S. C., & Engelke, D. R. (2008). A protein-only RNase P in human mitochondria. *Cell, 135*(3), 412-414. doi:10.1016/j.cell.2008.10.010

Wan, J., Steffen, J., Yourshaw, M., Mamsa, H., Andersen, E., Rudnik-Schöneborn, S., . . . Jen, J. C. (2016). Loss of function of SLC25A46 causes lethal congenital

pontocerebellar hypoplasia. *Brain, 139*(11), 2877-2890. doi:10.1093/brain/aww212

Wibom, R., Lasorsa, F. M., Töhönen, V., Barbaro, M., Sterky, F. H., Kucinski, T., . . . Wedell, A. (2009). AGC1 deficiency associated with global cerebral hypomyelination. *N Engl J Med, 361*(5), 489-495. doi:10.1056/NEJMoa0900591

Wohlrab, H., & Flowers, N. (1982). pH gradient-dependent phosphate transport catalyzed by the purified mitochondrial phosphate transport protein. *J Biol Chem, 257*(1), 28-31.

Wright, E. M. (2013). Glucose transport families SLC5 and SLC50. *Mol Aspects Med, 34*(2-3), 183-196. doi:10.1016/j.mam.2012.11.002

Writzl, K., Maver, A., Kovačič, L., Martinez-Valero, P., Contreras, L., Satrustegui, J., . . . Hennekam, R. C. (2017). De Novo Mutations in SLC25A24 Cause a Disorder Characterized by Early Aging, Bone Dysplasia, Characteristic Face, and Early Demise. *Am J Hum Genet, 101*(5), 844-855. doi:10.1016/j.ajhg.2017.09.017

Wu, M., Gu, J., Guo, R., Huang, Y., & Yang, M. (2016). Structure of Mammalian Respiratory Supercomplex I1III2IV1. *Cell, 167*(6), 1598-1609.e1510. doi:10.1016/j.cell.2016.11.012

Xu, W., Barrientos, T., & Andrews, N. C. (2013). Iron and copper in mitochondrial diseases. *Cell Metab, 17*(3), 319-328. doi:10.1016/j.cmet.2013.02.004

Yasuda, T., Yamaguchi, N., Kobayashi, K., Nishi, I., Horinouchi, H., Jalil, M. A., . . . Saheki, T. (2000). Identification of two novel mutations in the SLC25A13 gene and detection of seven mutations in 102 patients with adult-onset type II citrullinemia. *Hum Genet, 107*(6), 537-545.

Zhang, C. Y., Baffy, G., Perret, P., Krauss, S., Peroni, O., Grujic, D., . . . Lowell, B. B. (2001). Uncoupling protein-2 negatively regulates insulin secretion and is a major link between obesity, beta cell dysfunction, and type 2 diabetes. *Cell, 105*(6), 745-755.

Zhang, M., Mileykovskaya, E., & Dowhan, W. (2002). Gluing the respiratory chain together. Cardiolipin is required for supercomplex formation in the inner mitochondrial membrane. *J Biol Chem, 277*(46), 43553-43556. doi:10.1074/jbc.C200551200

Zhang, M., Wang, B., Ni, Y. H., Liu, F., Fei, L., Pan, X. Q., . . . Guo, X. R. (2006). Overexpression of uncoupling protein 4 promotes proliferation and inhibits apoptosis and differentiation of preadipocytes. *Life Sci, 79*(15), 1428-1435. doi:10.1016/j.lfs.2006.04.012

Chapter 2

The ADP/ATP carrier regulates mitochondrial translation

Sections of this chapter are derived from:

Oluwaseun B. Ogunbona, Matthew G Baile, Steven M. Claypool (2018). Cardiomyopathy-associated mutation in the ADP/ATP carrier reveals translation-dependent regulation of cytochrome *c* oxidase activity. *Mol Biol Cell* **(In Revision)**

ABSTRACT

How the absence of the major mitochondrial ADP/ATP carrier in yeast, Aac2p, results in a specific defect in cytochrome *c* oxidase (COX; complex IV) activity is a long-standing mystery. Aac2p physically associates with respiratory supercomplexes, which include complex IV, raising the possibility that its activity is dependent on its association with Aac2p. Here, we have leveraged a transport-dead pathogenic *AAC2* point mutant to determine the basis for the reduced COX activity in the absence of Aac2p. The steady state levels of complex IV subunits encoded by the mitochondrial genome are significantly reduced in the absence of Aac2p function, whether its association with respiratory supercomplexes is preserved or not. This diminution in COX amounts is not caused by a reduction in the mitochondrial genome copy number or the steady state level of its transcripts and does not reflect a defect in complex IV assembly. Instead, the absence of Aac2p activity, genetically or pharmacologically, results in an aberrant pattern of mitochondrial translation. Interestingly, compared to the complete absence of Aac2p, the complex IV-related defects are greater in mitochondria expressing the transport-inactive Aac2p mutant. Our results highlight a critical role for Aac2p transport in mitochondrial translation whose disturbance uniquely impacts cytochrome *c* oxidase.

INTRODUCTION

Life is energetically costly. The major energy currency in cells comes in the form of ATP, most of which is produced in the mitochondrion by the combined activities of a series of inner membrane proton pumps (complexes I, III, IV, and V), the last of which physiologically works in reverse. This process, which is known as oxidative phosphorylation (OXPHOS), additionally requires two mitochondrial carrier proteins, the phosphate carrier (Pic) and the ADP/ATP carrier (Aac). A symporter, Pic couples the downhill flow of protons across the inner membrane to the transport of phosphate into the mitochondrial matrix (Wohlrab & Flowers, 1982). Aac mediates the exchange of ADP into for ATP out of the matrix, a process that is driven by the electrical gradient across the inner membrane that is established by the electron transport chain (Klingenberg, 2008). Thus, Pic and Aac utilize the chemical and electrical components of the electrochemical gradient, respectively, to provide the substrates, Pi and ADP, needed by complex V to make ATP. By reducing the electrochemical gradient, Pic and Aac make it easier for complexes I, III and IV to pump protons. Further, their transport activity is a core feature of respiratory control, the classic mode of OXPHOS regulation. In the absence of ADP (or Pi), complex V is unable to couple the downhill flow of protons to the synthesis of ATP. This increases the electrochemical gradient to a level that effectively shuts off further proton pumping. Upon the addition of ADP and its transport into the matrix by Aac, complex V function resumes, decreasing the electrochemical gradient and thus increasing the activity of the respiratory complexes. As such, the OXPHOS machinery, Pic, and Aac are functionally co-dependent.

In humans, ADP/ATP carriers are called adenine nucleotide translocases (ANT). There are three Aac isoforms in yeast and four ANT isoforms in human. All of these isoforms are encoded by distinct genes. The four human ANT isoforms display a tissue-specific and yet partially overlapping expression pattern. ANT1 is the predominant isoform in the heart and skeletal muscle (Stepien, Torroni, Chung, Hodge, & Wallace, 1992), ANT2 is highly-expressed in regenerative tissues such as kidney and liver, ANT3 is ubiquitously expressed at low baseline levels, and ANT4 is contained in testis (Doerner et al., 1997; Dolce, Scarcia, Iacopetta, & Palmieri, 2005; Dupont & Stepien, 2011; Stepien et al., 1992). Of the three yeast Aac isoforms, only Aac2p is required for OXPHOS (Lawson, Gawaz, Klingenberg, & Douglas, 1990). Aac1p and Aac3p are minor isoforms whose expression is repressed in hypoxic (Gavurníková, Sabova, Kissová, Haviernik, & Kolarov, 1996) or induced in anaerobic (Sabová, Zeman, Supek, & Kolarov, 1993) conditions, respectively.

ANT1 deficiency is implicated in various pathological states, such as hypertrophic cardiomyopathy, mitochondrial myopathy, lactic acidosis, progressive external ophthalmoplegia, facioscapulohumeral muscular dystrophy, and Sengers syndrome (Echaniz-Laguna et al., 2012; Fontanesi et al., 2004; Graham et al., 1997; Jordens et al., 2002; Kaukonen et al., 2000; Komaki et al., 2002; Palmieri et al., 2005; Sharer, 2005; Thompson et al., 2016). Mutations in *ANT2* have been associated with non-syndromic intellectual disability (Vandewalle et al., 2013) and cardiac noncompaction (Kokoszka et al., 2016) and its dysregulation associated with a Warburg metabolic phenotype (Maldonado et al., 2016). Presumably, the impacted tissues reflect the expression pattern of ANT isoforms. However, whether these pathologies all result simply from impaired

OXPHOS function or additionally include isoform specific activities unrelated to OXPHOS remains an open question.

It was demonstrated by us and others that Aac2p physically associates with the respiratory supercomplex (RSC), higher order assemblies of individual respiratory complexes (Acín-Pérez, Fernández-Silva, Peleato, Pérez-Martos, & Enriquez, 2008; Gu et al., 2016; Letts, Fiedorczuk, & Sazanov, 2016; Moreno-Lastres et al., 2012; Schägger & Pfeiffer, 2000; Wu, Gu, Guo, Huang, & Yang, 2016), as well as other mitochondrial carriers, but only in the context of mitochondrial membranes that contain the unique phospholipid cardiolipin (Claypool, Oktay, Boontheung, Loo, & Koehler, 2008; Dienhart & Stuart, 2008). Importantly, we have recently established that the interaction between the ADP/ATP carrier and the respiratory supercomplexes is evolutionarily conserved (Lu et al., 2017), implying that this association is functionally important. However, the functional significance of the Aac2p interaction with respiratory supercomplexes has not been provided.

The absence of Aac2p in yeast not only prevents OXPHOS but additionally results in a specific diminution in complex IV activity (Claypool et al., 2008; Dienhart & Stuart, 2008; Fontanesi et al., 2004; Heidkämper, Müller, Nelson, & Klingenberg, 1996; Müller, Basset, Nelson, & Klingenberg, 1996). The mechanistic basis for the reduced complex IV function when Aac2p is missing has not been established. In the present study, we have modeled a transport-dead pathogenic *ANT1* point mutant discovered in a patient with hypertrophic cardiomyopathy and mild myopathy in *AAC2* to determine whether the reduction in complex IV activity when Aac2p is missing reflects the absence of the interaction between Aac2p and components of the electron transport chain and/or the lack

of nucleotide transport (i.e. Aac2p function). Importantly, the functionally inactive A137D allele of *AAC2* (*aac2*^{A137D}) is expressed normally and still interacts with components of the yeast respiratory supercomplex. In the absence of Aac2p function, the expression levels of complex IV subunits that are encoded by the mitochondrial genome (and which form the catalytic core of the complex IV holoenzyme) are specifically reduced. This reduction in the levels of complex IV subunits is not caused by a decrease in mitochondrial genome copy number or levels of mitochondrial DNA transcripts, nor does it result from any alteration in complex IV assembly. Instead, mitochondrial translation is altered in the absence of Aac2p activity. Interestingly, compared to the complete absence of Aac2p, the complex IV-related defects are greater in mitochondria expressing the transport-inactive Aac2^{A137D}. Collectively, our results highlight the importance of Aac2p function for the normal translation of the mitochondrial encoded complex IV subunits and further underscore the significant role of Aac2p in regulating oxidative phosphorylation.

RESULTS

Aac2^{A137D} is non-functional but assembles like wild type Aac2p

In yeast, complex IV function is specifically impaired in the absence of Aac2p. Even though this was first documented over two decades ago (Heidkämper et al., 1996; Müller et al., 1996) and subsequently confirmed by multiple groups (Claypool et al., 2008; Dienhart & Stuart, 2008; Fontanesi et al., 2004), the underlying mechanism has never been provided. In principle, Aac2p could support full complex IV activity by either mediating the flux of ADP and ATP across the inner membrane (Heidkämper et al., 1996) and/or by virtue of its physical association with the respiratory supercomplexes (Claypool et al., 2008; Dienhart & Stuart, 2008). To distinguish between these possibilities, we decided to leverage a pathogenic allele of ANT1, ANT1^{A123D}, identified in a patient suffering from exercise intolerance, lactic acidosis, hypertrophic cardiomyopathy, and mild myopathy (Palmieri et al., 2005). Interestingly, although the mutant protein is expressed at normal levels, it fails to mediate uptake of ATP upon reconstitution of muscle-derived mitochondrial extracts into liposomes. Moreover, when modeled in the yeast ortholog, Aac2^{A137D} is expressed at wild type levels, lacks ADP/ATP exchange in reconstituted liposomes, and fails to support respiratory growth (Palmieri et al., 2005). However, the quaternary assembly of Aac2^{A137D} has not been documented. We reasoned that if Aac2^{A137D} retains its ability to interact with other proteins, including the RSCs, it would provide an ideal tool to determine exactly how Aac2p controls complex IV activity.

Using CRISPR-Cas9, genomic mutations were introduced in *AAC2* that either resulted in a premature stop codon (*aac2*Δ) or the expression of the *aac2^{A137D}* mutant allele (Figure 2.1A). These genetic modifications were introduced in the presence or absence of

Aac1p and Aac3p, to evaluate if the minor Aac isoforms could potentially compensate for the absence of Aac2p function. As anticipated (Palmieri et al., 2005), Aac2^{A137D} was expressed like wild type Aac2p but unable to support growth on respiratory media (Figure 2.1A and B). Next, Aac2^{A137D} assembly was compared to wild type Aac2p by blue native (BN)-PAGE (Figure 2.1C). Indeed, Aac2^{A137D} engaged in a normal range of complexes that were not influenced by the presence or absence of the minor Aac isoforms. Importantly, the Aac2^{A137D} -containing complexes included high molecular weight associations with respiratory supercomplexes that consist of a complex III dimer associated with 1-2 copies of complex IV. In the absence of Aac2p function (*aac2*Δ and *aac2^{A137D})*, the relative abundance of the small supercomplex (III_2IV) was increased and free complex III dimers were readily detected (Figure 2.1D and E). These alterations suggest that the steady state level of complex IV is perhaps limiting when Aac2p is non-functional. To directly determine the ability of Aac2^{A137D} to associate with respiratory supercomplexes, we established yeast strains in which a FLAG tag was genomically appended to the C-terminus of either the complex IV subunit, Cox8p, or the complex III subunit, Qcr10p (Figure 2.9). Indeed, Aac2^{A137D} was co-immunoprecipitated with either Cox8-3XFLAG (Figure 2.1F) or Qcr10-3XFLAG (Figure 2.9A). Finally, the levels of ADP and ATP in mitochondria were determined as a proxy of Aac2^{A137D} function. In the absence of Aac2p activity, the level of mitochondrial ATP was significantly reduced (Figure 2.1H) which resulted in an elevated ADP:ATP ratio (Figure 2.1I). Interestingly, ADP levels were only significantly decreased for *aac2^{A137D}* and not *aac2*Δ (Figure 2.1G). Combined, these results indicate that Aac2^{A137D} is an assembly-competent, transport-inactive molecular tool that can be used to probe the molecular basis for the reduced complex IV activity that occurs

when Aac2p is not expressed (Claypool et al., 2008; Dienhart & Stuart, 2008; Fontanesi et al., 2004; Heidkämper et al., 1996; Müller et al., 1996).

Impaired complex IV activity and expression in the absence of Aac2p function

With the goal of determining if complex IV activity is dependent on its physical association with Aac2p, we next compared complex IV function in mitochondria that express either transport-active Aac2p, the transport-inactive Aac2^{A137D}, or that lack Aac2p expression completely. To determine complex IV activity in isolation, the rate of cytochrome *c* oxidation was tracked spectrophotometrically using mitochondria solubilized with n-dodecyl β-D-maltoside (DDM), a detergent that separates respiratory supercomplexes into its individual components (Schägger, 2001) (Figure 2.2A). To assess complex IV function in intact, non-detergent solubilized mitochondria, the ascorbate-TMPD (N,N,N′,N′-tetramethyl-p-phenylenediamine) dependent basal and uncoupled respiration rates, the only measurements that are relevant in the absence of Aac2p function, were determined (Figure 2.2B and C). Regardless of the method, complex IV (Figure 2.2A-C), but not complex III (Figure 2.2D), activity was significantly reduced in mitochondria that lack Aac2p function. Interestingly, the level of complex IV activity supported by the transport-inactive Aac2^{A137D} was even lower than detected in *aac2*Δ (Figure 2.2A-C). Thus, the reduced complex IV activity in *aac2*Δ extracts stems from the absence of Aac2p–mediated ADP/ATP exchange and not from the lack of the Aac2p–respiratory supercomplex interaction.

Next, the relative abundance of various complex IV subunits was determined in isolated mitochondria (Figure 2.2E). In yeast, complex IV has eleven total subunits, three of which–Cox1p, Cox2p, and Cox3p–are encoded by the mitochondrial genome. The

steady state levels of all three mitochondrial DNA (mtDNA)-encoded complex IV subunits was significantly reduced in the absence of Aac2p function (Figure 2.2E and quantified in Figure 2.2F and 2.10). This impacted the abundance of other complex IV subunits encoded by the nuclear genome such as Cox5Ap and Cox4p. mtDNA encoded subunits of complex V (Atp6p and Atp9p) were also reduced when Aac2p activity is missing, although not as drastically as the complex IV subunits. The steady state amounts of nuclear-encoded subunits of complex III (except for Qcr7p which was affected in the *aac2*^{A137D} mutant but not in *aac2*Δ) and complex V, as well as markers of the outer membrane, inner membrane, and matrix compartments (Tom70p, Pic1p, and Kgd1p, respectively), were not altered when Aac2p was absent or non-functional. The relative decrease in steady state abundance of mtDNA-encoded complex IV subunits was roughly proportional to the reduction in complex IV activity observed in mitochondria when Aac2p was not expressed at all (25-61% decrease in expression *vs*. 43-59% decrease in activity). Similarly, complex IV activity was compromised proportionately to its expression, although to a greater extent in the transport-inactive *aac2*^{A137D} mutant (62-89% decrease in expression vs 59-76% decrease in activity). This suggests that it is more detrimental to express a non-functional version of Aac2p than to not express it at all. From these results, we conclude that Aac2p activity controls complex IV functionality by specifically affecting the levels of mtDNA-encoded subunits of cytochrome *c* oxidase.

Mitochondrial translation is altered in the absence of Aac2p function

The steady state level of a protein is dictated by how robustly it is produced combined with how stable it is once it is made. Therefore, to determine the basis for the reduced steady state levels of mtDNA-encoded complex IV subunits, we started at the

genetic source of these subunits and determined mitochondrial DNA copy number relative to the nuclear genome by qPCR. Consistent with the fact that *aac2*Δ yeast are so-called petite-negative (that is, yeast lacking Aac2p are unable to survive in the absence of the mtDNA) (Kovác, Lachowicz, & Slonimski, 1967), mtDNA copy number was not significantly altered in strains lacking Aac2p activity compared to strains that have Aac2p activity (Figure 2.3A). We next reasoned that a specific reduction in the levels of complex IV subunits encoded by mtDNA could stem from a defect in their transcription. However, the relative abundance of transcripts that encode for subunits of complex IV (*COX1-3*) or complex V (*ATP6* and *ATP9*) were not impacted by the presence or absence of Aac2p function (Figure 2.3B-F).

These results suggest that Aac2p function regulates the steady state accumulation of mtDNA-encoded complex IV subunits through a post-transcriptional mechanism(s). As such, the translation of mtDNA-encoded proteins was determined by tracking the incorporation of ^{35}S-methionine/cysteine in yeast cultured in the presence of cycloheximide to inhibit cytosolic translation (Figure 2.4A and 2.11A). In the absence of Aac2p activity, translation of Cox1p and Cox2p was reduced while curiously, translation of Atp6p and Atp9p was increased relative to Aac2p-expressing yeast (Figure 2.4A and 2.11A). This latter change resulted in a significantly reduced ratio of newly translated Cox3p to Atp6p in yeast devoid of Aac2p activity (Figure 2.4B). Translation of Var1p was similar amongst the different yeast strains (Figure 2.11B) and while the overall incorporation of ^{35}S-Met/Cys was greatest when Aac2p was not expressed, this was not statistically significant (Figure 2.11C). Next, pulse-chase experiments were performed to determine if the absence of Aac2p function altered the stability of newly translated

mtDNA-encoded polypeptides (Figure 2.4C). In the absence, but not the presence, of the minor Aac isoforms, the stability of Cox1p and Cox2p was compromised in the context of the transport-inactive Aac2^{A137D} mutant (Figure 2.4 E and F). However, since the steady state levels of Cox1p and Cox2p were similarly decreased in Aac2^{A137D} mitochondria with or without the minor Aac isoforms (Figure 2.3), it is unlikely that the stability of newly translated Cox1p and Cox2p significantly contributes to their reduced steady state levels. Instead, their translation appears to correlate more strongly with their final steady state abundance. In contrast, the stability of freshly translated Cox3p was decreased in Aac2^{A137D} mitochondria regardless of the presence of the minor Aac isoforms (Figure 2.4G). Surprisingly, the stability of newly translated Atp6p was increased when Aac2p function was lacking (Figure 2.4H). An increased translation of Atp6p (Figure 2.4A) combined with an enhanced stability of newly made polypeptide (Figure 2.4H) would be expected to result in increased steady state Atp6p levels, something that was not observed (Figure 2.2). Finally, in the presence, but not the absence, of the minor Aac isoforms, the turnover of Cob1p and Var1p was modestly but significantly increased when Aac2p is missing (*aac2*Δ) (Figure 2.4 I and J).

Overall, our results indicate that when Aac2p function is absent, mitochondrial translation is dysregulated such that the production of the complex IV subunits Cox1p and Cox2p, and the complex V subunits Atp6p and Atp9p, is decreased and increased, respectively. Further, our data suggest that the relatively lower steady state levels of mtDNA-encoded complex IV subunits in *aac2*^{A137D} versus *aac2*Δ mitochondria (Figure 2.3) may stem in part from a reduced stability of newly translated Cox3p in the former (Figure 2.4G).

Import and assembly of nuclear encoded subunits of cytochrome *c* oxidase is not disturbed in the absence of Aac2p function

The assembly of complexes III, IV, and V in yeast involves the coordinated incorporation of proteins from two genomes, and for the two respiratory complexes, the complement of prosthetic groups that endow them with the ability to move electrons. Current evidence suggests that the three mtDNA-encoded COX subunits form three independent modules of distinct composition (McStay, Su, Thomas, Xu, & Tzagoloff, 2013; McStay, Su, & Tzagoloff, 2013; Su, McStay, & Tzagoloff, 2014). The assembly of these modules is closely monitored and tightly regulated. For example, Mss51p is a Cox1p translational activator that additionally functions as a chaperone that physically stabilizes nascent Cox1p (Barrientos, Korr, & Tzagoloff, 2002; Mick et al., 2010; Perez-Martinez, Broadley, & Fox, 2003; Siep, van Oosterum, Neufeglise, van der Spek, & Grivell, 2000). When functioning as a chaperone, Mss51p is unable to act as a Cox1p translational enhancer. As such, Cox1p synthesis is directly linked to the fidelity of its assembly. The complex IV holoenzyme is generated by the association of the three fully assembled modules and any remaining subunits.

Since a defect in complex IV assembly can negatively feedback to reduce mitochondrial translation of complex IV subunits (Barrientos, Zambrano, & Tzagoloff, 2004; Perez-Martinez et al., 2003; Soto, Fontanesi, Liu, & Barrientos, 2012; Towpik, 2005), we reasoned that Aac2p function may be specifically important for the assembly of complex IV. To test this model, we compared the incorporation of newly imported subunits into complex IV and complex IV-containing supercomplexes in mitochondria that contain or lack Aac2p activity (Brandner et al., 2005). To monitor multiple stages of complex IV

assembly, we followed the import and assembly of radiolabeled Cox5Ap and Cox13p, which are integrated into the Cox1p (McStay, Su, Thomas, et al., 2013; McStay, Su, & Tzagoloff, 2013) and Cox3p (Su et al., 2014) modules, respectively (Figure 2.5A). Both precursors were imported into isolated mitochondria in a time and membrane-potential dependent manner regardless of the presence or absence of Aac2p function (Figure 2.5B and C). Further, their incorporation into complex IV and complex IV-containing respiratory supercomplexes was not impacted by the absence of Aac2p transport (Figure 2.5D and E). Interestingly, the incorporation of radiolabeled Cox5Ap into complex IV-containing complexes was increased in *aac2*Δ mitochondria compared to mitochondria expressing either transport-active or transport-inactive Aac2p. While the basis for this observation is presently unclear, it is unlikely to reflect reduced steady state levels of Cox5Ap which were normal in *aac2*Δ mitochondria (Figure 2.2E).

Altered mitochondrial translation in the absence of Aac2p function is reversible

Mss51p, a specific translational activator of *COX1* mRNA, is involved in complex IV biogenesis by regulating the synthesis of Cox1p (Siep et al., 2000). When Mss51p is trapped in a complex consisting of unassembled Cox1p and other proteins it is prevented from enhancing Cox1p translation (Barrientos et al., 2004; Fontanesi, Clemente, & Barrientos, 2011; Perez-Martinez et al., 2003; Perez-Martinez, Butler, Shingu-Vazquez, & Fox, 2009). Unlike its translational target and subsequent client Cox1p, Mss51p accumulated normally in the absence of Aac2p activity (Figure 2.6A). Next, the ability of overexpressed Mss51p to rescue mitochondrial protein synthesis in the absence of Aac2p function was determined (Figure 2.6B). However, mitochondrial translation was not altered when Mss51p was overexpressed regardless of the presence or absence of Aac2p

function (Figure 2.6B and 2.12A). These results indicate that the availability of Mss51p to serve as a *COX1* translational activator is not limiting in the absence of Aac2p activity. As such, the reduced translation of complex IV subunits that occurs when Aac2p function is missing does not derive from any changes in Mss51p expression and function.

Aim23p or mIF3p (mitochondrial translation initiation factor 3), the *Saccharomyces cerevisiae* homolog of the bacterial translation initiation factor 3 (IF3), has conserved and overlapping functions with human mIF3p (Atkinson et al., 2012; Kuzmenko et al., 2014). Translation initiation factors act at a critical point between the first (translation initiation) and last (ribosomal recycling) steps of the translational cycle, ensuring correct tRNA and mRNA selection; however, unlike translational activators, translation initiation factors do not directly interact with mRNAs (Kuzmenko et al., 2014). Aim23p disruption results in disturbed mitochondrial translation (Kuzmenko et al., 2016), similar to what we have observed in the absence of Aac2p function (Figure 2.3). As such, we investigated whether Aim23p is involved in the abnormal mitochondrial translation detected in absence of Aac2p function. However, not only was its steady state abundance normal in the absence of Aac2p activity (Figure 2.6C), overexpression of Aim23p failed to improve the Aac2p-related mitochondrial translation defect (Figure 2.6D and 2.12B). Thus, it would appear that the altered mitochondrial translation in the absence of Aim23p or Aac2p are mechanistically unrelated.

As a control, we determined the ability of overexpressed WT Aac2p to rescue the translational impairment that occurs when Aac2p function is absent. As expected, re-introduction of Aac2p increased the translation of mitochondrial encoded subunits of

complex IV (Figure 2.6, B and D) and restored their steady state amounts (Figure 2.12C) in both *aac2*Δ and *aac2*^{A137D} yeast.

Acute Aac2p inhibition alters mitochondrial translation

To gain further insight into how Aac2p function promotes normal mitochondrial translation, we asked whether acute inhibition of Aac2p activity using the membrane permeable Aac2p inhibitor, bongkrekic acid (BKA), could prevent the rescued translation of complex IV subunits provided by overexpressed WT Aac2p. Indeed, the increased translation of complex IV subunits was prevented by the inclusion of BKA in the context of either *aac2*^{A137D} rescued with overexpressed Aac2p (Figure 2.7 A and B) or the WT strain with endogenous or overexpressed Aac2p (Figure 2.7 C and D). Since this effect occurred after only 10 min of Aac2p inhibition, this suggests that the altered mitochondrial translation detected upon genetic inactivation of Aac2p function does not stem from compensatory processes and instead reflects a direct functional link between Aac2p mediated transport and normal mitochondrial translation.

Acute Aac2p inhibition reduces the stability of nascent Cox3p

The stability of nascent Cox3p was specifically decreased in Aac2^{A137D} mitochondria (Figure 2.4G). Since inhibition of WT Aac2p with BKA results in a protein that is expressed but non-functional, similar to Aac2^{A137D}, we determined if acute Aac2p inhibition also increases the turnover of newly translated Cox3p. We initially performed a series of experiments using *aac2*^{A137D} rescued with overexpressed Aac2p, with empty vector transformed WT and *aac2*^{A137D} yeast serving as controls (Figure 2.13). Surprisingly, the stability of Cox3p was unaffected by BKA in any of the tested strains (Figure 2.13E). However, the turnover of Cox3p was notably different in untransformed (Figure 2.4G)

versus empty vector (EV)-transformed WT yeast (Figure 2.13E). To determine if these discrepant results stem from the different media employed (e.g. rich media versus minimal auxotrophic selection media), we compared WT and *aac2*^{A137D} strains with/without empty vector, grown in either rich or synthetic media lacking leucine. Indeed, total translation of mtDNA was decreased in the EV-transformed strains compared to their untransformed relatives (Figure 2.14A). Further, Cox3p stability notably differed in the untransformed versus the EV-transformed WT strain (Figure 2.14E); Cox3p was notably more stable in the untransformed WT strain. These results indicate that both mtDNA translation and the stability of its newly produced polypeptides is sensitive to either the growth conditions used and/or the presence of an episomal plasmid.

Therefore, we asked if acute Aac2p inhibition with BKA increases the turnover of nascent Cox3p in untransformed WT and *aac2*^{A137D} yeast (Figure 2.8). Indeed, BKA treatment enhanced the turnover of Cox3p in the WT strain expressing endogenous Aac2p, although its rate of degradation was not as fast as in *aac2*^{A137D} yeast (Figure 2.8E). As expected, BKA treatment did not further increase the turnover of Cox3p in *aac2*^{A137D} yeast. The stability of other newly translated proteins was unaffected by acute Aac2p inhibition except for Atp6p, whose turnover was modestly increased in BKA-treated WT yeast (Figure 2.8 C-H). These results demonstrate that the stability of nascent Cox3p is dependent on Aac2p transport activity.

DISCUSSION

Consistent with its role as the main conduit for ADP and ATP across the inner membrane, yeast lacking Aac2p activity, due to gene deletion or destabilizing mutations (Heidkämper et al., 1996; Müller et al., 1996; Müller, Heidkämper, Nelson, & Klingenberg, 1997; Nelson, Lawson, Klingenberg, & Douglas, 1993), are unable to grow on respiratory media due to a complete block in OXPHOS (Lawson et al., 1990). What is perhaps surprising is that the absence of Aac2p specifically impairs the function of complex IV, but not complex III (Dienhart & Stuart, 2008) (Figure 2.2 A-D). Potential insight into the underlying mechanism, which has remained unresolved for over twenty years, was provided by the demonstration that Aac2p physically associates with respiratory supercomplexes consisting of complex III and IV (Claypool et al., 2008; Dienhart & Stuart, 2008). The goal of the present study was to determine if complex IV activity is dependent on its physical association with Aac2p or instead Aac2p-mediated ADP/ATP transport. Utilizing a transport-null Aac2p mutant to distinguish between these possibilities, we have established that robust complex IV function requires Aac2p-based transport and not its physical association. In fact, if anything, the transport-null allele, which retained its ability to associate with complex IV-containing supercomplexes, resulted in more severe phenotypes than when Aac2p was completely missing.

How does the absence of Aac2p activity specifically impair complex IV function? Initial insight into the underlying mechanism was that the steady state amount of all three complex IV subunits encoded by the mitochondrial genome was significantly reduced when Aac2p function is missing. As expected, the levels of mtDNA in strains lacking Aac2p function was normal (Kovác et al., 1967). In yeast, mitochondrial transcription can

be regulated by nucleotide levels through the ability of the mitochondrial RNA polymerase, Rpo41p, to sense fluctuations in ATP levels (Amiott & Jaehning, 2006; Asin-Cayuela & Gustafsson, 2007). However, even though the absence of Aac2p activity resulted in altered mitochondrial ADP and ATP levels and a disturbed ADP:ATP ratio, mtDNA transcript levels were not affected, consistent with a prior study (Kucejova, Li, Wang, Giannattasio, & Chen, 2008). While the abundance of mtDNA transcripts was normal in the absence of Aac2p function, their subsequent translation was not. Whereas the synthesis of Cox1-3p was reduced, the translation of mtDNA encoded complex V subunits was increased. Curiously, while the steady state amount of Cox1-3p mirrored their translation, this was not the case for the complex V subunits. Overall, these finding indicate that while mitochondrial translation is not globally impaired by the absence of Aac2p function, it is significantly dysregulated.

One potential explanation for the reduced translation of COX subunits when Aac2p activity is missing is that the assembly of complex IV, which is known to tightly regulate translation of subunits through feedback mechanisms, is impaired. For example, a 15-base pair deletion in human Cox3p which decreases its stability additionally reduces the synthesis and stability of Cox1p and Cox2p and impairs the assembly of complex IV (Hoffbuhr et al., 2000). In yeast, Cox1p synthesis is significantly decreased by mutations in *COX2* or the *COX3* translational activators, *PET54 and PET122*, in a way that appears to be mediated by the assembly status of complex IV (Shingú-Vázquez et al., 2010). However, not only was complex IV assembly normal at steady state, the kinetics of its assembly was the same in the presence or absence of Aac2p function. An assembly defect could lead to accumulation of unassembled polypeptides and/or assembly intermediates

which could become toxic if not resolved. However, deletion of Oma1p, which is involved in the degradation of unassembled subunits of complex IV in certain situations (Bestwick, Khalimonchuk, Pierrel, & Winge, 2010; Khalimonchuk, Jeong, Watts, Ferris, & Winge, 2012), did not rescue the steady state level of complex IV subunits when Aac2p function is missing (Figure 2.15). In humans, truncating mutations in *COX1* have been shown to destabilize other complex IV subunits via a mechanism that requires the activity of the *m*-AAA protease even though the truncated Cox1p polypeptide is still able to assemble with other complex IV subunits as well as other respiratory complexes (Hornig-Do et al., 2012). Unfortunately, potential roles for the two mitochondrial AAA proteases Yme1p and Yta10p/Yta12p have not been determined since loss of Aac2p function is synthetically lethal with *yme1*Δ (Wang, Salinas, Zuo, Kucejova, & Chen, 2008) and complex IV subunits do not accumulate in the absence of Yta10p/Yta12p (Arlt et al., 1998). These results suggest that the low steady state amounts of mtDNA-encoded complex IV subunits in the absence of Aac2p activity stems from their reduced translation and not to a complex IV assembly defect.

Interestingly, the complex IV-related perturbations were greater in the context of the transport-null Aac2p mutant than when Aac2p was entirely gone. This was not due to compensation by the minor Aac isoforms since the same trend was observed in the presence and absence of Aac1p and Aac3p. Interestingly, the stability of newly translated Cox3p was compromised in yeast expressing the inactive Aac2p mutant but not in yeast lacking Aac2p altogether. Similarly, inhibition of Aac2p with BKA, also specifically increased the turnover of Cox3p in WT yeast. We speculate that the reduced stability of nascent Cox3p may contribute to the more drastic decrease in steady state levels of mtDNA-encoded

complex IV subunits in *aac2*^{A137D} versus *aac2*Δ mitochondria. These results raise the possibility that a high ATP-demanding process exists that is required for the stability of newly made but unassembled Cox3p. Moreover, the increased turnover of nascent Cox3p only occurs when Aac2p is present but non-functional suggesting that Aac2p facilitates the degradation of Cox3p via an activity that is distinct from its role in ADP/ATP exchange. Another potential explanation for the more severe complex IV phenotype of the transport-null Aac2p mutant was based on the identification of Mss51p as a potential Aac2p binding partner (Claypool et al., 2008). If the ability of Mss51p to stimulate *COX1* translation is reduced when bound to Aac2p, then this could in turn help explain the relatively strong *aac2*^{A137D} phenotype. However, since Mss51p overexpression failed to improve *COX1* translation when Aac2p activity was missing, this latter scenario appears unlikely.

The altered pattern of translation we observed is similar to what has been reported for loss of function mutants of the mitochondrial translation initiation factor, Aim23p; the DEAD-box helicase and mitochondrial transcription elongation factor, Mss116p; and the protein subunit of mitochondrial RNase P, Rpm2p, which is involved in mitochondrial RNA processing and mitochondrial translation (De Silva et al., 2017; Kuzmenko et al., 2016; Stribinskis, Gao, Ellis, & Martin, 2001). We wondered if the absence of Aac2p function regulates mitochondrial translation in a way that is dependent on any of these mitochondrial proteins. Focusing on Aim23p, we asked if overexpression of this protein could rescue the impairment of mitochondrial translation that we observed in the absence of Aac2p function. Overexpression of Aim23p and Mss51p did not rescue the translation impairment suggesting that the absence of Aac2p function impacts mitochondrial translation in a way that does not involve either of these two proteins. Surprisingly, the

restored translation of complex IV subunits provided by overexpressed WT Aac2p was completely prevented by the inclusion of the Aac2p inhibitor, BKA. Since the chronic absence of Aac2p function significantly altered the mitochondrial ADP:ATP ratio (Figure 2.1I), these results imply that Aac2p-based transport has an active and direct role in mitochondrial translation that may involve a feedback mechanism that is sensitive to matricial nucleotide levels. Even though some of the regulatory mechanisms that control mitochondrial translation are notably different between yeast and metazoans (Kehrein, Bonnefoy, & Ott, 2013), it will be important to determine if mitochondrial translation in humans is similarly dependent on mitochondrial ADP/ATP transport. If this requirement is conserved, then this could provide novel insight into ANT-associated diseases (Echaniz-Laguna et al., 2012; Fontanesi et al., 2004; Graham et al., 1997; Jordens et al., 2002; Kaukonen et al., 2000; Komaki et al., 2002; Palmieri et al., 2005; Sharer, 2005; Thompson et al., 2016; Vandewalle et al., 2013)

MATERIALS AND METHODS

Yeast strains and growth conditions

All yeast strains used in this study were derived from GA74-1A (*MAT*a, *his3-11,15*, *leu2*, *ura3*, *trp1*, *ade8* [rho^{+}, mit^{+}]). *aac1*Δ::*TRP1* and *aac3*Δ::*HISMX6* were established by replacing the entire open reading frame of the gene using PCR-mediated gene replacement(Wach, Brachat, Pöhlmann, & Philippsen, 1994). *aac1*Δ*aac3*Δ (*MAT*a*, trp1*, *leu2, ura3, ade8, aac1*Δ::*TRP1*, *aac3*Δ::*HISMX6*) was generated from *aac1*Δ (*MAT*a*, his3-11,15, trp1*, *leu2, ura3, ade8, aac1*Δ::*TRP1*). *aac2*Δ, $aac2^{A137D}$, *aac1*Δ*aac3*Δ*aac2*Δ *aac1*Δ*aac3*Δ$aac2^{A137D}$ were generated from WT and *aac1*Δ*aac3*Δ strains using Homology-integrated CRISPR-Cas (HI-CRISPR) system as previously described but with slight modification (Bao et al., 2015; Ogunbona, Onguka, Calzada, & Claypool, 2017). Briefly, the CRISPR-Cas9 target for *AAC2* was selected using the web-based yeastriction (Mans et al., 2015) and Benchling CRISPR guide design tools. The CRISPR construct was designed to recognize residues 542-561 on the reverse strand of *AAC2* (position 1 is the adenine of the AUG site). A 99bp or 250bp homology repair template was designed to have homology arms on both sides flanking the Cas9 cutting site and incorporated an 8bp deletion or point mutations to generate *aac2*Δ and $aac2^{A137D}$, respectively. *oma1*Δ strains were generated from the corresponding parental strains as previously described (Ogunbona et al., 2017).

Cox8p and Qcr10p, subunits of complex IV and III respectively were endogenously tagged in WT, *aac2*Δ, $aac2^{A137D}$ strains on the C-terminal end with 3X FLAG epitope tag using PCR-mediated gene replacement (Wach et al., 1994). *COX5A* and *COX13* genomic sequence were amplified from GA74-1A yeast genomic DNA and cloned into pSP64.

Aac2p, Mss51^{F199I}p and Aim23p were overexpressed under the control of their native promoters in WT, *aac2*Δ, *aac2*^{A137D} strains. *AAC2* and *AIM23* were amplified from genomic DNA isolated from GA74-1A yeast using primers that hybridized approximately 380bp upstream of the predicted start codon and 140bp downstream of the predicted stop codon and cloned into pRS315 and pRS425 respectively. The constitutively active mutant form of *MSS51* (*MSS51*^{F199I}) (Barrientos et al., 2002; De Silva et al., 2017; Fontanesi et al., 2011) was subcloned into pRS425.

Yeast cells were grown in either YP-Sucrose (1% yeast extract, 2% peptone, 2% sucrose), YP-Dextrose (1% yeast extract, 2% peptone, 2% dextrose) or their synthetic (SC) media equivalent (containing 0.17% Yeast Nitrogen base minus amino acids, 0.5% Ammonium sulfate, 0.2% dropout mix containing required amino acids and 2% Sucrose or Dextrose). To assess the respiratory function of the different strains, overnight cultures grown in indicated media were spotted on solid media containing 2% dextrose or ethanol/glycerol (1% ethanol, 3% glycerol) and grown at 30ºC.

Measurement of Ascorbate-TMPD respiration rates

Oxygen consumption rates were measured using a Clark-type oxygen electrode as described before (Claypool et al., 2008), with some modifications. In brief, mitochondria (100 μg) were used as soon as possible after thawing on ice. 1 ml of respiration buffer (0.25 M sucrose, 0.25 mg/ml BSA, 20 mM KCl, 20 mM Tris-Cl, 0.5 mM EDTA, 4 mM KH_2PO_4, and 3 mM $MgCl_2$, pH 7.2) was added to a magnetically stirred 1.5 ml chamber with temperature controlled at 25°C and the signal representing the level of oxygen in the chamber allowed to equilibrate. Following addition of mitochondria, background respiration rate was recorded for about 30 seconds. Next, 1 mM ascorbate and 0.3 mM

TMPD were added simultaneously and the State 2 respiration recorded for 1 minute, before the addition of 50 μM ADP to initiate State 3 respiration. Once the added ADP was consumed, State 4 respiration was recorded for 2 minutes before 10 μM FCCP was added to induce uncoupling. Uncoupled respiration was measured for 2 minutes or until the oxygen level reached zero. As there is no ADP-stimulated respiration in the absence of Aac2p function, the basal respiration (State 2) and uncoupled respiration were calculated.

Spectrophotometric Activity Assay

Respiratory complex III and IV activities were measured as previously described (Dienhart & Stuart, 2008; Lu et al., 2017; Tzagoloff, Akai, & Needleman, 1975). Briefly, 5 μg of mitochondria solubilized in 0.5% (w/v) *n*-dodecyl β-D-maltoside (Anatrace) and spiked with protease inhibitors were added to reaction buffer (50 mM KPi, 2 mM EDTA, pH 7.4) with 0.08% (w/v) equine heart cytochrome *c* (Sigma). For complex III activity measurements, 1 mM KCN (prevents oxidation of cytochrome *c* by complex IV) and 100 μM decylubiquinol (an analog of coenzyme Q) were added before the reaction was initiated. The reduction or oxidation of cytochrome *c* was followed at 550 nm.

Mitochondrial ADP and ATP measurement

Mitochondrial nucleotide levels were measured using ApoSENSOR ADP/ATP bioluminescent assay kit (BioVision) according to the manufacturer's protocol. Briefly, luminescence of each crude mitochondrial sample was measured using a BMG Labtech Fluostar Omega microplate reader in the Luminescence mode. 50 μg of mitochondria were added to a mixture of ATP monitoring enzyme and nucleotide releasing buffer incubated at room temperature in a Greiner Bio-One Black flat-bottomed 96 well plate. To determine ATP level, luminescence values after 2 minutes of adding mitochondrial samples was

corrected by subtracting background luminescence. Thereafter, ADP converting enzyme that converts ADP to ATP was added and the ADP levels were determined as the change in luminescence after the converting enzyme was added.

DNA Extraction and Quantitative Real-time PCR (qPCR)

DNA was extracted as described (Hoffman, 2001). In brief, 15 units of A_{600} yeast cells grown for 24-48 hours in YP-Sucrose media were harvested, washed in sterile water and resuspended in 200 µl of breaking buffer (2% Triton X-100 (w/v), 1% SDS (w/v), 100 mM NaCl, 10 mM Tris pH 8.0, 1 mM EDTA pH 8.0). 0.3 g glass beads (~200-300 µl volume) and 200 µl phenol/chloroform/isoamyl alcohol was added and the tubes sealed with parafilm before vortexing at highest speed for 3 minutes. Next, 200 µl TE buffer pH 8.0 was added and the mixture vortexed briefly before centrifugation at maximum speed at room temperature for 5 minutes. The aqueous phase was then transferred to a new eppendorf tube, 1 ml of 100% ethanol added and then mixed by inversion. This was followed by centrifugation at 21,000 x *g* at room temperature for 3 minutes and the pellets were resuspended in 400 µl Tris-EDTA (TE) buffer, pH 8.0. 3 µl of 10 mg/ml RNAse A was added followed by incubation at 37ºC for 5 minutes before adding 10 µl of 4 M ammonium acetate and 1 ml 100% ethanol. Finally, DNA pellets were recovered by centrifugation at maximum speed at room temperature for 3 minutes, dried, and then resuspended in 30 µl TE buffer pH 8.0. The DNA were quantitated and stored at -80ºC. Prior to the analyses, the DNA was re-quantitated and used at 10 ng/µl as template in the qPCR reaction.

The FastStart Universal SYBR Green Master Rox (Roche) was used for qPCR performed according to the manufacturer's instructions. 50 ng of genomic DNA was used

as template and the following primers were used at 100 nM concentration in a 20 µl reaction: COX1 forward, 5′- CTACAGATACAGCATTTCCAAGA-3′; COX1 reverse, 5′-GTGCCTGAATAGATGATAATGGT-3′; ACT1 forward, 5′-GTATGTGTAAAGCCGGTTTTG-3′; ACT1 reverse, 5′-CATGATACCTTGGTGTCTTGG -3′. The reaction was done in technical duplicate with three biological replicates. No-template controls were included in every assay. After completion of thermocycling cycles in a QuantStudio 6 Flex Real-Time PCR System (Thermo Fisher), melting-curve data were collected to verify PCR specificity and the absence of primer dimers. The Ct value difference between the nuclear (ACT1) and mitochondrial (COX1) target were computed as a measure of the level of mitochondrial DNA copy number relative to nuclear genome. A strain lacking its mitochondrial genome (Rho null) was used as negative control in all experiments.

RNA Extraction and Reverse Transcription Quantitative Real-time PCR (RT-qPCR)

Total RNA was extracted using hot phenol extraction exactly as described (Amin-ul Mannan, Sharma, & Ganesan, 2009) except that yeast cells were grown in YP-Sucrose media. Following treatment with Turbo DNase to remove any contaminating genomic DNA (TURBO DNA-free™ Kit, Invitrogen), RNA was purified using a RNeasy MiniElute Cleanup Kit (Qiagen). 1 µg of RNA was reverse transcribed into cDNA using SuperScript™ VILO™ Master Mix (Invitrogen) according to the manufacturer's protocol. The qPCR was done as described above but using a 1:10 dilution of synthesized cDNA as template instead of genomic DNA. Additionally, we performed a minus-RT control, i.e. RNA not reverse-transcribed to cDNA to verify the absence of contaminating genomic DNA in RNA samples, in addition to a no-template control. TAF10 was used as a reference

gene (Teste, Duquenne, François, & Parrou, 2009). The primers used are TAF10 forward, 5′- ATATTCCAGGATCAGGTCTTCCGTAGC -3′, TAF10 reverse, 5′- GTAGTCTTCTCATTCTGTTGATGTTGTTGTTG -3′; COX1 forward, 5′- TGCCTGCTTTAATTGGAGGT -3′, COX1 reverse, 5′- GGTCCTGAATGTGCCTGAAT -3′; COX2 forward, 5′- TTCAGGATTCAGCAACACCA -3′; COX2 reverse, 5′- CAGCTGGAAAAATTGTTCAAATA -3′; COX3 forward, 5′- TCTTTGCTGGTTTATTCTGAGC -3′; COX3 reverse, 5′- CTGCGATTAAGGCATGATGA -3′; ATP6 forward, 5′- CCTGCTGGTACACCATTACC -3′; ATP6 reverse, 5′- AGCCCAGACATATCCCTGAA -3′; ATP9 forward, 5′- TTGGAGCAGGTATCTCAACAAT -3′; ATP9 reverse, 5′- GCTTCTGATAAGGCGAAACC -3′. The Ct values difference between the reference gene (nuclear encoded TAF10) and the mitochondrial targets were computed as a measure of the steady state mRNA levels in the strains. A strain lacking its mitochondrial genome (Rho null) was used as negative control in all experiments.

In Vivo Labeling of Mitochondrial Translation Products

Yeast cells pre-cultured overnight in either YP-Sucrose (1% yeast extract, 2% peptone, 2% sucrose) or when strains are maintaining plasmids, synthetic media (containing 0.17% Yeast Nitrogen base minus amino acids, 0.5% Ammonium sulfate, 0.2% dropout mix containing amino acids except Leucine, and 2% Sucrose) were re-inoculated and grown to an A_{600} of 0.4-1. Yeast cells were labeled, prepared, and resolved by SDS-PAGE as done before (Barrientos et al., 2002) with little modification. In brief, 3.2 units of A_{600} yeast cells were washed with 2 ml of metabolic labeling buffer (40 mM KPi, pH 6.0, 2% Sucrose, 2 g/L SC-Methionine) once and then incubated in the buffer for 5 minutes to allow

completion of in-progress translation. For BKA inhibition, the pH of the labeling buffer was adjusted to 5.0 with diluted HCl and BKA was added at 10 μM concentration. 0.2 mg/ml of freshly prepared cycloheximide was then added to stop cytoplasmic translation, followed by the addition of 62 μCi/ml Trans ^{35}S-Label (sku 015100907 MP Biomedical; 85% Methionine and 15% Cysteine). Labeling was performed at 30ºC in a water bath for up to 20 minutes. A mixture of non-radioactive 24.2 μM methionine and Cysteine (with 4 μg/ml Puromycin in the chase) was added to stop the radiolabeling. After different time points, 0.5 ml aliquots were collected, processed in freshly prepared diluted Rodel buffer (0.24 M NaOH, 0.14 M 2-Mercaptoethanol, 1.3 mM phenylmethylsulfonyl fluoride) on ice, and then tricarboxylic acid (TCA)-precipitated. Recovered pellets were washed first with 500 mM Tris base and then with distilled water. The final pellet samples were resuspended in a 1:1 mixture of 0.1 M NaOH:2X reducing sample buffer and resolved on custom-made 17.5% SDS-PAGE (Barrientos et al., 2002) and/or 12-16% SDS-PAGE gels (the former as first described (Barrientos et al., 2002) gave better separation of all the mitochondrial proteins except Atp8p and Atp9p; however, using 2X more of Ammonium persulfate [APS] and N,N,N',N'-tetramethylethane-1,2-diamine [TEMED] i.e. 0.098% w/v and 0.071% v/v respectively, gave a 17.5% SDS-PAGE that provided for resolution of all the mitochondrial proteins as seen in Figures 2.7 C and E, 2.8A, 2.13A and 2.14A). Gels were stained with commassie, destained, dried, and separated radiolabeled proteins visualized by autoradiography.

In organello import

This was done as described before (Brandner et al., 2005; Ogunbona et al., 2017) with little modification. In brief, radiolabeled Cox5Ap and Cox13p precursors were synthesized in a

coupled transcription/translation reaction (Promega TNT Kit Mix) using 104 µCi of Easy-Tag L-[^{35}S] methionine (PerkinElmer Life Sciences) and 5.2 µg of plasmid in a 260 µl reaction volume. Mitochondria (180 µg) were added to import buffer (0.6 M Sorbitol, 2 mM KH_2PO_4, 60 mM KCl, 50 mM HEPES, 10 mM $MgCl_2$, 2.5 mM EDTA pH 8.0, 5 mM L-Methionine, 10 mg/mL Fatty Acid free BSA) containing 2 mM ATP, 2 mM NADH and an energy-regenerating system (0.1 mg/ml Creatine Phosphokinase, 1 mM Creatine phosphate, 10 mM Succinate). Where indicated, the mitochondrial membrane potential was collapsed with 1 µM valinomycin and 5 µM carbonyl cyanide *m*-chlorophenyl hydrazine. Following addition of the radiolabeled precursor, import reactions were incubated at 30ºC. At the designated timepoints, import was stopped with an equal volume of ice-cold BB7.4 (0.6 M sorbitol and 20 mM HEPES-KOH, pH 7.4) that contained 40 µg/ml of trypsin to degrade non-imported precursors. After at least 30 minutes on ice, 100 µg/ml of soybean trypsin inhibitor was added to each reaction which were then split into two equal portions. To monitor import, mitochondria were recovered by spinning at 21,000 × *g* for 5 min at 4°C and resolved on 15% SDS-PAGE gels. To monitor assembly, the re-isolated mitochondria were solubilized in lysis buffer (1% (w/v) digitonin, 20 mM HEPE-KOH, pH 7.4, 100 mM NaCl, 20 mM Imidazole, 1 mM $CaCl_2$, 10% glycerol, 1 mM PMSF, 10 µM leupeptin, 2 µM pepstatin A) and resolved on 5-12% blue native-PAGE gels. Relative to each timempoint, 5% of imported precursors were resolved on 15% SDS-PAGE gels. Radioactive bands were visualized by phosphorimaging.

Antibodies

Most antibodies used in this study were generated in our laboratory or in the laboratories of J. Schatz (University of Basel, Basel, Switzerland) or C. Koehler (UCLA) and have been

described previously (Claypool, Whited, Srijumnong, Han, & Koehler, 2011; Hwang, Claypool, Leuenberger, Tienson, & Koehler, 2007; Ogunbona et al., 2017; Onguka, Calzada, Ogunbona, & Claypool, 2015; Whited, Baile, Currier, & Claypool, 2013). Other antibodies used were rabbit polyclonal against Atp4p (Dienhart & Stuart, 2008), Atp6p/Atp9p(Kabala, Lasserre, Ackerman, di Rago, & Kucharczyk, 2014), Mss51p(Barrientos et al., 2002), Cox5Ap(Liu & Barrientos, 2013), Qcr7p(Hildenbeutel et al., 2014) and Aim23p(Kuzmenko et al., 2016).

Miscellaneous

Isolation of mitochondria, 1D BN-PAGE, co-immunoprecipitation and immunoblotting were performed as previously described (Claypool, Dickinson, Yoshida, Lencer, & Blumberg, 2002; Claypool, McCaffery, & Koehler, 2006; Claypool et al., 2011; Ogunbona et al., 2017; Onguka et al., 2015). Band densitometry analyses were performed using Quantity One (Bio-Rad). Statistical comparisons were performed by using one or two-way analysis of variance (ANOVA) with Dunnett test correction (Sidak's test correction for data shown in Figures 2.8 C-H and 2.13 C-H) for multiple comparison in Prism 7 (GraphPad); $P \leq 0.05$ were deemed significant (ns $P > 0.05$; * $P \leq 0.05$; ** $P \leq 0.01$; *** $P \leq 0.001$; **** $P \leq 0.0001$). All graphs show the mean ± SEM.

ACKNOWLEDGEMENTS

We would like to thank Drs. Carla Koehler (UCLA), Antoni Barrientos (University of Miami), Jean-Paul Lasserre (University of Bordeaux), Alexander Tzagoloff (Columbia University), Martin Ott (Stockholm University) and Rosemary Stuart (Marquette University) for generous gift of antibodies, and Dr Flavia Fontanesi (University of Miami) for the gift of Mss51 plasmid. This work was supported by the National Institutes of Health grants (R01HL108882) to S.M.C and Biochemistry, Cellular, and Molecular Biology Program Training Grant (T32GM007445) to M.G.B and and pre-doctoral fellowships from the American Heart Association (15PRE24480066) to O.B.O and (10PRE3280013) to M.G.B. The authors declare no competing financial interests.

AUTHOR CONTRIBUTIONS

O.B.O, M.G.B., and S.M.C. designed and performed research; O.B.O and S.M.C. wrote the paper which was edited by M.G.B.

FIGURES

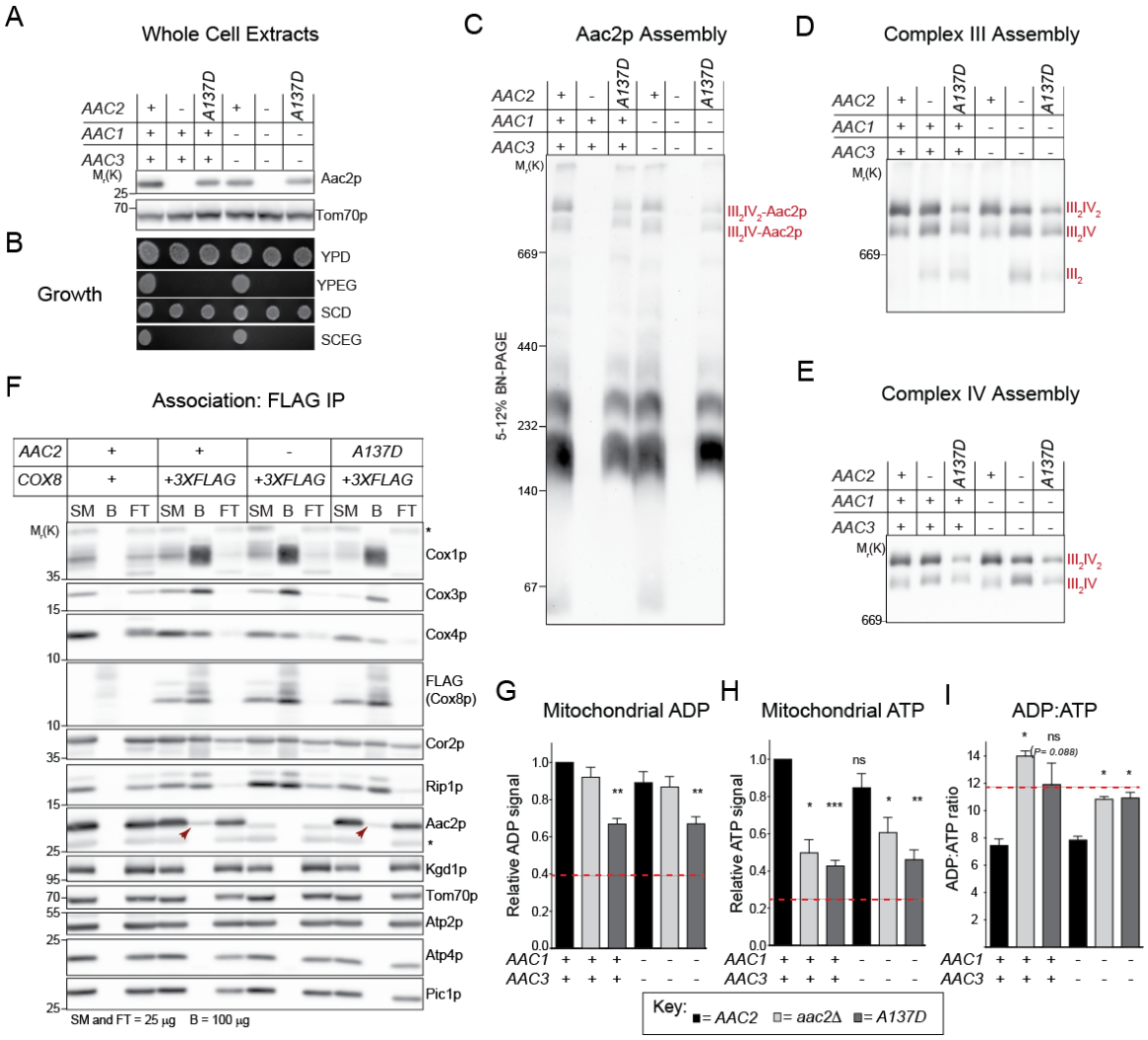

Figure 2.1. A non-functional Aac2p mutant is expressed and assembled normally. (A) Whole cell extracts from the indicated yeast strains were resolved by SDS-PAGE and immunoblotted for Aac2p. (B) Growth of the indicated strains on dextrose or ethanol-glycerol media at 30ºC for 3 days. n=3. (C) – (E) Mitochondria (50 µg protein) solubilized in 1.5% (w/v) digitonin were resolved by 5-12% 1D Blue Native (BN)–PAGE and (C) Aac2p, (D) complex III (Rip1p) and (E) complex IV (Cox4p) detected by immunoblot. n=3. (F) Following solubilization with 1.5% (w/v) digitonin, anti-FLAG resin was used to

immunoprecipitate Cox8-3XFLAG (subunit of complex IV) and the presence of co-purified respiratory supercomplex subunits determined by immunoblot; Kgd1p and Tom70p served as controls. SM, starting material; B, bound material; FT, non-binding flow through. n=3. *, non-specific bands. (G) ADP and (H) ATP levels in mitochondria. Luminescence values relative to wild type are shown. (I) Calculated mitochondrial ADP:ATP ratios. Mean ± SEM, n=4. Statistical difference relative to wild type is shown. The red dotted line refers to the values in a strain lacking mtDNA (rho null).

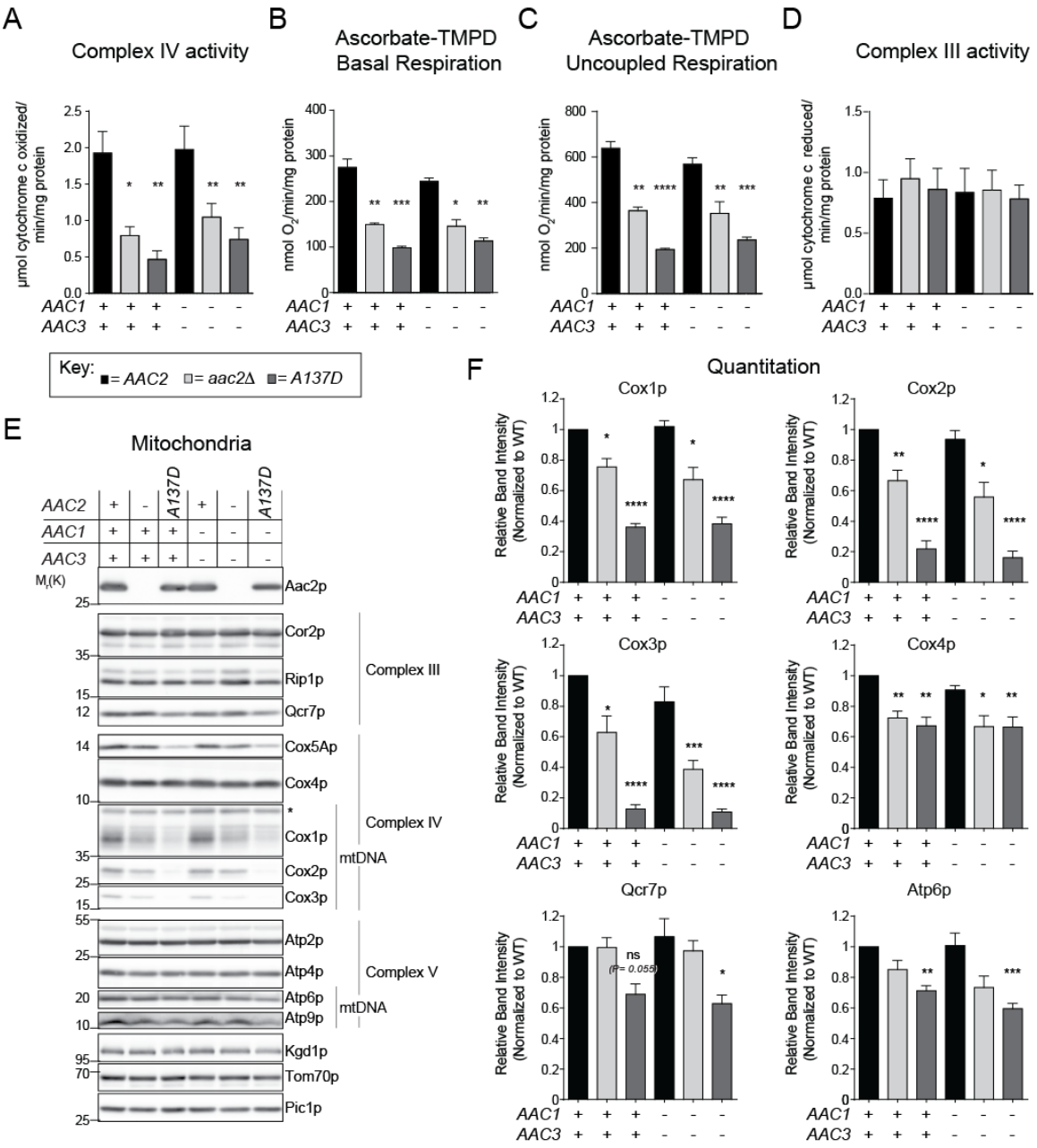

Figure 2.2. Oxidative phosphorylation is impaired in the absence of Aac2p function. (A) Spectrophotometric measurement of complex IV activity in DDM-solubilized mitochondria. Mean ± SEM, n=6. (B) Basal and (C) uncoupled respiration (+CCCP) in intact mitochondria using ascorbate + TMPD (donate electrons to complex IV) as substrate. Mean ± SEM, n=6. (D) Spectrophotometric measurement of complex III activity in DDM-solubilized mitochondria. Mean ± SEM, n=6. (E) Mitochondrial extracts were resolved by

SDS-PAGE and immunoblotted for various mitochondrial proteins- Kgd1p (matrix), Tom70p (outer membrane), Atp2p/Atp4p/Atp6p/Atp9p (Complex V), Pic1p (phosphate carrier) Cor2p/Rip1p/Qcr7p (Complex III), Cox1-4p/Cox5Ap (Complex IV), and Aac2p; *, non-specific band (F) Steady state levels of Cox1-4p, Qcr7p and Atp6p relative to WT were quantified. Mean ± SEM, n≥4. Statistical difference relative to wild type is shown for significant comparisons.

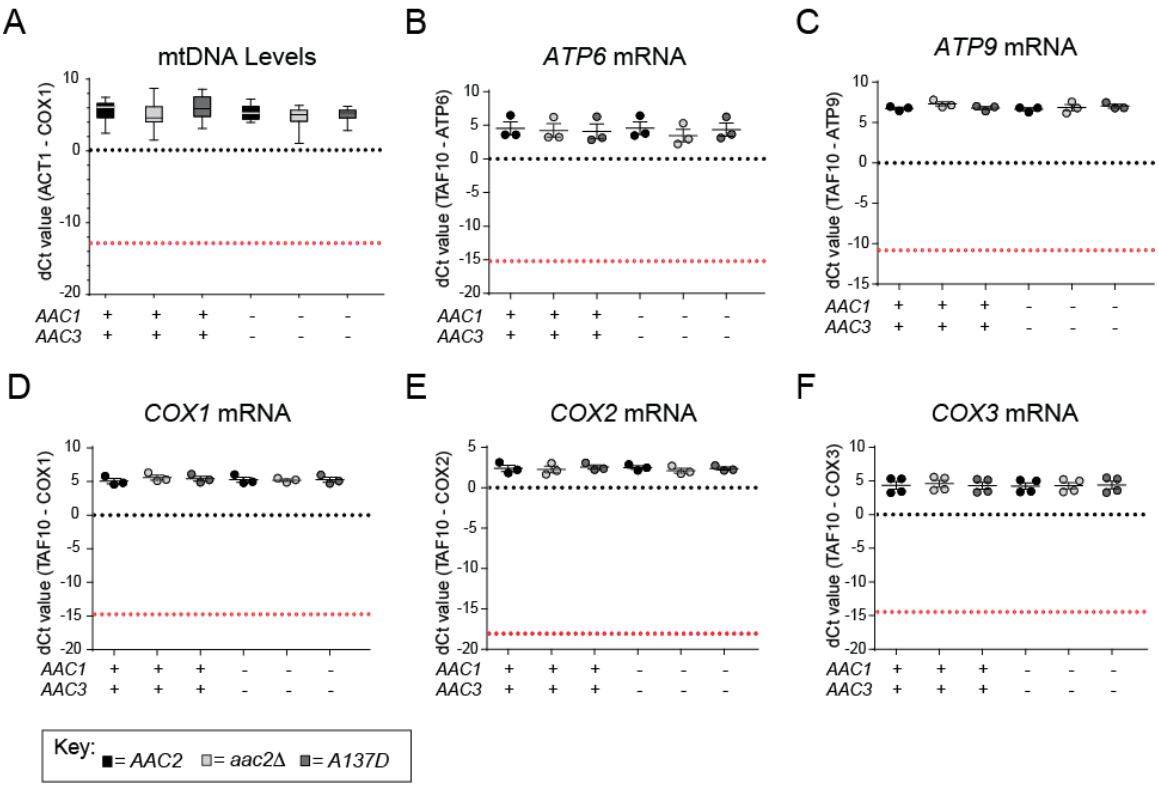

Figure 2.3. The regulation of mitochondrial genome encoded subunits of cytochrome *c* oxidase by Aac2p activity is post-transcriptional. (A) Boxplots showing mtDNA level in the indicated strains determined by quantitative polymerase chain reaction (qPCR) of COX1 in mtDNA and normalized to ACT1 in the nucleus. Whiskers represent 5th and 95th percentile. n=12 (B)–(F) Interleaved scatterplot showing the steady state transcript levels of mtDNA-encoded subunits determined by two step reverse transcription-quantitative PCR for Complex IV (COX1-3) and Complex V (ATP6, ATP9) subunits. TAF10 is a nuclear encoded reference gene. n≥3. The red dotted line refers to the calculated dCt values in a strain lacking mtDNA (rho null).

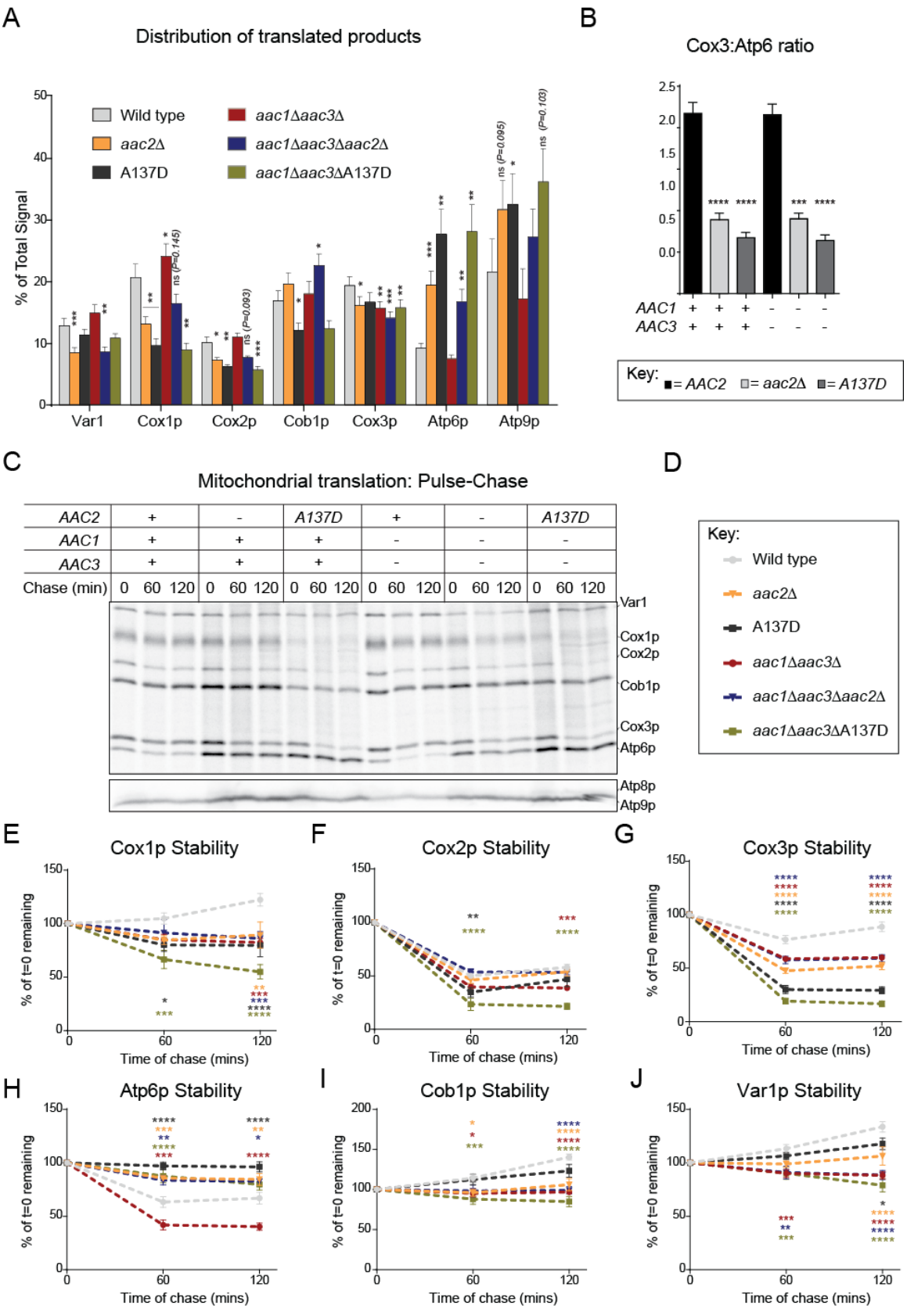
A
Distribution of translated products
% of Total Signal
Wild type
aac2Δ
A137D
aac1Δaac3Δ
aac1Δaac3Δaac2Δ
aac1Δaac3ΔA137D
Var1
Cox1p
Cox2p
Cob1p
Cox3p
Atp6p
Atp9p
B
Cox3:Atp6 ratio
AAC1
AAC3
Key: = AAC2 = aac2Δ = A137D
C
Mitochondrial translation: Pulse-Chase
AAC2
AAC1
AAC3
Chase (min)
Atp8p
D
Key:
Wild type
aac2Δ
A137D
aac1Δaac3Δ
aac1Δaac3Δaac2Δ
aac1Δaac3ΔA137D
E
Cox1p Stability
F
Cox2p Stability
G
Cox3p Stability
H
Atp6p Stability
I
Cob1p Stability
J
Var1p Stability
% of t=0 remaining
Time of chase (mins)

Figure 2.4. Aberrant mitochondrial translation in the absence of Aac2p function. (A) Yeast cultures were spiked with 62 µCi/ml 35S-methionine/cysteine and 0.2 mg/ml cycloheximide to inhibit cytosolic translation. After 10 and 20 minutes incubation at 30ºC, extracts were harvested, resolved by 12-16% SDS-PAGE (Figure 2.11A), and bands identified by phosphoimaging. The distribution of signals from all the mitochondrial encoded translated proteins is expressed as a percentage of the total signal for each experiment. Mean ± SEM, n=10 for everything (this includes the t=0 timepoints presented in the pulse-chase experiments in (C) except Atp9p, n=5). Only statistically significant comparisons relative to WT are displayed. (B) The ratio of Cox3p to Atp6p signals was quantitated. Mean ± SEM, n=10. (C) After 20 mins of pulse, 4 µg/ml puromycin and 24.2 µM methionine/cysteine were added and samples collected at t=0 and after 60 and 120 minutes of chase. Extracts were resolved on 17.5% (top) and 12-16% (bottom) SDS-PAGE, and bands identified by phosphoimaging. n=5. (D) Key for quantitations presented in (E)-(J). The relative signal for mitochondrial translated products in the pulse-chase experiment was quantified taking the signal at t=0 as 100%. Mean ± SEM, n=5. Significant differences of the percent remaining at t=60 and 120 minutes relative to wild type is shown.

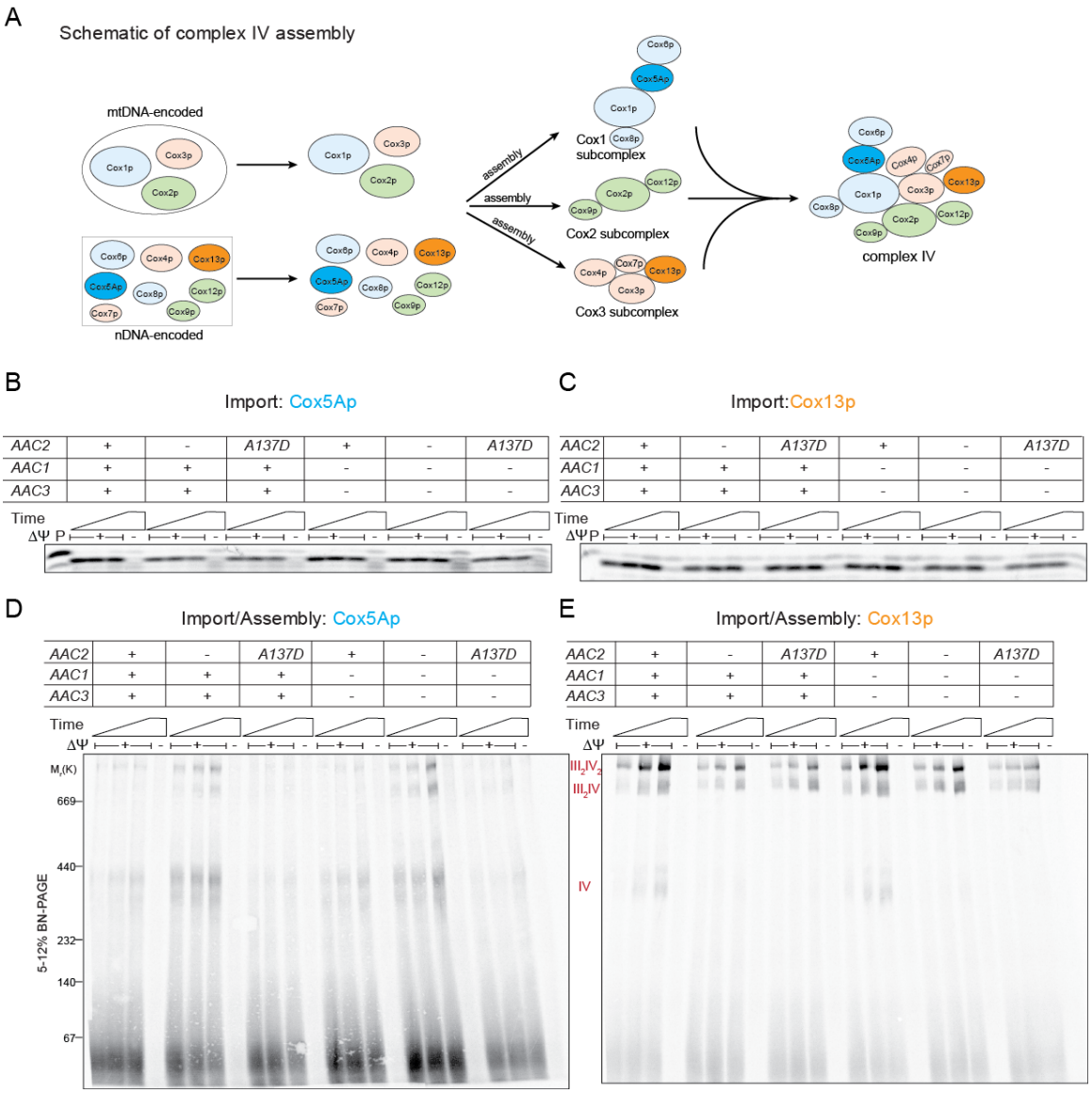

Figure 2.5. Assembly of cytochrome *c* oxidase is not impaired in the absence of Aac2p function. (A) Schematic of complex IV assembly (McStay et al., 2013a; McStay et al., 2013b; Su et al., 2014). An early assembly intermediate centered around Cox1p contains Cox5Ap. Cox13p is incorporated in the Cox3p-assembly module that is added later in the assembly process. Radiolabeled Cox5Ap (B and D) or Cox13p (C and E) was incubated with mitochondria from the indicated strains at 30°C and in the presence (+ΔΨ) or absence (-ΔΨ) of the electrochemical gradient across the inner membrane. Following incubation

for 5, 15, or45 minutes, non-imported precursors were removed with trypsin and the recovered mitochondria were resolved by 15% SDS-PAGE to monitor import (B and C) or solubilized in 1% (w/v) digitonin and resolved by BN–PAGE (D and E) to follow assembly post-import. Bands were identified by phosphoimaging. n=3. P, precursor (5% of each timepoint).

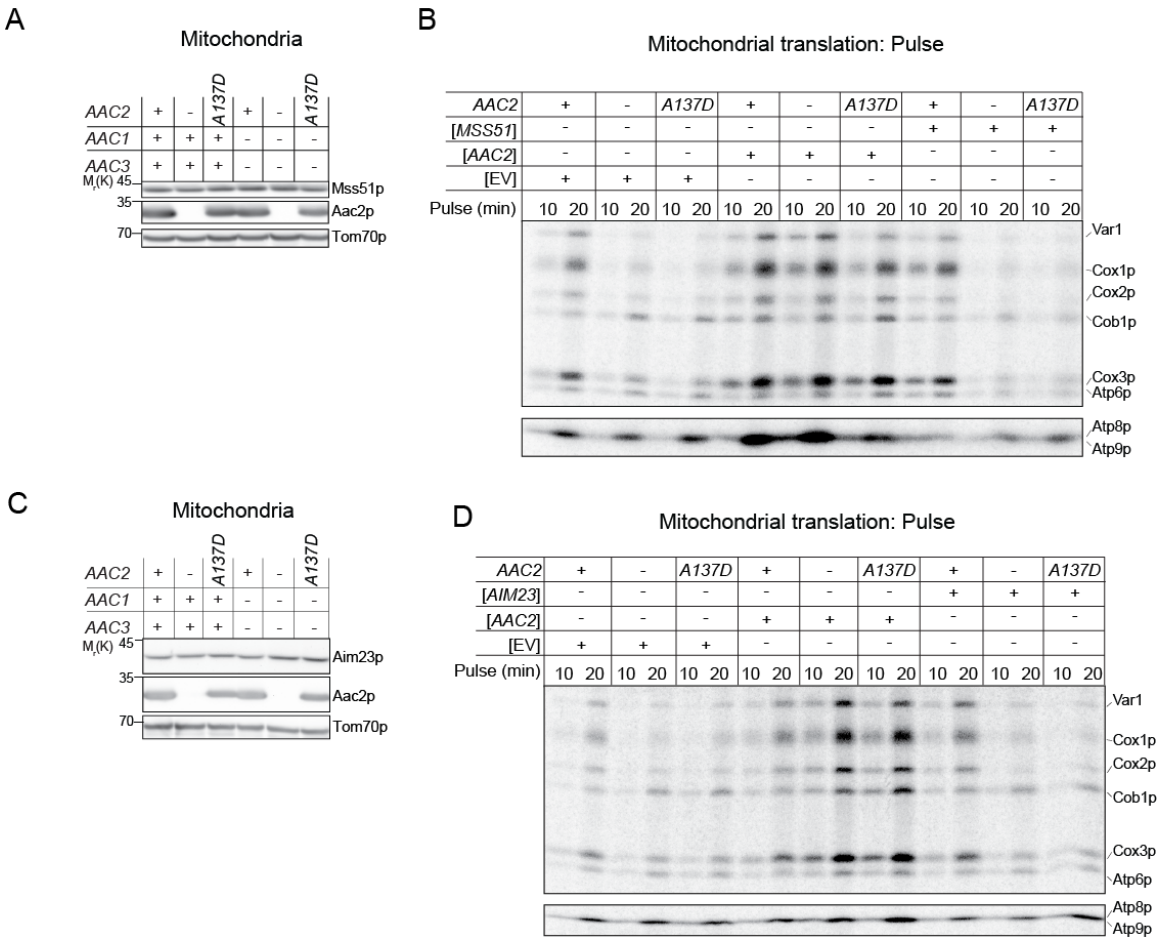

Figure 2.6. **Alteration of mitochondrial translation is rescued by overexpression of Aac2p.** (A) Mitochondrial extracts (50 µg) were resolved by SDS-PAGE and immunoblotted for Mss51p (translational activator for the COX1 mRNA) and Aac2p. n=6. (B) Mitochondrial translation was performed as in Figure 2.4. After 10 and 20 minutes incubation at 30°C, extracts were harvested, resolved by 17.5% SDS-PAGE, and bands identified by phosphoimaging. n=3. (C) Mitochondrial extracts (50 µg) were resolved by SDS-PAGE and immunoblotted for Aim23p (mitochondrial translation initiation factor) and Aac2p. n=4. (D) Mitochondrial translation after 10 and 20 minutes incubation. Following resolution by 17.5% SDS-PAGE, bands were identified by phosphoimaging. n=3.

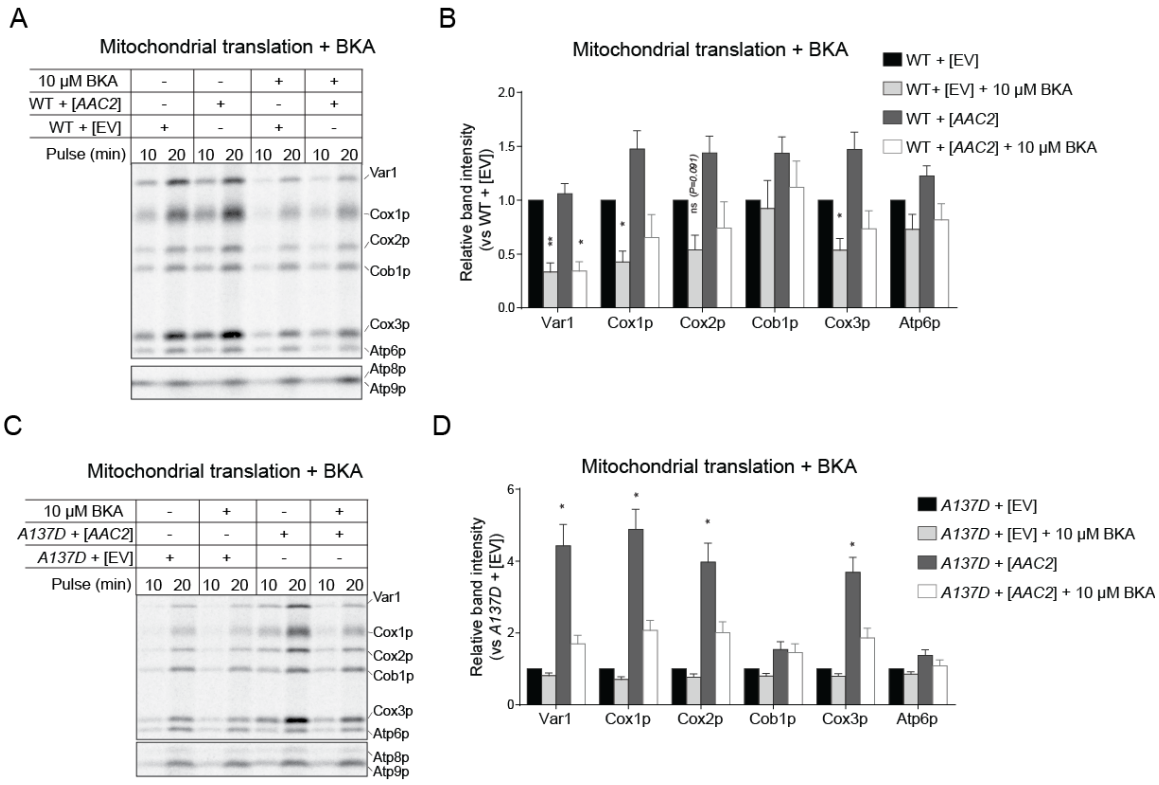

Figure 2.7. Mitochondrial translation is altered by acute Aac2p inhibition. (A) Mitochondrial translation was performed in the absence or presence of 10 µM BKA. Samples were harvested after 10 and 20 minutes of incubation, resolved by 17.5% SDS-PAGE, and bands identified by phosphoimaging. (B) The relative band intensities for the translated mitochondrial polypeptides in (A) were quantified and expressed as a ratio compared to the signal detected in the *A137D* strain transformed with empty vector (EV) in the absence of BKA. Mean ± SEM, n=4. Only statistically significant differences relative to *A137D* + [EV] in absence of BKA are displayed. (C) Mitochondrial translation was performed in the absence or presence of 10 µM BKA. Samples were harvested after 10 and 20 minutes incubation, resolved by 17.5% SDS-PAGE, and bands identified by phosphoimaging. (D) The relative band intensities for the translated mitochondrial polypeptides in (C) were quantified and expressed as a ratio compared to the signal

detected in the WT strain transformed with empty vector in the absence of BKA. Mean ± SEM, n=4. Only statistically significant differences relative to WT + [EV] in absence of BKA are displayed.

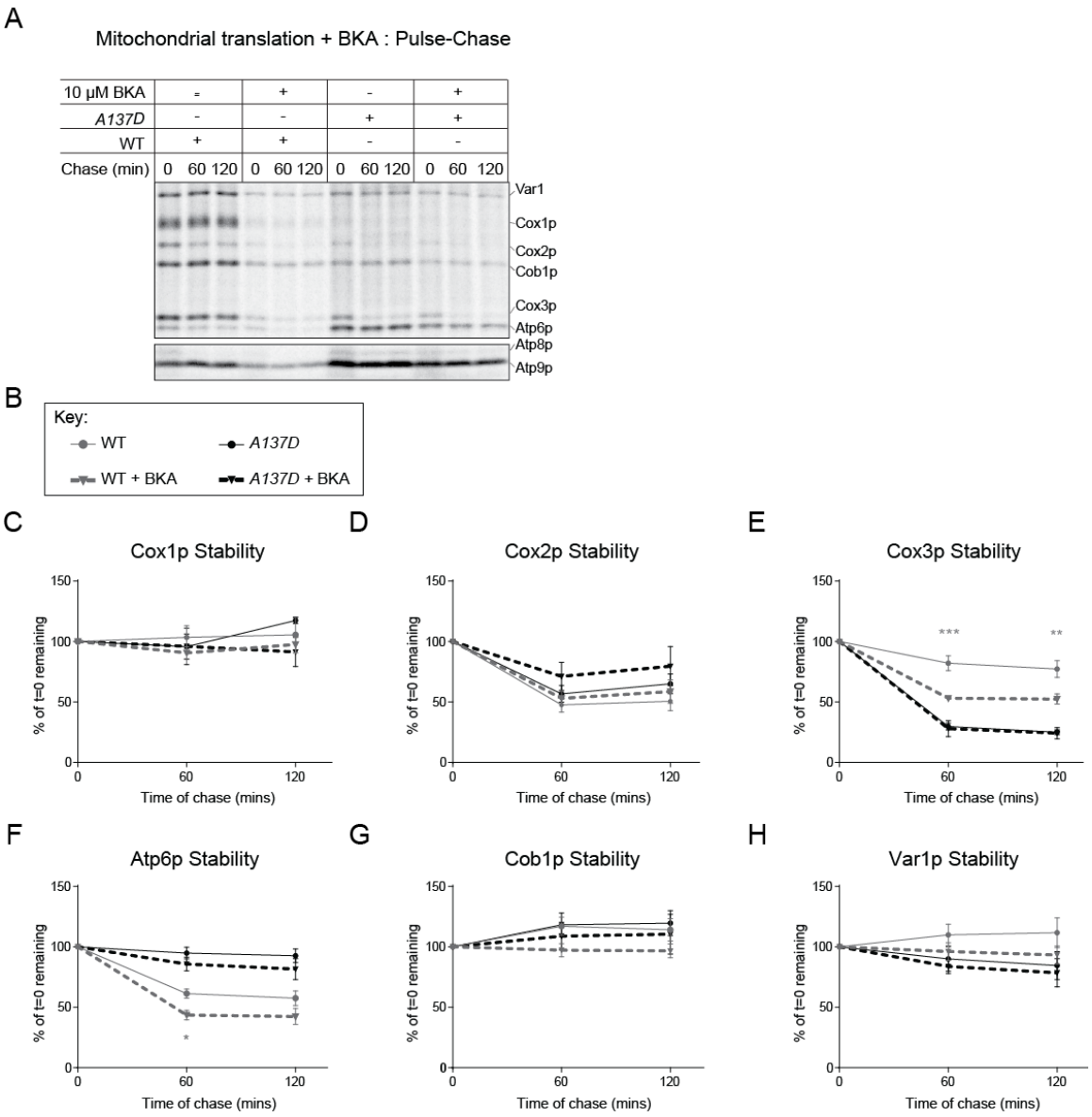

Figure 2.8. The stability of nascent Cox3p is reduced by acute Aac2p inhibition. (A) Mitochondrial translation was performed in the absence or presence of 10 µM BKA. After 20 mins of pulse, 4 µg/ml puromycin and 24.2 µM methionine/cysteine were added and samples collected at t=0 and after 60 and 120 minutes of chase. Extracts were resolved on 17.5% SDS-PAGE, and bands identified by phosphoimaging. (B) Key for quantitations presented in (C-H). The relative signal for mitochondrial translated products in the pulse-chase experiment was quantified taking the signal at t=0 as 100%. Mean ± SEM, n=4.

Significant differences (as determined by two-way ANOVA with Sidak's multiple comparison test) in BKA treated versus untreated samples is shown.

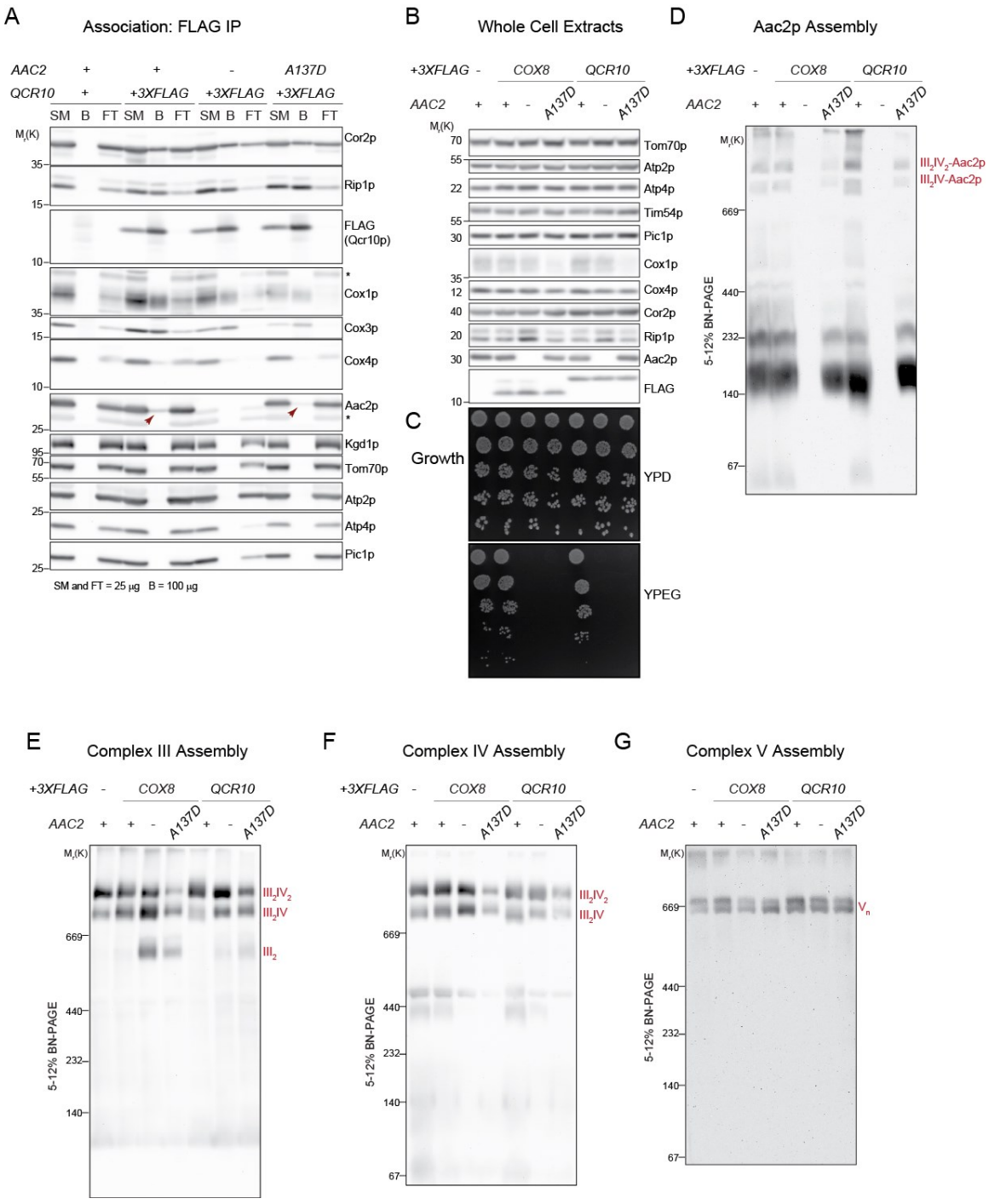

Figure 2.9. Epitope-tagged complex III and IV subunits are functional and assemble/associate normally. (A) Following solubilization with 1.5% (w/v) digitonin, anti-FLAG resin was used to immunoprecipitate Qcr10-3XFLAG (subunit of complex III) and the presence of co-purified respiratory supercomplex subunits determined by

immunoblot; Kgd1p and Tom70p served as controls. SM, starting material; B, bound material; FT, non-binding flow through. n=3. (B) Whole cell extracts for the indicated yeast strains were resolved by SDS-PAGE and immunoblotted for the indicated protein: Tom70p (outer membrane), Tim54p (inner membrane), Atp2p/Atp4p (Complex V), Pic1p (phosphate carrier), Cor2p/Rip1p (Complex III), Cox1p/Cox4p (Complex IV) and Aac2p. n=3. (C) Growth of the indicated strains on dextrose or ethanol-glycerol media at 30ºC for 3 days. n=3. (D) – (G) Mitochondria (50 μg protein) solubilized in 1.5% (w/v) digitonin were resolved by a 5-12% 1D BN–PAGE (D) Aac2p, (E) complex III (Rip1p), (F) complex IV (Cox4p) and (G) complex V (Atp2p) detected by immunoblot. n=3.

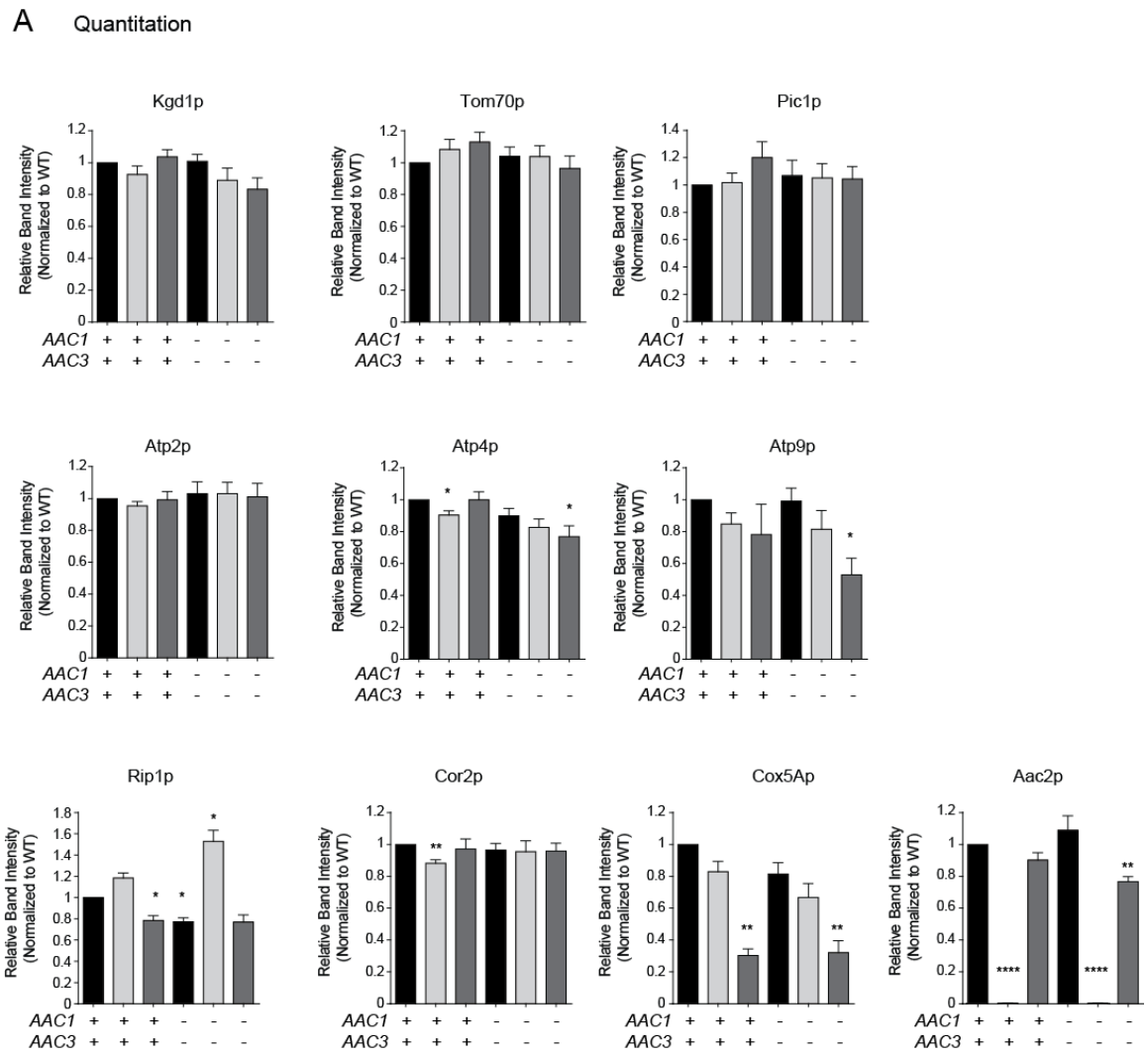

Figure 2.10. Steady states level of most mitochondrial proteins are not affected by Aac2p activity. (A) Steady state levels of Kgd1p, Tom70p, Pic1p, Atp2p, Atp4p, Atp9p, Rip1p, Cor2p, Cox5Ap and Aac2p, shown in Figure 2E, relative to WT are quantified. Mean ± SEM. Significant differences relative to wild type are shown.

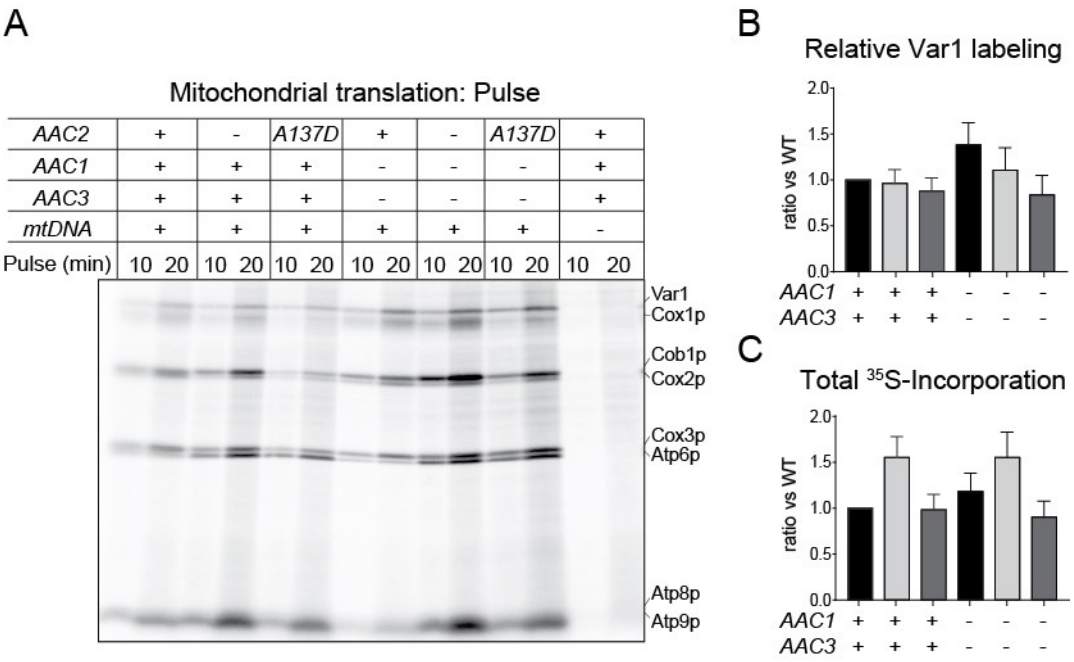

Figure 2.11. Aberrant mitochondrial translation in the absence of Aac2p function. (A) Yeast cultures were spiked with 62 µCi/ml 35S-methionine/cysteine and 0.2 mg/ml cycloheximide to inhibit cytosolic translation. After 10 and 20 minutes incubation at 30ºC, extracts were harvested, resolved by 12-16% SDS-PAGE, and bands identified by phosphoimaging. Quantification is shown in Figure 2.4A. (B) The incorporation of 35S into Var1p for indicated strains was expressed relative to WT. Mean ± SEM, n=10. There was no statistically significant difference in the Var1p labeling among the strains. (C) The total incorporation of 35S into all mitochondrial translated polypeptides was summed and expressed relative to WT. Mean ± SEM, n=10. There was no statistically significant difference in the total 35S- incorporation among the strains.

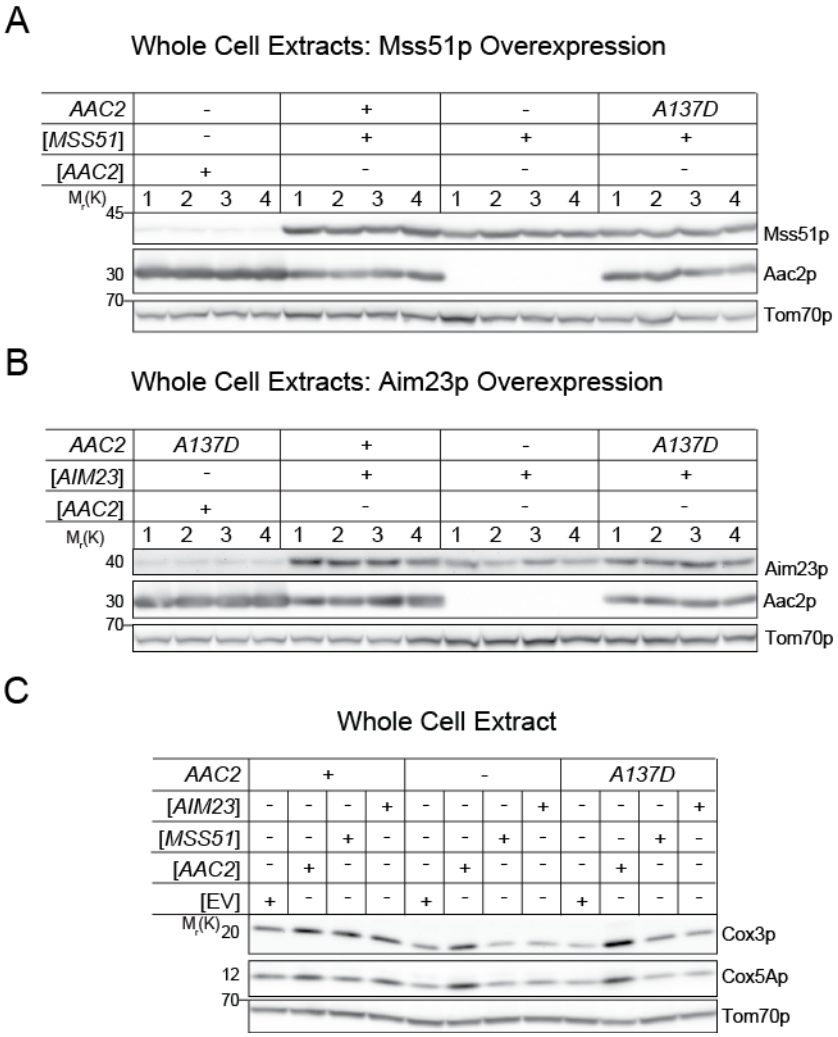

Figure 2.12. Mitochondrial translation is altered by acute Aac2p inhibition. Whole cell extracts for the indicated yeast strains were resolved by SDS-PAGE and immunoblotted for (A) Mss51p (translational activator for the COX1 mRNA) or (B) Aim23p (mitochondrial translation initiation factor); Tom70p served as loading control. n=4. (C) Whole cell extracts for the indicated yeast strains were resolved by SDS-PAGE and immunoblotted for the indicated protein- Tom70p (outer membrane), Cox3p/Cox5Ap (complex IV). n=5.

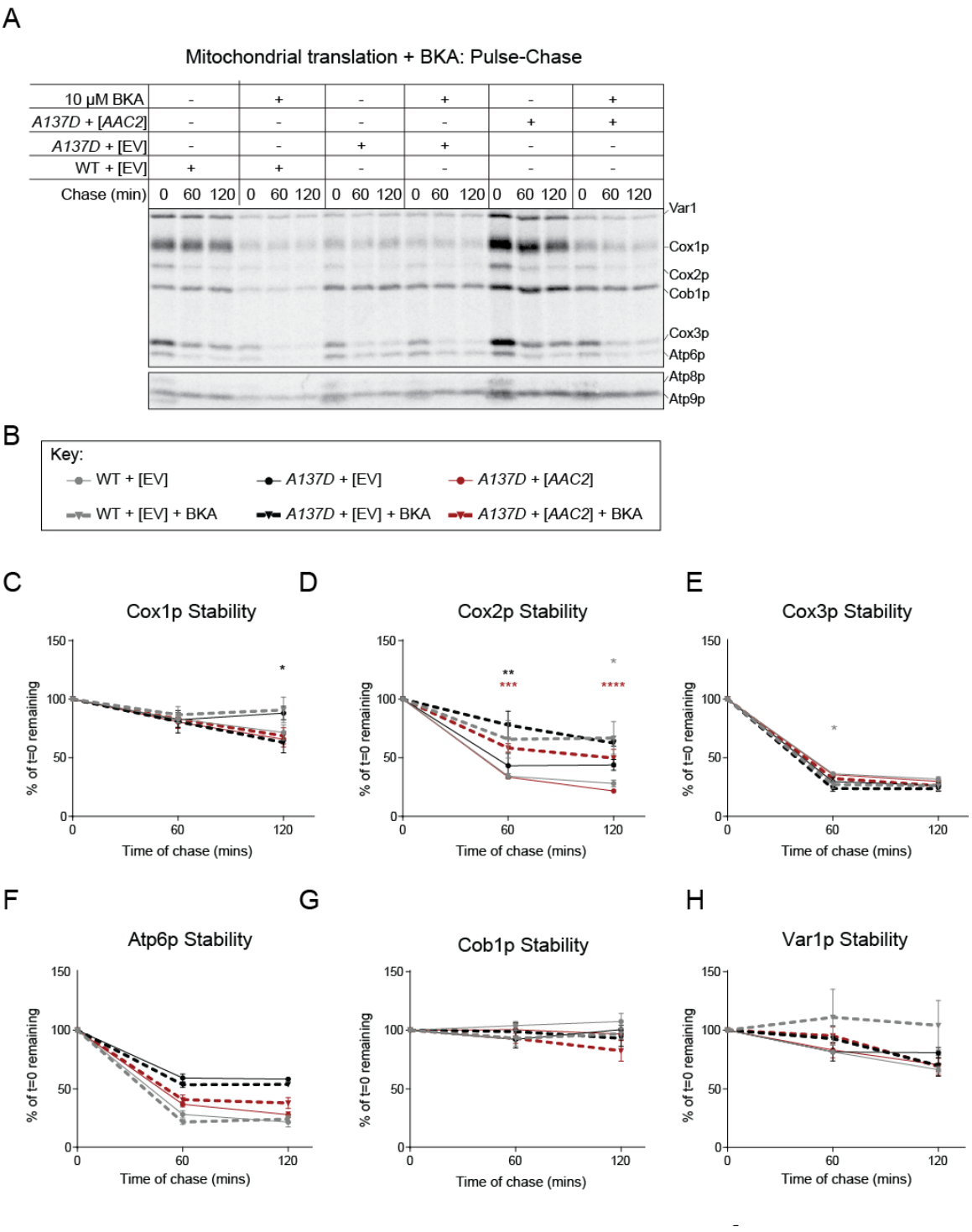

Figure 2.13. Turnover of synthesized mitochondrial protein upon acute Aac2p inhibition in the plasmid-based setting. (A) Mitochondrial translation in the absence or presence of 10 µM BKA. After 20 mins of pulse, 4 µg/ml puromycin and 24.2 µM

methionine/cysteine were added and samples collected at t=0 and after 60 and 120 minutes of chase. Extracts were resolved on 17.5% SDS-PAGE, and bands identified by phosphoimaging. (B) Key for quantitations presented in (C)-(H). (C)-(H) The relative signal for mitochondrial translated products in the pulse-chase experiment was quantified taking the signal at t=0 as 100%. Mean ± SEM, n=4. Significant differences (as determined by two-way ANOVA with Sidak's multiple comparison test) of the percent remaining at t=60 and 120 minutes in experiment with *vs* without BKA treatment is shown

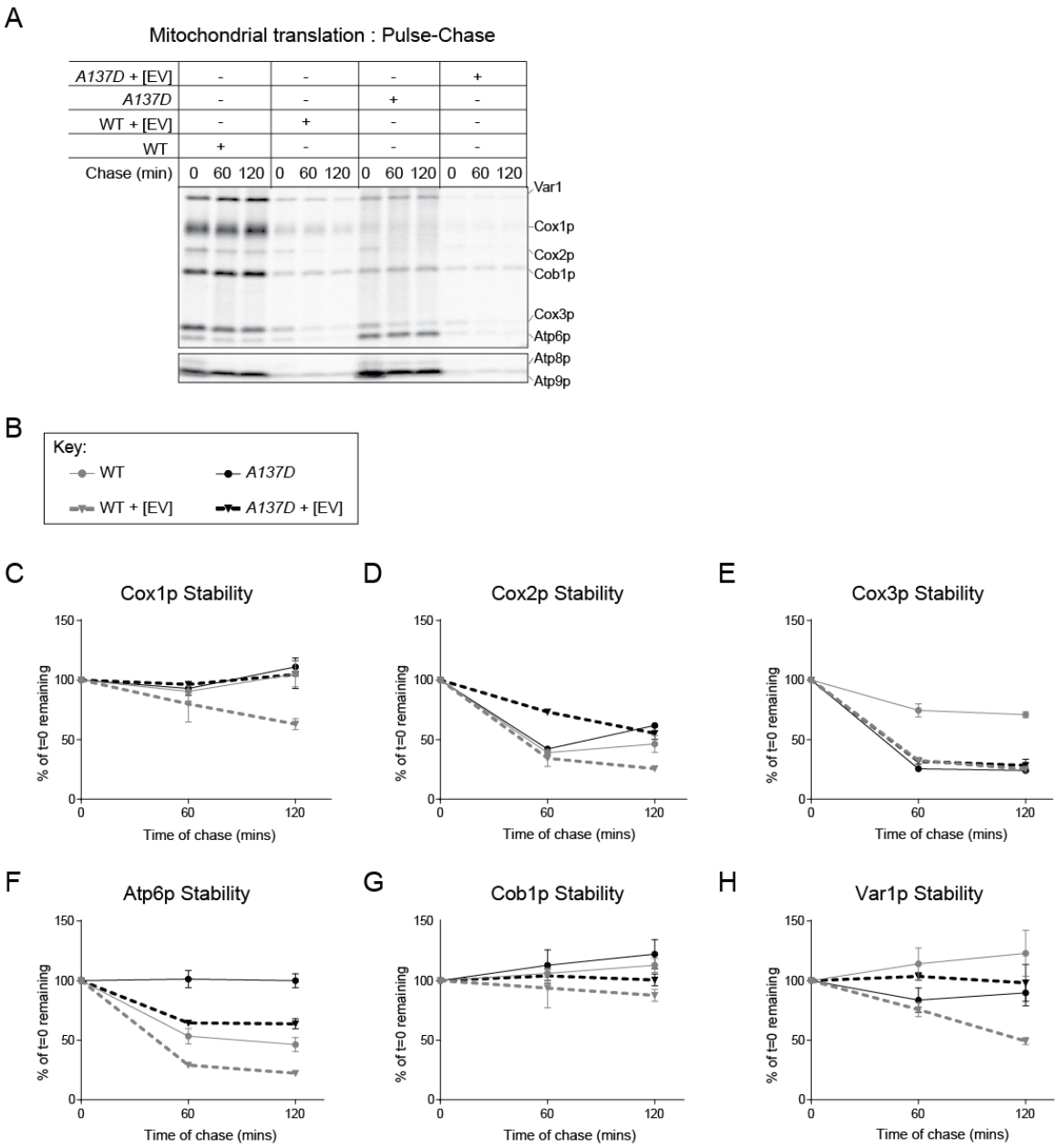

Figure 2.14. Plasmid maintenance reduces mitochondrial translation and decreases the stability of newly translated Cox3p when Aac2p is functional. (A) After 20 mins of pulse, 4 µg/ml puromycin and 24.2 µM methionine/cysteine were added and samples

collected at t=0 and after 60 and 120 minutes of chase. Extracts were resolved on 17.5% SDS-PAGE, and bands identified by phosphoimaging. (B) Key for quantitations presented in (C-H). The relative signal for mitochondrial translated products in the pulse-chase experiment was quantified taking the signal at t=0 as 100%. Mean ± SEM, n=2. No statistical analysis was done.

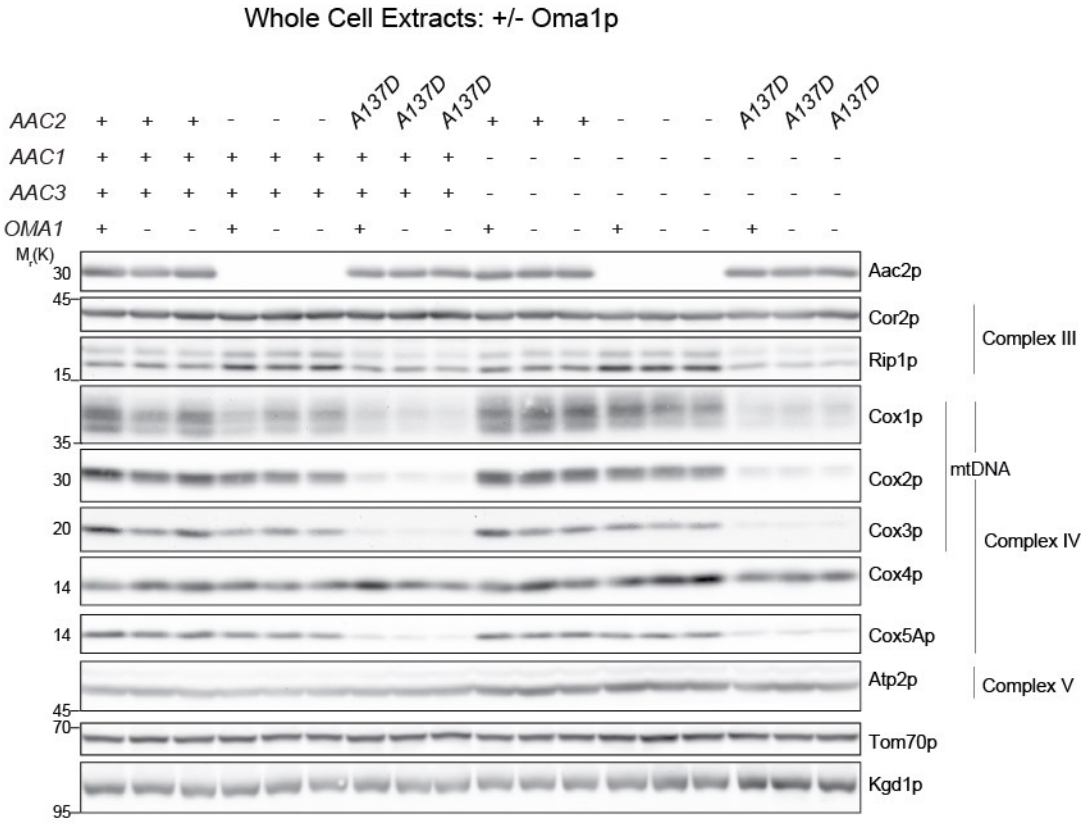

Figure 2.15. *OMA1* disruption does not rescue the steady states level of complex IV subunits. Whole cell extracts for the indicated yeast strains were resolved by SDS-PAGE and immunoblotted for the indicated protein: Kgd1p(matrix), Tom70p (outer membrane), Atp2p (Complex V) Cor2p/Rip1p (Complex III), Cox1-4p/Cox5Ap (Complex IV) and Aac2p. n=3.

REFERENCES

Acín-Pérez, R., Fernández-Silva, P., Peleato, M. L., Pérez-Martos, A., & Enriquez, J. A. (2008). Respiratory active mitochondrial supercomplexes. *Mol Cell, 32*(4), 529-539. doi:10.1016/j.molcel.2008.10.021

Amin-ul Mannan, M., Sharma, S., & Ganesan, K. (2009). Total RNA isolation from recalcitrant yeast cells. *Anal Biochem, 389*(1), 77-79. doi:10.1016/j.ab.2009.03.014

Amiott, E. A., & Jaehning, J. A. (2006). Mitochondrial transcription is regulated via an ATP "sensing" mechanism that couples RNA abundance to respiration. *Mol Cell, 22*(3), 329-338. doi:10.1016/j.molcel.2006.03.031

Arlt, H., Steglich, G., Perryman, R., Guiard, B., Neupert, W., & Langer, T. (1998). The formation of respiratory chain complexes in mitochondria is under the proteolytic control of the m-AAA protease. *EMBO J, 17*(16), 4837-4847. doi:10.1093/emboj/17.16.4837

Asin-Cayuela, J., & Gustafsson, C. M. (2007). Mitochondrial transcription and its regulation in mammalian cells. *Trends Biochem Sci, 32*(3), 111-117. doi:10.1016/j.tibs.2007.01.003

Atkinson, G. C., Kuzmenko, A., Kamenski, P., Vysokikh, M. Y., Lakunina, V., Tankov, S., . . . Hauryliuk, V. (2012). Evolutionary and genetic analyses of mitochondrial translation initiation factors identify the missing mitochondrial IF3 in S. cerevisiae. *Nucleic Acids Res, 40*(13), 6122-6134. doi:10.1093/nar/gks272

Bao, Z., Xiao, H., Liang, J., Zhang, L., Xiong, X., Sun, N., . . . Zhao, H. (2015). Homology-integrated CRISPR-Cas (HI-CRISPR) system for one-step multigene disruption in Saccharomyces cerevisiae. *ACS Synth Biol, 4*(5), 585-594. doi:10.1021/sb500255k

Barrientos, A., Korr, D., & Tzagoloff, A. (2002). Shy1p is necessary for full expression of mitochondrial COX1 in the yeast model of Leigh's syndrome. *EMBO J, 21*(1-2), 43-52.

Barrientos, A., Zambrano, A., & Tzagoloff, A. (2004). Mss51p and Cox14p jointly regulate mitochondrial Cox1p expression in Saccharomyces cerevisiae. *EMBO J, 23*(17), 3472-3482. doi:10.1038/sj.emboj.7600358

Bestwick, M., Khalimonchuk, O., Pierrel, F., & Winge, D. R. (2010). The role of Coa2 in hemylation of yeast Cox1 revealed by its genetic interaction with Cox10. *Mol Cell Biol, 30*(1), 172-185. doi:10.1128/MCB.00869-09

Brandner, K., Mick, D. U., Frazier, A. E., Taylor, R. D., Meisinger, C., & Rehling, P. (2005). Taz1, an outer mitochondrial membrane protein, affects stability and assembly of inner membrane protein complexes: implications for Barth Syndrome. *Mol Biol Cell, 16*(11), 5202-5214. doi:10.1091/mbc.E05-03-0256

Claypool, S. M., Dickinson, B. L., Yoshida, M., Lencer, W. I., & Blumberg, R. S. (2002). Functional reconstitution of human FcRn in Madin-Darby canine kidney cells requires co-expressed human beta 2-microglobulin. *J Biol Chem, 277*(31), 28038-28050. doi:10.1074/jbc.M202367200

Claypool, S. M., McCaffery, J. M., & Koehler, C. M. (2006). Mitochondrial mislocalization and altered assembly of a cluster of Barth syndrome mutant tafazzins. *J Cell Biol, 174*(3), 379-390. doi:10.1083/jcb.200605043

Claypool, S. M., Oktay, Y., Boontheung, P., Loo, J. A., & Koehler, C. M. (2008). Cardiolipin defines the interactome of the major ADP/ATP carrier protein of the mitochondrial inner membrane. *J Cell Biol, 182*(5), 937-950. doi:10.1083/jcb.200801152

Claypool, S. M., Whited, K., Srijumnong, S., Han, X., & Koehler, C. M. (2011). Barth syndrome mutations that cause tafazzin complex lability. *J Cell Biol, 192*(3), 447-462. doi:10.1083/jcb.201008177

De Silva, D., Poliquin, S., Zeng, R., Zamudio-Ochoa, A., Marrero, N., Perez-Martinez, X., . . . Barrientos, A. (2017). The DEAD-box helicase Mss116 plays distinct roles in mitochondrial ribogenesis and mRNA-specific translation. *Nucleic Acids Res, 45*(11), 6628-6643. doi:10.1093/nar/gkx426

Dienhart, M. K., & Stuart, R. A. (2008). The yeast Aac2 protein exists in physical association with the cytochrome bc1-COX supercomplex and the TIM23 machinery. *Mol Biol Cell, 19*(9), 3934-3943. doi:10.1091/mbc.E08-04-0402

Doerner, A., Pauschinger, M., Badorff, A., Noutsias, M., Giessen, S., Schulze, K., . . . Schultheiss, H. P. (1997). Tissue-specific transcription pattern of the adenine nucleotide translocase isoforms in humans. *FEBS Lett, 414*(2), 258-262.

Dolce, V., Scarcia, P., Iacopetta, D., & Palmieri, F. (2005). A fourth ADP/ATP carrier isoform in man: identification, bacterial expression, functional characterization and tissue distribution. *FEBS Lett, 579*(3), 633-637. doi:10.1016/j.febslet.2004.12.034

Dupont, P. Y., & Stepien, G. (2011). Computational analysis of the transcriptional regulation of the adenine nucleotide translocator isoform 4 gene and its role in spermatozoid glycolytic metabolism. *Gene, 487*(1), 38-45. doi:10.1016/j.gene.2011.07.024

Echaniz-Laguna, A., Chassagne, M., Ceresuela, J., Rouvet, I., Padet, S., Acquaviva, C., . . . Mousson de Camaret, B. (2012). Complete loss of expression of the ANT1 gene causing cardiomyopathy and myopathy. *J Med Genet, 49*(2), 146-150. doi:10.1136/jmedgenet-2011-100504

Fontanesi, F., Clemente, P., & Barrientos, A. (2011). Cox25 teams up with Mss51, Ssc1, and Cox14 to regulate mitochondrial cytochrome c oxidase subunit 1 expression and assembly in Saccharomyces cerevisiae. *J Biol Chem, 286*(1), 555-566. doi:10.1074/jbc.M110.188805

Fontanesi, F., Palmieri, L., Scarcia, P., Lodi, T., Donnini, C., Limongelli, A., . . . Viola, A. M. (2004). Mutations in AAC2, equivalent to human adPEO-associated ANT1 mutations, lead to defective oxidative phosphorylation in Saccharomyces cerevisiae and affect mitochondrial DNA stability. *Hum Mol Genet, 13*(9), 923-934. doi:10.1093/hmg/ddh108

Gavurníková, G., Sabova, L., Kissová, I., Haviernik, P., & Kolarov, J. (1996). Transcription of the AAC1 gene encoding an isoform of mitochondrial ADP/ATP carrier in Saccharomyces cerevisiae is regulated by oxygen in a heme-independent manner. *Eur J Biochem, 239*(3), 759-763.

Graham, B. H., Waymire, K. G., Cottrell, B., Trounce, I. A., MacGregor, G. R., & Wallace, D. C. (1997). A mouse model for mitochondrial myopathy and cardiomyopathy resulting from a deficiency in the heart/muscle isoform of the adenine nucleotide translocator. *Nat Genet, 16*(3), 226-234. doi:10.1038/ng0797-226

Gu, J., Wu, M., Guo, R., Yan, K., Lei, J., Gao, N., & Yang, M. (2016). The architecture of the mammalian respirasome. *Nature, 537*(7622), 639-643. doi:10.1038/nature19359

Heidkämper, D., Müller, V., Nelson, D. R., & Klingenberg, M. (1996). Probing the role of positive residues in the ADP/ATP carrier from yeast. The effect of six arginine mutations on transport and the four ATP versus ADP exchange modes. *Biochemistry, 35*(50), 16144-16152. doi:10.1021/bi960668j

Hildenbeutel, M., Hegg, E. L., Stephan, K., Gruschke, S., Meunier, B., & Ott, M. (2014). Assembly factors monitor sequential hemylation of cytochrome b to regulate mitochondrial translation. *J Cell Biol, 205*(4), 511-524. doi:10.1083/jcb.201401009

Hoffbuhr, K. C., Davidson, E., Filiano, B. A., Davidson, M., Kennaway, N. G., & King, M. P. (2000). A pathogenic 15-base pair deletion in mitochondrial DNA-encoded

cytochrome c oxidase subunit III results in the absence of functional cytochrome c oxidase. *J Biol Chem, 275*(18), 13994-14003.

Hoffman, C. S. (2001). Preparation of yeast DNA. *Curr Protoc Mol Biol, Chapter 13*, Unit13.11. doi:10.1002/0471142727.mb1311s39

Hornig-Do, H. T., Tatsuta, T., Buckermann, A., Bust, M., Kollberg, G., Rötig, A., . . . Wiesner, R. J. (2012). Nonsense mutations in the COX1 subunit impair the stability of respiratory chain complexes rather than their assembly. *EMBO J, 31*(5), 1293-1307. doi:10.1038/emboj.2011.477

Hwang, D. K., Claypool, S. M., Leuenberger, D., Tienson, H. L., & Koehler, C. M. (2007). Tim54p connects inner membrane assembly and proteolytic pathways in the mitochondrion. *J Cell Biol, 178*(7), 1161-1175. doi:10.1083/jcb.200706195

Jordens, E. Z., Palmieri, L., Huizing, M., van den Heuvel, L. P., Sengers, R. C., Dörner, A., . . . Smeitink, J. A. (2002). Adenine nucleotide translocator 1 deficiency associated with Sengers syndrome. *Ann Neurol, 52*(1), 95-99. doi:10.1002/ana.10214

Kabala, A. M., Lasserre, J. P., Ackerman, S. H., di Rago, J. P., & Kucharczyk, R. (2014). Defining the impact on yeast ATP synthase of two pathogenic human mitochondrial DNA mutations, T9185C and T9191C. *Biochimie, 100*, 200-206. doi:10.1016/j.biochi.2013.11.024

Kaukonen, J., Juselius, J. K., Tiranti, V., Kyttälä, A., Zeviani, M., Comi, G. P., . . . Suomalainen, A. (2000). Role of adenine nucleotide translocator 1 in mtDNA maintenance. *Science, 289*(5480), 782-785.

Kehrein, K., Bonnefoy, N., & Ott, M. (2013). Mitochondrial protein synthesis: efficiency and accuracy. *Antioxid Redox Signal, 19*(16), 1928-1939. doi:10.1089/ars.2012.4896

Khalimonchuk, O., Jeong, M. Y., Watts, T., Ferris, E., & Winge, D. R. (2012). Selective Oma1 protease-mediated proteolysis of Cox1 subunit of cytochrome oxidase in assembly mutants. *J Biol Chem, 287*(10), 7289-7300. doi:10.1074/jbc.M111.313148

Klingenberg, M. (2008). The ADP and ATP transport in mitochondria and its carrier. *Biochim Biophys Acta, 1778*(10), 1978-2021. doi:10.1016/j.bbamem.2008.04.011

Kokoszka, J. E., Waymire, K. G., Flierl, A., Sweeney, K. M., Angelin, A., MacGregor, G. R., & Wallace, D. C. (2016). Deficiency in the mouse mitochondrial adenine nucleotide translocator isoform 2 gene is associated with cardiac noncompaction. *Biochim Biophys Acta, 1857*(8), 1203-1212. doi:10.1016/j.bbabio.2016.03.026

Komaki, H., Fukazawa, T., Houzen, H., Yoshida, K., Nonaka, I., & Goto, Y. (2002). A novel D104G mutation in the adenine nucleotide translocator 1 gene in autosomal dominant progressive external ophthalmoplegia patients with mitochondrial DNA with multiple deletions. *Ann Neurol, 51*(5), 645-648. doi:10.1002/ana.10172

Kovác, L., Lachowicz, T. M., & Slonimski, P. P. (1967). Biochemical genetics of oxidative phosphorylation. *Science, 158*(3808), 1564-1567.

Kucejova, B., Li, L., Wang, X., Giannattasio, S., & Chen, X. J. (2008). Pleiotropic effects of the yeast Sal1 and Aac2 carriers on mitochondrial function via an activity distinct from adenine nucleotide transport. *Mol Genet Genomics, 280*(1), 25-39. doi:10.1007/s00438-008-0342-5

Kuzmenko, A., Atkinson, G. C., Levitskii, S., Zenkin, N., Tenson, T., Hauryliuk, V., & Kamenski, P. (2014). Mitochondrial translation initiation machinery: conservation and diversification. *Biochimie, 100*, 132-140. doi:10.1016/j.biochi.2013.07.024

Kuzmenko, A., Derbikova, K., Salvatori, R., Tankov, S., Atkinson, G. C., Tenson, T., . . . Hauryliuk, V. (2016). Aim-less translation: loss of Saccharomyces cerevisiae mitochondrial translation initiation factor mIF3/Aim23 leads to unbalanced protein synthesis. *Sci Rep, 6*, 18749. doi:10.1038/srep18749

Lawson, J. E., Gawaz, M., Klingenberg, M., & Douglas, M. G. (1990). Structure-function studies of adenine nucleotide transport in mitochondria. I. Construction and genetic analysis of yeast mutants encoding the ADP/ATP carrier protein of mitochondria. *J Biol Chem, 265*(24), 14195-14201.

Letts, J. A., Fiedorczuk, K., & Sazanov, L. A. (2016). The architecture of respiratory supercomplexes. *Nature, 537*(7622), 644-648. doi:10.1038/nature19774

Liu, J., & Barrientos, A. (2013). Transcriptional regulation of yeast oxidative phosphorylation hypoxic genes by oxidative stress. *Antioxid Redox Signal, 19*(16), 1916-1927. doi:10.1089/ars.2012.4589

Lu, Y. W., Acoba, M. G., Selvaraju, K., Huang, T. C., Nirujogi, R. S., Sathe, G., . . . Claypool, S. M. (2017). Human adenine nucleotide translocases physically and functionally interact with respirasomes. *Mol Biol Cell, 28*(11), 1489-1506. doi:10.1091/mbc.E17-03-0195

Maldonado, E. N., DeHart, D. N., Patnaik, J., Klatt, S. C., Gooz, M. B., & Lemasters, J. J. (2016). ATP/ADP Turnover and Import of Glycolytic ATP into Mitochondria in Cancer Cells Is Independent of the Adenine Nucleotide Translocator. *J Biol Chem, 291*(37), 19642-19650. doi:10.1074/jbc.M116.734814

Mans, R., van Rossum, H. M., Wijsman, M., Backx, A., Kuijpers, N. G., van den Broek, M., . . . Daran, J. M. (2015). CRISPR/Cas9: a molecular Swiss army knife for simultaneous introduction of multiple genetic modifications in Saccharomyces cerevisiae. *FEMS Yeast Res, 15*(2). doi:10.1093/femsyr/fov004

McStay, G. P., Su, C. H., Thomas, S. M., Xu, J. T., & Tzagoloff, A. (2013). Characterization of assembly intermediates containing subunit 1 of yeast cytochrome oxidase. *J Biol Chem, 288*(37), 26546-26556. doi:10.1074/jbc.M113.498592

McStay, G. P., Su, C. H., & Tzagoloff, A. (2013). Modular assembly of yeast cytochrome oxidase. *Mol Biol Cell, 24*(4), 440-452. doi:10.1091/mbc.E12-10-0749

Mick, D. U., Vukotic, M., Piechura, H., Meyer, H. E., Warscheid, B., Deckers, M., & Rehling, P. (2010). Coa3 and Cox14 are essential for negative feedback regulation of COX1 translation in mitochondria. *J Cell Biol, 191*(1), 141-154. doi:10.1083/jcb.201007026

Moreno-Lastres, D., Fontanesi, F., García-Consuegra, I., Martín, M. A., Arenas, J., Barrientos, A., & Ugalde, C. (2012). Mitochondrial complex I plays an essential role in human respirasome assembly. *Cell Metab, 15*(3), 324-335. doi:10.1016/j.cmet.2012.01.015

Müller, V., Basset, G., Nelson, D. R., & Klingenberg, M. (1996). Probing the role of positive residues in the ADP/ATP carrier from yeast. The effect of six arginine mutations of oxidative phosphorylation and AAC expression. *Biochemistry, 35*(50), 16132-16143. doi:10.1021/bi960667r

Müller, V., Heidkämper, D., Nelson, D. R., & Klingenberg, M. (1997). Mutagenesis of some positive and negative residues occurring in repeat triad residues in the ADP/ATP carrier from yeast. *Biochemistry, 36*(50), 16008-16018. doi:10.1021/bi971867l

Nelson, D. R., Lawson, J. E., Klingenberg, M., & Douglas, M. G. (1993). Site-directed mutagenesis of the yeast mitochondrial ADP/ATP translocator. Six arginines and one lysine are essential. *J Mol Biol, 230*(4), 1159-1170. doi:10.1006/jmbi.1993.1233

Ogunbona, O. B., Onguka, O., Calzada, E., & Claypool, S. M. (2017). Multitiered and cooperative surveillance of mitochondrial Phosphatidylserine Decarboxylase 1. *Mol Cell Biol*. doi:10.1128/MCB.00049-17

Onguka, O., Calzada, E., Ogunbona, O.B., & Claypool, S.M. (2015). Phosphatidylserine decarboxylase 1 autocatalysis and function does not require a mitochondrial-specific factor. *Journal of Biological Chemistry, 290*(20), 12744-12752. doi:10.1074/jbc.M115.641118

Palmieri, L., Alberio, S., Pisano, I., Lodi, T., Meznaric-Petrusa, M., Zidar, J., . . . Zeviani, M. (2005). Complete loss-of-function of the heart/muscle-specific adenine nucleotide translocator is associated with mitochondrial myopathy and cardiomyopathy. *Hum Mol Genet, 14*(20), 3079-3088. doi:10.1093/hmg/ddi341

Perez-Martinez, X., Broadley, S. A., & Fox, T. D. (2003). Mss51p promotes mitochondrial Cox1p synthesis and interacts with newly synthesized Cox1p. *EMBO J, 22*(21), 5951-5961. doi:10.1093/emboj/cdg566

Perez-Martinez, X., Butler, C. A., Shingu-Vazquez, M., & Fox, T. D. (2009). Dual functions of Mss51 couple synthesis of Cox1 to assembly of cytochrome c oxidase in Saccharomyces cerevisiae mitochondria. *Mol Biol Cell, 20*(20), 4371-4380. doi:10.1091/mbc.E09-06-0522

Sabová, L., Zeman, I., Supek, F., & Kolarov, J. (1993). Transcriptional control of AAC3 gene encoding mitochondrial ADP/ATP translocator in Saccharomyces cerevisiae by oxygen, heme and ROX1 factor. *Eur J Biochem, 213*(1), 547-553.

Schägger, H. (2001). Respiratory chain supercomplexes. *IUBMB Life, 52*(3-5), 119-128. doi:10.1080/15216540152845911

Schägger, H., & Pfeiffer, K. (2000). Supercomplexes in the respiratory chains of yeast and mammalian mitochondria. *EMBO J, 19*(8), 1777-1783. doi:10.1093/emboj/19.8.1777

Sharer, J. D. (2005). The adenine nucleotide translocase type 1 (ANT1): a new factor in mitochondrial disease. *IUBMB Life, 57*(9), 607-614. doi:10.1080/15216540500217735

Shingú-Vázquez, M., Camacho-Villasana, Y., Sandoval-Romero, L., Butler, C. A., Fox, T. D., & Pérez-Martínez, X. (2010). The carboxyl-terminal end of Cox1 is required for feedback assembly regulation of Cox1 synthesis in Saccharomyces cerevisiae mitochondria. *J Biol Chem, 285*(45), 34382-34389. doi:10.1074/jbc.M110.161976

Siep, M., van Oosterum, K., Neufeglise, H., van der Spek, H., & Grivell, L. A. (2000). Mss51p, a putative translational activator of cytochrome c oxidase subunit-1 (COX1) mRNA, is required for synthesis of Cox1p in Saccharomyces cerevisiae. *Curr Genet, 37*(4), 213-220.

Soto, I. C., Fontanesi, F., Liu, J., & Barrientos, A. (2012). Biogenesis and assembly of eukaryotic cytochrome c oxidase catalytic core. *Biochim Biophys Acta, 1817*(6), 883-897. doi:10.1016/j.bbabio.2011.09.005

Stepien, G., Torroni, A., Chung, A. B., Hodge, J. A., & Wallace, D. C. (1992). Differential expression of adenine nucleotide translocator isoforms in mammalian tissues and during muscle cell differentiation. *J Biol Chem, 267*(21), 14592-14597.

Stribinskis, V., Gao, G. J., Ellis, S. R., & Martin, N. C. (2001). Rpm2, the protein subunit of mitochondrial RNase P in Saccharomyces cerevisiae, also has a role in the translation of mitochondrially encoded subunits of cytochrome c oxidase. *Genetics, 158*(2), 573-585.

Su, C. H., McStay, G. P., & Tzagoloff, A. (2014). The Cox3p assembly module of yeast cytochrome oxidase. *Mol Biol Cell, 25*(7), 965-976. doi:10.1091/mbc.E13-10-0575

Teste, M. A., Duquenne, M., François, J. M., & Parrou, J. L. (2009). Validation of reference genes for quantitative expression analysis by real-time RT-PCR in Saccharomyces cerevisiae. *BMC Mol Biol, 10*, 99. doi:10.1186/1471-2199-10-99

Thompson, K., Majd, H., Dallabona, C., Reinson, K., King, M. S., Alston, C. L., . . . Taylor, R. W. (2016). Recurrent De Novo Dominant Mutations in SLC25A4 Cause Severe Early-Onset Mitochondrial Disease and Loss of Mitochondrial DNA Copy Number. *Am J Hum Genet, 99*(6), 1405. doi:10.1016/j.ajhg.2016.11.001

Towpik, J. (2005). Regulation of mitochondrial translation in yeast. *Cell Mol Biol Lett, 10*(4), 571-594.

Tzagoloff, A., Akai, A., & Needleman, R. B. (1975). Assembly of the mitochondrial membrane system: isolation of nuclear and cytoplasmic mutants of Saccharomyces

cerevisiae with specific defects in mitochondrial functions. *J Bacteriol, 122*(3), 826-831.

Vandewalle, J., Bauters, M., Van Esch, H., Belet, S., Verbeeck, J., Fieremans, N., . . . Froyen, G. (2013). The mitochondrial solute carrier SLC25A5 at Xq24 is a novel candidate gene for non-syndromic intellectual disability. *Hum Genet, 132*(10), 1177-1185. doi:10.1007/s00439-013-1322-3

Wach, A., Brachat, A., Pöhlmann, R., & Philippsen, P. (1994). New heterologous modules for classical or PCR-based gene disruptions in Saccharomyces cerevisiae. *Yeast, 10*(13), 1793-1808.

Wang, X., Salinas, K., Zuo, X., Kucejova, B., & Chen, X. J. (2008). Dominant membrane uncoupling by mutant adenine nucleotide translocase in mitochondrial diseases. *Hum Mol Genet, 17*(24), 4036-4044. doi:10.1093/hmg/ddn306

Whited, K., Baile, M. G., Currier, P., & Claypool, S. M. (2013). Seven functional classes of Barth syndrome mutation. *Hum Mol Genet, 22*(3), 483-492. doi:10.1093/hmg/dds447

Wohlrab, H., & Flowers, N. (1982). pH gradient-dependent phosphate transport catalyzed by the purified mitochondrial phosphate transport protein. *J Biol Chem, 257*(1), 28-31.

Wu, M., Gu, J., Guo, R., Huang, Y., & Yang, M. (2016). Structure of Mammalian Respiratory Supercomplex I1III2IV1. Cell, 167(6), 1598-1609.e1510. doi:10.1016/j.cell.2016.11.012

Chapter 3

Conclusions and Future Directions

Solute carrier and Mitochondrial Carrier Family

The MCF is a big family of proteins with members serving a lot of metabolic functions with numerous pathophysiologic implications. Several members have emerging roles in the biogenesis of cytochrome *c* oxidase. My thesis work uncovered a novel mitochondrial translation-dependent mode of regulation that tightly links complex IV expression to Aac2p transport activity. Additional studies are needed to probe the molecular details of the regulation provided by other members that have been linked to cytochrome *c* oxidase biogenesis and determine if a similar regulatory mechanism exists in humans.

Translation-dependent regulation of cytochrome *c* oxidase

A long standing enigma in the field of mitochondrial biology has been the molecular mechanisms for the regulation of cytochrome *c* oxidase activity by Aac2p (Claypool, Oktay, Boontheung, Loo, & Koehler, 2008; Dienhart & Stuart, 2008; Fontanesi et al., 2004; Heidkämper, Müller, Nelson, & Klingenberg, 1996; Müller, Basset, Nelson, & Klingenberg, 1996). Given the recently discovered interaction between Aac2p and RSCs (Claypool et al., 2008; Dienhart & Stuart, 2008), the major goal of my dissertation work was to understand whether Aac2p function and/or its interaction with RSCs is important for optimal complex IV activity. Interestingly, we found a role for Aac2p in the optimal translation of mitochondrial genome encoded subunits of cytochrome *c* oxidase (Figure 2.4). While this provides an explanation for the regulation of the complex's activity, it also functionally links nucleotide transport/metabolism to mitochondrial translation and the discovery opens up further lines of inquiry.

It is still unclear what the direct connection between Aac2p function and complex IV biogenesis pathway is. Perhaps the connection is a direct consequence of an altered ADP/ATP ratio in the mitochondrial matrix (Figure 2.1I). Further experiments are needed to test this hypothesis. It will be important to ascertain how the ADP and ATP levels in the mitochondrial matrix correlate with mitochondrial translation inhibition brought about by BKA. Measuring ATP and ADP levels in the mitochondria directly could be done using live-cell reporting with a fluorescent biosensor such as PercevalHR (Tantama, Martínez-François, Mongeon, & Yellen, 2013) which can be further modified to direct it to the mitochondrial matrix thus enabling one to monitor nucleotide changes in this compartment in real time.

It is also unclear as to why the translation of the subunits of the ATP synthase (complex V) are increased in the absence of Aac2p function. It could be a compensatory mechanism since assembly of respiratory complexes are linked to their synthesis. Also interesting is that the increase in the translational synthesis of the ATP synthase subunits is not reflected at the steady state level, at least for Atp6p and Atp9p (Figure 2.2E). The activity of the ATP synthase has also not been measured so it is unknown if there is a concomitant increase in the activity of the complex. While it appears that the assembly of synthesized complex IV subunits into the holoenzyme is not impaired, it is presently unknown why Cox5Ap incorporation into the respiratory complexes is increased in the absence of Aac2p compared to wild type and the non-functional Aac2p strains (Figure 2.5D).

Cox3p stability appears to be compromised in strains expressing the non-functional Aac2p, Aac2^{A137D} (Figure 2.4G). The reason for this is presently elusive and could be due

to the action of a mitochondrial protease. We initially focused on Oma1p, a mitochondrial protease that has been shown to degrade unassembled complex IV subunits in many different settings (Bestwick, Khalimonchuk, Pierrel, & Winge, 2010; Khalimonchuk, Jeong, Watts, Ferris, & Winge, 2012). However, Oma1p ablation did not rescue the level of affected cytochrome *c* oxidase subunits (Figure 2.15). Nevertheless, it is possible that other mitochondrial proteases are involved. In particular, the two ATP-dependent proteases of the IM and the mitochondrial matrix, the *i*-AAA (Yme1/Mgr protein complex) and *m*-AAA proteases (Yta10/12 complex) respectively, warrant further investigation given their pre-eminent roles in enforcing mitochondrial quality control on either side of the IM.

Why would the COX subunit be turned over faster in the absence of Aac2p function? Potentially, the augmented rate of Cox3p degradation reflects the existence of a novel ATP dependent step in the COX assembly pathway. Alternatively, perhaps the stability of newly synthesized Cox3p subunit(s) is itself energy demanding. Will elimination of the protease restore the steady state levels and possibly increase the amount and activity of cytochrome *c* oxidase? Mitochondrial proteases are important quality control machinery and their role in this regard has been extensively reviewed (Baker, Tatsuta, & Langer, 2011; Fischer, Hamann, & Osiewacz, 2012). Recently, we uncovered a role for Yme1p and Oma1p in enforcing quality control of a mitochondrial lipid synthesizing enzyme, Psd1p (Ogunbona, Onguka, Calzada, & Claypool, 2017). This interesting story is appended as Chapter 4 of this work.

Finally, in mammals, the multiple ANT isoforms (ANT1-4) have tissue-specific expression although their biological roles in the different tissues have not be defined. It will thus be important to determine the role and contribution of each ANT isoforms to OXPHOS

regulation and whether the dependence of mitochondrial translation and complex IV biogenesis on nucleotide transport that we discovered in yeast similarly occurs in the mammal system.

References

Baker, M. J., Tatsuta, T., & Langer, T. (2011). Quality control of mitochondrial proteostasis. *Cold Spring Harb Perspect Biol, 3*(7). doi:10.1101/cshperspect.a007559

Bestwick, M., Khalimonchuk, O., Pierrel, F., & Winge, D. R. (2010). The role of Coa2 in hemylation of yeast Cox1 revealed by its genetic interaction with Cox10. *Mol Cell Biol, 30*(1), 172-185. doi:10.1128/MCB.00869-09

Claypool, S. M., Oktay, Y., Boontheung, P., Loo, J. A., & Koehler, C. M. (2008). Cardiolipin defines the interactome of the major ADP/ATP carrier protein of the mitochondrial inner membrane. *J Cell Biol, 182*(5), 937-950. doi:10.1083/jcb.200801152

Dienhart, M. K., & Stuart, R. A. (2008). The yeast Aac2 protein exists in physical association with the cytochrome bc1-COX supercomplex and the TIM23 machinery. *Mol Biol Cell, 19*(9), 3934-3943. doi:10.1091/mbc.E08-04-0402

Fischer, F., Hamann, A., & Osiewacz, H. D. (2012). Mitochondrial quality control: an integrated network of pathways. *Trends Biochem Sci, 37*(7), 284-292. doi:10.1016/j.tibs.2012.02.004

Fontanesi, F., Palmieri, L., Scarcia, P., Lodi, T., Donnini, C., Limongelli, A., . . . Viola, A. M. (2004). Mutations in AAC2, equivalent to human adPEO-associated ANT1 mutations, lead to defective oxidative phosphorylation in Saccharomyces cerevisiae and affect mitochondrial DNA stability. *Hum Mol Genet, 13*(9), 923-934. doi:10.1093/hmg/ddh108

Heidkämper, D., Müller, V., Nelson, D. R., & Klingenberg, M. (1996). Probing the role of positive residues in the ADP/ATP carrier from yeast. The effect of six arginine mutations on transport and the four ATP versus ADP exchange modes. *Biochemistry, 35*(50), 16144-16152. doi:10.1021/bi960668j

Khalimonchuk, O., Jeong, M. Y., Watts, T., Ferris, E., & Winge, D. R. (2012). Selective Oma1 protease-mediated proteolysis of Cox1 subunit of cytochrome oxidase in assembly mutants. *J Biol Chem, 287*(10), 7289-7300. doi:10.1074/jbc.M111.313148

Müller, V., Basset, G., Nelson, D. R., & Klingenberg, M. (1996). Probing the role of positive residues in the ADP/ATP carrier from yeast. The effect of six arginine mutations of oxidative phosphorylation and AAC expression. *Biochemistry, 35*(50), 16132-16143. doi:10.1021/bi960667r

Ogunbona, O. B., Onguka, O., Calzada, E., & Claypool, S. M. (2017). Multitiered and cooperative surveillance of mitochondrial Phosphatidylserine Decarboxylase 1. *Mol Cell Biol*. doi:10.1128/MCB.00049-17

Chapter 4

Quality control of mitochondrial phosphatidylethanolamine synthesis

Sections of this chapter are derived from:

*Ogunbona, O. B., *Onguka, O., Calzada, E., & Claypool, S. M. (2017). Multitiered and cooperative surveillance of mitochondrial Phosphatidylserine Decarboxylase 1. *Mol Cell Biol*. doi:10.1128/MCB.00049-17

* = co-first author

SUMMARY

Phosphatidylserine decarboxylase 1 (Psd1p), an ancient enzyme that converts phosphatidylserine to phosphatidylethanolamine in the inner mitochondrial membrane, must undergo an autocatalytic self-processing event to gain activity. Autocatalysis severs the protein into a large membrane anchored β subunit that non-covalently associates with the small α subunit on the intermembrane space side of the inner membrane. Here, we determined that a temperature sensitive (*ts*) *PSD1* allele is autocatalytically impaired and that its fidelity is closely monitored throughout its life cycle by multiple mitochondrial quality control proteases. Interestingly, the proteases involved in resolving misfolded $Psd1^{ts}$ vary depending on its autocatalytic status. Specifically, the degradation of a $Psd1^{ts}$ precursor unable to undergo autocatalysis requires the unprecedented cooperative and sequential action of two inner membrane proteases, Oma1p and Yme1p. In contrast, upon heat-exposure post-autocatalysis, $Psd1^{ts}$ β subunits accumulate in protein aggregates that are resolved by Yme1p acting alone while the released α subunit is degraded in parallel by an unidentified protease. Importantly, the stability of endogenous Psd1p is also influenced by Yme1p. We conclude that Psd1p, the key enzyme required for the mitochondrial pathway of phosphatidylethanolamine production, is closely monitored at several levels and by multiple mitochondrial quality control mechanisms present in the intermembrane space.

INTRODUCTION

In an aqueous environment, the amphipathic chemistry of phospholipids drives the formation of lipid bilayers. These bilayers encapsulate the cell and its internal compartments and are indispensable for life. As one of the major membrane phospholipids, phosphatidylethanolamine (PE) is of fundamental importance for cell physiology with numerous emerging links to human pathology. PE serves as a precursor to the major cellular phospholipid, phosphatidylcholine (Summers, Letts, McGraw, & Henry, 1988) and is a critical component of glycosylphosphatidylinositol anchors (Menon & Stevens, 1992), the cleavage furrow (Emoto et al., 1996), and autophagy (Ichimura et al., 2000). In bacteria, PE can dictate membrane protein topology and function (Bogdanov & Dowhan, 2012). Defects in PE levels have been linked to Alzheimer's (Nesic et al., 2012), Parkinson's (Wang et al., 2014), and liver diseases (van der Veen, Lingrell, da Silva, Jacobs, & Vance, 2014). In spite of its clear physiologic importance, there remain significant gaps in our basic understanding of PE metabolism, including detailed mechanistic information concerning the enzymes responsible for its synthesis.

Of the four cellular pathways of PE production, two are essential for mammalian development and are differentially localized to the endoplasmic reticulum (ER) or the mitochondrion (Fullerton, Hakimuddin, & Bakovic, 2007; Steenbergen et al., 2005). The role of mitochondria in lipid synthesis is rarely mentioned despite the fact that it is second only to the ER in this functional capacity. Phospholipids made in the mitochondrion are phosphatidic acid (PA), cytidine diphosphate-diacylglycerol, phosphatidylglycerol, cardiolipin (CL), and PE (Lu & Claypool, 2015; Osman, Voelker, & Langer, 2011). Yeast express two phosphatidylserine decarboxylases, Psd1p and Psd2p, which produce PE by

decarboxylating phosphatidylserine (PS). Psd1p is localized in the mitochondrion (Y. Tamura et al., 2012; Trotter, Pedretti, & Voelker, 1993) while Psd2p resides in the endomembrane system (Gulshan, Schmidt, Shahi, & Moye-Rowley, 2008; Trotter & Voelker, 1995). Psd1p is conserved from bacteria to humans while Psd2p is only found in yeast. Yeast lacking both Psd1p and Psd2p (*psd1*Δ*psd2*Δ) are ethanolamine auxotrophs and require ethanolamine supplementation to produce PE by the ER localized CDP-ethanolamine pathway, the second major cellular pathway of PE biosynthesis.

Psd1p is encoded within the nucleus and imported into the mitochondrion post-synthesis as a zymogen (Trotter et al., 1993). Its maturation requires three proteolytic processing steps, the last of which is executed by Psd1p itself and essential to generate an active decarboxylase. This self-processing event, termed autocatalysis, separates the enzyme into two subunits, α and β, and generates a pyruvoyl prosthetic group at the NH_2-terminus of the α subunit that is absolutely required for enzymatic activity (Li & Dowhan, 1988, 1990; Satre & Kennedy, 1978). Autocatalysis occurs within a conserved LGST motif between the glycine and the serine residues through a process of serinolysis (Choi, Augagneur, Ben Mamoun, & Voelker, 2012; Horvath et al., 2012; Kuge, Saito, Kojima, Akamatsu, & Nishijima, 1996; Li & Dowhan, 1988, 1990; Onguka, Calzada, Ogunbona, & Claypool, 2015). The α subunit remains non-covalently associated with the β subunit, which is anchored to the mitochondrial inner membrane so that PS decarboxylation occurs on the intermembrane space (IMS) side (Horvath et al., 2012). Aside from the conserved LGST motif, mechanistic insight into this essential self-cleaving event is limited.

We recently showed that Psd1p re-routed to the secretory pathway undergoes autocatalysis normally and is capable of rescuing the ethanolamine auxotrophy of

*psd1*Δ*psd2*Δ yeast (Onguka, Calzada, Ogunbona, & Claypool, 2015). As such, unique mitochondrial factors–protein, lipid, or other–are not required for Psd1p autocatalysis. Thus, as long as it is anchored in a membrane, everything that is needed for Psd1p autocatalysis is encoded within the polypeptide itself. Based on these results, we hypothesized that membrane anchorage of Psd1p promotes a tertiary structure that is critical for autocatalysis. As such, mutations outside the conserved LGST motif that disrupt this postulated structure would be predicted to impair autocatalysis.

With the goal of identifying novel motifs required for Psd1p autocatalysis and function, we investigated the molecular basis of the temperature-sensitive behavior of a *PSD1* allele ($Psd1^{ts}$) that has four missense mutations in the β subunit (Birner, Nebauer, Schneiter, & Daum, 2003). We hypothesized that the temperature sensitivity of $Psd1^{ts}$ was due to a defect in autocatalysis which we demonstrate to indeed be the case. Our additional results indicate that the fidelity of $Psd1^{ts}$ is closely monitored by multiple mitochondrial quality control proteases. Interestingly, the efficient degradation of the $Psd1^{ts}$ precursor requires the sequential activity of two distinct proteases with Oma1p working prior to Yme1p. In contrast, post-autocatalysis, Yme1p, which is not required for the rapid turnover of the small α subunit, is able to degrade the mature $Psd1^{ts}$ β subunit alone. We conclude that key enzyme required for the mitochondrial pathway of phosphatidylethanolamine production, Psd1p, is closely monitored at several levels and by multiple mitochondrial quality control mechanisms present in the IMS. These results further underscore the efficiency and dedication of the quality control machinery towards the preservation of membrane homeostasis within the mitochondrion.

RESULTS

Defective autocatalysis of a temperature sensitive PSD1 allele

Using error prone PCR, a temperature sensitive (*ts*) *PSD1* allele was previously established that has a growth defect at the non-permissive temperature of 37ºC (Birner et al., 2003). Psd1^{ts} harbors four missense mutations – K356R, F397L, E429G, and M448T– in the β subunit (Figure 4.1A). However, the molecular basis for the thermolability of Psd1^{ts} has never been established. We hypothesized that the introduced mutations may disrupt Psd1p autocatalysis at the restrictive temperature which would in turn prevent it from functioning in mitochondrial PE synthesis. Consistent with the original characterization of the *ts* allele (Birner et al., 2003), Psd1^{ts} supported growth of the *psd1*Δ*psd2*Δ strain in the absence of ethanolamine at 22ºC and 30ºC, but failed to do so at 37ºC (Figure 4.1B). Wild type (WT) Psd1p rescued growth of *psd1*Δ*psd2*Δ yeast in the absence of ethanolamine at all temperatures. Consistent with our hypothesis, whereas WT Psd1p was properly matured into separate β and α subunits following growth at each temperature, Psd1^{ts} had a mild autocatalytic defect at permissive temperature (22ºC) that was exacerbated at 30ºC. Following overnight growth at the restrictive temperature (37ºC), even the Psd1^{ts} precursor was not detected by immunoblot (Figure 4.1C). Interestingly, even though Psd1^{ts} α and mature β subunits were not detected by immunoblot when grown at 30ºC (Figure 4.1C), there is apparently still enough functional enzyme present to rescue the ethanolamine auxotrophy of the *psd1*Δ*psd2*Δ strain at this temperature (Figure 4.1B). Indeed, an analysis of mitochondrial phospholipids revealed that Psd1^{ts} significantly increased PE levels relative to the parental *psd1*Δ*psd2*Δ strain following overnight growth at 22ºC and 30ºC, but not at 37ºC (Figure 4.1, D and E).

Next, radiolabeled WT and *ts* Psd1 precursors were incubated with wild type mitochondria and their import and processing followed as a function of time, temperature (22ºC, 30ºC, or 37ºC), and the presence and absence of a membrane potential (Figure 4.1F). Psd1p precursor harboring a S463A mutation in the conserved LGST motif served as an autocatalysis-defective control (Onguka et al., 2015). As expected, WT Psd1p was imported into mitochondria and underwent autocatalysis in a time and membrane-potential dependent manner at every temperature tested. In contrast, $Psd1^{ts}$ was imported into mitochondria but failed to undergo autocatalysis at any temperature. Thus, *in organello* import studies of $Psd1^{ts}$ revealed a severe defect in autocatalysis even when incubated at what is a permissive temperature *in vivo*. We conclude that the four mutations introduced into the β subunit of the *ts* allele inactivate Psd1p function at the restrictive temperature by disrupting its autocatalysis.

Psd1p is a self-processing serine protease before becoming a decarboxylase

The fact that ER-targeted Psd1p undergoes autocatalysis and is functional *in vivo* (Onguka et al., 2015) indicates that everything needed for autocatalysis is self-contained within the polypeptide. Currently, the only structural motif that is known to be required for autocatalysis across many species is the conserved LGST motif (Choi et al., 2012; Horvath et al., 2012; Kuge et al., 1996; Li & Dowhan, 1988, 1990; Onguka et al., 2015). A fundamental question regarding the autocatalytic mechanism is what makes Ser463 of the LGST motif a strong nucleophile. We postulated that Psd1p serinolysis involves a catalytic triad consisting of an acid and a base present within the polypeptide. Indeed, three bases (His residues, *green*) and twelve acids (Asp, Asn, Glu, and Gln) are conserved in the β subunit of Psd1p from bacteria to humans (Figure 4.2A). Of the three conserved bases,

only mutation of His345 prevented autocatalysis (Figure 4.2B) and failed to support growth of the *psd1*Δ*psd2*Δ strain in the absence of ethanolamine (Figure 4.2C). Interestingly, His345 is flanked by the four mutations present in the *ts* allele (Figure 4.2A, *red dashes*) suggesting a plausible mechanism for how they disturb the autocatalytic process. Similar to the H345A and S463A mutants, a D210A Psd1p mutant was autocatalytically impaired and nonfunctional (Figure 4.2, D and E). These results suggest that Ser463-His345-Asp210 of yeast Psd1p form a catalytic triad typical of serine proteases. In sum, Psd1p initially functions as a self-processing serine protease whose activity unmasks its final PS decarboxylase activity.

Psd1^{ts} is an unstable polypeptide with destabilized intramolecular interactions

The mutations in Psd1^{ts} disturbed the autocatalytic process before it occurred. We wondered if these same mutations could disrupt Psd1^{ts} when shifted to the restrictive temperature post-autocatalysis. To determine the relative stability of WT and *ts* Psd1p at different temperatures, *in vivo* degradation assays were performed (Figure 4.3A). Following growth at permissive temperature to allow autocatalysis of Psd1^{ts}, cycloheximide was added to inhibit new cytosolic protein synthesis and the cultures were either maintained at 22^{o}C or shifted to 30^{o}C or 37^{o}C prior to ascertaining the abundance of Psd1p α and β subunits at varying times by immunoblot. Wild type Psd1p α and β subunits were relatively stable at each temperature (Figure 4.3, B-E). At permissive temperature, both Psd1^{ts} subunits were stable similar to WT Psd1p (Figure 4.3, B and C). In contrast, upon shifting to 30^{o}C or 37^{o}C, the stability of both Psd1^{ts} subunits was significantly reduced compared to WT Psd1p (Figure 4.3, B, D, and E). Interestingly, at 37^{o}C the α subunit of Psd1^{ts} disappeared faster than its β subunit. To extend these results, mitochondria

isolated from *psd1*Δ*psd2*Δ yeast grown at permissive temperature and expressing either WT or *ts* Psd1p were incubated at 30ºC or 37ºC for up to an hour prior to determining the levels of Psd1p α and β subunits by immunoblot (Figure 4.3, F-H). As observed *in vivo* (Figure 4.3, B and E), the steady state abundance of the Psd1^{ts} α subunit decreased more rapidly at 37ºC than the β subunit, which was itself less stable than its WT counterpart (Figure 4.3H). This suggests that at higher temperature the Psd1^{ts} β subunit might be partially unfolded leading to the release of the α subunit. Further, these results implicate mitochondrial proteases in the temperature-dependent reduction in Psd1^{ts} levels.

To begin to assess the folding status of Psd1^{ts}, a blue native-PAGE (BN-PAGE) analysis was performed. BN-PAGE is a gentle electrophoretic technique that can resolve intact protein complexes, thus providing information on the quaternary structure of a protein. Post-autocatalysis, the α and β subunits of Psd1p remain non-covalently associated. Consistent with this, both the α and β subunits of WT Psd1p co-migrated in a discrete complex of >669 kDa (Figure 4.4A, *red arrows* in the *top panels*) and as diffuse complexes centered around 140 kDa (Figure 4.4A, *red lines* in the *top panels*). In contrast, Psd1^{ts} α subunit-containing complexes were absent which caused the Psd1^{ts} β subunit-containing complexes to be slightly downshifted compared to WT (Figure 4.4A, *gray lines* in the *top right panel*). Given that its steady state abundance as determined following SDS-PAGE was similar to WT Psd1p (Figure 4.4A, *bottom panels*), the failure to detect Psd1^{ts} α subunit-containing complexes indicates that the Psd1^{ts} β and α subunit interaction is destabilized in BN-PAGE. Since the α subunit is only ~10 kDa, it would not likely be resolved in this gel system. To directly determine if the non-covalent interaction between the α and β subunits of Psd1^{ts} post-autocatalysis is impaired, 3XFLAG tagged Psd1p α was

immunoprecipitated from mitochondria isolated from yeast grown at permissive temperature and the presence of co-purified β subunit determined (Figure 4.4B). Indeed, in contrast to WT Psd1p, the β subunit of the *ts* allele was only weakly co-purified with the α subunit and a significant fraction of Psd1^{ts} β was instead detected in the unbound flow thru (Figure 4.4C). These results indicate that the interaction of the α and β subunits of Psd1^{ts} is compromised even at permissive temperature.

The α and β subunits are co-dependent

At elevated temperatures, the α subunit of Psd1^{ts} exhibited a faster rate of decay than the β subunit (Figure 4.3, E and H) suggesting that post-autocatalysis, the α subunit requires the β subunit for its stability. Whether the WT β subunit requires the α subunit for its stability has not been established. Therefore, we generated *in vivo* constructs that allow the α and the β subunits to be expressed separately (Figure 4.5A); the former targeted to the mitochondrial IMS using the mitochondrial targeting sequence from Cytochrome c1 (Glick et al., 1992). The constructs were either individually or in combination transformed into *psd1*Δ*psd2*Δ yeast. Whereas the α subunit was readily detected when expressed individually, the β subunit was virtually undetectable (Figure 4.5B). The failure of the β subunit to accumulate was not secondary to a defect in its mitochondrial import (Figure 4.5D). Interestingly, when both subunits were co-expressed, the steady state abundance of the β subunit was somewhat stabilized. To more rigorously test the ability of the α subunit to promote the stability of Psd1β *in trans*, *psd1*Δ*psd2*Δ yeast expressing Psd1β were re-transformed with either a plasmid encoding the IMS-directed α subunit subject to doxycycline repression or empty vector (Figure 4.5E). In this model, Psd1β levels were directly proportional to the amount of co-expressed IMS-α (Figure 4.5F). Since the catalytically essential pyruvoyl prosthetic group is generated by the autocatalytic process,

artificial separation of the two subunits, even if brought back together physically, failed to rescue growth of the *psd1*Δ*psd2*Δ strain in the absence of ethanolamine, as expected (Figure 4.5, C and G). Finally, we determined whether the capacity of IMS-α to promote the stability of Psd1β reflected their ability to physically interact *in trans*. Consistent with the idea that IMS-α promotes Psd1β stability through their non-covalent association, Psd1β was co-purified with 3XFLAG tagged IMS-α (Figure 4.5H). Interestingly, the ability of digitonin to extract Psd1β was improved when co-expressed with IMS-α (Figure 4.5I). The failure of digitonin to solubilize Psd1β when expressed in isolation could reflect its folding status and/or accumulation in insoluble protein aggregates. Taken together, these results indicate that pre-autocatalysis the β subunit requires the α subunit for its stability while post-autocatalysis, they are mutually co-dependent.

The i-AAA protease degrades Psd1^{ts} β subunit following its heat-induced aggregation

Yme1p forms the *i*-AAA protease which has a principal role in enforcing quality control within the mitochondrial IMS (Potting, Wilmes, Engmann, Osman, & Langer, 2010; Schreiner et al., 2012). It was previously reported that deletion of *YME1* augments Psd1p activity with a concomitant increase in mitochondrial PE levels (Nebauer, Schuiki, Kulterer, Trajanoski, & Daum, 2007). From these results it was postulated that Yme1p contributes to the proteolytic turnover of Psd1p although direct evidence of this was never provided. To ascertain if Yme1p is a determinant of Psd1p stability, *YME1* was deleted in the context of *psd1*Δ*psd2*Δ yeast expressing a given amount of WT or *ts* Psd1p (Figures 4.6A). Next, the expression of WT or *ts* Psd1p was compared following growth at 22ºC, 30ºC, and 37ºC in the presence or absence Yme1p (Figure 4.6B). Notably, in the absence of Yme1p, both WT and *ts* Psd1p precursor accumulated at every temperature (Figure

4.6B, β-α band detected by both antibodies) and the amount of WT α and β subunits detected at 37ºC was increased. The absence of Yme1p modestly rescued the autocatalytic defect of Psd1^{ts} at 30ºC but not 37ºC; at 37ºC three smaller COOH terminal containing Psd1^{ts} fragments accumulated (f1, f2, and f3). Deletion of Yme1p did not change the thermosensitivity of Psd1^{ts} (Figure 4.6C) or its assembly (Figure 4.6, D-F). These results suggest a role for Yme1p in Psd1p biogenesis, indicate that at elevated temperatures a fraction of WT Psd1p is degraded by Yme1p, and demonstrate that several Psd1^{ts} fragments are produced independent of Yme1p which is responsible for their normal removal.

When the temperature-dependent stability of WT and *ts* Psd1p was assessed post-autocatalysis *in vivo*, a striking Yme1p-dependent difference in the thermostability of the β and α subunits of Psd1^{ts} was identified (Figures 4.7, A-C). In the presence of Yme1p, the β and α subunits of Psd1^{ts} were degraded at roughly similar rates at elevated temperatures (α slightly faster than β as previously noted). However, in its absence, while the α subunit still rapidly disappeared at higher temperatures, the Psd1^{ts} β subunit was significantly stabilized (Figures 4.7, B and C). Importantly, the discordant behavior of the α and β subunits of Psd1^{ts} minus Yme1p was also observed upon *in vitro* incubation of isolated mitochondria at 37ºC (Figures 4.8, A-C). Yme1p has a documented role in resolving mitochondrial protein aggregates (Schreiner et al., 2012). Therefore, we speculated that at elevated temperatures, the folding of Psd1^{ts} β may be affected such that its interaction with α is compromised causing it to adopt an aggregation-prone state. To test this idea, the α/β association and aggregation state of WT and *ts* Psd1p was determined in isolated mitochondria kept on ice or incubated as indicated at 37ºC. The α/β association of WT and *ts* Psd1p was not noticeably affected at elevated temperatures although less total Psd1^{ts} α

and co-purified β was noted after 20min at 37ºC (Figure 4.8D). In the presence or absence of Yme1p, WT Psd1p (both subunits) was almost completely extracted by digitonin even following a 1 hr heat treatment (Figures 4.8, E-G). In contrast, whereas both *ts* subunits were readily solubilized by digitonin in the presence or absence of Yme1p when kept on ice, after only 1 hr at 37ºC, a significant fraction of Psd1^{ts} β, but not α, accumulated in TX-100 resistant protein aggregates (*red arrowheads* in Figure 4.8E, quantified in F and G). Surprisingly, the heat-induced aggregation of Psd1^{ts} β occurred even in the context of Yme1p. Given that the levels of the *ts* β subunit were decreased by ~ 77% after only 2hrs growth at 37ºC (Figure 4.3E), this suggests that aggregation of Psd1^{ts} β proceeds, and likely provokes, its ultimate removal by Yme1p. Taken together, our results support the following model (Figure 4.8H): Upon exposure to heat, Psd1^{ts} β subunits are partially denatured such that they rapidly accumulate in protein aggregates that are eventually resolved by Yme1p. The Psd1^{ts} β aggregates do not include the α subunit which is instead rapidly degraded by an unidentified mitochondrial protease upon its release from β.

Evidence of role for Yme1p in the life cycle of endogenous Psd1p

We sought to obtain evidence for the involvement of Yme1p in the stability and/or folding of endogenous Psd1p. Since the levels of WT α and β subunits detected at 37ºC was increased in the absence of Yme1p (Figure 4.6B), we first determined the expression of endogenous Psd1p following growth of WT and *yme1*Δ yeast at 30ºC and 37ºC (Figure 4.9A).

Next, we determined the aggregation status of endogenous Psd1p in WT and *yme1*Δ mitochondria isolated following growth at 30ºC or 37ºC in the presence or absence of new protein synthesis (Figure 4.9C, -/+ CHX). Very little Psd1p was detected in aggregates in

mitochondria isolated from WT yeast grown at 30ºC (Figure 4.9, C and D). In contrast, more Psd1p was aggregated when *yme1*Δ yeast were grown at this temperature, although the observed difference just failed to reach significance. Interestingly, when WT yeast were grown at 37ºC, significantly more Psd1p, as well as additional integral inner membrane proteins, was present in aggregates. In contrast, the proportion of Psd1p detected in aggregates in *yme1*Δ mitochondria did not change following growth at this temperature. Combined, these results suggest that Yme1p has a routine role in monitoring the status of Psd1p (and other inner membrane proteins), that its capacity to perform this function is impaired and/or overwhelmed at elevated temperature, and that its absence shifts the mitochondrial proteostatic equilibrium under normal growth conditions to a stressed state.

In the absence of new protein synthesis, the amount of Psd1p detected in aggregates did not change in mitochondria purified from WT and *yme1*Δ yeast, regardless of the incubation temperature (Figure 4.9, C and E). Since the proportion of Psd1p in aggregates was increased following growth of WT yeast at 37ºC with continued protein synthesis (Figure 4.9D), this suggests that the stability of mature Psd1p is not overtly sensitive to elevated temperature, a conclusion that is reinforced by the *yme1*Δ-based results. Overall, our findings support the conclusion that Yme1p is an important determinant of WT Psd1p stability. Further, they underscore the difficulty of addressing this issue in *yme1*Δ yeast that express endogenous Psd1p and highlight the value of using the *ts* Psd1p allele as a tool to isolate the importance of Yme1p, and perhaps additional quality control proteases, in monitoring Psd1p fidelity.

The removal of the Psd1^{ts} precursor requires the sequential action of two mitochondrial proteases

The three COOH terminal containing Psd1^{ts} fragments (f1, f2, and f3) that accumulated at 37^{o}C in the absence of Yme1p required continued protein synthesis (Figure 4.10A). This, combined with the simple fact that they by definition represent NH_2-terminal truncations, indicates that they are products of the Psd1^{ts} precursor. We initially hypothesized that as a serine protease, perhaps these fragments were generated by inappropriate Psd1^{ts} self-proteolysis. To test this postulate, related isogenic yeast strains were established using HI-CRISPR that express a set amount of *ts*, S463A (cannot perform autocatalysis (Figure 4.2, B and D)), or *ts*-S463A Psd1p, in the presence or absence of Yme1p (Figure 4.10B). However, a *ts* mutant unable to perform autocatalysis (*ts*-S463A) still generated these fragments (Figure 4.10, C and D), indicating that a mitochondrial protease(s) is instead likely responsible for their production.

With the goal of identifying the mitochondrial protease responsible for generating the Psd1^{ts} precursor-derived fragments, we focused on Oma1p, a stress-activated mitochondrial protease that resides in the inner membrane (Baker et al., 2014; Bohovych, Donaldson, Christianson, Zahayko, & Khalimonchuk, 2014; Rainbolt, Lebeau, Puchades, & Wiseman, 2016; Rainbolt, Saunders, & Wiseman, 2015). Using HI-CRISPR, a series of related isogenic yeast strains were established that express a set amount of WT or *ts* Psd1p in the absence of Yme1p, Oma1p, or both (Figure 4.11A). With respect to its temperature-dependent expression, maturation, and stability, WT Psd1p was insensitive to the loss of Oma1p (Figures 4.11B and 4.12, A, C, and D). Additionally, the absence of Oma1p, singly or in combination with Yme1p, did not change the thermosensitivity of Psd1^{ts} (Figure 4.11D) or its autocatalytic competency at the permissive temperature (Figure 4.11C). However, when Oma1p was missing, either by itself or together with Yme1p, the *ts* Psd1p

precursor accumulated at 37ºC while two of the three COOH terminal containing Psd1^{ts} fragments (f1 and f3) did not (Figure 4.11C, *white arrowheads*). Interestingly, post-autocatalysis, the temperature-dependent stability of both Psd1^{ts} subunits was unaffected by deletion of Oma1p (Figures 4.12, B-D). In sum, these results indicate that the degradation of a Psd1^{ts} precursor unable to undergo autocatalysis depends on the cooperative and sequential action of two inner membrane proteases, Oma1p and Yme1p (Figure 4.11E).

Oma1p-dependent generation of f1 and f3 is temperature-independent

When Yme1p is missing, the abundance of fragments f1 and f3 was increased for *ts*-S463A regardless of temperature (Figure 4.10D). This suggests that the *ts* mutations negatively impact the stability of the S463A-Psd1p precursor. Moreover, their accumulation implies that this Oma1p-dependent process can occur at both permissive and non-permissive temperatures, if in fact f1 and f3 from *ts*-S463A are produced downstream of Oma1p. To directly test this possibility, related isogenic yeast strains were established that express a set amount of *ts*, S463A, or *ts*-S463A Psd1p in the presence or absence of Yme1p (Figure 4.10B) or Oma1p (Figure 4.13, A and B). In Yme1p-replete yeast, fragment f1 was not detected for S463A and even though the amount of precursor was significantly lower following growth at 37ºC (Figure 4.13C, *white arrows*), none of the COOH-terminal containing fragments accumulated (Figures 4.10D and 4.13C). When Yme1p is not expressed, fragments f1 and f3 produced from S463A accumulated at 37ºC, providing evidence that they are degraded, but not produced, by Yme1p (Figure 4.13C, *white arrowheads*). In the absence of Oma1p, fragment f1 was not detected and the amount of f3 was reduced for S463A. For *ts*-S463A, the absence of Yme1p increased the abundance

of the *ts*-S463A precursor and fragments f1 and f3 regardless of temperature. In contrast, in the absence of Oma1p, fragment f1 was not detected and the amount of f3 was reduced for *ts*-S463A, again at both incubation temperatures (Figure 4.13, B and C, *white arrowheads*). Thus, the Oma1p-dependent generation of fragments f1 and f3 does not require thermal stress since it can occur at both permissive and non-permissive temperatures (Figure 4.13D).

The generation of f1 and f3 depends on Oma1p and requires structural perturbation of the Psd1p precursor

Finally, we wanted to determine if Oma1p activation alone is sufficient to drive the accumulation of f1 and f3 fragments from the S463A autocatalytic mutant (Figure 4.14A). Three types of stress have been shown to activate Oma1p in yeast (Bohovych et al., 2014): oxidative stress (hydrogen peroxide), membrane potential depolarization (CCCP), and membrane potential hyperpolarization (complex V inhibitor, oligomycin). As such, the ability of these agents to provoke the degradation of S463A, as well as WT and *ts* Psd1p, was determined at 22ºC (S463A and *ts* Psd1p) or 30ºC (WT Psd1p) (Figures 4.14, B-D). None of these Oma1p-activating agents either decreased the levels of the S463A precursor or increased the amounts of f1 and f3 fragments detected (Figure 4.14D). Collectively, these results indicate that activation of Oma1p by itself is insufficient to drive the degradation of the Psd1p precursor (WT, *ts*, or S463A).

DISCUSSION

Until recently, the LGST motif was the only structural motif known to be required for Psd1p autocatalysis. In this study we tested the hypothesis that mutations outside the conserved LGST motif that disturb generation of an autocatalytically competent tertiary structure would interfere with this essential self-activating event. To test this postulate, we initially focused on a previously established *ts* allele of *PSD1* that has four missense mutations in the β subunit (Birner et al., 2003) and whose temperature sensitive mechanism had not been established. Indeed, here we demonstrated that the failure of the Psd1^{ts} allele to rescue the ethanolamine auxotrophy of the *psd1*Δ*psd2*Δ strain at restrictive temperatures was due to a severe autocatalytic defect. Interestingly, the four missense mutations in Psd1^{ts} cluster near a conserved histidine (His345) that, together with Asp210 and Ser463 of the LGST motif, we demonstrated forms a classic Ser-His-Asp catalytic triad. We thus speculate that the *ts*-associated mutations compromise the ability of the Psd1^{ts} precursor to adopt a folded structure that properly juxtaposes the catalytic triad and enables autocatalysis. Our results confirm and extend conclusions derived from recent *in vitro* studies with membrane anchorless *Plasmodium knowlesi* Psd1 (Choi, Duraisingh, Marti, Ben Mamoun, & Voelker, 2015) by demonstrating that the initial serine protease activity of Psd1p is evolutionarily conserved and occurs in its native membrane environment *in vivo*.

Post-autocatalysis, the missense mutations destabilize Psd1^{ts}. Even when not exposed to heat, the four missense mutations in the *ts* β subunit weaken its non-covalent interaction with α. Further, fully processed Psd1^{ts} that was allowed to accumulate at permissive temperature was rapidly degraded upon shifting to restrictive temperature. Both

in vivo and in isolated mitochondria, the stability of the α subunit of Psd1^{ts} was more sensitive to heat than its β subunit. This is perhaps not surprising given its small size and the fact that it is anchored to the IMS side of the inner membrane through its non-covalent interaction with the β subunit, an association that is impaired for Psd1^{ts}. To probe the relationship of α and β further, we artificially separated the two parts of Psd1p and expressed them in isolation or together. In the absence of only 38 amino acids that form the COOH terminus of the Psd1p precursor and which are destined to become the α subunit, Psd1β was hardly detected. This suggests that the ability of Psd1β to fold properly is dependent on its COOH terminus. Indeed, the importance of the α subunit for Psd1β folding and stability is evidenced by the fact that an IMS-directed α subunit increased the steady state abundance of Psd1β *in trans*. Given their co-dependence, it is tempting to speculate that Psd1p function could be tightly regulated by factors that decrease the stability of the interaction between the α and β subunits. Released α subunit would be quickly removed by an as yet unidentified mitochondrial protease and since it contains the essential pyruvoyl group, Psd1p activity would be abruptly turned off.

Our efforts to identify the mitochondrial protease(s) responsible for the efficient removal of Psd1^{ts} at elevated temperatures revealed a striking difference that varied depending on the autocatalytic status of Psd1^{ts}. Whereas post-autocatalysis, Yme1p activity alone is sufficient to clear aggregated *ts* β subunits, pre-autocatalysis, Oma1p activity generates two NH_2-terminally truncated fragments that are then fully degraded by Yme1p. To our knowledge this is the first demonstration that two mitochondrial proteases function sequentially and cooperatively to degrade a terminally misfolded protein. The identity of the protease(s) working parallel to Yme1p and responsible for the rapid turnover of *ts* α at

elevated temperatures remains unresolved. An intriguing aspect of our findings is the requirement for Oma1p in resolving the misfolded Psd1^{ts} precursor but not fully matured *ts* β given that both contain the same NH_2-terminal regions. The basis for this is not immediately clear but may reflect the misfolded state obtained for an enzyme that has never properly folded *versus* one that has.

Oma1p was originally identified using a *ts* allele of Oxa1p, a polytopic inner membrane protein (Kaser, Kambacheld, Kisters-Woike, & Langer, 2003). Similar to our study, it was shown that Oma1p lacks the ability to completely degrade Oxa1^{ts} and instead generates proteolytic fragments which are normally resolved by the matrix-facing *m*-AAA protease. These results were taken as evidence that Oma1p has overlapping activity with the *m*-AAA protease, hence its name. However, it is possible that, similar to our results with the Psd1^{ts} precursor, in fact Oma1p functions upstream of the *m*-AAA protease to promote the degradation of Oxa1^{ts} at non-permissive temperature. If correct, then these results together raise the possibility that Oma1p has a general role in facilitating the disposal of proteins that are either unable to fold correctly or become misfolded because of stress.

Given that Oma1p is activated by stress (Baker et al., 2014; Bohovych et al., 2014; Rainbolt et al., 2016; Rainbolt et al., 2015), we initially expected that its involvement in the turnover of the Psd1^{ts} precursor would be temperature-dependent since 37^{o}C is deemed a stressful temperature for yeast. However, the Oma1p-dependent accumulation of f1 and f3 fragments from *ts*-S463A Psd1p in the absence of Yme1p was as evident at 22^{o}C as at 37^{o}C (Figures 4.10D and 4.13C). Thus, the temperature-dependent activation of Oma1p is not required to explain our results. Moreover, exogenous addition of Oma1p-activating

agents did not drive the accumulation of f1 and f3, or the diminution of *ts*-S463A (or WT and *ts*) precursor, at permissive temperature. When combined, these results suggest that Oma1p only detects Psd1p that has not undergone autocatalysis and that has been structurally perturbed, as in the case of unprocessed *ts* Psd1p at non-permissive temperature or the *ts*-S463A variant regardless of temperature. While the accumulation of f1 and f3 is Oma1p-dependent, it is unclear if Oma1p itself needs to be activated. Potentially, a small fraction of Oma1p is always basally active (Figure 4.14E, Model 1). According to this scenario, Oma1p can respond whenever a suitable substrate is encountered. Alternatively, perhaps the folding status of a substrate can itself trigger Oma1p activation (Figure 4.14E, Model 2). In this case, any treatment that perturbs the structure of a potential substrate would have the innate capacity to stimulate a protease involved in its subsequent clearance.

In mammals, OMA1 and YME1L work in parallel to regulate mitochondrial dynamics by processing long isoforms of OPA1, a dynamin-related GTPase that mediates inner membrane fusion, into short forms (Anand et al., 2014; Duvezin-Caubet et al., 2006; Ehses et al., 2009; Griparic, Kanazawa, & van der Bliek, 2007; Head, Griparic, Amiri, Gandre-Babbe, & van der Bliek, 2009; Song, Chen, Fiket, Alexander, & Chan, 2007). However, where and when these proteases cleave OPA1 and the functional consequences of their processing are different. Robust OXPHOS activity stimulates inner membrane fusion that requires YME1L mediated cleavage of OPA1 (Mishra, Carelli, Manfredi, & Chan, 2014). In contrast, when mitochondrial function is challenged by various types of stress, inner membrane fusion is inhibited by the complete processing of long OPA1 isoforms at a different site by OMA1 (Anand et al., 2014; Baker et al., 2014; Griparic et al., 2007; Head et al., 2009; Korwitz et al., 2016). Intriguingly, following mitochondrial

depolarization, YME1L and OMA1 reciprocally degrade each other depending on cellular ATP levels (Rainbolt et al., 2016; Rainbolt et al., 2015). Cleavage of a long OPA1 isoform is performed by YME1L or OMA1 but not by both proteases (Anand et al., 2014; Ehses et al., 2009; Griparic et al., 2007; Head et al., 2009; Song et al., 2007). In contrast, we demonstrate here that Oma1p and Yme1p function sequentially to cooperatively degrade a common substrate that if left unresolved could compromise mitochondrial proteostasis. Thus, it would appear that depending on the substrate and/or cellular context, Yme1p and Oma1p can work alone, together, or antagonistically to ensure mitochondrial health.

Our work extends an emerging story of an intimate relationship between mitochondrial phospholipid metabolism and the quality control machinery therein. Mitochondrial phospholipid synthesis requires transport pathways for lipid precursors and products across the aqueous IMS and leaflets of a bilayer. Ups1p and Ups2p, each in association with Mdm35p (Potting et al., 2010; Yasushi Tamura, Iijima, & Sesaki, 2010), contribute to the flux of PA and PS across the IMS by grabbing their lipid ligands in the outer membrane and transporting them to the inner membrane (Aaltonen et al., 2016; Connerth et al., 2012; Miyata, Watanabe, Tamura, Endo, & Kuge, 2016). In so doing, they help provide substrates for CL and PE synthesis. Interestingly, both Ups proteins have, for mitochondrial proteins, unusually short half-lives which is explained by their constitutive degradation by Yme1p and/or Atp23p (Potting et al., 2010). Previously, we demonstrated that Yme1p has a critical role in degrading certain Barth syndrome associated mutants of the monolyso-CL transacylase, tafazzin which retain some enzymatic activity but are prone to aggregation (Claypool, Whited, Srijumnong, Han, & Koehler, 2011). And in the present study we have documented a role for Yme1p in the biogenesis of Psd1p (the Psd1p

precursor accumulates in its absence), the turnover of an aggregation-prone allele of the β subunit post-autocatalysis, and the stability of endogenously expressed WT Psd1p. Further, we demonstrated that two proteases, Oma1p and Yme1p, work sequentially to remove a Psd1^{ts} precursor that is unable to fully mature. A common feature for these lipid-related proteins is that they each work in or at the boundary between the hydrophilic surface and hydrophobic core of membranes, a denaturing environment. As such, we posit that the structurally destabilizing environment in which mitochondrial lipid metabolizing and transport proteins work has provoked the mitochondrial quality control machinery as a whole to evolve multiple means to monitor their fidelity.

Very recently, a novel tumor suppressor, LACTB, was discovered that when overexpressed in certain cancer cell lines, reduces cell proliferation and increases cellular differentiation *via* a mechanism that is at least in part explained by a significant decrease in the levels of PISD, the mammalian Psd1p equivalent (Keckesova et al., 2017). Importantly, the decrease in PISD abundance is post-transcriptionally mediated and results in significant reductions in certain PE and lyso-PE species. However, the actual mechanism of PISD turnover was not determined. These findings clearly establish that the post-transcriptional regulation of PISD is clinically relevant. Moving forward, it will be interesting to determine if some of the proteolytic pathways that we have identified in yeast using *ts* Psd1p are harnessed in certain physiological and/or pathophysiological contexts to regulate mammalian PISD levels, and by extension, the phenotype of cells.

MATERIALS AND METHODS

Yeast strains and growth conditions

All yeast strains used in this study were derived from GA74-1A (*MAT*a, *his3-11,15*, *leu2*, *ura3*, *trp1*, *ade8* [*rho*$^{+}$, *mit*$^{+}$]). *psd1*Δ (*MAT*a*, trp1*, *leu2, ura3, ade8, psd1*Δ::*HISMX6*), *psd1*Δ*psd2*Δ (*MAT*a, *leu2, ura3, ade8, psd1*Δ::*TRP1*, *psd2*Δ::*HISMX6*), and *yme1*Δ (*MAT*a*, trp1*, *leu2, ura3, ade8, yme1*Δ::*HISMX6*) have been described previously (Hwang, Claypool, Leuenberger, Tienson, & Koehler, 2007; Onguka et al., 2015). *psd1*Δ*psd2*Δ*yme1*Δ and *psd1*Δ*psd2*Δ*oma1*Δ were generated by taking *psd1*Δ*psd2*Δ or *psd1*Δ*psd2*Δ with WT, *ts*, *S463A*, or *ts-S463A PSD1* integrated into the Leu2 locus and using a CRISPR-cas9 gene block targeted against *YME1 or OMA1*. Specifically, *yme1* and *oma1* knockout were achieved using the Homology-Integrated CRISPR-Cas (HI-CRISPR) system (Bao et al., 2015). The plasmid pCRCT was a gift from Huimin Zhao (Addgene plasmid # 60621). The CRISPR-Cas9 target for *YME1*and *OMA1* were selected using the yeastriction (yeastriction.tnw.tudelft.nl) (Mans et al., 2015) and Benchling (www.benchling.com) online CRISPR guide design tools. The CRISPR construct was designed to recognize residues 12-31 on the forward strand of *YME1* and residues 118-137 on the reverse strand of *OMA1* (position 1 is the adenine of the AUG site). A 100bp homology repair template was designed to have 50bp homology arms on both sides flanking the Cas9 cutting site and incorporated an 8bp deletion so as to induce a frame shift mutation as described (Bao et al., 2015). *psd1*Δ*psd2*Δ*yme1*Δ*oma1*Δ strains were generated from the corresponding *psd1*Δ*psd2*Δ*yme1*Δ strains. The spacer sequences (including the CRISPR-Cas9 target and the homology repair template) were ordered as gBlocks (Integrated DNA Technologies) and assembled into the pCRCT plasmid using the Golden

Gate assembly method (Engler, Gruetzner, Kandzia, & Marillonnet, 2009). *OMA1* disruption was confirmed by DNA sequencing.

Yeast cells were grown in either rich lactate (1% yeast extract, 2% tryptone, 0.05% dextrose, 2% lactic acid, 3.4 mM $CaCl_2$-$2H_20$, 8.5 mM NaCl, 2.95 mM $MgCl_2$-$6H_20$, 7.35 mM KH_2P0_4, 18.7 mM NH_4Cl, pH 5.5) or YPD (1% yeast extract, 2% peptone, 2% dextrose). To assess the function of the assorted Psd1p constructs and mutants, overnight cultures grown in YPD were spotted on synthetic complete dextrose plates in the absence or presence of 2 mM ethanolamine, and grown at 30ºC or the indicated temperature. Steady state labeling of mitochondrial phospholipids was achieved by growing yeast for 24 hours at the indicated temperature in synthetic complete dextrose medium supplemented with 2 mM choline and 2.5 μCi/ml $^{32}P_i$. To activate Oma1p, starter cultures grown in YPD at the permissive temperature were used to inoculate fresh tubes with 1 OD_{600}/2ml YPD, which were spiked with nothing, 4 mM H_2O_2, 45 μM carbonyl cyanide *m*-chlorophenyl hydrazine, or 4 μM Oligomycin, and then incubated for 4 hours at 22ºC (*ts* and S463A Psd1p) or 30 ºC (WT Psd1p), shaking at 220 rpm, prior to yeast protein extraction.

Psd1p with a COOH-terminal 3XFLAG tag subcloned into pRS315 and pRS305 or harboring 6 COOH-terminal methionines and subcloned into pSP64 have been described (Onguka et al., 2015). The 6 Methionine residues added to the COOH-terminus allow detection of the α subunit post-autocatalysis in *in vitro* experiments while the addition of the 3XFLAG tag enables detection of the α subunit post-autocatalysis *in vivo*. *PSD1* point mutations were generated by overlap extension (Ho, Hunt, Horton, Pullen, & Pease, 1989) using pRS305Psd3XFLAG as template. The temperature sensitive *PSD1* allele (K356R, F397L, E429G, and M448T) was described previously (Birner et al., 2003) and assembled

here in the context of pRS305Psd3XFLAG by overlap extension. Psd1β was generated by introducing a stop codon immediately after Gly462 and cloned into pRS315. To target the α subunit to the IMS, α-3XFLAG (starting at S463) was placed downstream of the first 64 amino acids of cytochrome c1 but still under control of the *PSD1* promoter by overlap extension and cloned into pRS316. IMS-α was subcloned into pCM189 to allow Doxycycline based repression. For inducible expression of IMS-α, starter cultures grown in SC-Leu-Ura + Ethanolamine (0.17% yeast nitrogen base, 0.5% ammonium sulfate, 0.2% drop out mix complete, 2 mM ethanolamine, 2% dextrose) were used to inoculate fresh SC-Leu-Ura +Ethanolamine cultures, with or without 10 μg/ml doxycycline, which were grown overnight shaking at 220 rpm at 30ºC.

***In organello* import**

Radiolabeled precursors were produced using an SP6 Quick Coupled Transcription/Translation system (Promega) spiked with ^{35}S Easy-Tag (PerkinElmer). Import of radiolabeled precursors utilized mitochondria isolated from D273-10B grown in rich lactate and was performed as described previously (Claypool et al., 2011; Onguka et al., 2015). Where indicated, valinomycin (1 μM) and carbonyl cyanide *m*-chlorophenyl hydrazine (5 μM) were added 5 min prior to precursor addition to collapse the mitochondrial proton motive force. Upon addition of radiolabeled precursor, import reactions were incubated at the designated temperature. At the indicated times, import was stopped with an equal volume of ice-cold BB7.4 (0.6 M sorbitol and 20 mM Hepes-KOH, pH 7.4), and mitochondria were re-isolated by spinning at 21,000 *xg* for 5 min at 4°C. 100% of each time point and 5% of imported precursors were resolved on 15% SDS-PAGE gels and analyzed by phosphoimaging.

In vivo degradation experiments

In vivo degradation experiments were performed as previously described (Claypool et al., 2011). In brief, following growth at the permissive temperature, fresh tubes were inoculated with 6 OD_{600}/3ml YPD and incubated for 5 minutes at the permissive temperature. Cycloheximide was added to a final concentration of 200 μg/ml to inhibit cytosolic protein synthesis and cultures incubated at the indicated temperature shaking at 220 rpm. At each time point, 1 OD_{600} equivalents was transferred to a tube containing an equal volume of ice-cold 2X azide mix (20-mM NaN3 and 0.5 mg/ml BSA). Cells were collected (845 *xg* for 10 min at 4°C), the supernatant removed, and the pellets stored at -80ºC until all the time points were harvested. Proteins were extracted and SDS-PAGE and immunoblot performed as previously described (Claypool, Dickinson, Yoshida, Lencer, & Blumberg, 2002; Claypool, McCaffery, & Koehler, 2006).

In organello heat shock assay

Mitochondria isolated from yeast grown at permissive temperature were incubated at the indicated temperature for the designated times. Mitochondria were harvested by spinning at 21,000 *xg* for 5 min at 4°C and either further analyzed or resuspended in reducing sample buffer, boiled at 100ºC for 5 minutes, resolved on custom made 10-16% SDS-PAGE gels, and analyzed by immunoblot.

Immunoprecipitation

Mitochondria (0.2 mg) were solubilized (2.5 mg/ml) for 30 min on ice with 20 mM Hepes-KOH, pH 7.4, 20 mM imidazole, 10% glycerol, 100 mM NaCl, and 1 mM $CaCl_2$, supplemented with 1.5% (wt/vol) digitonin (Biosynth International, Inc.) and protease inhibitors (1 mM PMSF,10 μM leupeptin, and 2 μM pepstatin A). Clarified extracts

(21,000 *xg* for 30 min at 4°C) were diluted to 0.24% digitonin with lysis buffer base and incubated with 15µl anti FLAG Affinity Gel (Genscript) rotating at 4ºC for 2hrs. Following a low speed spin, 0.1 mg of unbound material was transferred to a tube, TCA precipitated and processed for SDS-PAGE. The bound material was subjected to three 10 minute washes (1st: 0.1% Digitonin Wash buffer; 2nd: 0.1% Digitonin Wash buffer with 250 mM NaCl; 3rd: 0.1% Digitonin No Salt) and processed for SDS-PAGE.

Antibodies

Most antibodies used in this study were generated in our laboratory or in the laboratories of J. Schatz (University of Basel, Basel, Switzerland) or C. Koehler (UCLA) and have been described previously (Claypool et al., 2011; Hwang et al., 2007; Onguka et al., 2015; Y. Tamura et al., 2012; Whited, Baile, Currier, & Claypool, 2013). Other antibodies used were mouse anti-FLAG (clone M2, Sigma), horseradish peroxidase–conjugated (Fig. 2, 4, 5, 6D, 6E, and 8D) or fluorescent-conjugated (Fig. 1C, 3B, 3F, 6B, 7A, 8B, 8E, 9C, 10A, 10D, 11B, 11C, 12A,12D, 13C, and 14, B-D) secondary antibodies (Pierce).

Miscellaneous

Isolation of mitochondria, 1D BN-PAGE, detergent-based aggregation, phospholipid analyses, and immunoblotting were performed as previously described (Claypool, Boontheung, McCaffery, Loo, & Koehler, 2008; Claypool et al., 2006; Claypool et al., 2011; Hwang et al., 2007; Onguka et al., 2015; Y. Tamura et al., 2012; Whited et al., 2013). Statistical comparisons were performed by *t* test or one-way analysis of variance (ANOVA) with Holm-Sidak pairwise comparison using SigmaPlot 11 software (Systat Software, San Jose, CA); $P \leq 0.05$ were deemed significant. All graphs show the mean ± S.E.M.

ACKNOWLEDGEMENTS

We would like to thank Drs. Jeff Schatz and Carla Koehler for antibodies, Dr. Sin Urban (JHMI) for the suggestion that the serine of the LGST motif may be part of a catalytic triad, and Pingdewinde N. Sam and James O. Owusu (Department of Physiology, Johns Hopkins University School of Medicine) for technical assistance. This work was supported by National Institutes of Health Grants (R01GM111548) to S.M.C. and Biochemistry, Cellular, and Molecular Biology Program Training Grant (T32GM007445) to O.O. and E.C., and a pre-doctoral fellowship from the American Heart Association (15PRE24480066) to O.B.O. The authors declare no competing financial interests.

FIGURES

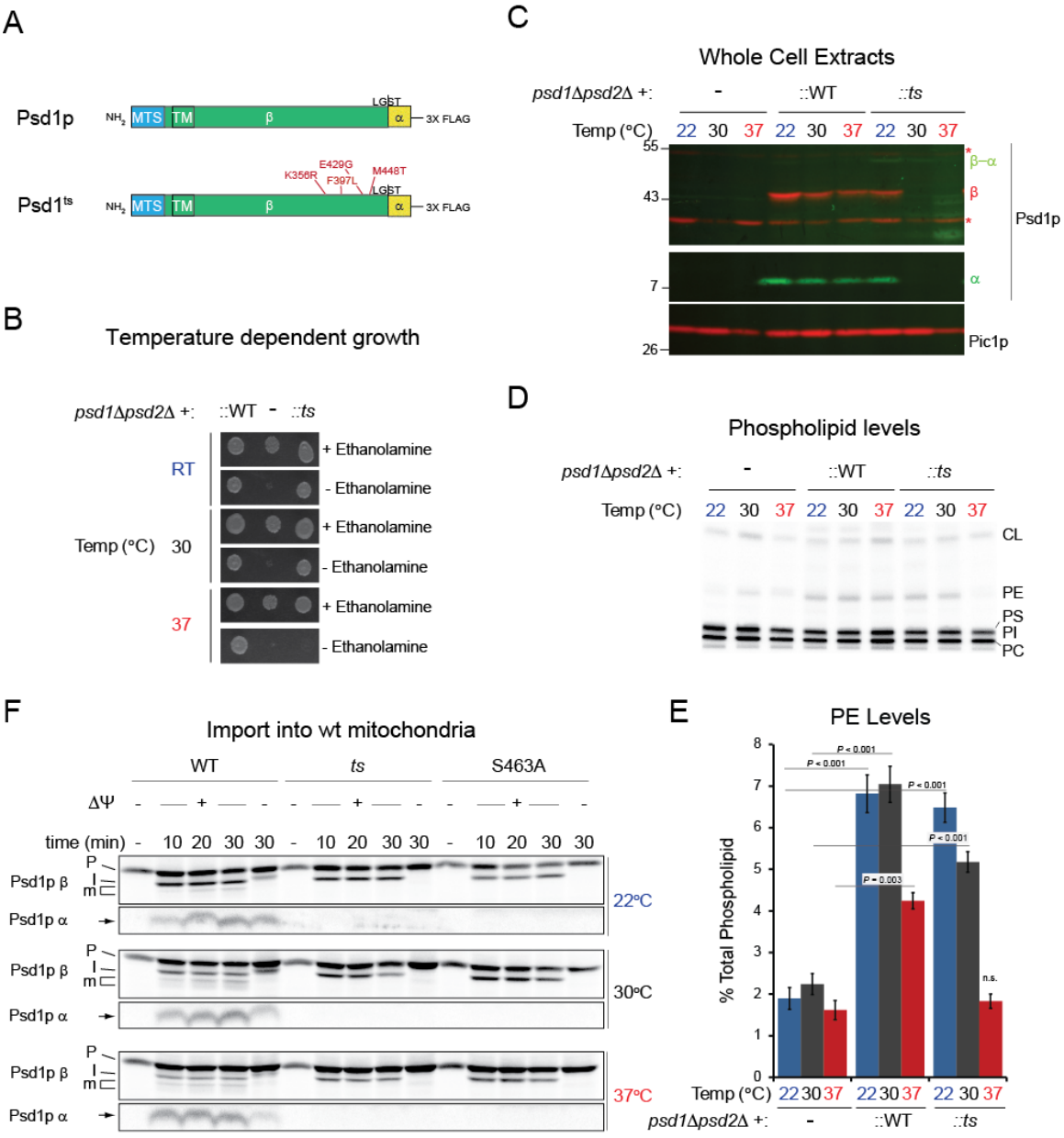

Figure 4.1. Psd1^{ts} has a temperature sensitive autocatalytic defect. (A) Schematic of *in vivo* Psd1p constructs. The missense mutations in Psd1^{ts} are indicated. MTS, mitochondrial targeting signal; TM, transmembrane domain. (B) The indicated strains pre-cultured at 22ºC were spotted onto synthetic complete dextrose (SCD) +/- 2mM ethanolamine and incubated at 22ºC, 30ºC, or 37ºC for 3 days. (C) The α and β subunits of

Psd1p were analyzed by immunoblot in whole cell extracts isolated from cultures grown at the indicated temperature; Pic1p served as a loading control. β-α, Psd1p that has not performed autocatalysis. (D) After steady-state labeling with $^{32}P_i$ in SCD +/- 2mM choline at the designated temperature, phospholipids were extracted from mitochondria isolated from the indicated strains and separated by TLC. The migration of phospholipids is indicated (PC, phosphatidylcholine; PI, phosphatidylinositol; CL, cardiolipin. (E) The relative abundance of PE was determined for each strain at each temperature and is expressed as a % of the total phospholipid for each strain at a given temperature (mean ± SEM, $n = 6$). For the 22ºC and 30ºC samples, significant differences were determined by One Way ANOVA, with Holm–Sidak pairwise comparisons and are indicated; for the 37ºC samples, the indicated significant differences were determined by Kruskal-Wallis One Way ANOVA on Ranks**,** with Tukey Test pairwise comparisons. n.s. = Not Significant. (F) *In vitro* import of [^{35}S] methionine-labeled WT, *ts*, or S463A Psd1p autocatalytic mutant into wild type mitochondria at 22ºC, 30ºC, and 37ºC and in the presence (+ΔΨ) or absence (-ΔΨ) of the proton motive force across the inner membrane. 5% of each precursor (-) and 100% of every time point were analyzed. P, precursor; I, import intermediate; m, mature β subunit.

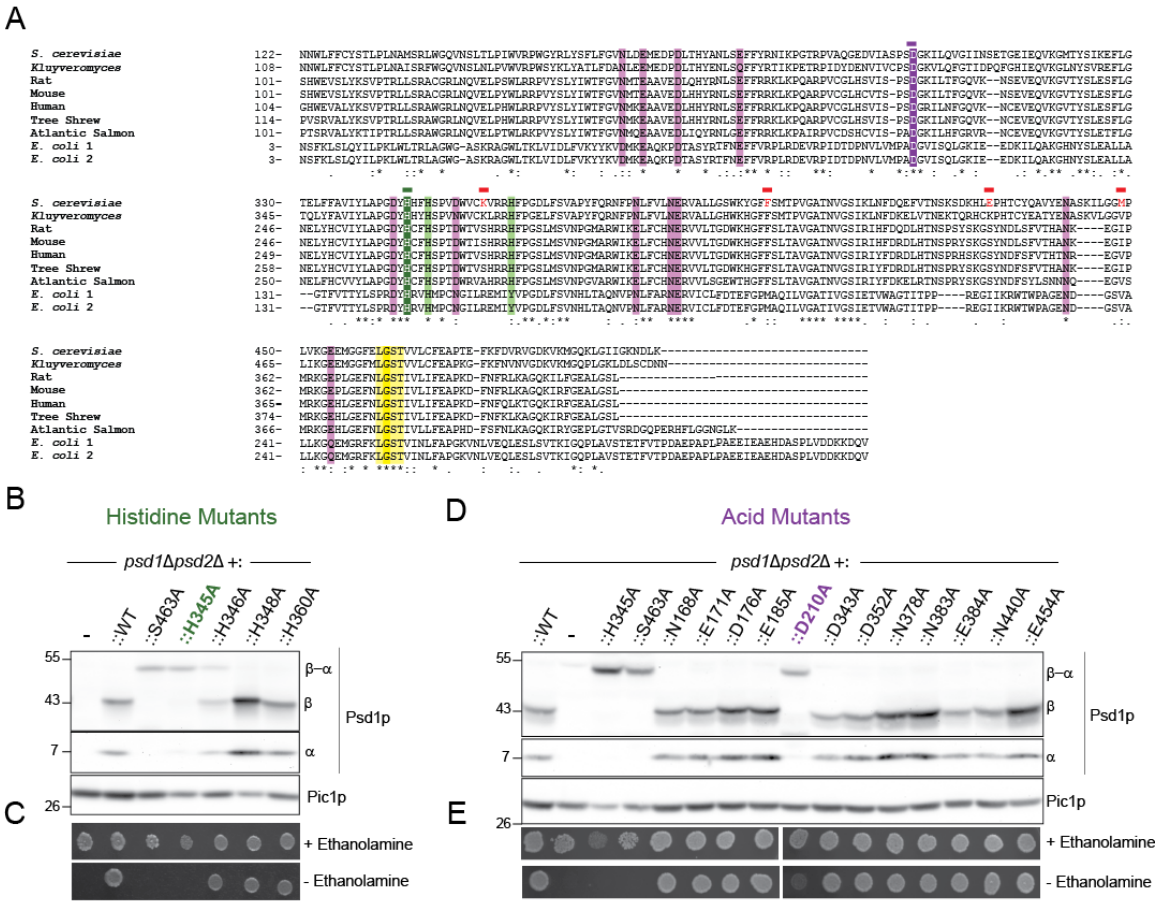

Figure 4.2. Identification of an (auto)catalytic triad in Psd1p. (A) Clustal Omega sequence alignment of Psd1p from the indicated species. Conserved potential bases (His residues; highlighted in *green*) and acids (Asp, Asn, Glu, and Gln; highlighted in *purple*) are indicated. The LGST motif is shown in *yellow*. The position of the four missense alleles present in Psd1^{ts} are marked with *red line*. The determined base His345 and acid Asp210 are designated with darker shading and *green* and *purple lines*. (B and D) *psd1*Δ*psd2*Δ yeast (-) and *psd1*Δ*psd2*Δ yeast transformed with the indicated Psd1p construct were grown overnight in SCD supplemented with 2 mM ethanolamine. The α and β subunits of Psd1p were detected in whole cell extracts by immunoblot; Pic1p served as a loading control. (C and E) *psd1*Δ*psd2*Δ yeast (-) and *psd1*Δ*psd2*Δ yeast transformed with the indicated Psd1p

constructs were spotted onto SCD plates +/- 2 mM ethanolamine and incubated at 30ºC for 4 days.

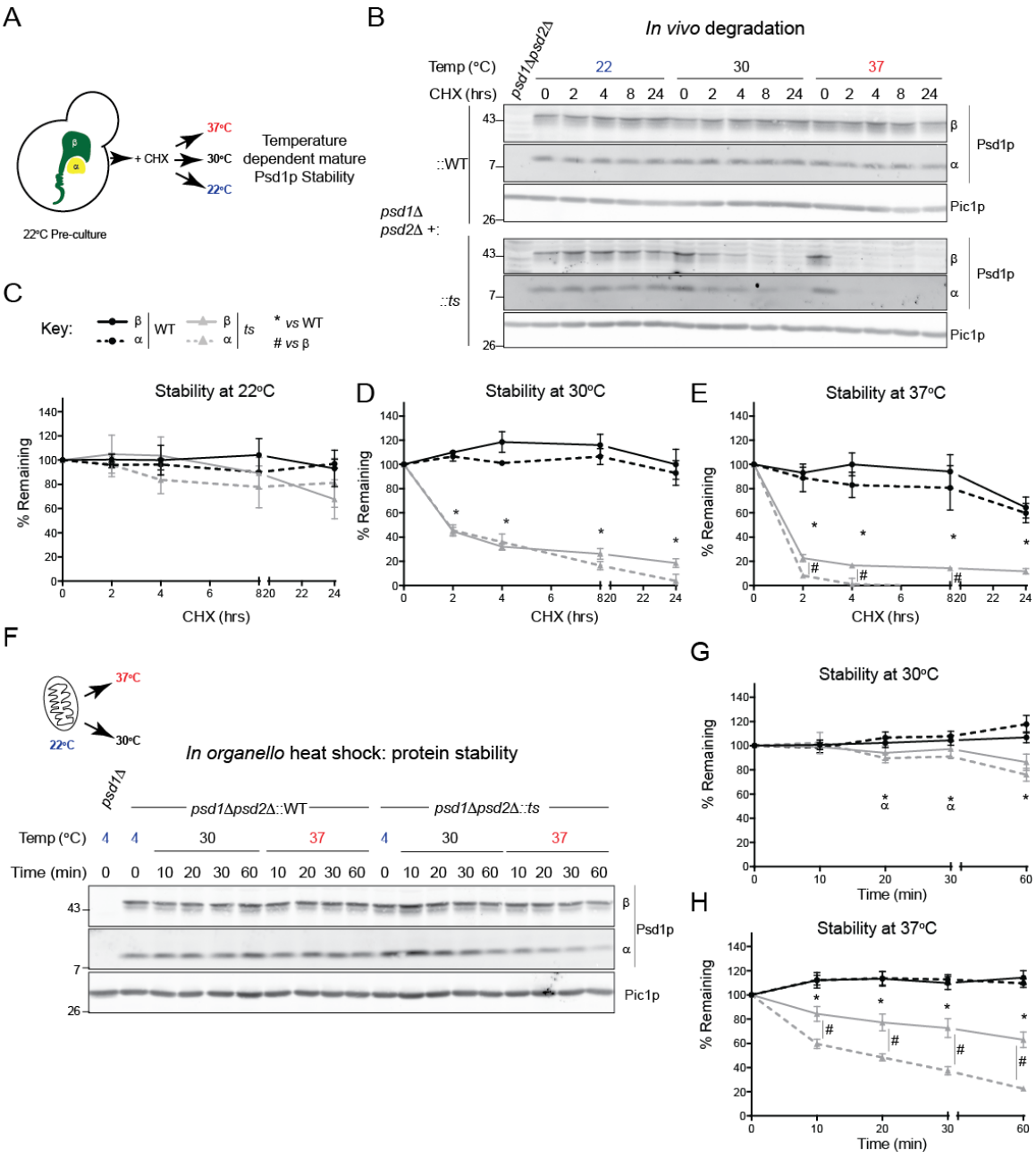

Figure 4.3. Psd1^{ts} is unstable at non-permissive temperature. (A) *In vivo* degradation assay. (B) Whole cell extracts were isolated at the designated times following growth at the indicated temperature in the presence of cycloheximide (CHX). Samples were resolved by SDS-PAGE and immunoblotted as indicated. The α and β subunits of WT and *ts* Psd1p remaining at each timepoint at (C) 22ºC, (D) 30ºC, and (E) 37ºC were quantified and

plotted as the % of protein remaining compared to t = 0. Mean ± SEM, *n*=4 * and # P≤0.05 (Student's t-test). (F) Mitochondria isolated from *psd1*Δ*psd2*Δ expressing WT or *ts* Psd1p at 22ºC were heat treated as indicated. Following incubation for the designated times, mitochondria were recovered and 50 μg resolved by SDS-PAGE and immunoblotted as indicated. The % of Psd1 β and α subunit remaining at each timepoint at (G) 30ºC and (H) 37ºC was quantified. Mean ± SEM, *n*=6 * and # P≤0.05 (Student's t-test).

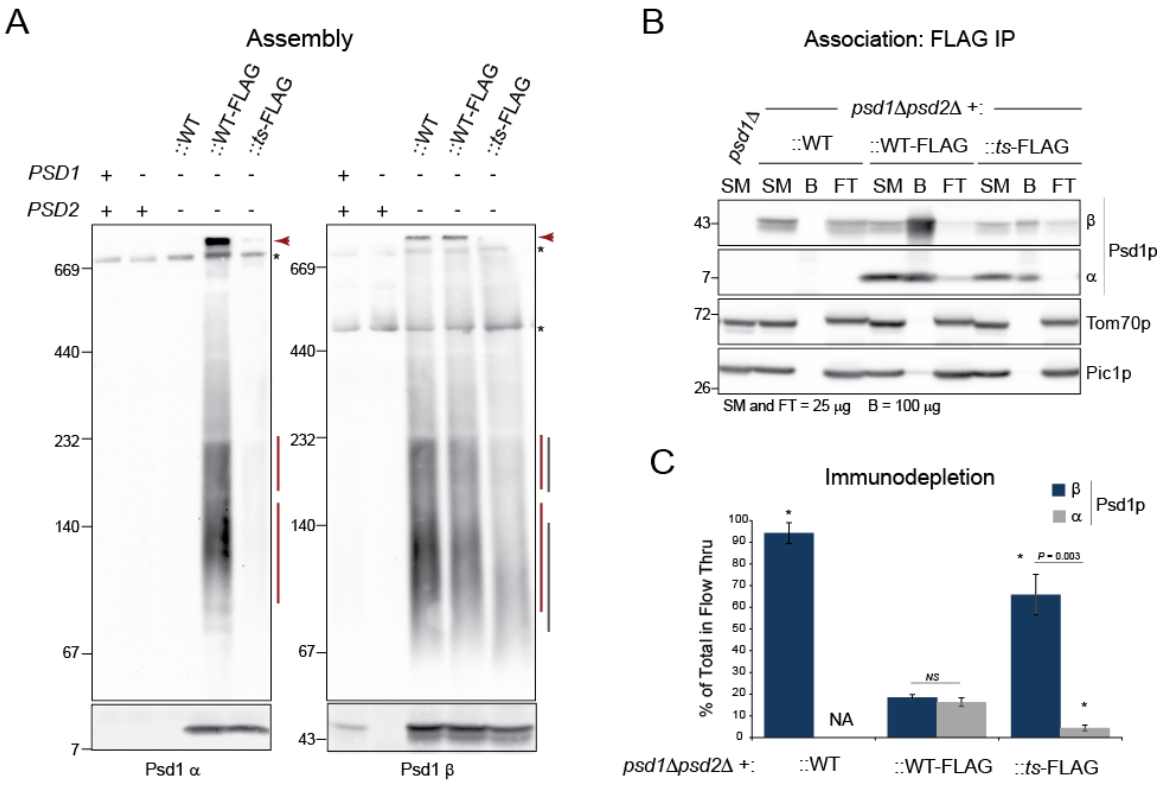

Figure 4.4. Association of α and β subunits is destabilized in Psd1^{ts}. (A) Mitochondria isolated at permissive temperature from *psd1*Δ*psd2*Δ yeast expressing FLAG tagged WT or *ts* Psd1p, or untagged WT Psd1p, were solubilized with 1.5% (wt/vol) digitonin, separated by 6-16% BN-PAGE, and immunoblotted for the α or β subunit. *Lower panels* show immunoblots following SDS-PAGE. *Red arrows* and *lines* mark Psd1p complexes that are detected by antibodies against both the α and β subunits; *gray lines* designate *ts* Psd1p complexes that migrate faster and are only detected with the β subunit antisera; *asterisks* highlight background bands identified in *psd1*Δ mitochondrial extracts. (B) Following solubilization with 1.5% (wt/vol) digitonin, anti-FLAG resin was used to immunoprecipitate the FLAG tagged α subunit and the presence of co-purified β determined by immunoblot; Tom70p and Pic1p served as controls. SM, starting material; B, bound material; FT, non-binding flow thru. (C) The percentage of each subunit detected

in the non-binding flow thru was determined as follows: FT/SM x 100, where FT is the volume of Psd1p α or β subunit detected in the flow thru and SM is the volume associated with the corresponding starting material. Mean ± SEM, *n*=3. Student's t-test were used to compare the α and β subunits. * P<0.001 versus FLAG tagged WT Psd1p (One-way ANOVA, with Holm-Sidak pairwise comparisons).

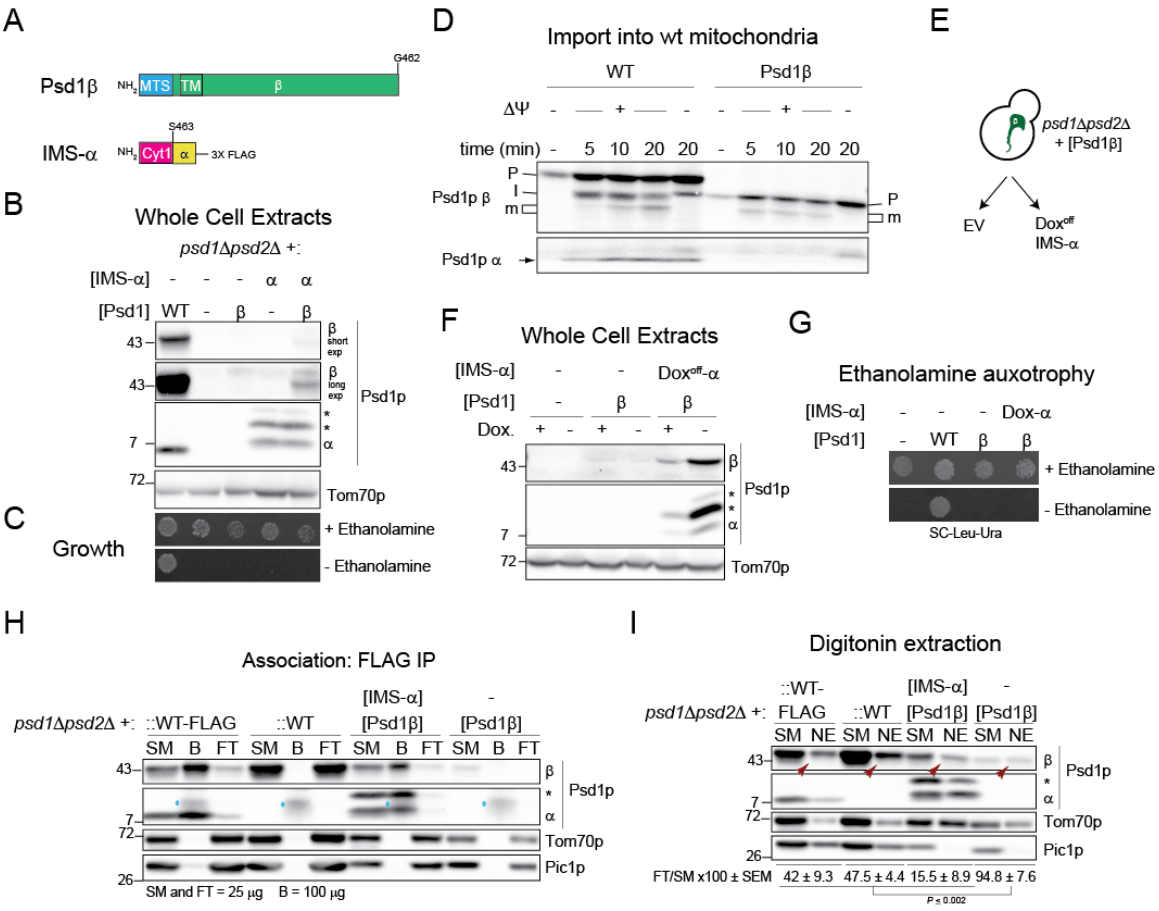

Figure 4.5. Pre-autocatalysis, Psd1 β requires α for stability. (A) Schematic of *in vivo* constructs to individually express the β and α subunits. The stop-transfer signal of cytochrome c1 is indicated in *pink*. (B) Whole cell extracts from *psd1*Δ*psd2*Δ yeast transformed as indicated were resolved by SDS-PAGE and immunoblotted for the α and β subunits; Tom70p served as a loading control. * highlight IMS-targeted α subunit that has not been fully processed. (C) In parallel, the same yeast were spotted onto SC-Leu-Ura +/- 2mM ethanolamine and incubated at 30ºC for 3 days. (D) *In vitro* import of [^{35}S] methionine-labeled WT or Psd1 β into wild type mitochondria at 30ºC in the presence (+ΔΨ) or absence (-ΔΨ) of the proton motive force. 5% of each precursor (-) and 100% of every time point were analyzed. P, precursor; I, import intermediate; m, mature β subunit. (E) *psd1*Δ*psd2*Δ expressing Psd1β were transformed further as indicated. (F) Immunoblots

for the α and β subunits in the indicated whole cell extracts; Tom70p served as a loading control. * highlight IMS-targeted α subunit that has not been fully processed. (G) In parallel, the same yeast were spotted onto SC-Leu-Ura +/- 2mM ethanolamine and incubated at 30^{o}C for 3 days. (H) Following solubilization of the designated mitochondria with 1.5% (wt/vol) digitonin, anti-FLAG resin was used to immunoprecipitate the FLAG tagged α subunit and the presence of co-purified β determined by immunoblot; Tom70p and Pic1p served as controls. SM, starting material; B, bound material; FT, non-binding flow thru. A background band detected in each Bound lane detected in the FLAG immunoblot is marked with a *blue circle*. (I) To determine digitonin solubilization efficiency, 25 μg of starting material (SM) and non-extracted (NE) pellet post-digitonin solubilization was resolved by SDS-PAGE and immunoblotted as indicated. A decreased signal intensity in the NE lanes (*red arrowheads*) relative to the corresponding SM lanes reflects the fraction of each protein that was extracted by digitonin. The percentage of Psd1 β not extracted by digitonin is shown below the *bottom panel* and was determined as follows: NE/SM x 100, where NE is the volume of Psd1 β subunit detected in NE and SM is the volume associated with the corresponding starting material. Mean ± SEM, n=3 Significant differences were measured by One-way ANOVA, with Holm-Sidak pairwise comparisons.

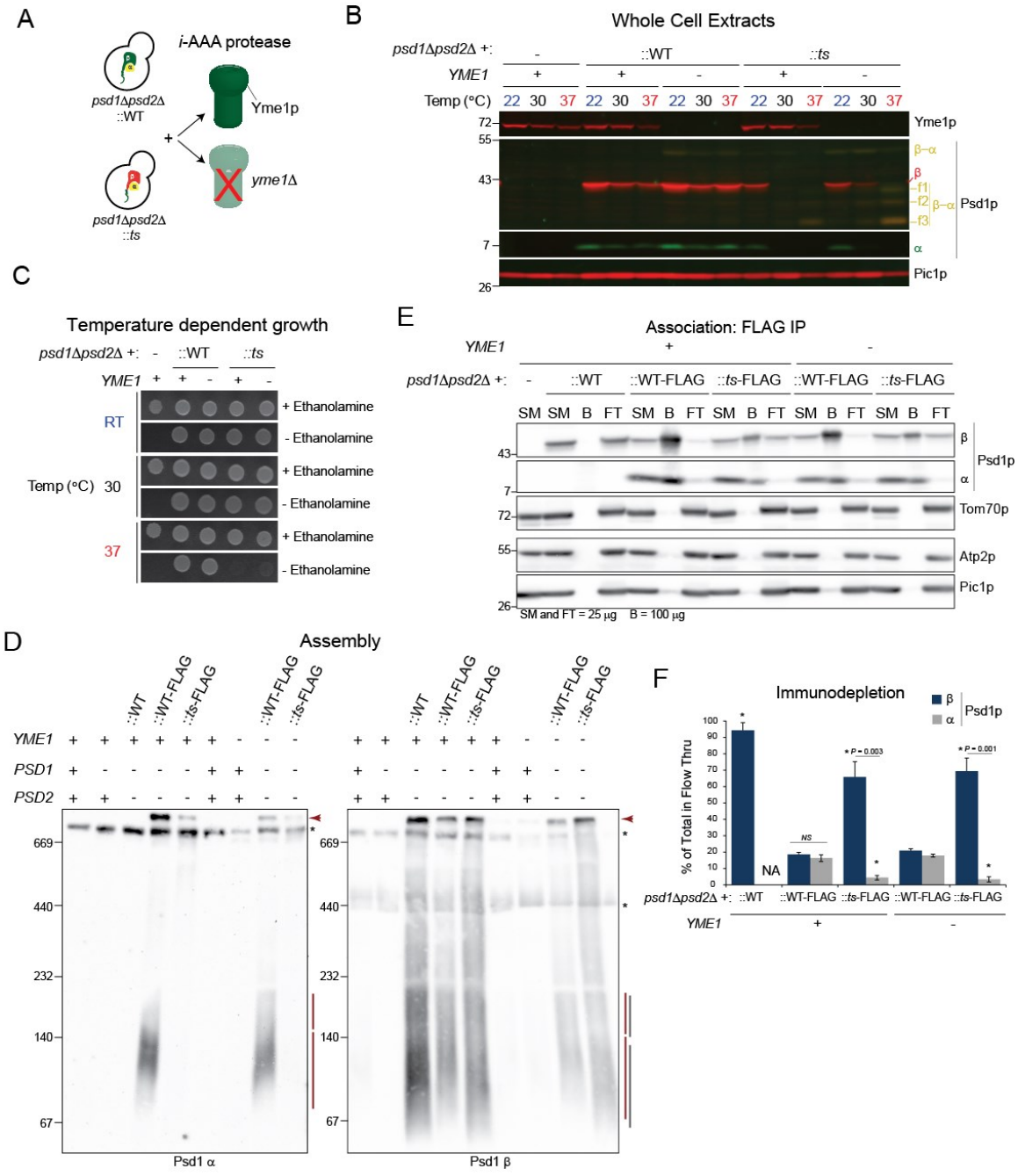

Figure 4.6. Three COOH terminal containing Psd1^{ts} fragments accumulate in the absence of Yme1p. (A) Schematic for generating strains expressing a set amount of WT or *ts* Psd1p in the presence or absence of Yme1p. (B) Immunoblots for Yme1p and the α and β subunits of WT and *ts* Psd1p in the indicated whole cell extracts from yeast grown at listed temperature; Pic1p served as a loading control. β-α, Psd1p that has not performed

autocatalysis. f1, f2, and f3, COOH terminal containing Psd1^{ts} fragments. (C) The indicated strains pre-cultured at 22ºC were spotted onto SCD +/- 2mM ethanolamine and incubated at 22ºC, 30ºC, or 37ºC for 3 days. (D) Mitochondria isolated at permissive temperature from *psd1*Δ*psd2*Δ yeast expressing FLAG tagged WT or *ts* Psd1p, or untagged WT Psd1p, in presence or absence of Yme1p, were solubilized with 1.5% (wt/vol) digitonin, separated by 6-16% BN-PAGE, and immunoblotted for the α subunit or β subunit. *Red arrows* and *lines* mark Psd1p complexes that are detected by antibodies against both the α and β subunits; *gray lines* designate *ts* Psd1p complexes that migrate faster and are only detected with the β subunit antisera; *asterisks* highlight background bands identified in Δ*psd1* mitochondrial extracts. (E) Following solubilization with 1.5% (wt/vol) digitonin, anti-FLAG resin was used to immunoprecipitate the FLAG tagged α subunit and the presence of co-purified β determined by immunoblot; Tom70p, Atp2p, and Pic1p served as controls. SM, starting material; B, bound material; FT, non-binding flow thru. (F) The percentage of each subunit detected in the non-binding flow thru was determined as follows: FT/SM x 100, where FT is the volume of Psd1p α or β subunit detected in the flow thru and SM is the volume associated with the corresponding starting material. Mean ± SEM, n=3 Student's t-test were used to compare the α and β subunits. * P<0.001 versus FLAG tagged WT Psd1p (One-way ANOVA, with Holm–Sidak pairwise comparisons).

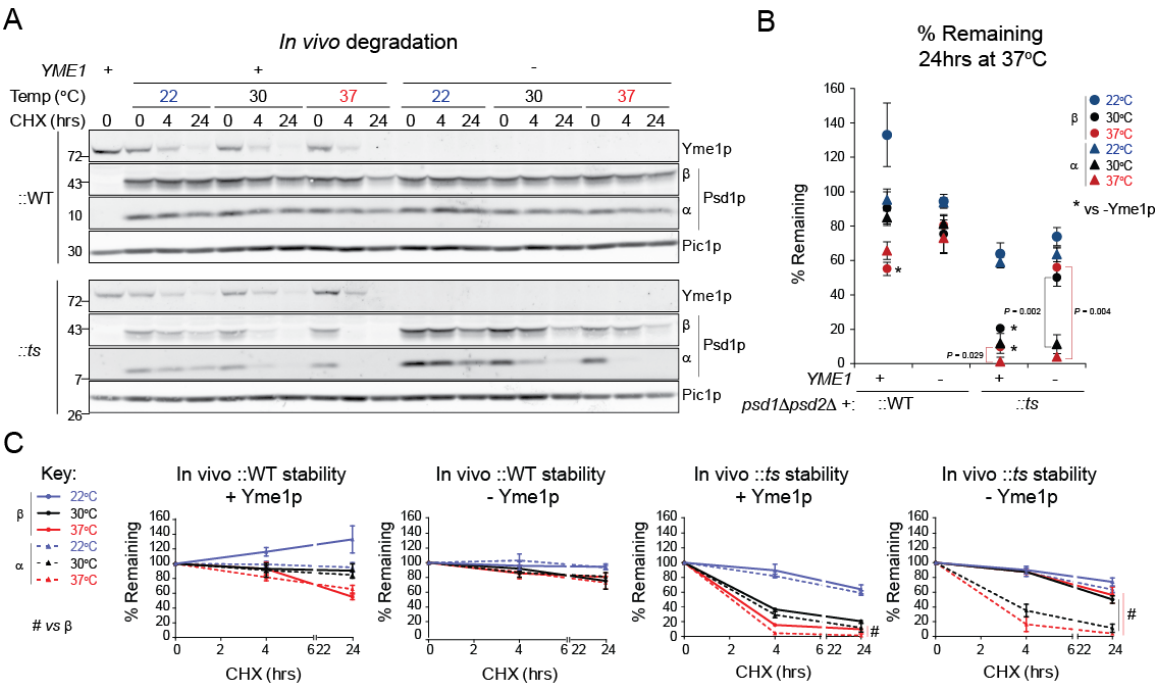

Figure 4.7. Yme1p is responsible for the rapid turnover of *ts* β but not *ts* α. (A) *In vivo* degradation assay. Whole cell extracts were isolated at the designated times following growth at the indicated temperature in the presence of CHX. Samples were resolved by SDS-PAGE and immunoblotted as indicated. (B) The % of α and β subunits remaining after 24hrs at 37°C for WT and *ts* Psd1p in the presence or absence of Yme1p was quantified. Mean ± SEM, *n*=4 * P≤0.05 (Student's t-test). (C) The % of α and β subunits remaining for WT and *ts* Psd1p at each timepoint +/- Yme1p was quantified. Mean ± SEM, *n*=4 # P≤0.05 (Student's t-test).

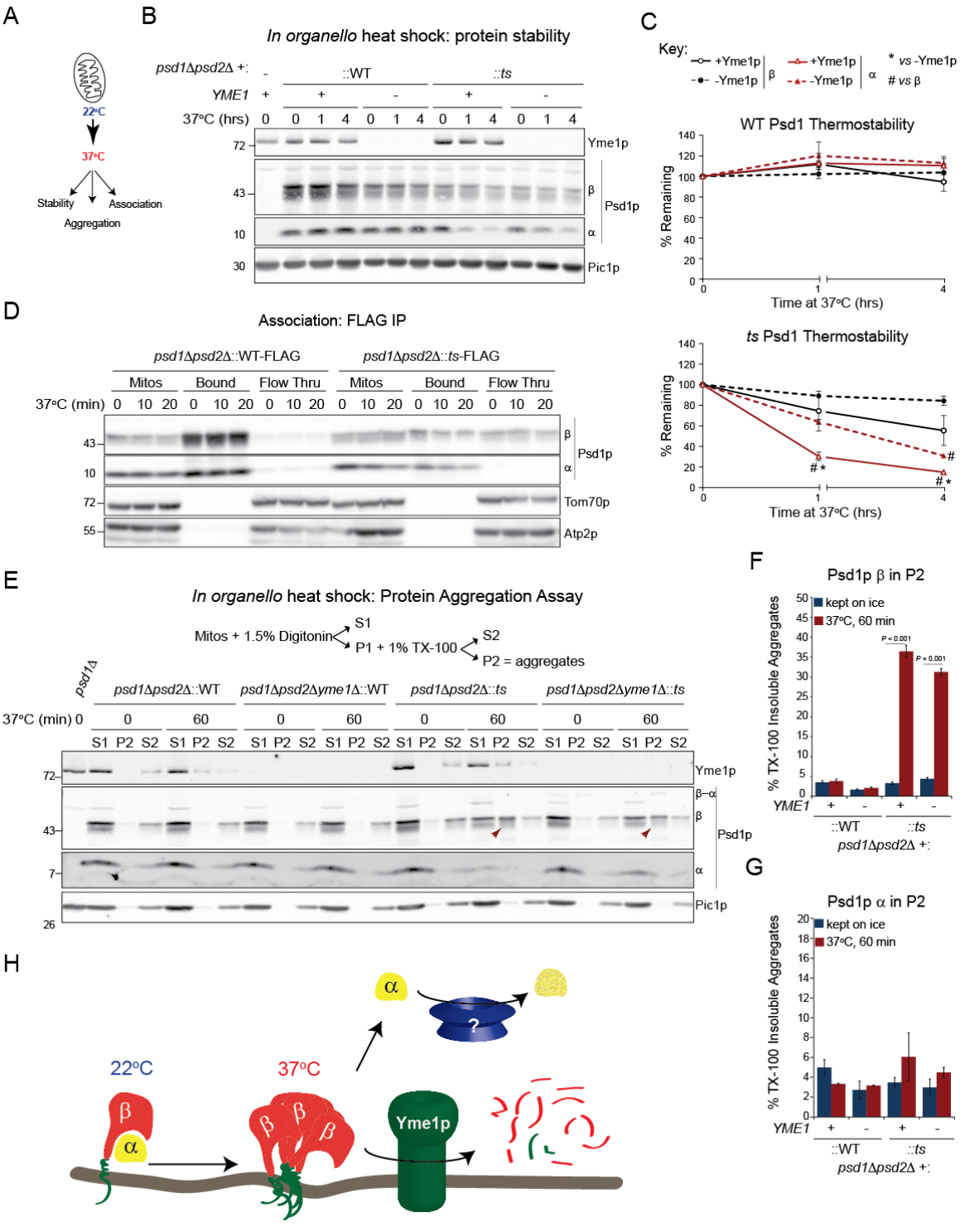

Figure 4.8. *ts* β subunit aggregates require Yme1p for their removal. (A) Schematic for assays performed in isolated mitochondria heat treated or not. (B) Mitochondria were isolated from the indicated yeast strains grown at 22ºC. Following incubation for the

designated times at 37ºC, mitochondria were recovered and 50 μg resolved by SDS-PAGE and immunoblotted as indicated. (C) The % of α and β subunits remaining for WT and *ts* Psd1p at each timepoint +/- Yme1p was quantified. Mean ± SEM, *n*=3. (D) Mitochondria incubated for the designated times at 37ºC were solubilized with 1.5% (wt/vol) digitonin, the FLAG tagged α subunit captured with anti-FLAG resin, and the presence of co-purified β determined by immunoblot; Tom70p and Atp2p served as controls. SM, starting material; B, bound material; FT, non-binding flow through. (E) Mitochondria were kept on ice or incubated at 37ºC for 1hr prior to performing a sequential detergent solubilization assay to detect protein aggregation. Fractions were resolved by SDS–PAGE and immunoblotted as indicated. (F and G) The percentage of WT and *ts* β subunit (F) and α subunit (G) in TX-100-insoluble aggregates was determined. Mean ± SEM; *n* = 3 (H) When shifted to high temperatures, the β subunit of $Psd1^{ts}$ forms aggregates that are resolved by Yme1p. The α subunit is not included in the *ts* β subunit aggregates and is rapidly degraded by an unidentified protease.

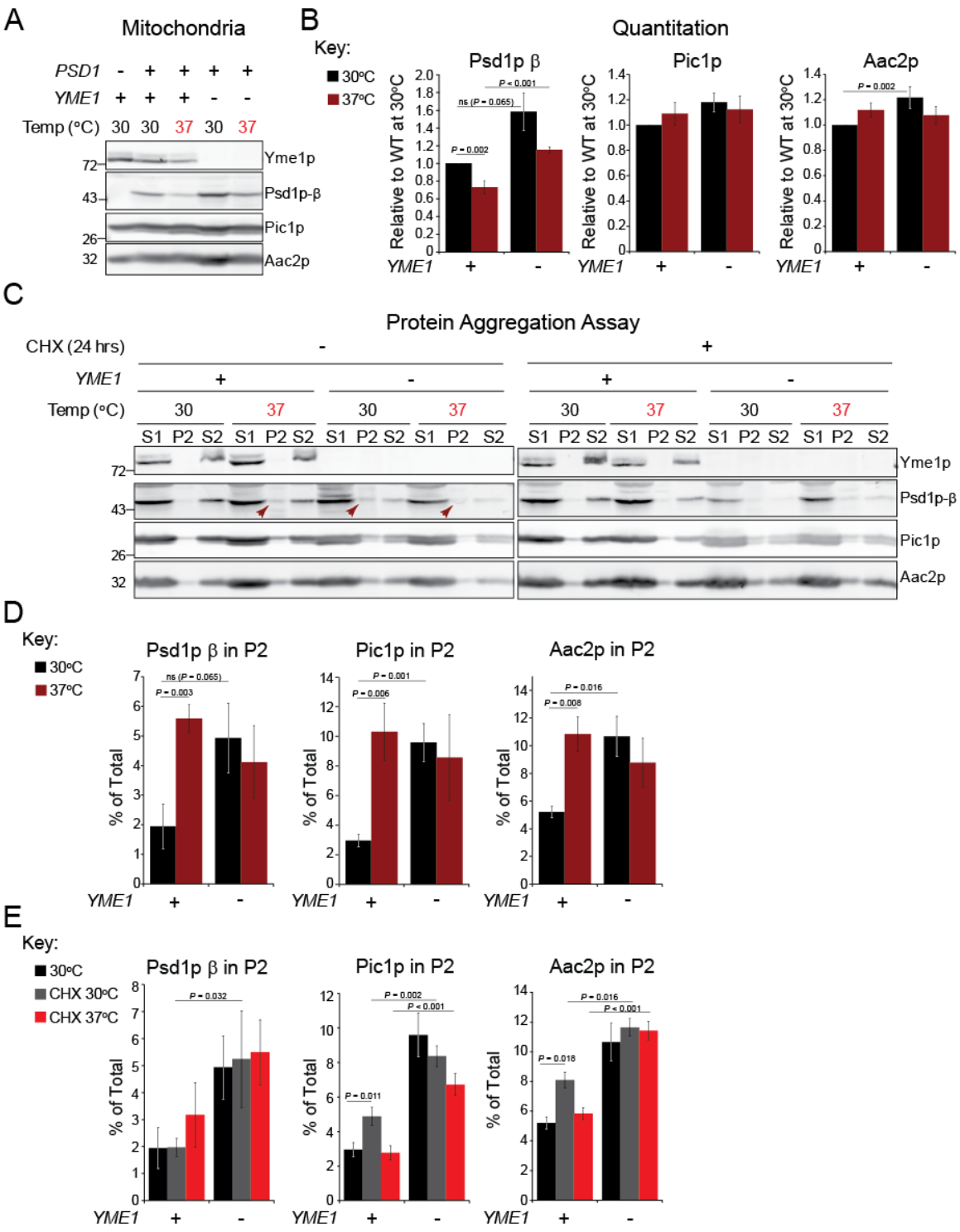

Figure 4.9. Evidence that Yme1p is important for endogenous Psd1p fidelity. (A) Mitochondria (50µg) from WT and *yme1*Δ yeast grown at the indicated temperature were immunoblotted as designated. (B) Densitometry analyses of protein steady state levels

from mitochondrial extracts from Figure 9A. Expression relative to WT at 30ºC ± SEM *n* = 6 for Psd1p and Aac2p and *n* = 3 for Pic1p. Significant differences were determined by Student's t-test and are indicated; if Normality or Equal Variance tests failed, significant differences were instead determined by Mann-Whitney Rank Sum Test (C) Mitochondria were isolated from WT and *yme1*Δ yeast grown at the indicated temperature in the absence (*left panels*) or presence of CHX for 24hrs (*right panels*) and protein aggregation determined using the sequential detergent solubilization assay. Fractions were resolved by SDS–PAGE and immunoblotted as indicated. (D) The percentage of Psd1p β subunit, Pic1p, and Aac2p in TX-100-insoluble aggregates following growth of WT and *yme1*Δ yeast at 30ºC or 37ºC in absence of CHX was determined. Mean ± SEM; *n* = 5 (E) The percentage of Psd1p β subunit, Pic1p, and Aac2p in TX-100-insoluble aggregates following growth of WT and *yme1*Δ yeast for 24hrs at 30ºC or 37ºC in presence of CHX was determined. Mean ± SEM; *n* = 5 Significant differences in D and E were determined by One Way ANOVA, with Holm–Sidak pairwise comparisons and are indicated; if Normality or Equal Variance tests failed, significant differences were instead determined by Kruskal-Wallis One Way ANOVA on Ranks**,** with Tukey Test pairwise comparisons. n.s. = Not Significant.

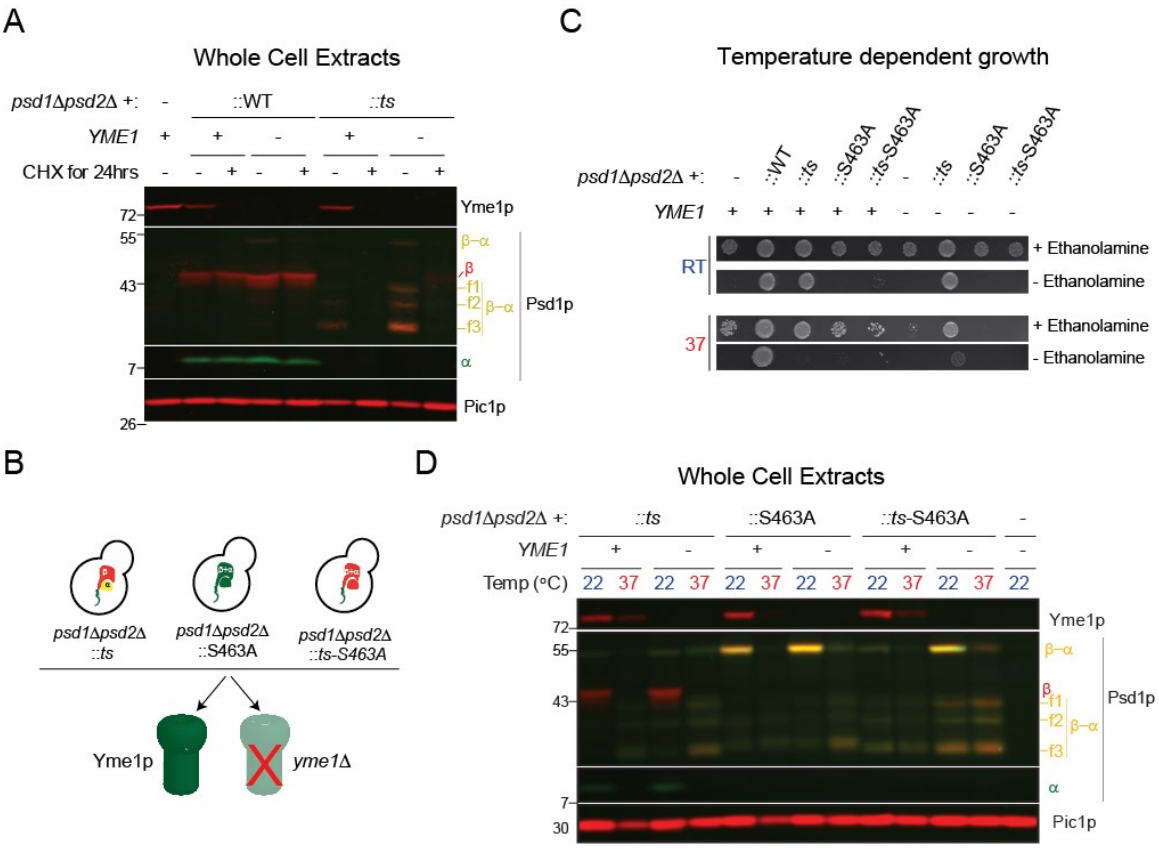

Figure 4.10. The three COOH terminal containing Psd1^{ts} fragments are not generated by aberrant self-proteolysis. (A) Immunoblots for Yme1p and the α and β subunits of WT and *ts* Psd1p in the indicated whole cell extracts from yeast grown at 37ºC for 24hrs with or without CHX; Pic1p served as a loading control. (B) Schematic for generating strains expressing a set amount of *ts*, S463A, or *ts*-S463A Psd1p in the presence or absence of Yme1p. (C) The indicated strains pre-cultured at 22ºC were spotted onto SCD +/- 2mM ethanolamine and incubated at 22ºC or 37ºC for 5 days. (D) Immunoblots for Yme1p and the α and β subunits of *ts,* S463A, and *ts*-S463A Psd1p in the indicated whole cell extracts from yeast grown at listed temperature; Pic1p served as a loading control. β-α, Psd1p that has not performed autocatalysis. f1, f2, and f3, COOH terminal containing Psd1p fragments.

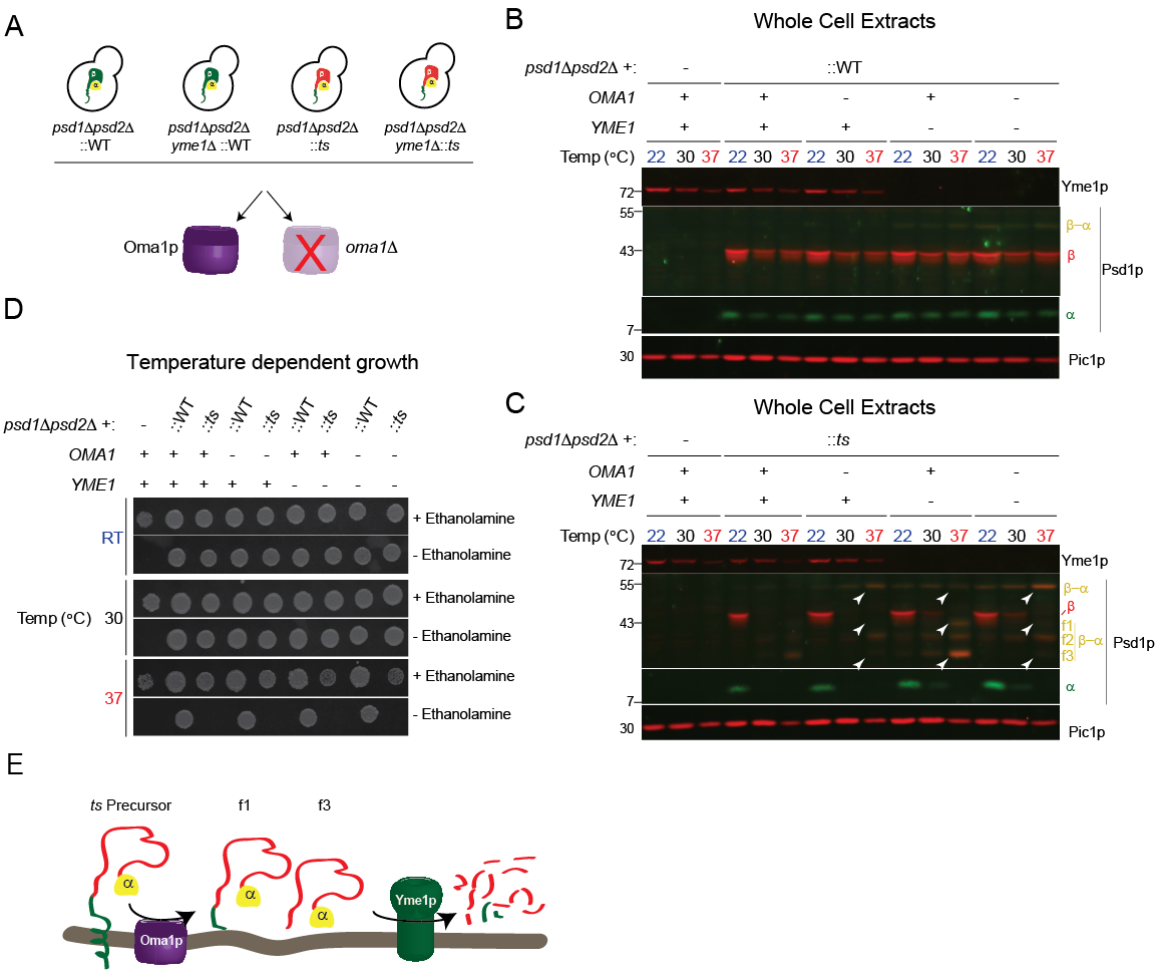

Figure 4.11. Oma1p and Yme1p work sequentially to degrade the Psd^{ts} precursor. (A) Schematic for generating strains expressing a set amount of WT or *ts* Psd1p in the presence or absence of Oma1p and/or Yme1p. (B and C) Immunoblots for Yme1p and the α and β subunits of (B) WT Psd1p or (C) *ts* Psd1p in whole cell extracts from the indicated yeast grown at listed temperature; Pic1p served as a loading control. (D) The indicated strains pre-cultured at 22ºC were spotted onto SCD +/- 2mM ethanolamine and incubated at 22ºC, 30ºC, or 37ºC. (E) When Psd1^{ts} is unable to adopt an autocatalytically competent tertiary structure at restrictive temperature, Oma1p generates two COOH-terminal containing fragments that are then completely degraded by Yme1p.

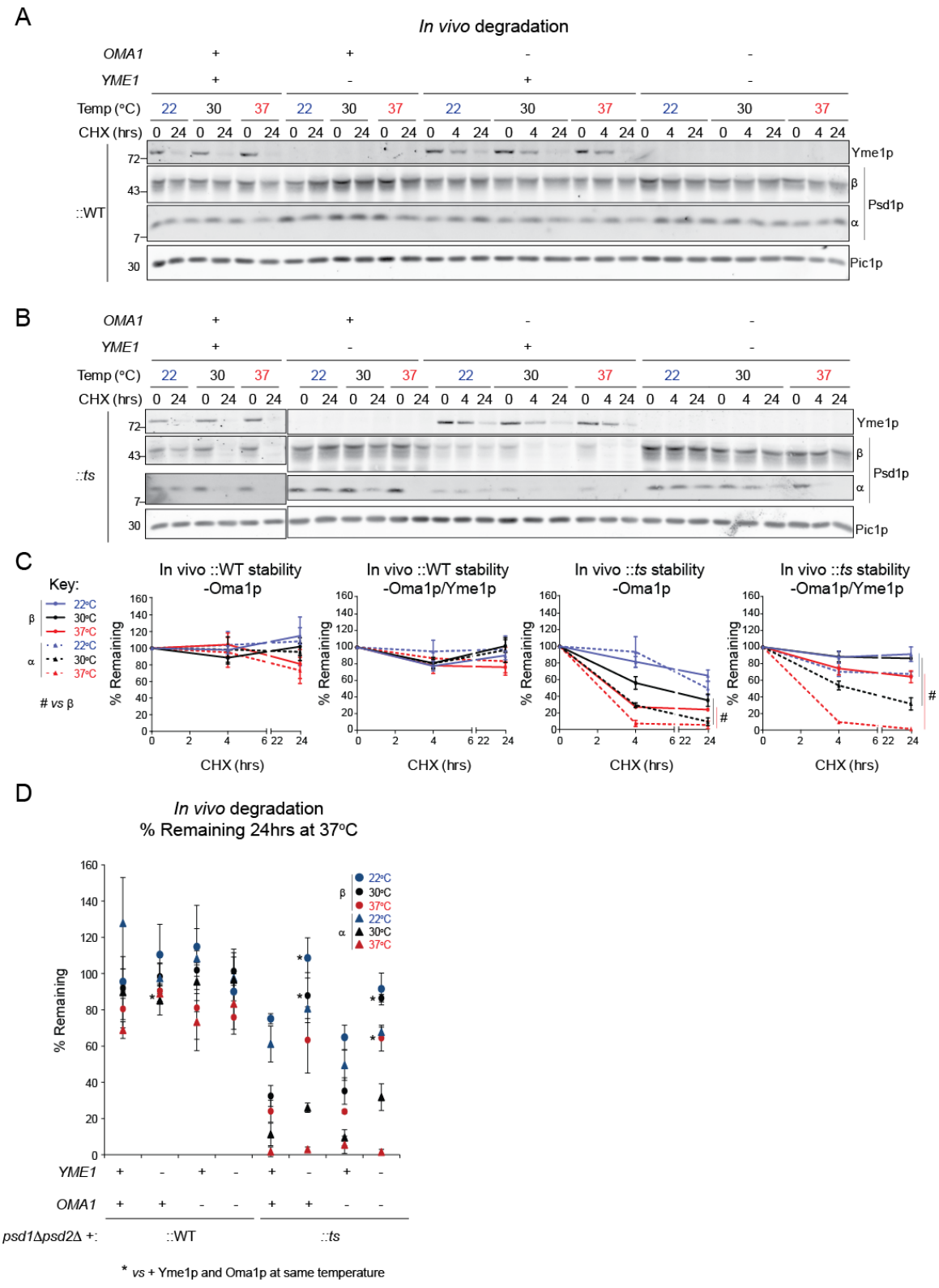

Figure 4.12. Oma1p is not required for the degradation of either *ts* subunit post-

autocatalysis. (A and B) *In vivo* degradation assay. Whole cell extracts from yeast expressing (A) WT Psd1p or (B) *ts* Psd1p were isolated at the designated times following growth at the indicated temperature in the presence of CHX. Samples were resolved by SDS-PAGE and immunoblotted as indicated. (C) The % of α and β subunits remaining for WT and *ts* Psd1p at each time point in the absence of Oma1p or the combined absence of Oma1p and Yme1p was quantified. Mean ± SEM, n=4 # P≤0.05 (Student's t-test). (D) The % of α and β subunits remaining after 24hrs at 37ºC for WT and *ts* Psd1p in the presence or absence of Oma1p and/or Yme1p was quantified. Mean ± SEM, n=4 * P≤0.05 (Student's t-test).

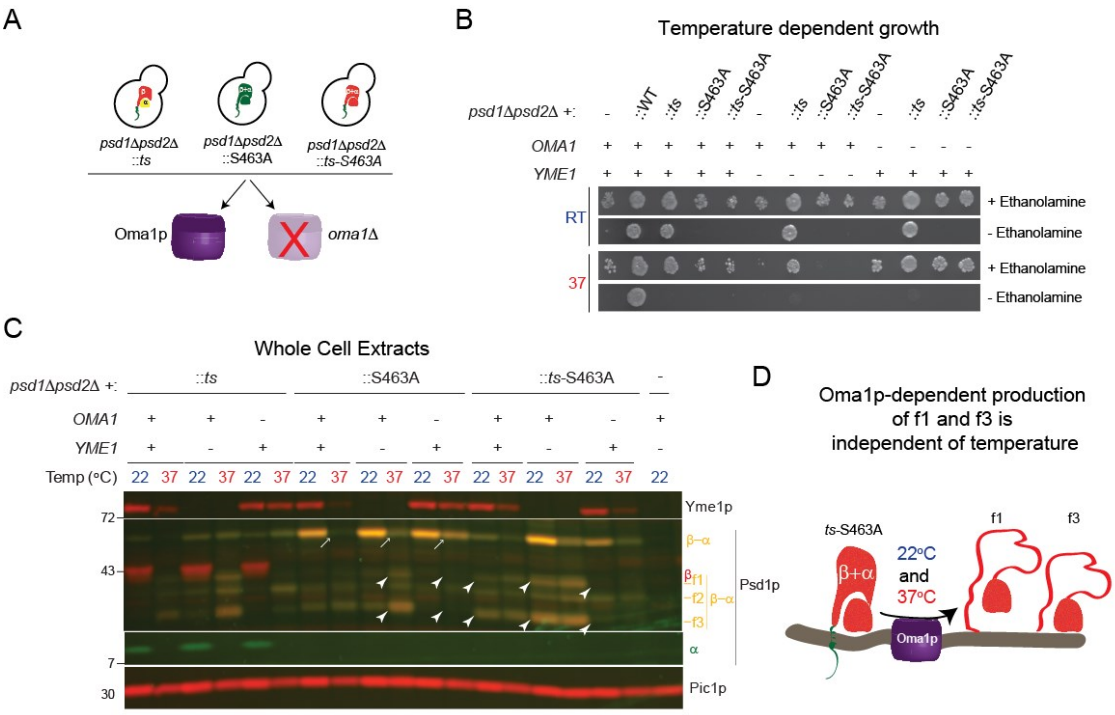

Figure 4.13. Oma1p-dependent generation of f1 and f3 can occur at 22ºC. (A) Schematic for generating strains expressing a set amount of *ts*, S463A, or *ts*-S463A Psd1p in the presence or absence of Oma1p. (B) The indicated strains pre-cultured at 22ºC were spotted onto SCD +/- 2mM ethanolamine and incubated at 22ºC or 37ºC for 5 days. (C) Immunoblots for Yme1p and the α and β subunits of *ts,* S463A, and *ts*-S463A Psd1p in the indicated whole cell extracts from yeast grown at listed temperature; Pic1p served as a loading control. β-α, Psd1p that has not performed autocatalysis. f1, f2, and f3, COOH terminal containing Psd1p fragments. (D) The Oma1p-dependent accumulation of f1 and f3 fragments from *ts*-S463A Psd1p occurs at both 22ºC and 37ºC.

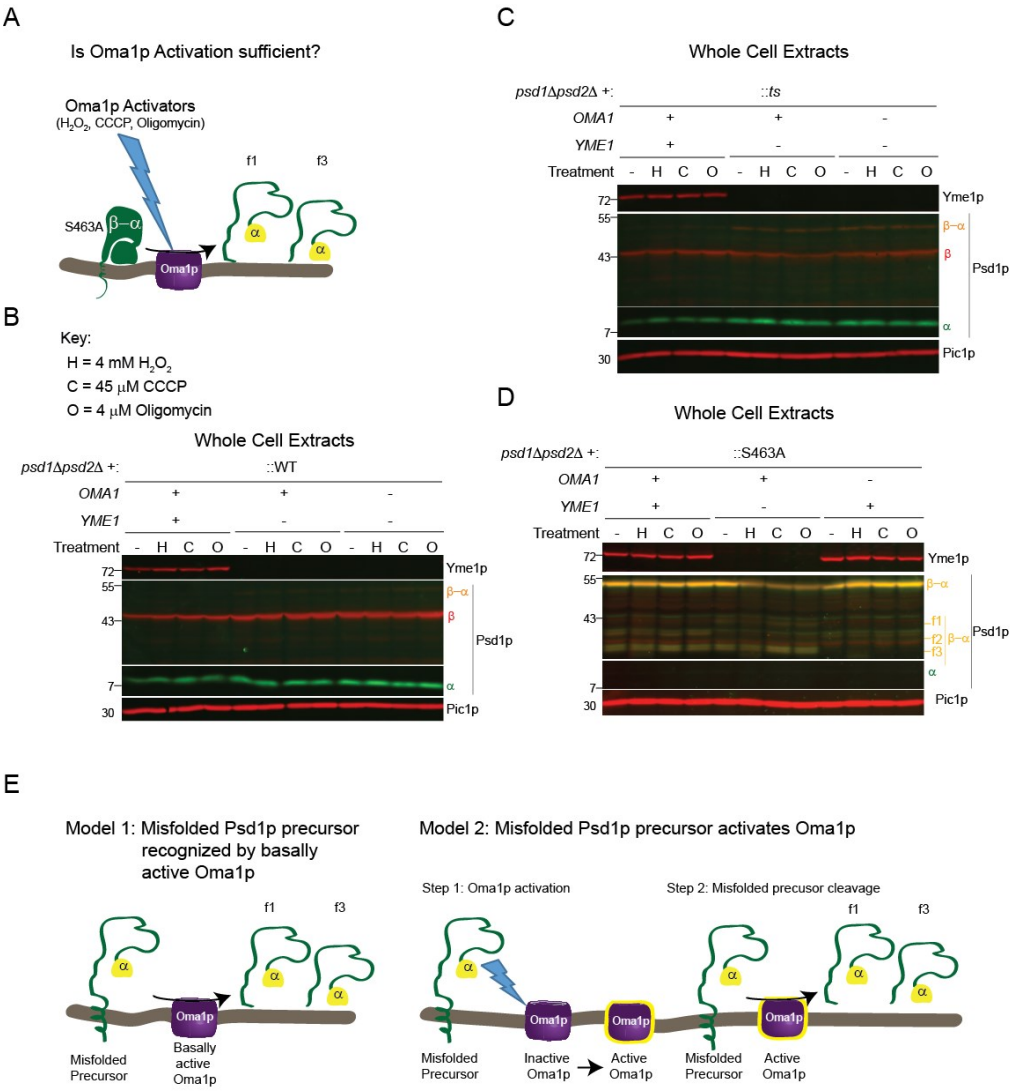

Figure 4.14. Oma1p activation is not sufficient to drive the accumulation of f1 and f3. (A) Can known Oma1p-activating agents result in the accumulation of f1 and f3 fragments from the autocatalytic mutant S463A Psd1p? (B-D) Immunoblots for Yme1p and the α and β subunits of (B) WT, (C) *ts*, and (D) S463A Psd1p in whole cell extracts from yeast grown at 22ºC (*ts* and S463A) or 30ºC (WT Psd1p) in the absence or presence of 4 mM H_2O_2, 45 μM CCCP, or 4 μM Oligomycin for 4hrs; Pic1p served as a loading control. β-α, Psd1p that has not performed autocatalysis. f1, f2, and f3, COOH terminal containing Psd1p fragments. (E) Two possible models that explain the generation of f1 and f3 from misfolded

Psd1p precursor. According to Model 1, some fraction of Oma1p is always basally active and thus available to degrade misfolded Psd1p precursor in the absence of any overt mitochondrial stress. In Model 2, the misfolded Psd1p precursor itself is the signal that activates inactive Oma1p thus initiating its own removal.

REFERENCES

Aaltonen, M. J., Friedman, J. R., Osman, C., Salin, B., di Rago, J. P., Nunnari, J., . . . Tatsuta, T. (2016). MICOS and phospholipid transfer by Ups2-Mdm35 organize membrane lipid synthesis in mitochondria. *J Cell Biol, 213*(5), 525-534. doi:doi: 10.1083/jcb.201602007

Anand, R., Wai, T., Baker, M. J., Kladt, N., Schauss, A. C., Rugarli, E., & Langer, T. (2014). The i-AAA protease YME1L and OMA1 cleave OPA1 to balance mitochondrial fusion and fission. *J Cell Biol, 204*(6), 919-929. doi:doi: 10.1083/jcb.201308006

Baker, M. J., Lampe, P. A., Stojanovski, D., Korwitz, A., Anand, R., Tatsuta, T., & Langer, T. (2014). Stress-induced OMA1 activation and autocatalytic turnover regulate OPA1-dependent mitochondrial dynamics. *EMBO J, 33*(6), 578-593. doi:doi: 10.1002/embj.201386474

Bao, Z., Xiao, H., Liang, J., Zhang, L., Xiong, X., Sun, N., . . . Zhao, H. (2015). Homology-integrated CRISPR-Cas (HI-CRISPR) system for one-step multigene disruption in Saccharomyces cerevisiae. *ACS Synth Biol, 4*(5), 585-594. doi:doi: 10.1021/sb500255k

Birner, R., Nebauer, R., Schneiter, R., & Daum, G. (2003). Synthetic lethal interaction of the mitochondrial phosphatidylethanolamine biosynthetic machinery with the prohibitin complex of Saccharomyces cerevisiae. *Mol Biol Cell, 14*(2), 370-383. doi:doi: 10.1091/mbc.E02-05-0263

Bogdanov, Mikhail, & Dowhan, William. (2012). Lipid-dependent Generation of Dual Topology for a Membrane Protein. *Journal of Biological Chemistry, 287*(45), 37939-37948. doi:doi: 10.1074/jbc.M112.404103

Bohovych, Iryna, Donaldson, Garrett, Christianson, Sara, Zahayko, Nataliya, & Khalimonchuk, Oleh. (2014). Stress-triggered Activation of the Metalloprotease Oma1 Involves Its C-terminal Region and Is Important for Mitochondrial Stress Protection in Yeast. *Journal of Biological Chemistry, 289*(19), 13259-13272. doi:doi: 10.1074/jbc.M113.542910

Choi, J. Y., Augagneur, Y., Ben Mamoun, C., & Voelker, D. R. (2012). Identification of gene encoding Plasmodium knowlesi phosphatidylserine decarboxylase by genetic complementation in yeast and characterization of in vitro maturation of encoded enzyme. *J Biol Chem, 287*(1), 222-232. doi:doi: 10.1074/jbc.M111.313676

Choi, J. Y., Duraisingh, M. T., Marti, M., Ben Mamoun, C., & Voelker, D. R. (2015). From Protease to Decarboxylase: THE MOLECULAR METAMORPHOSIS OF PHOSPHATIDYLSERINE DECARBOXYLASE. *J Biol Chem, 290*(17), 10972-10980. doi:doi: 10.1074/jbc.M115.642413

Claypool, S. M., Boontheung, P., McCaffery, J. M., Loo, J. A., & Koehler, C. M. (2008). The cardiolipin transacylase, tafazzin, associates with two distinct respiratory components providing insight into Barth syndrome. *Mol. Biol. Cell, 19*(12), 5143-5155 PMCID: PMC2592642. doi:E08-09-0896 [pii]10.1091/mbc.E08-09-0896

Claypool, S. M., Dickinson, B. L., Yoshida, M., Lencer, W. I., & Blumberg, R. S. (2002). Functional reconstitution of human FcRn in Madin-Darby canine kidney cells

requires co-expressed human beta 2-microglobulin. *J Biol Chem, 277*(31), 28038-28050. doi:doi: 10.1074/jbc.M202367200

Claypool, S. M., McCaffery, J. M., & Koehler, C. M. (2006). Mitochondrial mislocalization and altered assembly of a cluster of Barth syndrome mutant tafazzins. *J Cell Biol, 174*(3), 379-390 doi:doi: 10.1083/jcb.200605043

Claypool, S. M., Whited, K., Srijumnong, S., Han, X., & Koehler, C. M. (2011). Barth syndrome mutations that cause tafazzin complex lability. *J Cell Biol, 192*(3), 447-462 doi:doi: 10.1083/jcb.201008177

Connerth, M., Tatsuta, T., Haag, M., Klecker, T., Westermann, B., & Langer, T. (2012). Intramitochondrial transport of phosphatidic acid in yeast by a lipid transfer protein. *Science, 338*(6108), 815-818. doi:doi: 10.1126/science.1225625

Duvezin-Caubet, S., Jagasia, R., Wagener, J., Hofmann, S., Trifunovic, A., Hansson, A., . . . Reichert, A. S. (2006). Proteolytic processing of OPA1 links mitochondrial dysfunction to alterations in mitochondrial morphology. *J Biol Chem, 281*(49), 37972-37979. doi:doi: 10.1074/jbc.M606059200

Ehses, S., Raschke, I., Mancuso, G., Bernacchia, A., Geimer, S., Tondera, D., . . . Langer, T. (2009). Regulation of OPA1 processing and mitochondrial fusion by m-AAA protease isoenzymes and OMA1. *J Cell Biol, 187*(7), 1023-1036. doi:doi: 10.1083/jcb.200906084

Emoto, Kazuo, Kobayashi, Toshihide, Yamaji, Akiko, Aizawa, Hiroyuki, Yahara, Ichiro, Inoue, Keizo, & Umeda, Masato. (1996). Redistribution of phosphatidylethanolamine at the cleavage furrow of dividing cells

during cytokinesis. *Proceedings of the National Academy of Sciences, 93*(23), 12867-12872.

Engler, C., Gruetzner, R., Kandzia, R., & Marillonnet, S. (2009). Golden gate shuffling: a one-pot DNA shuffling method based on type IIs restriction enzymes. *PLoS One, 4*(5), e5553. doi:doi: 10.1371/journal.pone.0005553

Fullerton, M. D., Hakimuddin, F., & Bakovic, M. (2007). Developmental and metabolic effects of disruption of the mouse CTP:phosphoethanolamine cytidylyltransferase gene (Pcyt2). *Mol Cell Biol, 27*(9), 3327-3336. doi:doi: 10.1128/MCB.01527-06

Glick, Benjamin S., Brandt, Anders, Cunningham, Kyle, Müller, Sabina, Hallberg, Richard L., & Schatz, Gottfried. (1992). Cytochromes c1 and b2 are sorted to the intermembrane space of yeast mitochondria by a stop-transfer mechanism. *Cell, 69*(5), 809-822. doi:http://dx.doi.org/10.1016/0092-8674(92)90292-K

Griparic, L., Kanazawa, T., & van der Bliek, A. M. (2007). Regulation of the mitochondrial dynamin-like protein Opa1 by proteolytic cleavage. *J Cell Biol, 178*(5), 757-764. doi:doi: 10.1083/jcb.200704112

Gulshan, K., Schmidt, J. A., Shahi, P., & Moye-Rowley, W. S. (2008). Evidence for the bifunctional nature of mitochondrial phosphatidylserine decarboxylase: role in Pdr3-dependent retrograde regulation of PDR5 expression. *Mol Cell Biol, 28*(19), 5851-5864. doi:doi: 10.1128/MCB.00405-08

Head, B., Griparic, L., Amiri, M., Gandre-Babbe, S., & van der Bliek, A. M. (2009). Inducible proteolytic inactivation of OPA1 mediated by the OMA1 protease in mammalian cells. *J Cell Biol, 187*(7), 959-966. doi:doi: 10.1083/jcb.200906083

Ho, S. N., Hunt, H. D., Horton, R. M., Pullen, J. K., & Pease, L. R. (1989). Site-directed mutagenesis by overlap extension using the polymerase chain reaction. *Gene, 77*(1), 51-59.

Horvath, S. E., Bottinger, L., Vogtle, F. N., Wiedemann, N., Meisinger, C., Becker, T., & Daum, G. (2012). Processing and topology of the yeast mitochondrial phosphatidylserine decarboxylase 1. *J Biol Chem, 287*(44), 36744-36755. doi:doi: 10.1074/jbc.M112.398107

Hwang, D. K., Claypool, S. M., Leuenberger, D., Tienson, H. L., & Koehler, C. M. (2007). Tim54p connects inner membrane assembly and proteolytic pathways in the mitochondrion. *J Cell Biol, 178*(7), 1161-1175. doi:doi: 10.1083/jcb.200706195

Ichimura, Yoshinobu, Kirisako, Takayoshi, Takao, Toshifumi, Satomi, Yoshinori, Shimonishi, Yasutsugu, Ishihara, Naotada, . . . Ohsumi, Yoshinori. (2000). A ubiquitin-like system mediates protein lipidation. *Nature, 408*(6811), 488-492.

Kaser, M., Kambacheld, M., Kisters-Woike, B., & Langer, T. (2003). Oma1, a novel membrane-bound metallopeptidase in mitochondria with activities overlapping with the m-AAA protease. *J Biol Chem, 278*(47), 46414-46423. doi:doi: 10.1074/jbc.M305584200

Keckesova, Z., Donaher, J. L., De Cock, J., Freinkman, E., Lingrell, S., Bachovchin, D. A., . . . Weinberg, R. A. (2017). LACTB is a tumour suppressor that modulates lipid metabolism and cell state. *Nature, 543*(7647), 681-686. doi:10.1038/nature21408

Korwitz, A., Merkwirth, C., Richter-Dennerlein, R., Troder, S. E., Sprenger, H. G., Quiros, P. M., . . . Langer, T. (2016). Loss of OMA1 delays neurodegeneration by

preventing stress-induced OPA1 processing in mitochondria. *J Cell Biol, 212*(2), 157-166. doi:doi: 10.1083/jcb.201507022

Kuge, O., Saito, K., Kojima, M., Akamatsu, Y., & Nishijima, M. (1996). Post-translational processing of the phosphatidylserine decarboxylase gene product in Chinese hamster ovary cells. *Biochem J, 319 (Pt 1)*, 33-38.

Li, Q. X., & Dowhan, W. (1988). Structural characterization of Escherichia coli phosphatidylserine decarboxylase. *J Biol Chem, 263*(23), 11516-11522.

Li, Q. X., & Dowhan, W. (1990). Studies on the mechanism of formation of the pyruvate prosthetic group of phosphatidylserine decarboxylase from Escherichia coli. *J Biol Chem, 265*(7), 4111-4115.

Lu, Y. W., & Claypool, S. M. (2015). Disorders of phospholipid metabolism: an emerging class of mitochondrial disease due to defects in nuclear genes. *Front Genet, 6*, 3. doi:doi: 10.3389/fgene.2015.00003

Mans, R., van Rossum, H. M., Wijsman, M., Backx, A., Kuijpers, N. G., van den Broek, M., . . . Daran, J. M. (2015). CRISPR/Cas9: a molecular Swiss army knife for simultaneous introduction of multiple genetic modifications in Saccharomyces cerevisiae. *FEMS Yeast Res, 15*(2). doi:doi: 10.1093/femsyr/fov004

Menon, A K, & Stevens, V L. (1992). Phosphatidylethanolamine is the donor of the ethanolamine residue linking a glycosylphosphatidylinositol anchor to protein. *Journal of Biological Chemistry, 267*(22), 15277-15280.

Mishra, P., Carelli, V., Manfredi, G., & Chan, D. C. (2014). Proteolytic cleavage of Opa1 stimulates mitochondrial inner membrane fusion and couples fusion to oxidative phosphorylation. *Cell Metab, 19*(4), 630-641. doi:doi: 10.1016/j.cmet.2014.03.011

Miyata, N., Watanabe, Y., Tamura, Y., Endo, T., & Kuge, O. (2016). Phosphatidylserine transport by Ups2-Mdm35 in respiration-active mitochondria. *J Cell Biol, 214*(1), 77-88. doi:doi: 10.1083/jcb.201601082

Nebauer, R., Schuiki, I., Kulterer, B., Trajanoski, Z., & Daum, G. (2007). The phosphatidylethanolamine level of yeast mitochondria is affected by the mitochondrial components Oxa1p and Yme1p. *FEBS J, 274*(23), 6180-6190. doi:EJB6138 [pii]doi: 10.1111/j.1742-4658.2007.06138.x

Nesic, Iva, Guix, Francesc X., Vennekens, Krist'l, Michaki, Vasiliki, Van Veldhoven, Paul P., Feiguin, Fabian, . . . Wahle, Tina. (2012). Alterations in phosphatidylethanolamine levels affect the generation of Aβ. *Aging Cell, 11*(1), 63-72. doi:doi: 10.1111/j.1474-9726.2011.00760.x

Onguka, O., Calzada, E., Ogunbona, O. B., & Claypool, S. M. (2015). Phosphatidylserine decarboxylase 1 autocatalysis and function does not require a mitochondrial-specific factor. *J Biol Chem, 290*(20), 12744-12752. doi:doi: 10.1074/jbc.M115.641118

Osman, C., Voelker, D. R., & Langer, T. (2011). Making heads or tails of phospholipids in mitochondria. *J Cell Biol, 192*(1), 7-16. doi:doi: 10.1083/jcb.201006159

Potting, C., Wilmes, C., Engmann, T., Osman, C., & Langer, T. (2010). Regulation of mitochondrial phospholipids by Ups1/PRELI-like proteins depends on proteolysis and Mdm35. *EMBO J, 29*(17), 2888-2898. doi:doi: 10.1038/emboj.2010.169

Rainbolt, T. K., Lebeau, J., Puchades, C., & Wiseman, R. L. (2016). Reciprocal Degradation of YME1L and OMA1 Adapts Mitochondrial Proteolytic Activity during Stress. *Cell Rep, 14*(9), 2041-2049. doi:doi: 10.1016/j.celrep.2016.02.011

Rainbolt, T. K., Saunders, J. M., & Wiseman, R. L. (2015). YME1L degradation reduces mitochondrial proteolytic capacity during oxidative stress. *EMBO Rep, 16*(1), 97-106. doi:doi: 10.15252/embr.201438976

Satre, M, & Kennedy, E P. (1978). Identification of bound pyruvate essential for the activity of phosphatidylserine decarboxylase of Escherichia coli. *Journal of Biological Chemistry, 253*(2), 479-483.

Schreiner, B., Westerburg, H., Forne, I., Imhof, A., Neupert, W., & Mokranjac, D. (2012). Role of the AAA protease Yme1 in folding of proteins in the intermembrane space of mitochondria. *Mol Biol Cell, 23*(22), 4335-4346. doi:doi: 10.1091/mbc.E12-05-0420

Song, Z., Chen, H., Fiket, M., Alexander, C., & Chan, D. C. (2007). OPA1 processing controls mitochondrial fusion and is regulated by mRNA splicing, membrane potential, and Yme1L. *J Cell Biol, 178*(5), 749-755. doi:doi: 10.1083/jcb.200704110

Steenbergen, R., Nanowski, T. S., Beigneux, A., Kulinski, A., Young, S. G., & Vance, J. E. (2005). Disruption of the phosphatidylserine decarboxylase gene in mice causes embryonic lethality and mitochondrial defects. *J Biol Chem, 280*(48), 40032-40040. doi:doi: 10.1074/jbc.M506510200

Summers, E F, Letts, V A, McGraw, P, & Henry, S A. (1988). Saccharomyces cerevisiae cho2 mutants are deficient in phospholipid methylation and cross-pathway regulation of inositol synthesis. *Genetics, 120*(4), 909-922.

Tamura, Y., Onguka, O., Hobbs, A. E., Jensen, R. E., Iijima, M., Claypool, S. M., & Sesaki, H. (2012). Role for two conserved intermembrane space proteins, Ups1p and

Ups2p, [corrected] in intra-mitochondrial phospholipid trafficking. *J Biol Chem, 287*(19), 15205-15218 doi:doi: 10.1074/jbc.M111.338665

Tamura, Yasushi, Iijima, Miho, & Sesaki, Hiromi. (2010). Mdm35p imports Ups proteins into the mitochondrial intermembrane space by functional complex formation. *EMBO J, 29*(17), 2875-2887. doi:http://www.nature.com/emboj/journal/v29/n17/suppinfo/emboj2010149a_S1.html

Trotter, P. J., Pedretti, J., & Voelker, D. R. (1993). Phosphatidylserine decarboxylase from Saccharomyces cerevisiae. Isolation of mutants, cloning of the gene, and creation of a null allele. *J Biol Chem, 268*(28), 21416-21424.

Trotter, P. J., & Voelker, D. R. (1995). Identification of a non-mitochondrial phosphatidylserine decarboxylase activity (PSD2) in the yeast Saccharomyces cerevisiae. *J Biol Chem, 270*(11), 6062-6070.

van der Veen, J. N., Lingrell, S., da Silva, R. P., Jacobs, R. L., & Vance, D. E. (2014). The concentration of phosphatidylethanolamine in mitochondria can modulate ATP production and glucose metabolism in mice. *Diabetes, 63*(8), 2620-2630. doi:10.2337/db13-0993

Wang, S., Zhang, S., Liou, L. C., Ren, Q., Zhang, Z., Caldwell, G. A., . . . Witt, S. N. (2014). Phosphatidylethanolamine deficiency disrupts alpha-synuclein homeostasis in yeast and worm models of Parkinson disease. *Proc Natl Acad Sci U S A, 111*(38), E3976-3985. doi:10.1073/pnas.1411694111

Whited, K., Baile, M. G., Currier, P., & Claypool, S. M. (2013). Seven functional classes of Barth syndrome mutation. *Hum Mol Genet, 22*(3), 483-492 doi:doi: 10.1093/hmg/dds447

Oluwaseun B Ogunbona **March 28, 2018**

Educational History:

Ph.D.	2018	**Program:** Cellular and Molecular Physiology (CMP) **Mentor:** Steven M. Claypool, Ph.D.	Johns Hopkins University School of Medicine, Baltimore
MBBS	2013	Medicine and Surgery	College of Medicine, University of Lagos, Nigeria
B.Sc	2009	Physiology	College of Medicine, University of Lagos, Nigeria

Medical Licensure/Certification:

2017	Certificate Number: 0-939-821-5	Educational Commission for Foreign Medical Graduates

Research Experience:

Research Rotation	2014	Laboratory of Frank Bosmans, Ph.D.	Johns Hopkins University School of Medicine
Research Rotation	2014	Laboratory of Roger Reeves, Ph.D.	Johns Hopkins University School of Medicine
Research Rotation	2013	Laboratory of Guang W Wong, Ph.D.	Johns Hopkins University School of Medicine

Undergraduate Research	2008-2009	Laboratory of Prof Olusoga Sofola, MBBS, PhD	College of Medicine, University of Lagos, Nigeria

Scholarships and Fellowships:

Predoctoral Fellowship	2015-2017	15PRE24480066	American Heart Association

Awards and Honors:

2018	Alicia Showalter Reynolds Young Investigator Award	Johns Hopkins University School of Medicine
2017	Minority Travel Fellowship Award	The American Physiological Society (APS) and Janssen Pharmaceutical Companies of Johnson & Johnson
2017	Cardiovascular Outreach Award	American Heart Association
2017	Student Scholars Award	The American Thoracic Society
2014	Program for Excellence in Science – Sponsored membership (2014-2017)	American Association for the Advancement of Science (AAAS) /Science

Publications:

1. **Ogunbona, O. B.,** Baile, M. G., & Claypool, S. (2018). Cardiomyopathy-associated mutation in the ADP/ATP carrier reveals translation-dependent regulation of cytochrome c oxidase activity. Manuscript in revision at Molecular Biology of the Cell.

2. Kandasamy, S., Lu, Y., Acoba, M. G., **Ogunbona, O.,** Claypool, S. (2018). Cardiolipin and respiratory supercomplex-dependent oligomerization of the major mitochondrial ADP/ATP carrier in yeast. Manuscript in review at Journal of Biological Chemistry.

3. ***Ogunbona, O. B.,** *Onguka, O., Calzada, E., & Claypool, S. M. (2017). Multitiered and cooperative surveillance of mitochondrial Phosphatidylserine Decarboxylase 1. Mol Cell Biol. doi:10.1128/MCB.00049-17; *= co-first author

4. Onguka, O., Calzada, E., **Ogunbona, O.B.,** & Claypool, S.M. (2015). Phosphatidylserine decarboxylase 1 autocatalysis and function does not require a mitochondrial-specific factor. Journal of Biological Chemistry, 290(20), 12744-12752. doi:10.1074/jbc.M115.641118

5. **Ogunbona, O.,** Okafor, I., & Sekoni, A. (2013). Knowledge and practice of blood donation among university undergraduates. Highland Medical Research Journal, 13(1), 26-30.

Abstracts:

1. **Ogunbona, O.B.,** Baile, M.G., & Claypool, S. (2017). Cardiomyopathy-associated point mutation in the ADP-ATP carrier reveals translation-dependent regulation of cytochrome c oxidase activity in yeast. American Heart Association Basic Cardiovascular Scientific Sessions, held July 10-13, 2017, at the Hilton Portland & Executive Tower hotel in Portland, Oregon.

2. **Ogunbona, O.B.,** Baile, M.G., & Claypool, S. (2017). Cardiomyopathy-associated point mutation in the ADP-ATP carrier reveals translation-dependent regulation of cytochrome c oxidase activity in yeast. FASEB Mitochondrial meeting on Mitochondrial Biogenesis and Dynamics in Health, Disease and Aging held at Marriott West Palm Beach, 1001 Okeechobee Boulevard, West Palm Beach, Florida, from May 21-26, 2017

3. **Ogunbona, O.B.,** Baile, M.G., & Claypool, S. (2017). Regulation of the yeast mitochondrial respiratory complex IV activity by the major isoform of the ADP-ATP carrier (1007.3). The FASEB Journal, 31 (1 Supplement), 1007.3

4. **Ogunbona O.,** Baile M., & Claypool, S. (2015) Mechanisms of regulation of mitochondrial cytochrome c oxidase by the ADP/ATP carrier. FASEB Mitochondrial meeting on Mitochondrial Biogenesis and Dynamics in Health, Disease and Aging held at Marriott West Palm Beach, 1001 Okeechobee Boulevard, West Palm Beach, Florida, from May 17-22, 2015

5. Onguka, O., **Ogunbona, O.,** & Claypool, S. (2015). Identifying novel motifs required for Phosphatidylserine Decarboxylase Autocatalysis and Function. "Lipids, Molecular & Cellular Biology of" Gordon Research Conference Abstract # 6576. July 26-31, 2015, Waterville Valley, NH

6. Onguka, O., **Ogunbona, O.,** & Claypool, S. (2014). Defining the molecular requirements for phosphatidylserine decarboxylase activation (757.3). The FASEB Journal, 28 (1 Supplement), 757.3

Teaching Experience:

1. Pathways and Regulation, Teaching Assistant for the Biochemistry, Cellular and Molecular Biology Graduate Course Program, Spring 2015, 2016, 2017 and 2018

2. Organ Physiology, Teaching Assistant for the Physiology and Pharmacology Graduate Student Course, Spring 2015, 2016 and 2017

3. Cell Physiology section of Scientific Foundations of Medicine (including Macromolecules, Cell Physiology, Metabolism, Genetics, Pharmacology, Foundations in Histology & Pathobiology), Teaching Assistant for Medical Student Year I Course (MS-I) Fall 2015.